Discretisation of Hodge Laplacians in the Elasticity Complex



Francis R. A. Aznaran

The Queen's College

University of Oxford

A thesis submitted for the examination of

Doctor of Philosophy

Trinity 2022

Abstract

The elasticity differential complex associated with a 2- or 3-dimensional domain is a sequence of function spaces connected by differential operators, which together encode topological properties of the domain. Associated with any complex is a sequence of partial differential equations, known as the Hodge Laplace equations, which include and generalise many important elliptic equations arising in continuum mechanics. This thesis addresses the discretisation of the Sobolev spaces and Hodge Laplacian problems associated with the elasticity complex using finite elements. We demonstrate the broad utility of such efforts via applications to linear elasticity, linear irreversible thermodynamics, and defect elasticity.

First, we address the classical problem of enforcing the symmetry and div-conformity of the elastic stress tensor. The exactly symmetric Arnold–Winther elements were one of the key early breakthroughs of the finite element exterior calculus, but have never been systematically implemented, as their dual bases are not preserved by the Piola pullback; we develop abstract transformation theory which enables the first robust and composable implementations of these exotic elements. We then apply these tensor-valued elements to discretise the viscous stress in the compressible Stokes equations, a crucial coupling variable for the incorporation of convection into modelling the molecular diffusion of multicomponent single-phase fluids. We derive a novel variational formulation, called the *Stokes–Onsager–Stefan–Maxwell* system, with appropriate finite element discretisations which represent the first ever rigorous numerics for the coupling of non-ideal multicomponent diffusion with compressible convective flow. Finally, we turn our attention to the discretisation of the strain space in the elasticity complex, and analyse the *incompatibility operator* acting on strain tensor fields; the Hodge Laplacian boundary value problem we study comprises initial steps towards a canonical well-posed model of linearised defect elasticity.

Acknowledgements

I gratefully acknowledge the teaching and financial support provided by the EPSRC Centre for Doctoral Training in Partial Differential Equations: Analysis and Applications [grant number EP/L015811/1], as well as financial support and work experience provided by The MathWorks, Inc.

I thank my parents, Eileen M. Reynolds and Antonio J. Aznarán Vigo.

I thank for their guidance and patience my supervisors Patrick Farrell and Endre Süli, and my collaborators Rob Kirby and Kaibo Hu.

I thank my various examiners Kathryn Gillow, Alain Goriely, José Carrillo de la Plata, and Colin Cotter.

Finally, I thank my friends through thick and thin (global pandemics notwithstanding) Alexei Gazca-Orozco, John Papadopoulos, Maike Meier, Pablo Brubeck, Jonah Duncan, James Kohout, Chris Irving, my collaborator Alex Van-Brunt, officemates Gonzalo Gonzalez de Diego and Nic Boullé, Johannes Forkel, all of OU Cross Country Club, and the Beatroots.

Contents

0 Introduction **1**

0.1 The elasticity complex 1

0.2 The abstract Hodge Laplacian 3

0.2.1 Some less abstract Hodge Laplacians 4

0.3 Contributions and structure 6

1 Finite elements for symmetric stress tensors **8**

1.1 Motivations: continuum mechanics and finite element transformation theory 10

1.2 The stress tensor in linear elasticity 11

1.2.1 Continuum-mechanical context and problem formulation . . . 11

1.2.2 Stress components and the incompressible limit 14

1.2.3 Numerical enforcement of symmetry 15

1.2.4 The Arnold–Winther elements 18

1.3 Piola transformation theory 22

1.3.1 Domain geometry and pullbacks 22

1.3.2 Transformation of components and their moments 24

1.3.3 Transforming Piola-inequivalent elements 27

1.4 Piola-mapped tensor elements 30

1.4.1 The nonconforming AW element 30

1.4.2 The conforming AW element 32

1.4.3 Scale-invariance and conditioning 33

1.4.4 Preservation of the constraints 34

1.5 Traction conditions in the Hellinger–Reissner principle with Nitsche's method 36

1.6 An exterior calculus perspective 42

1.6.1 Uniform construction of the pullbacks 42

1.6.2 Kernel-capturing and robust multigrid 46

1.7 Multigrid for the Hellinger–Riessner system 47
1.8 Numerical examples 49
1.8.1 Manufactured solutions 49
1.8.2 Li, 2018 52

2 Application to linear irreversible thermodynamics 56
2.1 Overview of the Stokes–Onsager–Stefan–Maxwell system 57
2.1.1 Convection-diffusion in multicomponent flows 57
2.1.2 Thermodynamic setting and the Onsager–Stefan–Maxwell system 60
2.1.3 Stokes momentum balance 62
2.1.4 Augmentation of the transport matrix and Stokes momentum balance 63
2.1.5 The chemical potential and the thermodynamic equation of state 64
2.1.6 Coupled problem statement 66
2.1.7 Relation to existing numerical literature 67
2.2 Variational formulation 68
2.2.1 Pressure regularity in the stress complex 68
2.2.2 Fully coupled nonlinear variational formulation 70
2.3 Linearisation and well-posedness 74
2.3.1 Generalised Picard scheme 74
2.3.2 Well-posedness of the linearised system 76
2.4 Discretisation 80
2.4.1 Structure-preservation and well-posedness 80
2.4.2 Error estimates 82
2.4.3 Examples of suitable finite elements 83
2.5 Numerical experiments 85
2.5.1 Validation with manufactured solutions 85
2.5.2 Convergence of thermodynamic forces and the pressure gradient 87
2.5.3 Microfluidic mixing of benzene and cyclohexane 88

3 The strain Hodge Laplacian 91
3.1 Motivations: Kröner's theory of defect elasticity 92
3.2 Problem formulation 94
3.2.1 A strain-displacement formulation 94
3.2.2 Comparison to the linear models of van Goethem et al. 95
3.3 The incompatibility operator 97
3.3.1 Green's formulae 97

3.3.2 Traces and exactness . . . 98
3.3.3 A remark on abstract Hilbert traces . . . 100
3.4 Discrete incompatibility and the Regge element . . . 101
3.4.1 The Regge finite element . . . 102
3.4.2 Discrete Green's formulae . . . 104
3.4.3 Codimension-2 curvature . . . 105
3.5 Interior penalisation in $H(\mathrm{inc})$ . . . 106
3.5.1 A codimension-1 approach . . . 106
3.5.2 A discrete Poincaré inequality . . . 107

4 Concluding remarks and outlook **111**
4.1 Exotic finite elements . . . 111
4.1.1 Solvers for symmetry-enforcing discretisations . . . 112
4.1.2 Symmetric elements and Piola transforms in 3D . . . 112
4.1.3 The curvilinear case . . . 113
4.2 Multicomponent diffusion . . . 113
4.2.1 Refinements of the model . . . 114
4.2.2 Multicomponent CFD . . . 114
4.2.3 Preconditioning . . . 114
4.3 The incompatibility operator and defect elasticity . . . 114
4.4 How far can we take the FEEC and the Hodge Laplace concept? . . . 115
4.4.1 Construction of finite element complexes . . . 115
4.4.2 General relativity . . . 116
4.4.3 Implicitly-constituted continuum mechanics . . . 116
4.4.4 Nonlinear complexes of Riemannian geometry . . . 116

References **118**

Notation

Spaces and sets

Ω	an open, bounded, and polytopal (polygonal or polyhedral) subset of $\mathbb{R}^{d\in\{2,3\}}$ with Lipschitz boundary
$\mathbb{M}$	the space $\mathbb{R}^{d\times d}$ of $d \times d$ matrices
$\mathbb{S}$	its symmetric subspace $\mathbb{R}^{d\times d}_{\text{sym}}$
$\mathbb{K}$	its skew-symmetric subspace $\mathbb{R}^{d\times d}_{\text{skw}}$
$\mathbb{T}$	its deviatoric (traceless) subspace $\ker(\text{tr})$
$W^{k,p}(\Omega;\mathbb{X})$ ($L^p(\Omega;\mathbb{X})$ when $k=0$)	the standard Sobolev space with domain Ω and codomain the vector space $\mathbb{X}$
$L^2_0(\Omega)$	$\{f \in L^2(\Omega) \mid \fint_\Omega f \,\mathrm{d}x = 0\}$
H^k	$W^{k,2}$
$H(\text{op};\mathbb{X})$ or $H(\text{op},\Omega;\mathbb{X})$	$\{f \in L^2(\Omega;\mathbb{X}) \mid \text{op}(f) \in L^2\}$
$H_\Gamma(\text{op};\mathbb{X})$	$\{f \in H(\text{op};\mathbb{X}) \mid T(f) = 0 \text{ on } \Gamma\}$, where $\Gamma \subseteq \partial\Omega$ and T is the trace operator associated with op[1]
$H_0(\text{op};\mathbb{X})$	$H_{\partial\Omega}(\text{op};\mathbb{X})$
$C^\infty_c(\Omega;\mathbb{X})$	the space of smooth $\mathbb{X}$-valued functions with compact support in Ω
$\mathcal{D}'(\Omega;\mathbb{X})$	the space of $\mathbb{X}$-valued distributions[2]
$\mathcal{P}_k(\Omega;\mathbb{X})$	the space of $\mathbb{X}$-valued polynomials of total degree at most $k \geq 0$ on Ω
$\mathcal{T}_h$	a triangulation of Ω with mesh size h
CG_k	the continuous Lagrange element space $\{p \in C^0(\Omega) \mid p\|_K \in \mathcal{P}_k(K)\ \forall\ K \in \mathcal{T}_h\}$
DG_k	the discontinuous Lagrange element space $\{p \in L^\infty(\Omega) \mid p\|_K \in \mathcal{P}_k(K)\ \forall\ K \in \mathcal{T}_h\}$
$\text{dom}(\cdot)$	domain of an unbounded linear operator
$\ker(\text{op};V), \text{im}(\text{op};V)$	kernel and image of op when defined on domain V

Quantities

h	small characteristic mesh size

[1] This space is well-defined for $\Gamma, \partial\Omega$ of sufficient regularity. In general, $H_0(\text{op};\mathbb{X})$ may be defined as $\overline{C^\infty_0(\Omega;\mathbb{X})}^{\|\cdot\|_{\text{op}}}$, in analogy to the space $W^{k,p}_0$.

[2] This is the dual of $\mathcal{D}(\Omega;\mathbb{X}) = C^\infty_c(\Omega;\mathbb{X})$ with respect to the locally convex topology induced by the family of seminorms $\{\sup_K \|\partial^\alpha \cdot\|\}_{K,\alpha}$ indexed by compact subsets $K \subseteq \Omega$ and multiindices α.

$\mathbf{n}$	the outward-pointing unit normal to $\partial\Omega$
$\mathbb{I}$	the identity matrix $\mathbb{I}_{d\times d} \in \mathbb{M}$
Relations	
$\lesssim$	domination up to a constant which may depend on mesh regularity but not on h
$\twoheadrightarrow$	surjection
$\oplus\!\!\!\!-_H$	direct sum, orthogonal with respect to the Hilbert space H
Operators and functionals	
sym	$\frac{1}{2}(\cdot + \cdot^\top)$, the symmetric part of a matrix
sph	$\frac{\mathrm{tr}(\cdot)}{d}\mathbb{I}$, the spherical part of a matrix
dev	$\cdot - \mathrm{sph}(\cdot)$, the deviator (traceless part) of a matrix
$\mathrm{div}, \mathrm{curl}, \mathrm{rot}$	classical divergence, curl, and rotation operators, defined row-wise for higher-order tensor fields
∇^2	Hessian
op_h	operator applied element-wise
$(\cdot,\cdot)_H$	inner product of the Hilbert space H
P_X	the H-orthogonal projection onto the closed subspace $X \subseteq H$
$\|\cdot\|$	ℓ^2-norm on $\mathbb{X}$
$\|\cdot\|_{k,\Omega}$ or $\|\cdot\|_k$ (/ $\|\cdot\|_{k,\Omega}$ or $\|\cdot\|_k$)	canonical graph norm (/seminorm) on $H^k(\Omega;\mathbb{X})$
$\|\cdot\|_{\mathrm{op},\Omega}$ or $\|\cdot\|_{\mathrm{op}}$	canonical graph norm on $H(\mathrm{op};\mathbb{X})$, $\|\cdot\|^2_{\mathrm{op}} := \|\cdot\|^2_0 + \|\mathrm{op}(\cdot)\|^2_0$
$⨍_\Omega$	the integral mean $\frac{1}{\lvert\Omega\rvert}\int_\Omega$
$\langle\cdot,\cdot\rangle_\Gamma$	the $(H^{-1/2}\times H^{1/2}_{00})(\Gamma;\mathbb{X})$ dual pairing[11, p. 13]

Chapter 0

Introduction

0.1 The elasticity complex

The unifying theme of this thesis is the discretisation of the linear elasticity complex, and the simulation of continuum mechanics problems thus enabled.

A *complex* is a sequence of vector spaces connected by linear operators, such that the image of each map lies in the kernel of the next. Over the last twenty years, complexes of function spaces have played an increasingly central role in the development of structure-preserving numerical methods in the framework of the *finite element exterior calculus* (FEEC) [19]. For example, the de Rham complex associated with a bounded Lipschitz domain $\Omega \subseteq \mathbb{R}^3$ is well-known in computational electromagnetism:

$$0 \longrightarrow \mathbb{R} \xrightarrow{\subseteq} C^\infty(\Omega) \xrightarrow{\nabla} C^\infty(\Omega;\mathbb{R}^3) \xrightarrow{\text{curl}} C^\infty(\Omega;\mathbb{R}^3) \xrightarrow{\text{div}} C^\infty(\Omega) \longrightarrow 0, \tag{0.1.1}$$

or with Sobolev regularity (the 'L^2 de Rham complex')

$$0 \longrightarrow \mathbb{R} \xrightarrow{\subseteq} H^1(\Omega) \xrightarrow{\nabla} H(\text{curl}) \xrightarrow{\text{curl}} H(\text{div}) \xrightarrow{\text{div}} L^2(\Omega) \longrightarrow 0. \tag{0.1.2}$$

For the finite element simulation of continuum mechanics problems which require discretisation of these various spaces, it is natural to consider discrete analogues of (0.1.2). The central insight of the FEEC is that, by identification of these spaces of vector calculus with spaces of differential forms on Ω, viewed as a Riemannian manifold, the resulting finite element methods are able to preserve much of the topological and algebraic structure encoded in the complexes.

The most elementary example of this phenomenon is as follows. Notice that the composition of adjacent operators in (0.1.1) vanishes; the sequence is called *exact* if the kernel of each operator is precisely the image of the previous. It can be shown that (0.1.1), (0.1.2) are exact if and only if Ω is contractible, a structure which is

desirable to preserve with a finite element subcomplex; if one can construct a finite element subcomplex which is also exact, and can be connected to the original (0.1.2) via appropriate interpolants or projections to form a commuting diagram, then typically a wealth of information results. Such structure-preservation is rewarded by, for example, simplified proofs of error estimates and unisolvency of dual bases, clarification of links between different finite elements (providing clues to construct new or more regular elements), the inheritance at the discrete level of Hodge decompositions (which generalise the classical Helmholtz decomposition of vector fields), inf-sup conditions, and generalised Poincaré inequalities for each operator. The characterisation of discretised differential operators also plays a role in the construction of robust multigrid smoothers, as we shall detail in §1.6.2 and §1.7.

Elasticity has been a particular success story of the FEEC via the study of the *elasticity complexes*, which arise in several areas of continuum mechanics, as well as general relativity [11]; for now, we write them down without reference to differential forms, but will consider such geometric identifications in §1.6.1. The elasticity complex with Sobolev regularity in 3D is given by

$$0 \longrightarrow \underset{\substack{\text{rigid}\\ \text{motions}}}{RM} \xrightarrow{\subseteq} \underset{\text{displacement}}{H^1(\Omega;\mathbb{R}^3)} \xrightarrow{\varepsilon} \underset{\text{strain}}{H(\text{inc};\mathbb{S})} \xrightarrow{\text{inc}} \underset{\text{stress}}{H(\text{div};\mathbb{S})} \xrightarrow{\text{div}} \underset{\text{load}}{L^2(\Omega;\mathbb{R}^3)} \longrightarrow 0, \tag{0.1.3}$$

where ε denotes the symmetric gradient and $\text{inc} := \text{curl} \circ \top \circ \text{curl}$ denotes the *incompatibility operator*, which in 2D is scalar-valued as $\text{inc} := \text{rot}\,\text{rot}$.[3] In 2D, one has the *stress complex*

$$0 \longrightarrow \mathcal{P}_1(\Omega) \xrightarrow{\subseteq} \underset{\text{potentials}}{H^2(\Omega)} \xrightarrow{\text{airy}} \underset{\text{stress}}{H(\text{div};\mathbb{S})} \xrightarrow{\text{div}} \underset{\text{load}}{L^2(\Omega;\mathbb{R}^2)} \longrightarrow 0. \tag{0.1.4}$$

Here airy denotes the formal adjoint to scalar-valued inc in 2D, which assigns to a scalar potential ϕ its matrix-valued Airy stress function, the cofactor of its Hessian,

$$\text{airy}\,\phi := \mathbf{curl}\,\text{curl}\,\phi = \begin{pmatrix} \dfrac{\partial^2\phi}{\partial y^2} & -\dfrac{\partial^2\phi}{\partial x \partial y} \\ -\dfrac{\partial^2\phi}{\partial x \partial y} & \dfrac{\partial^2\phi}{\partial x^2} \end{pmatrix}, \tag{0.1.5}$$

which is identically symmetric and divergence-free.

Taking the adjoint of a complex of Sobolev spaces in practice 'adds' (or by duality, removes) boundary conditions. Modulo such boundary conditions, the formal adjoint

[3] The $\frac{d(d+1)}{2}$-dimensional space RM of *infinitesimal rigid body motions of linear elasticity* is given in 2D by $\{\mathbf{x} \mapsto \mathbf{a} + b\mathbf{x}^\perp \mid \mathbf{a} \in \mathbb{R}^2, b \in \mathbb{R}\}$ and in 3D by $\{\mathbf{x} \mapsto \mathbf{a} + \mathbf{b} \times \mathbf{x} \mid \mathbf{a}, \mathbf{b} \in \mathbb{R}^3\}$.

to (0.1.4) is the *strain complex*

$$0 \longrightarrow \underset{\substack{\text{rigid}\\ \text{motions}}}{RM} \xrightarrow{\subseteq} \underset{\text{displacement}}{H^1(\Omega;\mathbb{R}^2)} \xrightarrow{\varepsilon} \underset{\text{strain}}{H(\text{inc};\mathbb{S})} \xrightarrow{\text{inc}} \underset{\substack{\text{incompatibility}\\ /\text{curvature}}}{L^2(\Omega)} \longrightarrow 0. \tag{0.1.6}$$

0.2 The abstract Hodge Laplacian

Before motivating the study of the Hodge Laplacian problems associated with a sequence, we require the following abstract definition.

Definition 0.2.1. [12, p. 33][50] A *closed Hilbert complex* is a sequence of Hilbert spaces (called *base spaces*)

$$\ldots \xrightleftharpoons{} W^{k-1} \underset{(\mathrm{d}^{k-1})^*}{\overset{\mathrm{d}^{k-1}}{\rightleftarrows}} W^k \underset{(\mathrm{d}^{k})^*}{\overset{\mathrm{d}^{k}}{\rightleftarrows}} W^{k+1} \underset{(\mathrm{d}^{k+1})^*}{\overset{\mathrm{d}^{k+1}}{\rightleftarrows}} \ldots \tag{0.2.1}$$

connected by closed, densely defined linear operators d^k with the property that $\mathrm{im}(\mathrm{d}^k) \subseteq \ker(\mathrm{d}^{k+1})$. Denoting by $V^k := \mathrm{dom}(\mathrm{d}^k)$ the dense subspace of W^k on which d^k is defined (the *domain space*), we define the associated *domain complex* as

$$\ldots \xrightleftharpoons{} V^{k-1} \underset{(\mathrm{d}^{k-1})^*}{\overset{\mathrm{d}^{k-1}}{\rightleftarrows}} V^k \underset{(\mathrm{d}^{k})^*}{\overset{\mathrm{d}^{k}}{\rightleftarrows}} V^{k+1} \underset{(\mathrm{d}^{k+1})^*}{\overset{\mathrm{d}^{k+1}}{\rightleftarrows}} \ldots, \tag{0.2.2}$$

on which each d^k is bounded linear. Each V^k is then Hilbert with graph norm $\|\cdot\|^2_{V^k} := \|\cdot\|^2_{W^k} + \|\mathrm{d}^k \cdot\|^2_{W^{k+1}}$.

For example, the domain complex (0.1.3) has

$$0 \longrightarrow RM \xrightarrow{\subseteq} L^2(\Omega;\mathbb{R}^3) \xrightarrow{\varepsilon} L^2(\Omega;\mathbb{S}) \xrightarrow{\text{inc}} L^2(\Omega;\mathbb{S}) \xrightarrow{\text{div}} L^2(\Omega;\mathbb{R}^3) \longrightarrow 0 \tag{0.2.3}$$

as base complex; typically, the roles of the domain and base spaces are played by the Sobolev and ambient Lebesgue spaces respectively.

Associated with any closed Hilbert complex is a sequence of canonical partial differential equations, each associated with a space in the complex. Define the *Hodge Laplacian* operator

$$\mathcal{L}^k := (\mathrm{d}^k)^*\mathrm{d}^k + \mathrm{d}^{k-1}(\mathrm{d}^{k-1})^* \tag{0.2.4}$$

with domain

$$\mathrm{dom}(\mathcal{L}^k) = \{u \in V^k \cap V_k^* \mid \mathrm{d}^k u \in V_{k+1}^*, (\mathrm{d}^{k-1})^* u \in V^{k-1}\}, \tag{0.2.5}$$

where $V_k^* := \mathrm{dom}((\mathrm{d}^{k-1})^*)$. The *Hodge Laplace* (HL) problem

$$\mathcal{L}^k u = f \tag{0.2.6}$$

for given data $f \in W^k$ is a far-reaching generalisation of the classical Poisson problem which encompasses many famous PDEs of continuum mechanics, or their linearisations, within a single abstract framework. In addition to the strong form (0.2.6), one may also consider the equivalent *primal weak form*: seek $u \in V^k \cap V_k^*$ such that (dropping superscripts for clarity)

$$(\mathrm{d}u, \mathrm{d}v)_W + (\mathrm{d}^* u, \mathrm{d}^* v)_W = (f, v)_W \ \forall\ v \in V^k \cap V_k^*, \tag{0.2.7}$$

or the equivalent *mixed weak form*, employing the dual variable $\sigma = \mathrm{d}^* u \in V^{k-1}$: seek $(\sigma, u) \in V^{k-1} \times V^k$ such that

$$\begin{aligned} (\sigma, \tau)_W \quad & -(u, \mathrm{d}\tau)_W = 0 \quad && \forall\ \tau \in V^{k-1}, \\ (\mathrm{d}\sigma, v)_W \quad & +(\mathrm{d}u, \mathrm{d}v)_W = (f, v)_W \quad && \forall\ v \in V^k. \end{aligned} \tag{0.2.8}$$

The HL problem is well-posed provided the complex is exact, and otherwise only up to the kernel of the HL operator, the *harmonic forms* $\ker(\mathrm{d}^k; W^k)/\operatorname{im}(\mathrm{d}^{k-1}; W^{k-1}) \simeq \ker(\mathrm{d}^k; W^k) \cap \ker((\mathrm{d}^{k-1})^*; W^k)$ [12, p. 39]. It may be shown that the classical Poisson problem with homogeneous Dirichlet boundary conditions is precisely the HL problem associated with the final space $L^2(\Omega)$ of (0.1.2), while the Poisson problem with Neumann conditions is that associated with $H^1(\Omega)$.

The numerical solution of HL problems is a central topic of the FEEC. Bearing in mind the classic phenomenon of justifying or motivating a framework entirely using terminology from said framework, it is a natural problem to consider because, for example, it may be viewed as computing the *Hodge decomposition* $(\mathrm{d}^*\mathrm{d} + \mathrm{d}\mathrm{d}^*)u$ of the data f.

0.2.1 Some less abstract Hodge Laplacians

We exhibit some further examples.

- The mixed form (0.2.8) of the Poisson problem is well-known to be equivalent to Darcy's law for porous media flow, up to the identification of the symmetric positive definite permeability tensor with the identity.
- The HL associated with $H(\mathrm{curl})$ in (0.1.2), when $f \in \mathrm{curl}\, H_0(\mathrm{curl})$, gives rise to the *curlcurl problem with magnetic boundary conditions* of electromagnetics [12, p. 47].

- The Einstein–Bianchi formulation of general relativity linearised about Minkowski space may be obtained as the mixed weak form of the HL associated with $H_0(\mathrm{curl};\mathbb{S})$ in the Hessian complex with boundary conditions in 3D [162],

$$0 \longrightarrow H_0^2(\Omega) \xrightarrow{\nabla^2} H_0(\mathrm{curl};\mathbb{S}) \xrightarrow{\mathrm{curl}} H_0(\mathrm{div};\mathbb{T}) \xrightarrow{\mathrm{div}} L^2(\Omega;\mathbb{R}^3)/\mathrm{RT}_0 \longrightarrow 0, \tag{0.2.9}$$

  where RT_0 denotes the lowest-order Raviart–Thomas element.[4]

- The HL of the space $H_0^2(\Omega)$ in (0.2.9) is the biharmonic problem of plate elasticity [161].

- The Navier–Lamé displacement formulation of linear elasticity, whose displacement-pressure formulation is well-known to be formally equivalent to the Stokes equations of fluid dynamics in the incompressible limit, may be recovered as the primal formulation of the HL of the displacement space $H^1(\Omega;\mathbb{R}^d)$ in (0.1.3) or (0.1.6).

- The Hellinger–Reissner mixed stress-displacement formulation of linear elasticity may be viewed as the HL of the load space $L^2(\Omega;\mathbb{R}^d)$ in (0.1.3) or (0.1.4); we study this case in §1.

- The *Stokes complex* is a smoothing of the de Rham complex (0.1.2); in 3D with boundary conditions, this is given by

$$0 \longrightarrow H_0^2(\Omega) \xrightarrow{\nabla} H_0^1(\mathrm{curl}) \xrightarrow{\mathrm{curl}} H_0^1(\Omega;\mathbb{R}^3) \xrightarrow{\mathrm{div}} L_0^2(\Omega) \longrightarrow 0, \tag{0.2.10}$$

  where $H_0^1(\mathrm{curl}) := \{f \in H_0^1(\Omega;\mathbb{R}^3) \mid \mathrm{curl}\, f \in H^1(\Omega;\mathbb{R}^3), f\times\mathbf{n} = 0 \text{ on } \partial\Omega\}$ [152]. If (0.2.10) is taken to be its *own* base complex and $H_0^1(\Omega;\mathbb{R}^3)$ is endowed with norm $|\cdot|_1$, then the *in*compressible Stokes equations are the mixed weak form of the HL associated with $L_0^2(\Omega)$. Discrete preservation of the complex property $\mathrm{div}\, H_0^1(\Omega;\mathbb{R}^3) \subseteq L_0^2(\Omega)$ is well-known to be a starting point for exactly divergence-free velocity fields, implying mass conservation and pressure robustness [127].

- A remarkable example of the relevance of HL problems was recently found in [56], where the authors showed that the linear Cosserat elasticity model arises as the HL of a 'twisted' de Rham complex; a smoothed de Rham complex has also been found to arise naturally in relaxed micromorphic continuum models [173].

[4] Note that the sequence ending $\ldots \longrightarrow {}^{X}/_{Y} \longrightarrow 0$ may be equivalently be written as $\ldots \longrightarrow X \xrightarrow{P_Y} Y \longrightarrow 0$.

Motivated by the physical relevance which many HL problems enjoy, and the utility of the (comparatively understudied) elasticity complex in several areas of continuum mechanics, the overarching theme of this thesis is the discretisation of the Sobolev spaces and HL problems arising in the elasticity complex. Rather than explore the discretisation of the elastic HL problem in its abstract generality, we provide in-depth studies of three concrete instantiations:

- §1: the classical Hellinger–Reissner stress-displacement linear elasticity problem, which is the HL associated with the load space in the 2D stress complex (0.1.4);
- §2: stress-velocity-pressure compressible Stokes flow (corresponding to the same HL) and its coupling with molecular diffusion;
- returning to solid mechanics in §3[5]: the essentially unstudied HL arising from the strain space in the 2D strain complex (0.1.6) 'from scratch', which corresponds to a candidate linearised strain-displacement model of defect elasticity.

0.3 Contributions and structure

The work of this thesis is cleanly divided into three subtopics:

(i) In §1, we develop the generalised Piola transformation theory necessary to implement nonstandard elements discretising $H(\mathrm{div};\mathbb{S})$, prototypically the conforming and nonconforming Arnold–Winther elements [24, 25]. These famously solved an open problem in numerical elasticity by providing exactly symmetric approximations to the Cauchy stress tensor in the Hellinger–Reissner stress-displacement formulation of linear elasticity; this is precisely the mixed weak form of the Hodge Laplacian arising from the final (load) space $L^2(\Omega;\mathbb{R}^2)$ in the 2D stress elasticity complex (0.1.4), of which the Arnold–Winther elements form exact subcomplexes. We verify the correctness of this so-called *zany* transformation theory via numerical experiments with our implementations of these elements in the Firedrake finite element library [164]. We also demonstrate the effectiveness of appropriate multigrid smoothers for this system, prove convergence of Nitsche's method for the weak enforcement of traction conditions,

[5] as well as 'taking the adjoint and then one step to the right' in the 2D stress complex

and provide a uniform construction of all standard reference-to-physical Piola pullback maps using FEEC machinery.[6]

(ii) As is well-known, the equations of linear elasticity are essentially equivalent to the Stokes equations of fluid dynamics. In §2, we are therefore able to employ the Arnold–Winther elements to discretise compressible Stokes flow, for which a $H(\mathrm{div};\mathbb{S})$-conforming viscous stress tensor is shown to be a crucial coupling variable for the incorporation of convection into the Stefan–Maxwell model of multicomponent diffusion in the Onsager framework of linear irreversible thermodynamics. Thus, our abstract transformation theory for the discrete stress complex studied in §1 plays a role in enabling among the first rigorous computational coupling of convective fluid flow with multicomponent molecular diffusion, modelled by what we christen the *(Navier–)Stokes–Onsager–Stefan–Maxwell* system; for a general non-ideal fluid consisting of n species, this complex nonlinear model requires us to solve for $2n+3$ fields over Ω. This chapter details the formulation of this physical model, and of corresponding finite element schemes, which are provably consistent with the fundamental laws of thermodynamics. Practical applications include the microfluidic mixing of hydrocarbons.[7][8]

(iii) Finally in §3, we consider the discretisation of the Hodge Laplacian associated with the strain space in (0.1.3). This necessitates the discretisation of $H(\mathrm{inc};\mathbb{S})$, a task more subtle even than for $H(\mathrm{div};\mathbb{S})$ due to the high-order operators at play and very sparse existing work. Intriguingly, this problem draws connections between the FEEC and Kröner's classical theory of defects and incompatibility; we carry out the foundational functional and numerical analysis, in particular discontinuous Galerkin FEM, necessary for the eventual goal of a candidate well-posed linearised model of defect elasticity.[9]

We draw conclusions and indicate potential avenues of further research in §4.

[6] An abridged version of §1, but which includes similar theory enabling the implementation of and smoothers for the pressure-robust, $H(\mathrm{div})$-conforming (and H^1-nonconforming) Mardal–Tai–Winther element for Navier–Stokes–Darcy flow and (locking-free) primal linear elasticity [145], which discretises a 2D Stokes complex (0.2.10), has been accepted to the SMAI Journal of Computational Mathematics, with P. E. Farrell and R. C. Kirby [28].

[7] This chapter is drawn from a manuscript with A. J. Van-Brunt, P. E. Farrell, and C. W. Monroe [29].

[8] **Concerning authorship.** The work of §2 was carried out in collaboration with a peer, fellow DPhil candidate Alexander J. Van-Brunt. Where possible/practical, I have indicated the presence of any material and work attributable solely to him.

[9] This chapter is drawn from a manuscript currently in preparation with K. Hu [30].

Chapter 1

Finite elements for symmetric stress tensors

We consider the 2D stress complex (0.1.4) with, in general, mixed boundary conditions:

$$0 \longrightarrow \underset{\text{potentials}}{H^2_{\Gamma_N}(\Omega)} \xrightarrow{\text{airy}} \underset{\text{stress}}{H_{\Gamma_N}(\text{div};\mathbb{S})} \xrightarrow{-\text{div}} \underset{\text{load}}{L^2(\Omega;\mathbb{R}^2)} \longrightarrow 0, \tag{1.0.1}$$

which is exact on simply connected domains (as follows from [160, Theorem. 3.8]). Here $\partial\Omega = \Gamma_D \sqcup \Gamma_N$, and Γ_D, Γ_N are each relatively open and Lipschitz with $0 < |\Gamma_D|, |\Gamma_N| < |\partial\Omega|$. In the case $|\Gamma_N| = 0$, we replace (1.0.1) with

$$0 \longrightarrow \mathcal{P}_1(\Omega) \xrightarrow{\subseteq} \underset{\text{potentials}}{H^2(\Omega)} \xrightarrow{\text{airy}} \underset{\text{stress}}{H(\text{div};\mathbb{S})} \xrightarrow{-\text{div}} \underset{\text{load}}{L^2(\Omega;\mathbb{R}^2)} \longrightarrow 0, \tag{1.0.2}$$

and when $|\Gamma_D| = 0$ with

$$0 \longrightarrow \underset{\text{potentials}}{H^2_0(\Omega)} \xrightarrow{\text{airy}} \underset{\text{stress}}{H_0(\text{div};\mathbb{S})} \xrightarrow{-\text{div}} \underset{\text{load}}{L^2(\Omega;\mathbb{R}^2)/RM} \longrightarrow 0. \tag{1.0.3}$$

The base stress space $L^2(\Omega;\mathbb{S})$ is endowed with energy norm induced by the *compliance tensor* $\mathcal{A}$ [12, p. 107]; in dimension d and for fixed Lamé parameters λ, μ with $\lambda + \frac{2\mu}{d} > 0$, this is a symmetric, bounded, positive definite, 4^{th}-order tensor $\mathcal{A} : \mathbb{S} \to \mathbb{S}$ defined by

$$\mathcal{A}\sigma := \frac{1}{2\mu}\left(\sigma - \frac{\lambda}{2\mu + d\lambda}(\text{tr}\sigma)\mathbb{I}\right). \tag{1.0.4}$$

In general $\lambda(\mathbf{x}), \mu(\mathbf{x})$ can vary spatially within Ω, hence also can $\mathcal{A} = \mathcal{A}(\mathbf{x})$ provided that it is uniformly positive definite, but we consider the homogeneous isotropic case here, in which it is the above constant.

Writing down the Hodge Laplacian boundary value problem associated with the load space $L^2(\Omega;\mathbb{R}^2)$ in mixed weak form in (1.0.1), we obtain: for given $f \in L^2(\Omega;\mathbb{R}^2)$, seek $(\sigma, u) \in H_{\Gamma_N}(\mathrm{div};\mathbb{S}) \times L^2(\Omega;\mathbb{R}^2)$ satisfying

$$\begin{aligned} \int_\Omega \mathcal{A}\sigma : \tau + (\mathrm{div}\,\tau)\cdot u \,\mathrm{d}x &= 0 && \forall\ \tau \in H_{\Gamma_N}(\mathrm{div};\mathbb{S}), \\ \int_\Omega (\mathrm{div}\,\sigma)\cdot v \,\mathrm{d}x &= \int_\Omega f\cdot v \,\mathrm{d}x && \forall\ v \in L^2(\Omega;\mathbb{R}^2), \end{aligned} \tag{1.0.5}$$

which is precisely the classical Hellinger–Reissner principle, a formulation of linear elasticity which solves for the Cauchy stress σ and the displacement u.

The Hellinger–Reissner variational formulation of linear elasticity is successfully discretised by the Arnold–Winther (AW) elements [24, 25]; their development was one of the key early breakthroughs of the finite element exterior calculus. Despite their great utility, they are not available in standard finite element software, because their dual bases are not preserved under the Piola push-forward. In this chapter, we apply the novel transformation theory recently developed by Kirby [130] to devise the correct map for transforming their bases on a reference cell to a generic physical triangle. This enables the use of the AW elements, both conforming and nonconforming, in the widely-used Firedrake finite element software [164], composing with its advanced symbolic code generation and geometric multigrid functionality.

This chapter is structured as follows. In the next section, we describe the broad motivations of this chapter. Then in §1.2, we review the theory of linear elasticity, in particular stress-displacement formulations, and make note of existing efforts at the finite element approximation of such problems, before defining the AW families of elements in 2D. In §1.3, we provide notation used to define geometry and Piola mappings, summarise how different tensor components are transformed, and motivate and survey abstract transformation theory for general Piola-mapped elements. Afterwards in §1.4, we work this out in detail for the AW elements, by studying what the Piola transforms do to their dual spaces. A discussion of the application of the AW elements to linear elasticity follows in §1.5; in particular, we prove convergence of Nitsche's method for the imposition of traction boundary conditions. Then §1.6 provides a uniform construction of all standard Piola pullbacks using differential forms, and reviews the role of FEEC in the development of multigrid preconditioners, as discussed in §1.7, in which we apply patch-based multigrid algorithms to precondition the canonical Hellinger–Reissner system for the AW elements. We briefly discuss the implementation within the Firedrake code stack in §1.8 and exhibit numerical examples for our newly-enabled elements which verify the correctness of our theory.

1.1 Motivations: continuum mechanics and finite element transformation theory

Classically, the 2$^{\text{nd}}$-order Cauchy stress tensor acts as a measure of the force imposed on a body per unit area [63], but various notions of stress are also used to, for example, prove thermodynamical consistency of rate-type models in viscoelasticity [143], as a coupling field for electrical propagation in cardiac biomechanics [66], and for the experimental study of the Poynting effect in finite strain theory [43, 148].

The component matrix of the elastic stress tensor in solid mechanics is symmetric, but the preservation of symmetry is notoriously difficult to enforce in finite element discretisations, and so many methods initially proposed in the literature enforce symmetry only approximately, or as a postprocessing step. After decades of effort by many researchers, tensor-valued polynomial shape spaces for the stress-displacement formulation of linear elasticity which do strongly enforce symmetry and result in a stable and convergent discretisation were eventually discovered by Arnold and Winther [24, 25], but in the two decades since then, their implementations have either required the explicit element-by-element construction of the basis [61], or have been for one-off numerical experiments, such as for stress reconstruction or the design of error indicators [98, 148, 153, 167]. The FIAT library [129] has had partial support for this element, but the lack of reference mappings has prevented its use in practice [140, Ch. 3].

Indeed, the use of an abstract *reference element* is critical in the evaluation of finite element basis functions and their derivatives. One constructs, by some means, the basis functions on a particular fixed element only once, and obtains the basis functions on an arbitrary cell through a mapping. Moreover, this is not merely a theoretical consideration because this approach is faster than any alternative when assembling the enormous finite element matrices in the simulations offered by many modern code libraries [8, 33, 35, 140, 164, 184]. For scalar-valued function spaces, this mapping is usually a simple pullback (change of coordinates). However, vector-valued elements discretising $H(\text{div})$ or $H(\text{curl})$, as well as their tensor-valued counterparts, typically use instead the *Piola transformations* in order to facilitate enforcing appropriate continuity of only normal or tangential components.

The reference element paradigm is typically employed for elements that satisfy a kind of *equivalence*, where the reference element basis functions map directly to the physical element basis functions under the coordinate change. However, for many elements both classical and modern, including the AW elements, this is not the case, as

the degrees of freedom (DOFs) are 'mixed up' by the associated (Piola) push-forward in a cell-dependent manner. In [130], Kirby developed a general theory for obtaining the correct basis on each physical cell, in the case of affinely mapped cells. This approach gives the correct nodal basis as a linear combination of the mapped reference element basis functions. This linear combination turns out to be sparse, meaning that applying the theory incurs only a small additional cost during the finite element computation, ensuring that the use of these more exotic elements composes neatly with existing high-level automatic code generation software. Kirby and Mitchell [132] generalised the Firedrake [164] code stack to generate and employ this transformation, giving results for Morley, Hermite, Argyris, and Bell elements. The basis on the reference cell for each of these elements is constructed using FIAT [129]. We aim to extend this framework, colloquially called the *zany* transformation theory by its originators, to Piola-mapped $H(\mathrm{div};\mathbb{S})$ elements, with the conforming and nonconforming AW elements as representative examples.[10]

1.2 The stress tensor in linear elasticity

1.2.1 Continuum-mechanical context and problem formulation

The variational formulation of the linear theory of static elasticity is obtained by linearising with respect to the displacement in the equilibrium equations given by Cauchy's theorem, a fundamental result proved in 1823 [63]. As a result, no distinction is made between the Eulerian and Lagrangian configurations, and we assume the absence of nonlinearities both geometric and constitutive. This approximation is reasonable and provides acceptably accurate numerical models in many areas of engineering and design, from the placement of tiny springs in car suspensions [118, p. 380] to the structural analysis of massive offshore oil rigs [13, p. 4]. Moreover, this

[10] In some sense, these motivations are in reverse order. To discretise the elastic stress, FEEC-based elements which strongly enforce symmetry are so complicated that they merit their own tailored transformation theory to be properly implemented. On the other hand, we should clarify that structure-preservation (in the sense of enforcing symmetry) for linear elasticity is but a single application of a much broader story of research, which concerns the automatic and efficient generation of finite element codes which are themselves efficient, hidden behind high-level interpreted interfaces (such as the Unified Form Language [1]) which are flexible and do not require expertise to use, hence are concretely useful to the modern applied scientist. Such work is carried out in, among others, the communities of Firedrake [164] and FEniCS [140], who employ notions of software 'composability' and graph-theoretic mesh topology to efficiently automate the FEM within a unified framework. The transformation theory described here is but a small step near the end of this more elaborate process, in order that a user can perform simulations with the desirable property of exactly symmetric stresses. For details of these more advanced and far-reaching research agendas, see for example [129, 136, 164].

regime at least gives the basis on which to study nonlinear elastic models, for example via their Newton or Picard linearisations.

Apart from volumetric forces, such as gravity or those arising from the presence of an electromagnetic field, an external force can only be transmitted to a solid through its boundary [118, p. 7]. Given a subdomain of the solid with sufficiently smooth boundary, the *Cauchy stress* is *a priori* a vector quantity $\mathbf{T} = \mathbf{T}(\mathbf{x}, \mathbf{n})$, also called *traction*, defined as the infinitesimal force per unit area applied at a point $\mathbf{x}$ on the boundary of said subdomain, which depends also on the outward-pointing unit normal $\mathbf{n}$ [45, p. 250]. Assuming $\mathbf{T}$ is spatially continuous, part of the statement of Cauchy's theorem gives the existence of the Cauchy stress tensor σ, which satisfies

$$\mathbf{T}(\mathbf{x}, \mathbf{n}) = \sigma(\mathbf{x})\mathbf{n}. \tag{1.2.1}$$

In §1.6.1, we will see how this informs the interpretation of σ as a differential form.

For practical applications, one is often interested in computing this stress tensor with at least as much accuracy as the displacement [45, p. 297][40, p. 16], and hence, in mixed stress-displacement formulations in which the stress is computed directly rather than, for example, via numerical differentiation after the fact. The *mixed dual* stress-displacement formulation (1.0.5) on which we focus is a classical way to alleviate the well-known numerical phenomenon of volumetric locking in the incompressible limit [34, p. 354], which arises in both mixed and unmixed primal formulations. Finally, we note that in this small-strain regime, most other notions of elastic stress coincide with the Cauchy stress.

Remark 1.2.1. Having emphasised that the stress is a primary variable of interest, one may also consider an unmixed dual formulation in which the stress is the only unknown, but then compatibility conditions on the resulting strain formulated by Saint Venant [97, p. 84] have to be enforced: denoting by E the strain tensor computed from the stress tensor, these require $\operatorname{inc} E = 0$. Typically, this condition is impractical to impose in the variational formulation for finite element computations [185, p. 20], but will be discussed at greater length in §3.

Let $\Omega \subseteq \mathbb{R}^d$ be a polytopal elastic body; we focus on the planar case $d = 2$. Given an external body force $f \in L^2(\Omega; \mathbb{R}^d)$, displacement data $u_0 \in H^{1/2}_{00}(\Gamma_D; \mathbb{R}^d)$, and traction data $g \in H^{-1/2}(\Gamma_N; \mathbb{R}^d)$, we consider the minimisation of the *complementary*

energy[11]

$$\mathcal{J}(\sigma) = \frac{1}{2}\int_\Omega \mathcal{A}\sigma : \sigma \, \mathrm{d}x - \langle \sigma\mathbf{n}, u_0\rangle_{\Gamma_D} \tag{1.2.2}$$

among all stresses $\sigma \in H(\mathrm{div}; \mathbb{S})$ satisfying

$$\sigma\mathbf{n} = g \text{ on } \Gamma_N \text{ in the trace sense,} \tag{1.2.3}$$

constrained by the equilibrium equation

$$\mathrm{div}\, \sigma = f. \tag{1.2.4}$$

The displacement field $u \in L^2(\Omega; \mathbb{R}^d)$ may be thought of as the Riesz representative of the Lagrange multiplier for this equilibrium constraint, so equivalently, we seek stress-displacement pairs $(\sigma, u) \in H(\mathrm{div}; \mathbb{S}) \times L^2(\Omega; \mathbb{R}^d)$ with traction condition (1.2.3) which are critical points of the Hellinger–Reissner functional

$$\mathcal{H}(\sigma, u) = \mathcal{J}(\sigma) + \int_\Omega (\mathrm{div}\, \sigma - f) \cdot u \, \mathrm{d}x. \tag{1.2.5}$$

A stationary point (σ, u) satisfies

$$\begin{aligned} \int_\Omega \mathcal{A}\sigma : \tau + (\mathrm{div}\, \tau) \cdot u + (\mathrm{div}\, \sigma) \cdot v \, \mathrm{d}x = \int_\Omega f \cdot v \, \mathrm{d}x + \langle \tau\mathbf{n}, u_0\rangle_{\Gamma_D} \\ \forall \ (\tau, v) \in H_{\Gamma_N}(\mathrm{div}; \mathbb{S}) \times L^2(\Omega; \mathbb{R}^d), \end{aligned} \tag{1.2.6}$$

i.e. the saddle point system

$$\mathcal{A}\sigma = \varepsilon(u) \quad \text{in } \Omega, \qquad (\textit{constitutive relation}) \tag{1.2.7a}$$

$$\mathrm{div}\, \sigma = f \quad \text{in } \Omega, \qquad (\textit{conservation of linear momentum}) \tag{1.2.7b}$$

$$u = u_0 \quad \text{on } \Gamma_D, \qquad (\textit{prescribed displacement}) \tag{1.2.7c}$$

$$\sigma\mathbf{n} = g \quad \text{on } \Gamma_N, \qquad (\textit{prescribed surface traction}) \tag{1.2.7d}$$

sometimes called the Navier–Lamé equations. Here $\varepsilon(u) := \mathrm{sym}(\nabla u)$ represents the linearised strain. Well-posedness follows from uniform positive definiteness of $\mathcal{A}$, an appropriate inf-sup condition, and the standard Brezzi theorem, as long as $|\Gamma_D| > 0$ [40, p. 541]. The pure traction problem arising when $|\Gamma_D| = 0$ can also be treated subject to a compatibility condition on the data (see §1.5).

[11] Here as usual, the trace space $H^{-1/2}(\Gamma)$ for $\Gamma \subsetneq \partial\Omega$ has as predual the trace space

$$H^{1/2}_{00}(\Gamma) := \left\{ w|_\Gamma \;\middle|\; w \in H^1_{\partial\Omega\setminus\overline{\Gamma}}(\Omega) \right\} = \left\{ v \in H^{1/2}(\Gamma) \;\middle|\; \begin{array}{l}\text{the extension of } v \text{ to } \partial\Omega \\ \text{by zero lies in } H^{1/2}(\partial\Omega)\end{array} \right\} \subsetneq H^{1/2}(\Gamma).$$

Note that the constitutive relation (1.2.7a) may be formally inverted to give the stress in terms of certain derivatives of the displacement (i.e. "Hooke's law"):

$$\sigma = \mathbb{C}\varepsilon(u) = 2\mu\varepsilon(u) + \lambda(\mathrm{tr}\varepsilon(u))\mathbb{I}. \tag{1.2.8}$$

Here $\mathbb{C} = \mathcal{A}^{-1}$ is the *stiffness* (or *elasticity*) tensor. Note that the primal displacement formulation of linear elasticity is precisely the weak form of the unmixed HL equation associated with the displacement space $H^1(\Omega;\mathbb{R}^2)$ in the strain complex (0.1.6) dual to the stress complex (0.1.4). Philosophically, this primal formulation uses the stress-displacement equation (1.2.8) as a constitutive equation to *define* (and thus eliminate) the stress, while using the equilibrium equation (1.2.7b) to characterise minimisation of an associated quadratic Hookean strain-energy potential; by contrast, the mixed stress-displacement saddle point formulation (of which the primal displacement formulation is the displacement Schur complement) uses (1.2.7a) as an optimality condition which is equivalent to the stress-displacement relation (1.2.8), and the equilibrium equation (1.2.7b) and traction condition (1.2.7d) are used to restrict the class of admissible stresses. It is with this consideration that the Hellinger–Reissner principle was first proposed [97, p. 223][166].

1.2.2 Stress components and the incompressible limit

Observe that we may write

$$\mathcal{A} = \frac{1}{2\mu}\,\mathrm{dev} + \frac{1}{2\mu + d\lambda}\,\mathrm{sph}, \tag{1.2.9}$$

where the spherical part is also known as the *mean normal* stress and its deviator as the *isochoric* or *shear* stress. This orthogonal decomposition is useful in that, roughly speaking, the deviatoric component of the Cauchy stress is responsible for distorting the shape of the elastic body, while the spherical component is responsible for changes in volume [102, p. 94]. Moreover, since the trace of a tensor is independent of the coordinate system, this representation is the most coordinate-free description of the tensor field. In particular, passing to the incompressible regime in which $\lambda \gg \mu$ (or equivalently the Poisson ratio $\nu \nearrow \frac{1}{2}$), we have

$$\mathcal{A} \xrightarrow{\lambda\to\infty} \frac{1}{2\mu}\,\mathrm{dev}, \tag{1.2.10}$$

so that the use of the compliance tensor is in some sense advantageous since it at least admits a limit as $\lambda \to \infty$, unlike the elasticity tensor (1.2.8) which blows up, so our stress-strain relation (1.2.7a) remains valid in this limit. Since dev is not invertible, stress is no longer uniquely determined by strain in this regime.

Remark 1.2.2. For some classes of materials, it is not possible to write the stress explicitly in terms of the (linearised) strain as in (1.2.8), giving rise to the theory of implicitly-constituted solids. Our formulation (1.2.7a) is at least a starting point for such problems, since (as just explained) such a situation arises by passing to the incompressible limit.

Considering instead the spherical component by formally taking the trace of the constitutive equation (1.2.7a) and applying the parameter relation $\lambda = \frac{2\mu\nu}{1-2\nu}$, we find

$$\operatorname{div} u = \frac{\operatorname{tr}\sigma}{2\mu}\left(1 - \frac{d\lambda}{2\mu + d\lambda}\right) = \frac{d}{2\mu(1+(d-2)\nu)}(1-2\nu)\frac{\operatorname{tr}\sigma}{d}, \tag{1.2.11}$$

so the infinitesimal volume change, measured by the divergence of the displacement, is proportional to the first principal invariant of the Cauchy stress, which measures the arithmetic average of the principal stresses, the *mean stress*, but this dependence is removed in the incompressible limit $\nu \nearrow \frac{1}{2}$.

Finally, we note that in the case where the deformation is purely spherical, it is useful to identify the scale factor by which the Cauchy stress is a multiple of the identity tensor; this gives one way to define the *pressure* $p := -\frac{\operatorname{tr}\sigma}{d}$. In the case of pure displacement conditions ($|\Gamma_N| = 0$) which are moreover clamped ($u_0 \equiv 0$), we have, using (1.2.11),

$$\int_\Omega \operatorname{tr}\sigma \, \mathrm{d}x = \frac{2\mu(1+(d-2)\nu)}{1-2\nu}\int_\Omega \operatorname{div} u \, \mathrm{d}x = \frac{2\mu(1+(d-2)\nu)}{1-2\nu}\int_{\partial\Omega} u\cdot\mathbf{n} \, \mathrm{d}s = 0 \tag{1.2.12}$$

[45, p. 269], i.e. $\sigma \in H(\operatorname{div};\mathbb{S})/\mathbb{R}$, which comprises a compatibility condition on the stress space, clearly equivalent to $\int_\Omega p \, \mathrm{d}x = 0$ which is familiar from the classical Stokes problem.

1.2.3 Numerical enforcement of symmetry

That the Cauchy stress field σ is symmetric is equivalent to the conservation of angular momentum, and is called Cauchy's second law of motion. It is highly desirable but notoriously difficult to preserve in finite element discretisations; a further challenge arises from the requirement of $H(\operatorname{div};\mathbb{M})$-conformity as explained in the next section. Before defining the $H(\operatorname{div};\mathbb{S})$-discretising, exactly symmetric Arnold–Winther elements, we briefly review other approaches to the numerical enforcement of symmetry; for further references, see [40, Ch. 9.3–9.4].

Conventionally, symmetry is enforced weakly via $L^2(\Omega;\mathbb{M})$-orthogonality to a skew-symmetric subspace:

$$\int_\Omega \sigma : q \, \mathrm{d}x = 0 \quad \forall \, q \in Q, \tag{1.2.13}$$

where Q denotes some $\mathbb{K}$-valued Sobolev space; this is equivalent to symmetry at the continuous level, and so replacing Q with some finite element space constitutes a weak enforcement of symmetry. This approach encapsulates, for example, the PEERS element [16], and is typically incorporated into the formulation by a Lagrange multiplier, interpreted as the skew-symmetric *rotation tensor* $\omega = \operatorname{skw} \nabla u$.

Years after developing the AW elements, Arnold, Falk, and Winther [17] developed a new method in 3D in which symmetry is not imposed on the stress space directly, but weakly, as above. These elements were of lower order, and are based on the longer *elasticity complex with weak symmetry*, of which the weak imposition scheme is a HL problem; they identify these elements as somehow 'just the right' mixed elements for elasticity. Nevertheless, we still regard the original AW elements as of significant interest due to the exact imposition of symmetry.

Weak imposition of symmetry also fits naturally into the FOSLS (first order system least-squares) method by penalisation of asymmetry [54, 151]. Certainly, any tensor field σ satisfying (1.2.7a) must in particular be symmetric, but in fact, the paper [54] explicitly proves a bound on the skew-symmetric part in terms of the constitutive residual: for arbitrary $\tau \in L^2(\Omega;\mathbb{M})$ and $v \in H^1(\Omega;\mathbb{R}^d)$, we have

$$\| \operatorname{skw} \tau \|_0 \leq 2\mu \| \mathcal{A}\tau - \varepsilon(v) \|_0, \tag{1.2.14}$$

so that enforcing the constitutive equation in the least-squares functional penalises asymmetry at the continuous level, even without the term $\| \operatorname{skw} \sigma \|_0^2$ in the functional; this was demonstrated numerically in [53]. We remark however that the elementary estimate (1.2.14) may be crude for many common materials – for example, iron has shear modulus $\mu = \mathcal{O}(10^{10})$ in SI units. Practitioners of this method also suggest simply replacing the computed discrete stress with its symmetric part as a postprocessing step [54]: given an only weakly symmetric σ_h, use instead the projection $\sigma_h \longleftarrow \operatorname{sym}(\sigma_h)$.

A classical alternative is the use of *composite* elements [95], for which the stress is approximated on a mesh which is more refined than that used for the displacement – for example, the former may be obtained by barycentric refinement of triangles, or by

'Union-Jack' refinement of quadrilateral elements. Such *equilibrium methods* require that for a given pair (Σ_h, V_h), we have

$$\tau_h \in \Sigma_h \text{ and } (\operatorname{div} \tau_h, v_h)_{L^2} = 0 \ \ \forall\ v_h \in V_h \Longrightarrow \operatorname{div} \tau_h = 0 \text{ in } \Omega, \tag{1.2.15}$$

and that there exists a suitable interpolant π_h such that for all τ,

$$(\operatorname{div} \pi_h \tau, v_h)_{L^2} = (\operatorname{div} \tau, v_h)_{L^2} \tag{1.2.16}$$

[128]; these conditions can be used to prove inf-sup stability.

A very significant contribution are the TDNNS elements due to Schöberl and Pechstein (née Sinwel) [170]; We mentioned in §1.2.1 that the primal stress-displacement mixed formulation $(L^2 - H^1)$ can lead to locking; on the other hand, the dual mixed formulation we have used thus far $(H(\operatorname{div}) - L^2)$ is complicated by the enforcement of symmetry, and also of $H(\operatorname{div})$-conformity as described in the next section. The TDNNS approach attempts to seek an intermediate formulation between these, using for the stress $\{\tau \in L^2(\Omega; \mathbb{S}) \mid \operatorname{div}\operatorname{div} \tau \in H^{-1}(\Omega)\}$, and for the displacement $H(\operatorname{rot})$ in 2D or $H(\operatorname{curl})$ in 3D. This choice of displacement space arises naturally because taking the Lagrange multiplier associated with (1.2.13) to be $\omega \in Q := L^2(\Omega; \mathbb{K})$, then (in 2D)

$$\omega = \frac{1}{2} \begin{pmatrix} & 1 \\ -1 & \end{pmatrix} \operatorname{rot} u, \tag{1.2.17}$$

and hence $u \in H(\operatorname{rot})$; an analogous calculation holds in 3D. The corresponding weak form necessitates an appropriate interpretation of the dual pairing "$\langle \operatorname{div} \tau, v \rangle$". These elements can be demonstrated numerically to avoid locking, and work well for plate models and curved geometries, at the cost of the more complicated variational formulation. The discrete stress space consists of the symmetric tensor-valued polynomials of degree $k \geq 1$ whose normal-normal component $(\mathbf{n}^\top \tau \mathbf{n})$ is continuous across each edge, paired with a displacement space of the same degree whose tangential component is continuous; schematics are provided in Figure 1.1.

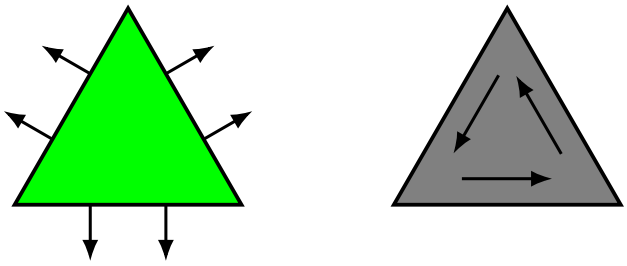


Figure 1.1: The Tangential-Displacement and Normal-Normal-Stress mixed element [170]. Thin arrows on the tensor diagram refer to a single tensor component in the given direction (e.g. $\mathbf{n}^\top \tau \mathbf{n}$).

Another exactly symmetric element is the Hellan–Herrmann–Johnson (HHJ) element, discretising $L^2(\Omega;\mathbb{S})$ and used classically for Kirchhoff plates. It consists of symmetric matrix-valued polynomials of degree $k \geq 0$, again with continuity of the normal-normal components. A schematic is provided in Figure 1.2.

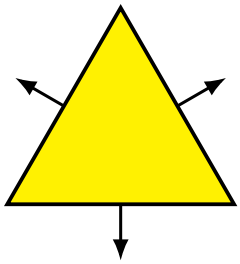


Figure 1.2: The Hellan–Herrmann–Johnson element [108, 109, 128].

This element is more natural for approximating the elastic *strain*, and will be discussed along with the related Regge symmetric finite element in §3.

The TDNNS elements are implemented in Netgen/NGSolve, while the HHJ element was introduced into FEniCS in [106] and later into Firedrake; as we will see, it follows from their type of DOFs that the Piola mapping works in the standard way for these elements, hence their implementations were possible without the theory we develop in this chapter.

Finally, we make note of the beautiful observation due to Gopalakrishnan and Guzmán [103] that for matrix polynomials of high enough degree, and with a mesh which either has a minimal angle condition, or is obtained via barycentric refinement of a quasiuniform mesh, one can define a stable method in which the skew-symmetric test space in (1.2.13) can be taken to be of the same degree as the stress trial space, i.e. weak symmetry happens to imply exact symmetry. The latter hypothesis is in obvious analogy to the exactly divergence-free Scott–Vogelius element used for incompressible fluid flow, and is proved using a result pertaining to that element.

1.2.4 The Arnold–Winther elements

Arnold and Winther proposed two exactly symmetric elements discretising $H(\mathrm{div};\mathbb{S})$ in 2D, one div-conforming (AW^{c}) [24] and the other nonconforming ($\mathrm{AW}^{\mathrm{nc}}$) [25]. We first consider the conforming element. Let K denote a generic triangle, with edges $\{\mathbf{e}_k\}_{k=1}^3$ and vertices $\{\mathbf{x}_k\}_{k=1}^3$.

In the lowest-order case, the space is locally the symmetric matrix-valued quadratic polynomials, augmented by solenoidal cubic bubbles:

$$\begin{aligned} \mathrm{AW}^{\mathrm{c}}(K) &= \{\tau \in \mathcal{P}_3(K;\mathbb{S}) \mid \operatorname{div}\tau \in \mathcal{P}_1(K;\mathbb{R}^2)\} \\ &= \mathcal{P}_2(K;\mathbb{S}) + \{\tau \in \mathcal{P}_3(K;\mathbb{S}) \mid \operatorname{div}\tau = 0\}. \end{aligned} \tag{1.2.18}$$

This is 24-dimensional, with DOFs

- the values of the three unique components of τ at each vertex of K,
- the moments of degree 0 and 1 of the normal-normal and normal-tangential components of τ on each edge,
- the constant moments of the three unique components of τ over K.

The associated local displacement space is $V_h(K) = \mathcal{P}_1(K;\mathbb{R}^2)$ which is 6-dimensional, with DOFs given by, for example, the values of the 2 components at 3 non-collinear points interior to K. Element diagrams for this lowest-order case which we consider are provided in Figure 1.3.

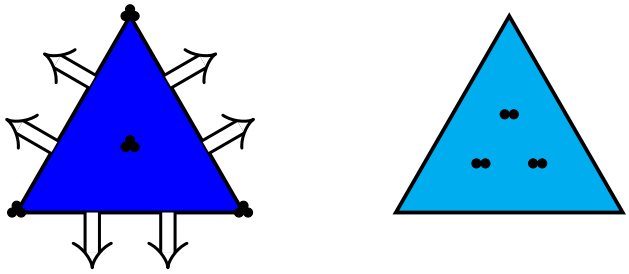


Figure 1.3: The conforming Arnold–Winther element [24], and the discontinuous Lagrange element for displacement with which it is paired. Thick arrows refer to both components of a tensor in a given direction (e.g. $\tau\mathbf{n}$ or $\tau\mathbf{t}$). A clutch of circles either indicates internal moments of each unique component or evaluation of each component at a point.

The global stress space Σ_h is then defined as the space of all tensor fields which belong element-wise to $\mathrm{AW}^{\mathrm{c}}(K)$, subject to the continuity conditions that the two lowest-order moments of the normal components are continuous across mesh edges, and that all components are continuous at mesh vertices; these DOFs associated to an edge and its endpoints uniquely determine the full normal component on that edge, so that when the local spaces are patched together in this manner, a globally $H(\operatorname{div},\Omega;\mathbb{S})$-conforming space results. The global displacement space V_h is simply defined as the piecewise linear vector fields with respect to the triangulation, subject to no interelement continuity conditions: $V_h = \mathrm{DG}_1(\mathcal{T}_h;\mathbb{R}^2)$.

We require some further technical definitions. For $m \geq 0$ let $\{\mu_i\}_{i=0}^m$ denote a *hierarchical basis* for the polynomial space $\mathcal{P}_m[0,1]$ – that is, such that the first $i+1$ entries form a basis for $\mathcal{P}_i[0,1]$. Some examples are the monomials or the Legendre polynomials, and the definition is extended to higher-dimensional domains in the obvious manner. Assume in addition that $\mu_0 \equiv 1$. Given an edge $\mathbf{e}_k$ of a triangle K, let $f : [0,1] \to \mathbf{e}_k$ be a diffeomorphism, and let μ_i^k be the mapping of μ_i from the unit interval to $\mathbf{e}_k$ by the 'standard pullback' $\mu_i^k := \mu_i \circ f^{-1}$ (see equation (1.3.3) below).

To introduce notation for the stress DOFs, we let

$$\ell^{k,i,j}(\tau) = \tau_{i,j}(\mathbf{x}_k) \tag{1.2.19}$$

denote evaluation of a particular component of the input τ at one of the vertices of triangle K. We define the boundary moments by

$$\ell^{\mathbf{n},\mathbf{s},i,k}(\tau) = \int_{\mathbf{e}_k} (\mathbf{n} \cdot \tau(s)\mathbf{s})\, \mu_i^k(s)\, \mathrm{d}s, \tag{1.2.20}$$

where $\mathbf{s} \in \{\mathbf{n}, \mathbf{t}\}$; for the HHJ element, we thus have nodes $\{\ell^{\mathbf{n},\mathbf{n},i,k}\}_{i=0}^1$ for each edge $\mathbf{e}_k$ of the triangle.

For the interior nodes, denoting by $\{\phi_i\}_i$ a hierarchically ordered basis over K (e.g. the bivariate monomials or Dubiner basis) with $\phi_0 \equiv 1$, we let $\tau_{n,i,j}$ denote the tensor with ϕ_n in the i,j entry and 0 elsewhere – a natural injection into the space of tensor-valued orthogonal polynomials. We let

$$\ell^{n,i,j}(\tau) = \int_K \tau(\mathbf{x}) : \tau_{n,i,j}(\mathbf{x})\ \mathrm{d}x. \tag{1.2.21}$$

Thus, DOFs for the AW^{c} space are given in full by $\{\ell^{k,1,1}, \ell^{k,1,2}, \ell^{k,2,2}\}_{k=1}^3$, $\{\ell^{\mathbf{n},\mathbf{n},i,k}, \ell^{\mathbf{n},\mathbf{t},i,k}\}_{i=0,k=1}^{1,\ 3}$, $\{\ell^{0,1,1}, \ell^{0,1,2}, \ell^{0,2,2}\}$.

The nonconforming stress element introduced in [25] avoids the somewhat unusual feature of vertex degrees of freedom and gives a cheaper (though slightly less accurate) method based on the space

$$\mathrm{AW}^{\mathrm{nc}}(K) = \{\tau \in \mathcal{P}_2(K;\mathbb{S}) \mid \mathbf{n}_k \cdot \tau \mathbf{n}_k \in \mathcal{P}_1(\mathbf{e}_k),\ \ 1 \leq k \leq 3\}\,. \tag{1.2.22}$$

This space, consisting of symmetric tensors of quadratic polynomials subject to a degree reduction in the normal-normal component on each edge, is 15-dimensional, and is determined by $\{\ell^{\mathbf{n},\mathbf{n},i,k}, \ell^{\mathbf{n},\mathbf{t},i,k}\}_{i=0,k=1}^{1,\ 3}$, $\{\ell^{0,1,1}, \ell^{0,1,2}, \ell^{0,2,2}\}$, i.e.

- the constant and linear moments of both the normal-normal and normal-tangential components on each edge,

- the constant moments of the three unique components on the interior.

It is again paired with the displacement space $V_h(K) = \mathcal{P}_1(K;\mathbb{R}^2)$; element diagrams are provided in Figure 1.4.

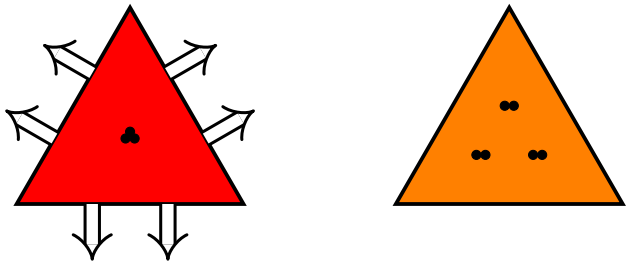


Figure 1.4: The nonconforming Arnold–Winther mixed element [25].

As for the AW^c element, the global stress space is then defined by agreement of the DOFs associated with each edge across that edge; these determine the normal-normal component on that edge, but not the full normal component, so that the resulting global space will be div-nonconforming. The global displacement space is again subject to no interelement continuity conditions, $V_h = \mathrm{DG}_1(\mathcal{T}_h;\mathbb{R}^2)$.

The Arnold–Winther elements were one of the first products of the then embryonic finite element exterior calculus [19]. Their novelty is that they form an exact subcomplex of the 2D stress complex (0.1.4), with commuting cochain projections:

$$\begin{array}{ccccccccc} 0 & \longrightarrow & \mathcal{P}_1(\Omega) & \xrightarrow{\subseteq} & H^2(\Omega) & \xrightarrow{\mathrm{airy}} & H(\mathrm{div};\mathbb{S}) & \xrightarrow{\mathrm{div}} & L^2(\Omega;\mathbb{R}^2) \longrightarrow 0 \\ & & \downarrow{\scriptstyle \mathrm{id}} & & \downarrow{\scriptstyle I_h} & & \downarrow{\scriptstyle \Pi_h} & & \downarrow{\scriptstyle P_h} \\ 0 & \longrightarrow & \mathcal{P}_1(\Omega) & \xrightarrow{\subseteq} & Q_h & \xrightarrow{\mathrm{airy}_h} & \Sigma_h & \xrightarrow{\mathrm{div}_h} & V_h \longrightarrow 0. \end{array} \tag{1.2.23}$$

Here, if (Σ_h, V_h) are either the conforming or nonconforming AW elements, Q_h is either the Argyris space (another element requiring nonstandard transformations) or a certain nonconforming approximation of $H^2(\Omega)$ respectively, I_h, Π_h are appropriate densely defined interpolants, and P_h is the L^2-projection, then it is proved in [24, 25] (see also [185]) that the above diagram is commuting, with exact rows whenever Ω is simply connected. Writing (1.2.16) as $\mathrm{div}_h\, \pi_h = P_{V_h}\, \mathrm{div}$, we see that the commutativity of (1.2.23) and the surjectivity of $\mathrm{div}_h : \Sigma_h \to V_h$ are simply modern restatements of the conditions (1.2.15)–(1.2.16) defining classical equilibrium methods.

In the next section, we discuss how finite element spaces are actually implemented, and see why this task has proved so difficult for the AW elements.

1.3 Piola transformation theory

1.3.1 Domain geometry and pullbacks

Let $\hat{K} \subset \mathbb{R}^2$ be a reference triangle with vertices $\{\hat{\mathbf{x}}_i\}_{i=1}^3$ and let K be a typical cell with vertices $\{\mathbf{x}_i\}_{i=1}^3$. We assume the diffeomorphism $F : \hat{K} \to K$ to be affine, as shown in Figure 1.5:

$$F(\hat{\mathbf{x}}) = J\hat{\mathbf{x}} + \mathbf{b}, \tag{1.3.1}$$

which of course depends on K, though highly structured meshes correspond to, for example, many maps differing only by the translation $\mathbf{b}$.

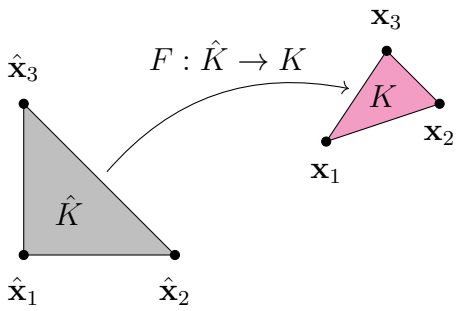


Figure 1.5: Affine mapping from a reference cell $\hat{K}$ to a typical cell K.

We now discuss the geometry of the physical and reference cells; this will make more precise some notation already used in the definition of the AW elements in §1.2.4. For local choices of indexing and orientation, we follow the convention in [168] as follows. Edge i of any triangle excludes the vertex i and is oriented from the lower-numbered vertex to the higher-numbered one. Each edge $\mathbf{e}$ is a column vector running between two vertices of a triangle, and is also used to denote the edge as a set. We define the unit tangent to edge $\mathbf{e}$ as $\mathbf{t} = \frac{\mathbf{e}}{\|\mathbf{e}\|}$, and to each edge associate its normal $\mathbf{n} = R\mathbf{t}$, where

$$R = \begin{pmatrix} & 1 \\ -1 & \end{pmatrix} \tag{1.3.2}$$

is clockwise rotation. Quantities and differential operators with $\hat{}$ are defined analogously for the reference element. Now clearly, the following statements are mutually exclusive:

- that all element boundaries have the same orientation as the reference boundary, and the unit normal is always outward-pointing, *or*
- that triangles sharing an edge will automatically agree on its direction (so that local and global direction coincide).

With the above convention, we have chosen the latter. In particular, F may reverse orientation. This greatly simplifies the required logic for assembly of finite element DOFs involving normal components. This convention can be extended to simplices of any dimension [21, 168].

The diffeomorphism (1.3.1) between the elements induces a map between corresponding function spaces in the obvious manner – to evaluate on the physical cell, we pull back to the reference cell and evaluate there: given a function $\hat{\phi}$ defined on $\hat{K}$, we define its *pullback* by

$$\phi := F^{-*}(\hat{\phi}) := \hat{\phi} \circ F^{-1}, \tag{1.3.3}$$

so that given a point $\mathbf{x} = F(\hat{\mathbf{x}})$, we can evaluate ϕ there as

$$\phi(\mathbf{x}) = \hat{\phi}(\hat{\mathbf{x}}). \tag{1.3.4}$$

For scalar-valued spaces, the pullback provides an isomorphism between $H^m(\hat{K})$ and $H^m(K)$ for $m \in \mathbb{Z}_{\geq 0}$; its use is very natural in the context of affine equivalent elements such as Lagrange or Crouzeix–Raviart. One can define their basis functions on a fixed reference element $\hat{K}$ and obtain the basis functions on any K by pullback. This can be adapted, with some technicalities, when affine equivalence fails [130]. Other shape spaces, such as the globally defined Rannacher–Turek quadrilateral element [163, Remarks 2 and 5], do not fall under the reference element paradigm.

When working with vector or tensor finite elements discretising Sobolev spaces such as $H(\mathrm{div})$ or $H(\mathrm{curl})$, it is helpful to work with the Piola mappings. As already used implicitly in §1.2, we note that elements of $H(\mathrm{div})$ have a well-defined normal trace, which moreover lies in $H^{-1/2}(\partial\Omega)$, and there is a corresponding Green's formula [40, Lemma 2.1.1]. A consequence is that piecewise polynomial vector fields will lie in $H(\mathrm{div})$ if and only if they have continuous normal traces across interfaces [40, Prop. 2.1.2]; applying this row-wise gives an analogous statement for $H(\mathrm{div};\mathbb{M})$ and $H(\mathrm{div};\mathbb{S})$. Hence, finite elements for $H(\mathrm{div})$-based spaces tend to include normal components as degrees of freedom, and these will be preserved by using the appropriate mapping.

This is seemingly a technicality at the level of function spaces, but also has a natural physical interpretation for the stress: $H(\mathrm{div};\mathbb{M})$-conformity means that the traction forces on a mesh face shared between two elements are in equilibrium.

Definition 1.3.1. (Vector and tensor contravariant Piola transforms). Let $\hat{K}, K \subseteq \mathbb{R}^d$, let $F : \hat{K} \to K$ be a diffeomorphism, and let $J(\hat{\mathbf{x}}) = \hat{\nabla} F(\hat{\mathbf{x}})$ be its Jacobian. The

contravariant Piola map takes $\hat{\Phi} : \hat{K} \to \mathbb{R}^d$ to $\Phi : K \to \mathbb{R}^d$ defined by

$$\mathcal{F}^{\text{div}}(\hat{\Phi}) := \tfrac{1}{\det J} J\hat{\Phi} \circ F^{-1}. \tag{1.3.5}$$

The *(double) contravariant Piola map* takes $\hat{\tau} : \hat{K} \to \mathbb{S}$ to $\tau : K \to \mathbb{S}$ by

$$\mathcal{F}^{\text{div,div}}(\hat{\tau}) := \tfrac{1}{(\det J)^2} J \left(\hat{\tau} \circ F^{-1}\right) J^\top. \tag{1.3.6}$$

The Piola transforms $\mathcal{F}^{\text{div}} : H(\text{div}, \hat{K}) \to H(\text{div}, K), \mathcal{F}^{\text{div,div}} : H(\text{div}, \hat{K}; \mathbb{S}) \to H(\text{div}, K; \mathbb{S})$ are well-defined and isomorphisms. Analogous considerations hold for $H(\text{rot}), H(\text{rot}; \mathbb{S}), H(\text{curl}), H(\text{curl}; \mathbb{S})$, tangential traces, and the *co*variant Piola mappings:

Definition 1.3.2. (Vector and tensor covariant Piola transforms). The *covariant Piola map* takes $\hat{\Phi} : \hat{K} \to \mathbb{R}^d$ to $\Phi : K \to \mathbb{R}^d$ by

$$\mathcal{F}^{\text{curl}}(\hat{\Phi}) := J^{-\top}\hat{\Phi} \circ F^{-1}. \tag{1.3.7}$$

The *(double) covariant Piola map* takes $\hat{\tau} : \hat{K} \to \mathbb{S}$ to $\tau : K \to \mathbb{S}$ by

$$\mathcal{F}^{\text{curl,curl}}(\hat{\tau}) := J^{-\top} \left(\hat{\tau} \circ F^{-1}\right) J^{-1}. \tag{1.3.8}$$

Unlike in the usual definition of the Piola map, the absolute value of the determinant is not taken in (1.3.5); this is explained in [168], which gives a thorough exposition of transforming and assembling vector finite elements in the case that the spaces and degrees of freedom are exactly preserved under the Piola mappings. The central contribution of this chapter is to adapt the techniques of [130] to handle $H(\text{div}; \mathbb{S})$ elements that are *not* exactly preserved under contravariant Piola mapping. This occurs, for example, when elements use degrees of freedom involving edge tangents or vertex values in addition to edge/face normals and internal ones, as in the case of the AW^{c} and AW^{nc} elements. This enables us to develop general and robust software implementations of these elements.

1.3.2 Transformation of components and their moments

We now review the relationship between the reference and physical element normals and tangents when F is affine. Suppose $i, j \in \{1, 2, 3\}$, $j < i$, so that the edge $\mathbf{e} = \mathbf{x}_i - \mathbf{x}_j$ joins vertices i and j of the physical element. Since $F(\hat{\mathbf{x}}_i) = \mathbf{x}_i$, we have

$$\mathbf{e} = \mathbf{x}_i - \mathbf{x}_j = J(\hat{\mathbf{x}}_i - \hat{\mathbf{x}}_j) = J\hat{\mathbf{e}}, \tag{1.3.9}$$

so

$$\|\mathbf{e}\|\mathbf{t} = \|\hat{\mathbf{e}}\|J\hat{\mathbf{t}}. \tag{1.3.10}$$

For the normal component, we use the identity $RJR^\top = (\det J)J^{-\top}$ (for all 2×2 matrices) to obtain

$$\|\mathbf{e}\|\mathbf{n} = \|\mathbf{e}\|R\mathbf{t} = R\mathbf{e} = RJ\hat{\mathbf{e}} = (\det J)J^{-\top}R\hat{\mathbf{e}} = (\det J)J^{-\top}\|\hat{\mathbf{e}}\|R\hat{\mathbf{t}} = (\det J)J^{-\top}\|\hat{\mathbf{e}}\|\hat{\mathbf{n}}. \tag{1.3.11}$$

It follows that the Jacobian maps reference tangents to physical ones (up to scale factor), but a slightly different map (1.3.11) is needed to obtain the physical normal from the reference one.

We can now deduce what the Piola map does to the various components of a tensor field. Let $\hat{\tau} : \hat{K} \to \mathbb{S}$ and $\tau = \mathcal{F}^{\text{div,div}}(\hat{\tau})$. At a point $\mathbf{x}$ on an edge $\mathbf{e} \subseteq \partial K$, the normal-normal component is preserved:

$$\begin{aligned}\|\mathbf{e}\|^2\mathbf{n}^\top\tau(\mathbf{x})\mathbf{n} &= \left((\det J)J^{-\top}\|\hat{\mathbf{e}}\|\hat{\mathbf{n}}\right)^\top \left(\frac{1}{(\det J)^2}J\hat{\tau}(\hat{\mathbf{x}})J^\top\right)\left(\|\hat{\mathbf{e}}\|(\det J)J^{-\top}\hat{\mathbf{n}}\right)\\ &= \|\hat{\mathbf{e}}\|^2\hat{\mathbf{n}}^\top\hat{\tau}(\hat{\mathbf{x}})\hat{\mathbf{n}}.\end{aligned} \tag{1.3.12}$$

On the other hand, the normal/tangential and double tangential components are not preserved, as direct calculations verify:

$$\|\mathbf{e}\|^2\mathbf{n}^\top\tau(\mathbf{x})\mathbf{t} = \left((\det J)J^{-\top}\|\hat{\mathbf{e}}\|\hat{\mathbf{n}}\right)^\top \left(\frac{1}{(\det J)^2}J\hat{\tau}(\mathbf{x})J^\top\right)\left(\|\hat{\mathbf{e}}\|J\hat{\mathbf{t}}\right) = \frac{\|\hat{\mathbf{e}}\|^2}{\det J}\hat{\mathbf{n}}^\top\hat{\tau}(\hat{\mathbf{x}})J^\top J\hat{\mathbf{t}}, \tag{1.3.13}$$

and

$$\|\mathbf{e}\|^2\mathbf{t}^\top\tau(\mathbf{x})\mathbf{t} = \left(\|\hat{\mathbf{e}}\|^2J\hat{\mathbf{t}}\right)^\top \left(\frac{1}{(\det J)^2}J\hat{\tau}(\hat{\mathbf{x}})J^\top\right)\left(\|\hat{\mathbf{e}}\|J\hat{\mathbf{t}}\right) = \frac{\|\hat{\mathbf{e}}\|^2}{(\det J)^2}\hat{\mathbf{t}}^\top J^\top J\hat{\tau}(\hat{\mathbf{x}})J^\top J\hat{\mathbf{t}}. \tag{1.3.14}$$

The tangential-normal component $\|\mathbf{e}\|^2\mathbf{t}^\top\tau(\mathbf{x})\mathbf{n}$ follows from (1.3.13) by symmetry. Evidently, it will be useful to further resolve $J^\top J\hat{\mathbf{t}}$ in terms of reference normal and tangential components. Define the orthogonal matrix

$$\hat{G} = \begin{pmatrix}\hat{\mathbf{n}} & \hat{\mathbf{t}}\end{pmatrix}. \tag{1.3.15}$$

Then, using $\mathbb{I} = \hat{G}\hat{G}^\top$,

$$J^\top J\hat{\mathbf{t}} = \hat{G}\underbrace{\hat{G}^\top J^\top J\hat{\mathbf{t}}}_{:=\begin{pmatrix}\tilde{\alpha}\\ \tilde{\beta}\end{pmatrix}} = \tilde{\alpha}\hat{\mathbf{n}} + \tilde{\beta}\hat{\mathbf{t}}. \tag{1.3.16}$$

Defining $\alpha = \frac{\tilde{\alpha}}{\det J}$ and $\beta = \frac{\tilde{\beta}}{\det J}$, then

$$\|\mathbf{e}\|^2 \mathbf{n}^\top \tau(\mathbf{x})\mathbf{t} = \|\hat{\mathbf{e}}\|^2 \hat{\mathbf{n}}^\top \hat{\tau}(\hat{\mathbf{x}}) \left(\alpha\hat{\mathbf{n}} + \beta\hat{\mathbf{t}}\right) = \|\hat{\mathbf{e}}\|^2 \left(\alpha\hat{\mathbf{n}}^\top \hat{\tau}(\hat{\mathbf{x}})\hat{\mathbf{n}} + \beta\hat{\mathbf{n}}^\top \hat{\tau}(\hat{\mathbf{x}})\hat{\mathbf{t}}\right), \quad (1.3.17)$$

and

$$\begin{aligned} \|\mathbf{e}\|^2 \mathbf{t}^\top \tau(\mathbf{x})\mathbf{t} &= \|\hat{\mathbf{e}}\|^2 \left(\frac{1}{\det J} J^\top J\hat{\mathbf{t}}\right)^\top \hat{\tau}(\hat{\mathbf{x}}) \left(\frac{1}{\det J} J^\top J\hat{\mathbf{t}}\right) \\ &= \|\hat{\mathbf{e}}\|^2 \left(\alpha\hat{\mathbf{n}} + \beta\hat{\mathbf{t}}\right)^\top \hat{\tau}(\hat{\mathbf{x}}) \left(\alpha\hat{\mathbf{n}} + \beta\hat{\mathbf{t}}\right) \\ &= \|\hat{\mathbf{e}}\|^2 \left(\alpha^2 \hat{\mathbf{n}}^\top \hat{\tau}(\hat{\mathbf{x}})\hat{\mathbf{n}} + 2\alpha\beta\hat{\mathbf{n}}^\top \hat{\tau}(\hat{\mathbf{x}})\hat{\mathbf{t}} + \beta^2 \hat{\mathbf{t}}^\top \hat{\tau}(\hat{\mathbf{x}})\hat{\mathbf{t}}\right). \end{aligned} \quad (1.3.18)$$

Remark 1.3.1. The tangential and tangential-tangential traces are well-defined at least on polynomial subspaces, and are included here for completeness.

We also wish to consider the transformation of integral moments against some function $\mu(\mathbf{x}) = \hat{\mu}(F^{-1}(\mathbf{x}))$, where $\hat{\mu} \in L^2(\hat{\mathbf{e}})$ will typically be a polynomial. Along an edge, the change of variables introduces a Jacobian factor $\frac{\|\mathbf{e}\|}{\|\hat{\mathbf{e}}\|}$, so by (1.3.12),

$$\|\mathbf{e}\| \int_{\mathbf{e}} \left(\mathbf{n}^\top \tau(s)\mathbf{n}\right) \mu(s)\, \mathrm{d}s = \|\hat{\mathbf{e}}\| \int_{\hat{\mathbf{e}}} \left(\hat{\mathbf{n}}^\top \hat{\tau}(\hat{s})\hat{\mathbf{n}}\right) \hat{\mu}(\hat{s})\, \mathrm{d}\hat{s}. \quad (1.3.19)$$

Similarly,

$$\|\mathbf{e}\| \int_{\mathbf{e}} \left(\mathbf{n}^\top \tau(s)\mathbf{t}\right) \mu(s)\, \mathrm{d}s = \|\hat{\mathbf{e}}\| \left(\alpha \int_{\hat{\mathbf{e}}} \left(\hat{\mathbf{n}}^\top \hat{\tau}(\hat{s})\hat{\mathbf{t}}\right) \hat{\mu}(\hat{s})\, \mathrm{d}\hat{s} + \beta \int_{\hat{\mathbf{e}}} \left(\hat{\mathbf{n}}^\top \hat{\tau}(\hat{s})\hat{\mathbf{t}}\right) \hat{\mu}(\hat{s})\, \mathrm{d}\hat{s}\right), \quad (1.3.20)$$

and

$$\begin{aligned} \|\mathbf{e}\| \int_{\mathbf{e}} \left(\mathbf{t}^\top \tau(s)\mathbf{t}\right) \mu(s)\, \mathrm{d}s = \|\hat{\mathbf{e}}\| \Bigg(\alpha^2 \int_{\hat{\mathbf{e}}} \left(\hat{\mathbf{n}}^\top \hat{\tau}(\hat{s})\hat{\mathbf{n}}\right) \hat{\mu}(\hat{s})\, \mathrm{d}\hat{s} + 2\alpha\beta \int_{\hat{\mathbf{e}}} \left(\hat{\mathbf{n}}^\top \hat{\tau}(\hat{s})\hat{\mathbf{t}}\right) \hat{\mu}(\hat{s})\, \mathrm{d}\hat{s} \\ + \beta^2 \int_{\hat{\mathbf{e}}} \left(\hat{\mathbf{t}}^\top \hat{\tau}(\hat{s})\hat{\mathbf{t}}\right) \hat{\mu}(\hat{s})\, \mathrm{d}\hat{s}\Bigg). \end{aligned} \quad (1.3.21)$$

It follows that bases for tensor-valued elements with boundary DOFs involving only normal-normal components can be directly mapped by the Piola transform; this is for example true of the TDNNS and HHJ elements. Since the AW elements also have boundary DOFs of other kinds, application of the Piola map alone will not result in the correct dual basis on each physical cell.

Remark 1.3.2. Many methods proposed after the seminal papers of Arnold and Winther [24, 25] were, in essence, attempts to construct improved versions of the AW elements. Among these, perhaps the most efficient are the Hu–Zhang elements [119–121], which strongly and stably enforce symmetry in any dimension; Arnold himself [12, p. 111] refers to these elements as "[m]ore efficient ... [and] applicable in any

dimension", and in the 2D conforming case, they have 18 local DOFs in comparison to AW^c's 24. The same authors recently provided a unified analysis of methods which strongly impose symmetry [114], using a generalised 4-field formulation of which both the Hu–Zhang and AW elements, among many others, are special cases. These elements also admit an interpretation in terms of the FEEC [71]. The Hu–Zhang elements employ tangential DOFs, and the Piola transformation theory which they therefore require would be very similar to that for the AW elements which we present here.

Remark 1.3.3. We briefly comment on the covariant case for $H(\mathrm{curl})$ elements. As is well-known, in 2D, $H(\mathrm{rot})$ and $H(\mathrm{div})$ are isomorphic by simple rotation, although the spaces are quite different in 3D; indeed, in dimensions strictly greater than 2, the analogous identification is always impossible for the vector-valued spaces [138, Prop. 4.1]. It follows that the transformation theory for $H(\mathrm{rot};\mathbb{S})$ and $H(\mathrm{curl};\mathbb{S})$ elements, at least in 2D, may be similar *mutatis mutandis* to what we present in this chapter.

1.3.3 Transforming Piola-inequivalent elements

Recall that, given an FE space V with $\dim V = n$ and a set of degrees of freedom (or *nodes*) $\{l_i\}_{i=1}^n \subseteq V^*$, there exists a unique *nodal basis* $\{\psi_i\}_{i=1}^n \subseteq V$ [48, p. 70] to which the $\{l_i\}$ are a cobasis, i.e. satisfying the Kronecker property

$$l_i(\psi_j) = \delta_{ij}. \tag{1.3.22}$$

We remark that this notion coincides with that of Riesz representative only when both bases are orthonormal.

It follows from identities such as (1.3.20) and (1.3.21) that FE spaces for $H(\mathrm{div};\mathbb{S})$ involving tangential degrees of freedom will not map nicely under the contravariant Piola transform – the reference element nodal basis will not map to the physical element one. In [130], Kirby developed abstract theory to address the simpler but analogous situation with the standard pullback. The broad strokes of the theory go through essentially unchanged if one replaces the regular pullback (1.3.3) with a Piola pullback; for self-containment, we summarise the key ideas here.

We let $\hat{\boldsymbol{\Phi}}$ be a (column) vector of elements of a function space $\hat{V}$ over $\hat{K}$. Let $\mathcal{F}^* : \hat{V} \to V$ denote some linear pullback operator (such as one of the Piola maps) taking $\hat{V}$ into a function space V defined on K. Define $\mathcal{F}^*(\hat{\Phi})$ componentwise, i.e.

$$\left(\mathcal{F}^*(\hat{\boldsymbol{\Phi}})\right)_j := \mathcal{F}^*(\hat{\boldsymbol{\Phi}}_j). \tag{1.3.23}$$

Then, if we take $\hat{\mathbf{\Psi}}$ to contain the nodal basis functions of $\hat{V}$ on the reference element and $\mathbf{\Psi}$ to contain the nodal basis of V defined on K, then it follows from identities such as (1.3.20) that

$$\mathcal{F}^*(\hat{\mathbf{\Psi}}) \neq \mathbf{\Psi}, \tag{1.3.24}$$

and note that equality still fails to hold up to permutation or scaling. If the pullback operator preserves the function space, providing an isomorphism between the instantiations V and $\hat{V}$, then in particular it preserves linear independence, so $\mathcal{F}^*(\hat{\mathbf{\Psi}})$ will be a basis – just not the nodal one. Consequently, there must exist a (cell-dependent) invertible matrix M such that

$$\mathbf{\Psi} = M\mathcal{F}^*(\hat{\mathbf{\Psi}}). \tag{1.3.25}$$

Hence, the correct physical nodal basis is simply obtained by computing the pullback of the reference basis, and then multiplying by M. If M is sparse, then application of this principle incurs only a small additional cost to the overall finite element computation.[12]

However, as we see from §1.3.2, it is natural to consider the effect of the pullback on the DOFs, rather than directly on the nodal basis. To consider instead how the dual spaces are transformed, denote by $N = \{\ell_i\}_i$ and $\hat{N} = \{\hat{\ell}_i\}_i$ (row) vectors of functionals on V and $\hat{V}$ respectively, and define the *dual* or *push-forward* $\mathcal{F}_* : V^* \to \hat{V}^*$ associated with $\mathcal{F}^*$ by

$$\mathcal{F}_*(\ell) := \ell \circ \mathcal{F}^*. \tag{1.3.26}$$

Now identifying an n-vector $\mathbf{\Phi} \in V^n$ with its componentwise image $\mathbf{\Phi}^{**} \in (V^{**})^n$ under the canonical embedding into the bidual, it induces an evaluation operator on vectors of dual functionals via the 'outer product' $N\mathbf{\Phi} := \mathbf{\Phi}^{**} \otimes N$, where

$$(\mathbf{\Phi}^{**} \otimes N)_{i,j} := \mathbf{\Phi}_j^{**}(\ell_i) = \ell_i(\mathbf{\Phi}_j). \tag{1.3.27}$$

This allows us to extend the push-forward (1.3.26) to vectors of functionals componentwise either in a manner analogous to (1.3.23), or equivalently as

$$\mathcal{F}_*(N) := N\mathcal{F}^* = \mathcal{F}^*(\cdot)^{**} \otimes N. \tag{1.3.28}$$

Choosing $N, \hat{N}$ to be the DOFs, then the Kronecker property (1.3.22) by which they are characterised is then simply expressed as

$$\Psi^{**} \otimes N = \mathbb{I} = \hat{\Psi}^{**} \otimes \hat{N}. \tag{1.3.29}$$

[12] With some effort, the theory can be extended to handle the situation when the pullback does not send $\hat{V}$ onto V, but none of our examples in the present work require this.

Moreover, this clarifies the transformation of the primal basis: expanding the desired physical basis in terms of the mapped reference basis, we have

$$\mathbf{\Psi}_j = \sum_{k=1}^{n} \theta_k^{(j)} \mathcal{F}^*(\hat{\mathbf{\Psi}}_k), \qquad j = 1, \dots, n, \tag{1.3.30}$$

so it follows from the Kronecker property (1.3.22) that

$$Q\Theta = \mathbb{I}, \tag{1.3.31}$$

where

$$Q = \mathcal{F}^*(\hat{\mathbf{\Psi}})^{**} \otimes N = \left(\ell_i(\mathcal{F}^*(\hat{\mathbf{\Psi}}_k))\right)_{i,k=1}^{n} \tag{1.3.32}$$

can be interpreted as a generalised Vandermonde matrix and

$$\Theta = Q^{-1} = \left(\theta_k^{(j)}\right)_{k,j=1}^{n} \tag{1.3.33}$$

has the vector of coefficients for $\mathbf{\Psi}_j$ with respect to $\{\mathcal{F}^*(\hat{\mathbf{\Psi}}_k)\}_k$ in column j.

Now by (1.3.24) and unisolvency of N, we have

$$\mathcal{F}^*(\hat{\Psi})^{**} \otimes N \neq \Psi^{**} \otimes N = \mathbb{I}, \tag{1.3.34}$$

so

$$\mathcal{F}_*(N)(\hat{\Psi}) = \mathcal{F}^*(\hat{\Psi})^{**} \otimes N \neq \mathbb{I} = \hat{\Psi}^{**} \otimes \hat{N} = \hat{N}\hat{\Psi}, \tag{1.3.35}$$

so in particular,

$$\mathcal{F}_*(N) \neq \hat{N}, \tag{1.3.36}$$

but as before, there must be an invertible P with

$$\hat{N} = P\mathcal{F}_*(N). \tag{1.3.37}$$

An important result of [130, Theorem 3.1] is that

$$M = P^\top \tag{1.3.38}$$

(as matrices of numbers). In other words, it is sufficient to relate the physical nodes and their push-forwards. As we will see in our examples, it can be more natural to find P^{-1} and then invert it by hand.

Remark 1.3.4. Proponents of the FEEC employ a refinement of the notion of DOFs in the classical Ciarlet triplet defining a finite element [19, Section 4][21][138, p. 11]. Rather than specifying a basis of the dual V^* of the shape space V, one can specify maps from V into subspaces of the duals of function spaces on arbitrary-codimensional

facets of the cell. Arguably, it is this geometric decomposition of V^*, rather than any particular basis for it, which is useful for defining the global FE space, since it makes more explicit the fact that the basis functions are associated with subsimplices, in order that interelement continuity conditions can be applied to patch together the local spaces on a mesh during the assembly process.[13]

1.4 Piola-mapped tensor elements

The general approach of the transformation theory developed in [130] is to build the nodal basis on K out of a linear combination of the mapped reference element basis functions. As explained in the previous subsection, for us the transformation of basis functions works by duality, considering instead the push-forward of nodes. It will be natural to begin with the nonconforming case, and then consider the inclusion of vertex DOFs for the conforming element. The existing implementations of these elements [58, 61] require a separate construction of the basis functions for each element, by inverting the Vandermonde matrix arising from the Piola pullback of the primal basis, as in equation (1.3.31).

1.4.1 The nonconforming AW element

We employ block notation to define vectors of the DOFs. For the nonconforming element, we define the vector of nodes associated with edge $\mathbf{e}_k$ by

$$N^{1,k} = \begin{pmatrix} \ell^{\mathbf{n},\mathbf{n},0,k} & \ell^{\mathbf{n},\mathbf{t},0,k} & \ell^{\mathbf{n},\mathbf{n},1,k} & \ell^{\mathbf{n},\mathbf{t},1,k} \end{pmatrix}^\top. \tag{1.4.1}$$

That is, we store the normal and tangential moments of order 0, followed by those of order 1. We collect the three internal DOFs in the vector

$$N^2 = \begin{pmatrix} \ell^{0,1,1} & \ell^{0,1,2} & \ell^{0,2,2} \end{pmatrix}^\top, \tag{1.4.2}$$

so that the nonconforming element has degrees of freedom $N = \begin{pmatrix} N^{1,1} & N^{1,2} & N^{1,3} & N^2 \end{pmatrix}^\top$, with an analogous definition and ordering of reference element degrees of freedom $\hat{N}^{1,k}, \hat{N}^2, \hat{N}$. Note that we have added superscripts of 1 and 2 to indicate the topological dimension associated with the DOFs.

[13] An alternative refinement is given by the notion of *finite element systems* due to Christiansen [68], which consist of, for each subsimplex T, a complex of spaces $A^k(T) \xrightarrow{\mathrm{d}} A^{k+1}(T) \xrightarrow{\mathrm{d}} \dots$ indexed by form degree and connected by the exterior derivative d; together with restriction maps to further subsimplices which commute with d, these complexes can be interpreted as a *presheaf* on the category of subsimplices [72, Remark 9]. However, we remark that typically, the existence and description of the 'next' space in such a sequence is itself a research question.

Now, we need to compute the Piola push-forward (denoted $\mathcal{F}_*$) of these nodes in terms of the reference element nodes, and thus build up sub-blocks of the matrix P^{-1}, where P is the change-of-basis matrix defined in (1.3.37).

So let $\hat{\tau}$ be defined over $\hat{K}$, $1 \leq k \leq 3$, and $i = 0$ or 1. Then by (1.3.19),

$$\begin{aligned}\mathcal{F}_*(\ell^{\mathbf{n},\mathbf{n},i,k})(\hat{\tau}) = \ell^{\mathbf{n},\mathbf{n},i,k}(\mathcal{F}^{\mathrm{div},\mathrm{div}}(\hat{\tau})) &= \int_{\mathbf{e}_k} (\mathbf{n} \cdot \mathcal{F}^{\mathrm{div},\mathrm{div}}(\hat{\tau})(s)\mathbf{n})\mu_i(s)\,\mathrm{d}s \\ &= \frac{\|\hat{\mathbf{e}}_k\|}{\|\mathbf{e}_k\|} \int_{\hat{\mathbf{e}}_k} (\hat{\mathbf{n}} \cdot \hat{\tau}(\hat{s})\hat{\mathbf{n}})\hat{\mu}_i(\hat{s})\,\mathrm{d}\hat{s} \\ &= \frac{\|\hat{\mathbf{e}}_k\|}{\|\mathbf{e}_k\|} \hat{\ell}^{\hat{\mathbf{n}},\hat{\mathbf{n}},i,k}(\hat{\tau}).\end{aligned} \tag{1.4.3}$$

So, normal-normal moment nodes are pushed forward exactly to the corresponding reference normal-normal modes. For the normal-tangential moments, (1.3.20) can be rewritten as

$$\|\mathbf{e}_k\|\mathcal{F}_*(\ell^{\mathbf{n},\mathbf{t},i,k})(\hat{\tau}) = \|\hat{\mathbf{e}}_k\| \left(\alpha^k \hat{\ell}^{\hat{\mathbf{n}},\hat{\mathbf{n}},i,k}(\hat{\tau}) + \beta^k \hat{\ell}^{\hat{\mathbf{n}},\hat{\mathbf{t}},i,k}(\hat{\tau})\right), \tag{1.4.4}$$

where the superscript k indicates association with edge k. It follows that

$$\mathcal{F}_*(N^{1,k}) = W^k \hat{N}^{1,k}, \tag{1.4.5}$$

where

$$W^k = \frac{\|\hat{\mathbf{e}}_k\|}{\|\mathbf{e}_k\|} \begin{pmatrix} 1 & & & \\ \alpha^k & \beta^k & & \\ & & 1 & \\ & & \alpha^k & \beta^k \end{pmatrix}, \tag{1.4.6}$$

which easily inverts to

$$\left(W^k\right)^{-1} = \frac{\|\mathbf{e}_k\|}{\|\hat{\mathbf{e}}_k\|} \begin{pmatrix} 1 & & & \\ -\frac{\alpha^k}{\beta^k} & \frac{1}{\beta^k} & & \\ & & 1 & \\ & & -\frac{\alpha^k}{\beta^k} & \frac{1}{\beta^k} \end{pmatrix}. \tag{1.4.7}$$

Applying now the push-forward to an internal DOF (recalling that $\phi_0 \equiv 1$):

$$\mathcal{F}_*(\ell^{0,i,j})(\hat{\tau}) = \int_K \mathcal{F}^{\mathrm{div},\mathrm{div}}(\hat{\tau}) : \tau_{0,i,j}\,\mathrm{d}x = \int_{\hat{K}} \frac{1}{\det J} \left(J\hat{\tau}J^\top\right)_{ij} \mathrm{d}\hat{x}. \tag{1.4.8}$$

Expanding out $J\hat{\tau}J^\top$ gives

$$\begin{pmatrix} J_{11}^2\hat{\tau}_{11} + 2J_{11}J_{12}\hat{\tau}_{12} + J_{12}^2\hat{\tau}_{22} & J_{11}J_{21}\hat{\tau}_{11} + (J_{11}J_{22} + J_{12}J_{21})\hat{\tau}_{12} + J_{12}J_{22}\hat{\tau}_{22} \\ * & J_{21}^2\hat{\tau}_{11} + 2J_{21}J_{22}\hat{\tau}_{12} + J_{22}^2\hat{\tau}_{22} \end{pmatrix}, \tag{1.4.9}$$

where the asterisk indicates equality due to symmetry. Using this in (1.4.8) gives

$$\begin{aligned}
\mathcal{F}_*(\ell^{0,1,1}) &= \frac{1}{\det J}\left(J_{11}^2\hat{\ell}^{0,1,1} + 2J_{11}J_{12}\hat{\ell}^{0,1,2} + J_{12}^2\hat{\ell}^{0,2,2}\right),\\
\mathcal{F}_*(\ell^{0,1,2}) &= \frac{1}{\det J}\left(J_{11}J_{21}\hat{\ell}^{0,1,1} + (J_{11}J_{22}+J_{12}J_{21})\hat{\ell}^{0,1,2} + J_{12}J_{22}\hat{\ell}^{0,2,2}\right),\\
\mathcal{F}_*(\ell^{0,2,2}) &= \frac{1}{\det J}\left(J_{21}^2\hat{\ell}^{0,1,1} + 2J_{21}J_{22}\hat{\ell}^{0,1,2} + J_{22}^2\hat{\ell}^{0,2,2}\right),
\end{aligned} \tag{1.4.10}$$

so that with

$$\tilde{W} = \begin{pmatrix} J_{11}^2 & 2J_{11}J_{12} & J_{12}^2 \\ J_{11}J_{21} & J_{11}J_{22}+J_{12}J_{21} & J_{12}J_{22} \\ J_{21}^2 & 2J_{21}J_{22} & J_{22}^2 \end{pmatrix} \tag{1.4.11}$$

and $\check{W} = \frac{1}{\det J}\tilde{W}$, we have

$$\mathcal{F}_*(N^2) = \check{W}\hat{N}^2. \tag{1.4.12}$$

Hence, overall,

$$P^{-1} = \begin{pmatrix} W^1 & & & \\ & W^2 & & \\ & & W^3 & \\ & & & \check{W} \end{pmatrix}, \tag{1.4.13}$$

which is readily inverted blockwise to find P. As a remark, the $\check{W}$ block is dense, but denoting its dependence on J by $\check{W} = \check{W}_J$, it is then easily checked that $\check{W}_J^{-1} = \check{W}_{J^{-1}}$, i.e. the inverse can be found by reversing the roles of K and $\hat{K}$.

1.4.2 The conforming AW element

We now turn to the fully conforming Arnold–Winther element. It has the same edge and internal nodes as the nonconforming element, but also includes vertex values. However, these transform in a very similar fashion to the internal moments just discussed. We collect the pointwise evaluation functionals for each vertex $\mathbf{x}_k$ into a small vector:

$$N^{0,k} = \begin{pmatrix} \ell^{k,1,1} & \ell^{k,1,2} & \ell^{k,2,2} \end{pmatrix}^\top, \tag{1.4.14}$$

and as for $\mathrm{AW}^{\mathrm{nc}}$, collect together the DOFs for the opposite edge:

$$N^{1,k} = \begin{pmatrix} \ell^{\mathbf{n},\mathbf{n},0,k} & \ell^{\mathbf{n},\mathbf{t},0,k} & \ell^{\mathbf{n},\mathbf{n},1,k} & \ell^{\mathbf{n},\mathbf{t},1,k} \end{pmatrix}^\top. \tag{1.4.15}$$

The internal DOFs are collected in

$$N^2 = \begin{pmatrix} \ell^{0,1,1} & \ell^{0,1,2} & \ell^{0,2,2} \end{pmatrix}^\top. \tag{1.4.16}$$

Again we order DOFs by topological dimension:

$$N = \begin{pmatrix} N^{0,1} & N^{0,2} & N^{0,3} & N^{1,1} & N^{1,2} & N^{1,3} & N^2 \end{pmatrix}^\top. \tag{1.4.17}$$

The edge and internal degrees of freedom are handled exactly as for the previous element. The Piola push-forward of a vertex functional gives

$$\mathcal{F}_*(\ell^{k,i,j})(\hat{\tau}) = \ell^{k,i,j}(\mathcal{F}^{\mathrm{div},\mathrm{div}}(\hat{\tau})) = \left(\frac{1}{(\det J)^2} J\hat{\tau}(\hat{\mathbf{x}}_k)J^\top\right)_{ij}. \tag{1.4.18}$$

This suggests that (except for very special geometry), the Piola transform will not send vertex-oriented basis functions on the reference element to their physical counterpart. However, using the expansion of $J\hat{\tau}J^\top$ given in (1.4.9), a very similar calculation as for the internal moments shows that (1.4.18) gives for each vertex

$$\mathcal{F}_*(N^{0,k}) = \breve{W}\hat{N}^{0,k}, \tag{1.4.19}$$

where now $\breve{W} = \frac{1}{(\det J)^2}\tilde{W}$, for which again $\breve{W}_J^{-1} = \breve{W}_{J^{-1}}$. Combining all of these push-forwards gives

$$\mathcal{F}_*(N) = \begin{pmatrix} \breve{W} & & & & & & \\ & \breve{W} & & & & & \\ & & \breve{W} & & & & \\ & & & W^1 & & & \\ & & & & W^2 & & \\ & & & & & W^3 & \\ & & & & & & \breve{W} \end{pmatrix} \hat{N}. \tag{1.4.20}$$

Again, the block-diagonal structure of the matrix makes it straightforward to invert and find P.

Remark 1.4.1. On near-degenerate cells, the analogues of blocks W^k such as (1.4.6) may be ill-conditioned, which could affect the accuracy with which basis functions are evaluated.

1.4.3 Scale-invariance and conditioning

For both elements considered, scale factors in the transformations do not matter for construction of the local space because a nonzero scaling of a unisolvent set remains unisolvent, but they are important for the global space due to the required continuity of DOFs between cells which share them. We remark that, in this sense, the AW internal DOFs (1.2.21) require no special treatment after being Piola-mapped, as they do not need to be shared between adjacent elements; as a result, replacing $\breve{W}$ with any nonsingular matrix in (1.4.13) or (1.4.20) would suffice for implementation.

It is natural to divide moment DOFs by some power of the facet measure; for example, replacing the internal DOF (1.2.21) by an integral mean would do away

with factors of $\det J$ in the transformation matrix. Such scale-invariance is implicit in the treatment of AW^{c} by Carstensen et al. [61], the Morley–Wang–Xu elements, and related H^3-nonconforming elements due to Wu and Xu [186] and would give a slightly different transformation matrix. Contravariant rescaling of DOFs gives neater expressions in the transformation theory but, more concretely, can improve the conditioning of the discrete system, as we now show; this extends [130, Section 5.1] to the AW elements.

Consider an AW^{c} basis function dual to a vertex DOF; it is unity at one vertex in one component and zero at other vertices, hence $\mathcal{O}(1)$ over the cell. An internal basis function integrates to unity over the cell, hence must be of size $\mathcal{O}(h^{-2})$; between these cases, a normal moment basis function over an edge must have size $\mathcal{O}(h^{-1})$ over that edge. Integrating the inner products which populate the global mass matrix, we obtain some entries (corresponding to pairs of vertex basis functions) of size $\mathcal{O}(h^2)$, others (corresponding to pairs of internal basis functions) of size $\mathcal{O}(h^{-2})$, and others in between. This leads to an $\mathcal{O}(h^{-4})$ condition number of the mass matrix; for $\mathrm{AW}^{\mathrm{nc}}$, this difference is $\mathcal{O}(h^{-2})$. By contrast, for Lagrange mass matrices, the condition number is $\mathcal{O}(1)$ under refinement.[14]

Instead of redefining the canonical AW DOFs, we propose *post hoc* rescaling of the DOFs (and hence the basis functions to which they are dual) on the physical cell; this is equivalent to postmultiplying the local transformation matrix P by a diagonal matrix whose diagonal entries are 1, h_K, or h_K^2 as appropriate, where h_K denotes a local averaged cell diameter on whose value the cells sharing the DOF agree. This rescaling is necessary to give an $\mathcal{O}(1)$ condition number for the mass matrix and prevent conditioning worse than $\mathcal{O}(h^{-2})$ for our overall system.

1.4.4 Preservation of the constraints

Our two spaces of interest can be characterised as standard polynomials of certain total degree, but subject to linear constraints. For example, shape functions in the local $\mathrm{AW}^{\mathrm{nc}}$ space (1.2.22) are quadratic, but constrained to have linear normal-normal components on cell edges. For each such condition, we may consider linear functionals on polynomials of total degree which vanish precisely on the subspace satisfying the

[14] When derivative DOFs are also present, as for example in the Hermite, Argyris, and Bell elements, one can use inverse inequalities to deduce analogous deterioration of conditioning [130]; in general, a basis function dual to an unnormalised moment of an sth order derivative over a r-dimensional facet will scale as $\mathcal{O}\left(h^{-(s+r)}\right)$.

constraint; the finite element space is therefore characterised as the intersection of the kernels of all these constraint functionals.

For the $\mathrm{AW}^{\mathrm{nc}}$ space, if $\tau \in \mathcal{P}_2(K;\mathbb{S})$, then $\mathbf{n}\cdot\tau\mathbf{n} \in \mathcal{P}_1(\mathbf{e})$ for a given edge $\mathbf{e}$ if and only if it is $L^2(\mathbf{e})$-orthogonal to any polynomial of degree exactly 2. Thus, within $\mathcal{P}_2(K;\mathbb{S})$, $\mathrm{AW}^{\mathrm{nc}}(K)$ has constraint functionals

$$\ell_k^c(\tau) = \int_{\mathbf{e}_k} (\mathbf{n}\cdot\tau(s)\mathbf{n})\mu_2^k(s)\,\mathrm{d}s, \qquad 1 \le k \le 3, \tag{1.4.21}$$

where μ_2^k is the quadratic Legendre polynomial on $\mathbf{e}_k$.

For the AW^{c} element, if $\tau \in \mathcal{P}_3(K;\mathbb{S})$ so that $v = \operatorname{div}\tau \in \mathcal{P}_2(K;\mathbb{R}^2)$, then $v \in \mathcal{P}_1(K;\mathbb{R}^2)$ if and only if v is $L^2(K)$-orthogonal to any choice of six vector-valued orthogonal polynomials of degree exactly 2. With respect to $\mathcal{P}_3(K;\mathbb{S})$, $\mathrm{AW}^{\mathrm{c}}(K)$ has constraint functionals

$$\ell_i^c(\tau) = \int_K (\operatorname{div}\tau(\mathbf{x}))\cdot\boldsymbol{\phi}_{i,j,k}(\mathbf{x})\mathrm{d}x, \qquad k = 1,2, \quad i+j=2, \tag{1.4.22}$$

where $\{\boldsymbol{\phi}_{i,j,k}\}_{k=1,i+j=2}^{2} \subseteq \mathcal{P}_2(K;\mathbb{R}^2)$ are the six Dubiner polynomials of degree exactly 2.

It is important to note that these constraints are preserved under Piola mappings; that is, if some tensor field satisfies the appropriate conditions on the reference element, then its Piola pullback will satisfy the analogous conditions on the physical element. For the $\mathrm{AW}^{\mathrm{nc}}$ space, in light of (1.3.12), reference element quadratic tensor fields with linear normal-normal components on edges will map to physical element fields with the same property. Similarly, the conforming AW^{c} element is subject to a loss-of-degree constraint on its divergence; denoting $\tau = \mathcal{F}^{\mathrm{div},\mathrm{div}}(\hat{\tau})$ for some symmetric $\hat{\tau}$ defined on the reference element, by a direct computation we have $\operatorname{div}\tau = \frac{1}{(\det J)^2} J\widehat{\operatorname{div}}\,\hat{\tau}$. It follows that the Piola map preserves the constraints in both cases.

All of the constraint functionals we use here are preserved (up to sign) under the Piola push-forward. Hence, the physical element function space is actually constructed by pullback, even if the basis functions are not preserved. This need not be the case – for example, the constraints on the C^1 Bell element are not preserved under affine pullback, requiring a fuller version of the transformation theory [130].

1.5 Traction conditions in the Hellinger–Reissner principle with Nitsche's method

The Arnold–Winther discretisation of the Hellinger–Reissner problem (1.2.7) is given by seeking the unique (σ_h, u_h) in one of the AW pairs $\Sigma_h \times V_h$ satisfying the stationarity condition of the discretised Hellinger–Riessner functional

$$\mathcal{H}_h(\sigma_h, u_h) := \mathcal{J}(\sigma_h) + \int_\Omega (\operatorname{div}_h \sigma_h - f) \cdot u_h \, \mathrm{d}x. \tag{1.5.1}$$

In the pure displacement case $|\Gamma_N| = 0$, for displacement data u_0, the stationarity condition has discrete weak form[15]

$$\begin{aligned} \int_\Omega \mathcal{A}\sigma_h : \tau_h + (\operatorname{div}_h \tau_h) \cdot u_h \, \mathrm{d}x &= \int_{\partial\Omega} (\tau_h \mathbf{n}) \cdot u_0 \, \mathrm{d}s \quad \forall \, \tau_h \in \Sigma_h, \\ \int_\Omega (\operatorname{div}_h \sigma_h) \cdot v_h \, \mathrm{d}x &= \int_\Omega f \cdot v_h \, \mathrm{d}x \qquad \forall \, v_h \in V_h. \end{aligned} \tag{1.5.2}$$

We now turn to the enforcement of traction conditions (1.2.3) for the Hellinger–Reissner problem, which for the dual formulation (1.2.6) are essential (i.e. strongly enforced); we consider a mixed boundary condition ($0 < |\Gamma_D|, |\Gamma_N| < |\partial\Omega|$), although the method may be extended to the pure traction case $|\Gamma_D| = 0$ subject to a quotient of the displacement space by the rigid motions, which moreover the data should annihilate as a compatibility condition, i.e. $\int_\Omega f \cdot v \, \mathrm{d}x + \langle g, v \rangle_{\partial\Omega} = 0 \; \forall \; v \in RM$.

The original AW papers [24, 25] only treated the case of the elastic body clamped everywhere on the boundary, i.e. $|\Gamma_N| = 0$ with homogeneous displacement data $u_0 \equiv 0$. For the conforming element, it is possible to set the traction boundary conditions on an edge $\mathbf{e}$ using only the DOFs associated with the closure of $\mathbf{e}$, since these uniquely determine the (projection onto $\mathcal{P}_1(\mathbf{e}; \mathbb{R}^2)$ of the) normal trace on $\mathbf{e}$. However, Carstensen et al. [61] identified (in particular, inhomogeneous) traction conditions as a substantial practical difficulty associated with the AW elements, due to delicate interdependence between DOFs at the boundary, which moreover depend on the shape of the boundary at a given boundary vertex; they were able to enforce them using nodal interpolation [59], Lagrange multipliers [61], or elimination of the boundary DOFs by condensation [58]. When the boundary condition is mixed but the traction data g is zero, the relevant trial and test space for the stress is

$$H_{\Gamma_N}(\operatorname{div}, \Omega; \mathbb{S}) = \{\tau \in H(\operatorname{div}, \Omega; \mathbb{S}) \mid \langle \tau \mathbf{n}, v \rangle_{\Gamma_N} = 0 \; \forall \; v \in H^1_{0,\Gamma_D}(\Omega; \mathbb{R}^2)\} \tag{1.5.3}$$

[15] From this subsection onwards in this thesis, we switch to the usual convention that the unit normal $\mathbf{n}$ to the boundary of Ω or a cell K is outward-pointing, simplifying arguments which employ integration by parts.

[40, Remark 2.1.3]. Wang [185, Lemma III.1] constructed an interpolant of Scott–Zhang type which preserves the traction-free condition on Γ_N under an elliptic regularity assumption, and which was used to prove a discrete inf-sup condition for this case, but no details of the discrete enforcement of this condition were offered in Pasciak and Wang's application of AW^c to the homogeneous pure traction problem in [159].

There is no clear way to enforce the traction condition in either the Arnold–Winther spaces or the weak formulation of Hellinger–Reissner. We therefore advocate a simpler approach, employing the classical Nitsche's method [154] to weakly enforce the condition. There is little literature on the application of Nitsche's method to the enforcement of essential boundary conditions in dual mixed problems. Our approach is similar to [52, 133] for the mixed Poisson problem; see also [171].

Given traction data g, we augment the Hellinger–Reissner functional (1.5.1) (with div replaced by div_h) over the discrete spaces $\Sigma_h \times V_h$ with a term incorporating the traction condition (to ensure consistency, since we do not impose the condition on the spaces), and a consistent, quadratic penalty term, seeking the critical point $(\sigma_h, u_h) \in \Sigma_h \times V_h$ of

$$\mathcal{H}_{h,\gamma}(\sigma_h, u_h) := \mathcal{H}_h(\sigma_h, u_h) - \int_{\Gamma_N} \mathbf{r}_h \cdot u_h \ \mathrm{d}s + \frac{\gamma}{2}\delta_h(\mathbf{r}_h), \tag{1.5.4}$$

where h denotes the characteristic mesh size, $\gamma > 0$ is an h-independent penalty parameter, $\mathbf{r}_h = \sigma_h \mathbf{n} - g$ denotes the traction residual, and

$$\delta_h(\mathbf{r}_h) := \frac{1}{h}\int_{\Gamma_N} \|\mathbf{r}_h\|^2 \,\mathrm{d}s \tag{1.5.5}$$

may be interpreted as a least-squares term penalising deviation from the traction condition.

The exact traction satisfies $\sigma\mathbf{n} = g$ in $H^{-1/2}(\Gamma_N;\mathbb{R}^2)$, but a penalty term δ_h in terms of the dual norm in $H^{-1/2}(\Gamma_N;\mathbb{R}^2)$ would not aid the analysis, nor is it practical to equivalently penalise the Riesz representative of $\mathbf{r}_h$ in $H^{1/2}_{00}(\Gamma_N;\mathbb{R}^2)$, or to work with the linearisation of such penalisations. To ensure consistency of the $L^2(\Gamma_N;\mathbb{R}^2)$-penalisation (1.5.5), we assume full elliptic regularity of the stress field by assuming that the solution (σ, u) to (1.2.6) satisfies $(\sigma, u) \in H^1(\Omega;\mathbb{S}) \times H^2(\Omega;\mathbb{R}^2)$, and that $g \in L^2(\Gamma_N;\mathbb{R}^2)$. The latter assumption typically holds in practice for the traction data (or some discrete approximation thereof), while the former holds in the homogeneous isotropic case if Ω is a convex polygon and $\mathcal{A}$ is smooth.

Remark 1.5.1. As already remarked, the exact displacement u satisfies an unmixed primal formulation of linear elasticity for which $u \in H^1(\Omega;\mathbb{R}^2)$, precisely the unmixed weak form of the HL equation associated with this space in the strain complex, and moreover in fact satisfies $\varepsilon(u) \in H(\mathrm{div};\mathbb{S})$ when viewed as the solution to the strong form. However, there is no gain in regularity for the stress field by passing to an alternative formulation.

Remark 1.5.2. The natural choice of exponent for h in (1.5.5) is $+1$ and not -1, by dimensionalisation and since we expect $\|\mathbf{r}_h\|^2_{0,\Gamma_N}$ to converge one order slower than $\|\mathbf{r}_h\|^2_{-1/2,\Gamma_N}$. However, the term with negative exponent is more naturally interpretable as a penalisation, and was found to be more effective in preliminary numerical experiments. This also informs the choice of discrete norms (1.5.8) below.

Convergence will be proved only for the AW^{c} element, but a computational example will be included also for $\mathrm{AW}^{\mathrm{nc}}$.

Let $\mathcal{T}_h$ denote a quasi-uniform triangulation of Ω, $\mathcal{E}_h^\circ$ the set of its internal edges, and Λ_h the set of its vertices.[16] Linearising the augmented functional (1.5.4) over the AW^{c} pair, we seek $(\sigma_h, u_h) \in \Sigma_h \times V_h$ satisfying

$$\begin{aligned} a_{h,\gamma}(\sigma_h,\tau_h) + b(\tau_h,u_h) &= \int_{\Gamma_D} \tau_h\mathbf{n}\cdot u_0 \ \mathrm{d}s + \frac{\gamma}{h}\int_{\Gamma_N} g\cdot\tau_h\mathbf{n}\ \mathrm{d}s \quad && \forall\ \tau_h\in\Sigma_h,\\ b(\sigma_h,v_h) &= \int_\Omega f\cdot v_h\ \mathrm{d}x - \int_{\Gamma_N} g\cdot v_h\,\mathrm{d}s && \forall\ v_h\in V_h, \end{aligned} \tag{1.5.6}$$

where

$$\begin{aligned} a_{h,\gamma}(\sigma_h,\tau_h) &:= \int_\Omega \mathcal{A}\sigma_h : \tau_h\ \mathrm{d}x + \frac{\gamma}{h}\int_{\Gamma_N}\sigma_h\mathbf{n}\cdot\tau_h\mathbf{n}\ \mathrm{d}s,\\ b(\tau_h,v_h) &:= \int_\Omega (\mathrm{div}\,\tau_h)\cdot v_h\ \mathrm{d}x - \int_{\Gamma_N}\tau_h\mathbf{n}\cdot v_h\ \mathrm{d}s. \end{aligned} \tag{1.5.7}$$

Define the $H^1(\Omega;\mathbb{S})\times H^1(\Omega;\mathbb{R}^2)$-based mesh-dependent norms

$$|||\tau_h|||_h^2 := \|\tau_h\|^2_{0,\Omega} + \frac{1}{h}\|\tau_h\mathbf{n}\|^2_{0,\Gamma_N}, \qquad \|v_h\|_h^2 := \|\varepsilon_h(v_h)\|_0^2 + \frac{1}{h}\sum_{\mathbf{e}\in\mathcal{E}_h^\circ}\|[\![v_h]\!]\|^2_{0,\mathbf{e}} + \frac{1}{h}\|v_h\|^2_{0,\Gamma_D}, \tag{1.5.8}$$

where $[\![\cdot]\!]$ on an interior edge $\mathbf{e} = \partial K \cap \partial K'$ denotes the jump $[\![v_h]\!] := v_h|_K - v_h|_{K'}$, and on an exterior edge $\mathbf{e}\subseteq\partial\Omega$ denotes the identity. We now prove well-posedness of the augmented discrete formulation (1.5.6) using the standard Brezzi conditions [40, Section 4.2.3]. We take $\gamma \geq 1$.

[16] We assume the edges of $\mathcal{T}_h$ align with the partition $\Gamma_D \cup \Gamma_N$, so that each external edge lies entirely in one of these.

Proposition 1.5.1. (Discrete well-posedness). *The augmented Nitsche system (1.5.6) is well-posed, uniformly in h, with respect to the norms (1.5.8).*

Proof. There exists $C_{\mathcal{A}} > 0$ with $\int_\Omega \mathcal{A}\tau : \tau \, \mathrm{d}x \leq C_{\mathcal{A}}^2 \|\tau\|_{0,\Omega}^2 \; \forall \; \tau \in L^2(\Omega;\mathbb{S})$. For $\sigma_h, \tau_h \in \Sigma_h, v_h \in V_h$, we have

$$|a_{h,\gamma}(\sigma_h, \tau_h)| \leq \max\{C_{\mathcal{A}}^2, \gamma\} |||\sigma_h|||_h |||\tau_h|||_h, \tag{1.5.9}$$

and

$$\begin{aligned} b(\tau_h, v_h) &= -\int_{\Gamma_N} \tau_h \mathbf{n} \cdot v_h \; \mathrm{d}s + \sum_{K \in \mathcal{T}_h} \int_\Omega (\operatorname{div} \tau_h) \cdot v_h \; \mathrm{d}x \\ &= \sum_K \left(\int_{\partial K} \tau_h \mathbf{n} \cdot v_h \; \mathrm{d}s - \int_K \varepsilon(v_h) : \tau_h \; \mathrm{d}x \right) - \int_{\Gamma_N} \tau_h \mathbf{n} \cdot v_h \; \mathrm{d}s \\ &= -\int_\Omega \varepsilon_h(v_h) : \tau_h \; \mathrm{d}x + \sum_{\mathbf{e} \in \mathcal{E}_h^\circ} \int_{\mathbf{e}} \tau_h \mathbf{n} \cdot [\![v_h]\!] \, \mathrm{d}s + \int_{\Gamma_D} \tau_h \mathbf{n} \cdot v_h \; \mathrm{d}s, \end{aligned} \tag{1.5.10}$$

so

$$|b(\tau_h, v_h)| \leq \|\varepsilon_h(v_h)\|_0 \|\tau_h\|_0 + \sum_{\mathbf{e} \in \mathcal{E}_h^\circ} \|\tau_h \mathbf{n}\|_{0,\mathbf{e}} \|[\![v_h]\!]\|_{0,\mathbf{e}} + \|\tau_h \mathbf{n}\|_{0,\Gamma_D} \|v_h\|_{0,\Gamma_D}. \tag{1.5.11}$$

By the scaling $\|\tau_h \mathbf{n}\|_{0,\mathbf{e}} \lesssim h^{-\frac{1}{2}} \|\tau_h\|_{0,K} \; \forall \; \mathbf{e} \subseteq \partial K$, we obtain

$$|b(\tau_h, v_h)| \lesssim |||\tau_h|||_h \|v_h\|_h. \tag{1.5.12}$$

Clearly, $a_{h,\gamma}$ is $|||\cdot|||_h$-coercive on all of Σ_h uniformly in h, provided $\gamma \geq 1$. Now fix $0 \neq u_h \in V_h$. Define $\tau_h \in \Sigma_h$ by the AW^c DOFs

$$\tau_h(\mathbf{x}) = 0 \qquad \forall \; \mathbf{x} \in \Lambda_h, \tag{1.5.13a}$$

$$\int_{\mathbf{e}} \tau_h \mathbf{n} \cdot w_h \; \mathrm{d}s = \frac{1}{h} \int_{\mathbf{e}} [\![u_h]\!] \cdot w_h \; \mathrm{d}s \qquad \forall \; \mathbf{e} \in \mathcal{E}_h^\circ, \forall \; \mathbf{e} \subseteq \Gamma_D, w_h \in \mathcal{P}_1(\mathbf{e};\mathbb{R}^2), \tag{1.5.13b}$$

$$\int_{\mathbf{e}} \tau_h \mathbf{n} \cdot w_h \; \mathrm{d}s = 0 \qquad \forall \; \mathbf{e} \subseteq \Gamma_N, w_h \in \mathcal{P}_1(\mathbf{e};\mathbb{R}^2), \tag{1.5.13c}$$

$$\int_K \tau_h : q_h \; \mathrm{d}x = -\int_K \varepsilon(u_h) : q_h \; \mathrm{d}x \quad \forall \; K \in \mathcal{T}_h, q_h \in \mathcal{P}_0(K;\mathbb{S}) = \mathbb{S}. \tag{1.5.13d}$$

Choosing $w_h = [\![u_h]\!] \in \mathcal{P}_1(\mathbf{e};\mathbb{R}^2)$ in (1.5.13b), $q_h = \varepsilon(u_h) \in \mathbb{S}$ in (1.5.13d) gives

$$\int_{\mathbf{e}} \tau_h \mathbf{n} \cdot [\![u_h]\!] \; \mathrm{d}s = \frac{1}{h} \|[\![u_h]\!]\|_{0,\mathbf{e}}^2 \; \forall \; \mathbf{e} \in \mathcal{E}_h^\circ, \qquad \int_{\mathbf{e}} \tau_h \mathbf{n} \cdot u_h \; \mathrm{d}s = \frac{1}{h} \|u_h\|_{0,\mathbf{e}}^2 \; \forall \; \mathbf{e} \subseteq \Gamma_D,$$
$$\int_K \tau_h : \varepsilon(u_h) \; \mathrm{d}x = -\|\varepsilon(u_h)\|_{0,K}^2 \; \forall \; K \in \mathcal{T}_h. \tag{1.5.14}$$

Using (1.5.10),

$$b(\tau_h, u_h) = -\sum_K \left(-\|\varepsilon(u_h)\|_{0,K}^2\right) + \sum_{\mathbf{e}\in\mathcal{E}_h^\circ} \frac{1}{h}\|[\![u_h]\!]\|_{0,\mathbf{e}}^2 + \sum_{\mathbf{e}\subseteq\Gamma_D} \frac{1}{h}\|u_h\|_{0,\mathbf{e}}^2 = \|u_h\|_h^2. \quad (1.5.15)$$

It remains to show that $\|u_h\|_h \gtrsim |||\tau_h|||_h$. For every $\mathbf{e} \subseteq \Gamma_N$, since the DOFs associated to an edge and its endpoints determine $\tau_h\mathbf{n}$ on that edge, we have $\tau_h\mathbf{n} = 0$ by (1.5.13a), (1.5.13c), so it suffices to show $\|u_h\|_h \gtrsim \|\tau_h\|_{0,\Omega}$. By (1.5.13b), (1.5.13d), we have $\pi_{\mathbf{e}}(\tau_h\mathbf{n}) = \frac{1}{h}[\![u_h]\!], \pi_K(\tau_h) = -\varepsilon(u_h)\ \forall\ \mathbf{e} \in \mathcal{E}_h^\circ, \mathbf{e} \subseteq \Gamma_D, K \in \mathcal{T}_h$, where $\pi_{\mathbf{e}} : L^2(\mathbf{e};\mathbb{R}^2) \to \mathcal{P}_1(\mathbf{e};\mathbb{R}^2), \pi_K : L^2(K;\mathbb{S}) \to \mathbb{S}$ are orthogonal projections. By equivalence of norms on $\widehat{\Sigma}_h$ on the reference cell $\hat{K}$, we have $\|\hat{\tau}_h\|_{0,\hat{K}}^2 \lesssim \sum_{\text{vertices } \hat{\mathbf{x}}\in\hat{K}} |\hat{\tau}_h(\hat{\mathbf{x}})|^2 + \sum_{\hat{\mathbf{e}}\subseteq\partial\hat{K}} \|\pi_{\hat{\mathbf{e}}}(\hat{\tau}\hat{\mathbf{n}})\|_{0,\hat{\mathbf{e}}}^2 + \|\pi_{\hat{K}}\hat{\tau}\|_{0,\hat{K}}^2$, so by a scaling argument we obtain $\|\tau_h\|_{0,K}^2 \lesssim \sum_{\mathbf{e}\subseteq\partial K} \frac{1}{h}\|[\![u_h]\!]\|_{0,\mathbf{e}}^2 + \|\varepsilon(u_h)\|_{0,K}^2$. This shows

$$\inf_{u_h\in V_h} \sup_{\tau_h\in\Sigma_h} \frac{b(\tau_h, u_h)}{|||\tau_h|||_h \|u_h\|_h} \gtrsim 1. \quad (1.5.16)$$

□

Remark 1.5.3. In analogy with the RT spaces considered in [52, 133], we have the useful equilibrium property $\operatorname{div}\Sigma_h \subseteq V_h$, but in disanalogy we in general have $(\Sigma_h|_{\mathbf{e}})\mathbf{n} \not\subseteq V_h|_{\mathbf{e}}$ on edges $\mathbf{e}$.

For error estimation, we employ intermediate approximants $\Pi_h\sigma, P_h u$, where $P_h : L^2(\Omega;\mathbb{R}^2) \to V_h$ denotes the orthogonal projection and $\Pi_h : H^1(\Omega;\mathbb{S}) \to \Sigma_h$ denotes the Clément-like interpolation operator constructed by Arnold and Winther [24], which enjoy the following approximation properties for all $(\tau, v) \in H^1(\Omega;\mathbb{S}) \times L^2(\Omega;\mathbb{R}^2)$: (i) $\operatorname{div}\Pi_h\tau = P_h \operatorname{div}\tau$ (as in a smoothed variant of the commuting diagram (1.2.23)); (ii) $(\Pi_h\tau)\mathbf{n} = \pi_{\mathbf{e}}(\tau\mathbf{n})$ on all edges $\mathbf{e}$; (iii) $\|\tau - \Pi_h\tau\|_{0,\Omega} \lesssim h^m\|\tau\|_{m,\Omega}, 1 \le m \le 3$; (iv) $\|v - P_h v\|_{0,\Omega} \lesssim h^m\|v\|_{m,\Omega}, 0 \le m \le 2$.

Lemma 1.5.1. (Local approximation in H^1). *For each $K \in \mathcal{T}_h$ and $\tau \in H^2(\Omega;\mathbb{S})$, we have*

$$\|\tau - \Pi_h\tau\|_{1,K} \lesssim h\|\tau\|_{2,S_K}, \quad (1.5.17)$$

where S_K is a patch of cells neighbouring K such that $\{S_K\}_{K\in\mathcal{T}_h}$ has the finite overlapping property $\sum_{S_K,K\in\mathcal{T}_h} \|\cdot\|_{0,S_K} \lesssim \|\cdot\|_{0,\Omega}$.

Proof. We adapt the proof of (iii) in [24], from which we recall that the error in Π_h may be written as $I - \Pi_h = (I - \Pi_h^0)(I - R_h)$, where $R_h : L^2(\Omega;\mathbb{S}) \to \Sigma_h \cap H^1(\Omega;\mathbb{S})$ is a Clément interpolant satisfying

$$\|\tau - R_h\tau\|_{j,K} \lesssim h^{m-j}\|\tau\|_{m,S_K}, \qquad 0 \le j \le 1, \quad j \le m \le 3, \quad (1.5.18)$$

and S_K is a patch of the required form, and $\Pi_h^0 : H^1(\Omega;\mathbb{S}) \to \Sigma_h$ is the canonical interpolation operator except at the vertices, at which $(\Pi_h^0\tau)(\mathbf{x}) := 0 \ \forall \ \mathbf{x} \in \Lambda_h$. It is easily checked that $\Pi_{\hat{K}}^0$, the restriction of Π_h^0 to a single cell $\hat{K}$, is bounded from $H^1(\hat{K};\mathbb{S})$ to $H^r(\hat{K};\mathbb{S})$ for all $r \geq 0$; choosing $r = 1$, by a scaling argument we obtain $\|\Pi_K^0\tau\|_{1,K} \lesssim h^{-1}\|\tau\|_{0,K} + \|\tau\|_{1,K}$, so

$$\|\Pi_h^0(I - R_h)\tau\|_{1,K} \lesssim h^{-1}\|(I - R_h)\tau\|_{0,K} + \|(I - R_h)\tau\|_{1,K} \lesssim h\|\tau\|_{2,S_K}, \tag{1.5.19}$$

which gives the result when combined with (1.5.18). □

We make an additional regularity assumption on the stress field for error analysis.

Proposition 1.5.2. (Convergence of stress in L^2). *Let $(\sigma, u) \in H^2(\Omega;\mathbb{S}) \times H^2(\Omega;\mathbb{R}^2)$. We have the error estimate*

$$\|\sigma - \sigma_h\|_0 \lesssim h(\gamma\|\sigma\|_{2,\Omega} + \|u\|_{2,\Omega}). \tag{1.5.20}$$

In particular, we expect the traction residual to converge as $\|\sigma_h\mathbf{n} - g\|_{0,\Gamma_N} = \mathcal{O}(h^{\frac{1}{2}})$.

Proof. By the Babuška condition associated with the well-posed system (1.5.6), applied to $(\sigma_h - \Pi_h\sigma, u_h - P_hu) \in \Sigma_h \times V_h$, there are $(\tau_h, v_h) \in \Sigma_h \times V_h$ with $|||\tau_h|||_h + \|v_h\|_h \leq 1$ and

$$|||\sigma_h - \Pi_h\sigma|||_h + \|u_h - P_hu\|_h \lesssim a_{h,\gamma}(\sigma_h - \Pi_h\sigma, \tau_h) + b(\tau_h, u_h - P_hu) + b(\sigma_h - \Pi_h\sigma, v_h) \tag{1.5.21}$$

which by consistency of the system (1.5.6) is equal to

$$\begin{aligned}
&a_{h,\gamma}(\sigma - \Pi_h\sigma, \tau_h) + b(\tau_h, u - P_hu) + b(\sigma - \Pi_h\sigma, v_h) \\
&\quad = a_{h,\gamma}(\sigma - \Pi_h\sigma, \tau_h) - \int_{\Gamma_N} \tau_h\mathbf{n} \cdot (u - P_hu)\,\mathrm{d}s \qquad \text{using (i), (ii)} \\
&\quad = \int_\Omega \mathcal{A}(\sigma - \Pi_h\sigma) : \tau_h \,\mathrm{d}x + \underbrace{\frac{\gamma}{h}\int_{\Gamma_N} (\sigma - \Pi_h\sigma)\mathbf{n} \cdot \tau_h\mathbf{n} \,\mathrm{d}s}_{(*)} - \int_{\Gamma_N} \tau_h\mathbf{n} \cdot (u - P_hu)\,\mathrm{d}s \\
&\quad = (\dagger).
\end{aligned} \tag{1.5.22}$$

By (ii), the term $(*)$ would vanish were it not for Remark 1.5.3. Employing multiplicative trace inequalities, approximation properties of P_h, and Lemma 1.5.1, we

have

$$
\begin{aligned}
(\dagger) &\lesssim \|\sigma - \Pi_h\sigma\|_0\|\tau_h\|_0 + \|\tau_h\|_{0,\Gamma_N}\left(\frac{\gamma}{h}\|(\sigma-\Pi_h\sigma)\mathbf{n}\|_{0,\Gamma_N} + \|u - P_h u\|_{0,\Gamma_N}\right)\\
&\lesssim h^2\|\sigma\|_{2,\Omega} + h^{\frac{1}{2}}\sum_{\mathbf{e}\subseteq\Gamma_N}\left(\frac{\gamma}{h}\|\sigma-\Pi_h\sigma\|_{0,\mathbf{e}} + \|u-P_hu\|_{0,\mathbf{e}}\right)\\
&\lesssim h^2\|\sigma\|_{2,\Omega} + h^{\frac{1}{2}}\sum_{K}\left(\frac{\gamma}{h}\|\sigma-\Pi_h\sigma\|_{0,K}^{\frac{1}{2}}\|\sigma-\Pi_h\sigma\|_{1,K}^{\frac{1}{2}} + \|u-P_hu\|_{0,K}^{\frac{1}{2}}\|u-P_hu\|_{1,K}^{\frac{1}{2}}\right)\\
&\lesssim h^2\|\sigma\|_{2,\Omega} + h^{\frac{1}{2}}\left(\frac{\gamma}{h}h\|\sigma\|_{1,\Omega}^{\frac{1}{2}}h^{\frac{1}{2}}\|\sigma\|_{2,\Omega} + h\|u\|_{2,\Omega}^{\frac{1}{2}}h^{\frac{1}{2}}\|u\|_{2,\Omega}^{\frac{1}{2}}\right)\\
&= h^2\|\sigma\|_{2,\Omega} + \gamma h\|\sigma\|_{2,\Omega} + h^2\|u\|_{2,\Omega},
\end{aligned}
\tag{1.5.23}
$$

so

$$
\begin{aligned}
\|\sigma-\sigma_h\|_0 &\leq \|\sigma-\Pi_h\sigma\|_0 + \|\sigma_h - \Pi_h\sigma\|_0 \lesssim h^2\|\sigma\|_2 + |||\sigma_h-\Pi_h\sigma|||_h + \|u_h - P_hu\|_h\\
&\lesssim h^2\|\sigma\|_2 + \gamma h\|\sigma\|_2 + h^2\|u\|_2.
\end{aligned}
\tag{1.5.24}
$$

□

1.6 An exterior calculus perspective

In this section, we consider the application of FEEC to Piola transformation theory, and to the construction of multigrid smoothers.

1.6.1 Uniform construction of the pullbacks

The Piola transforms (1.3.5)–(1.3.8) may be regarded as the analogy of the standard pullback (1.3.3) for $H(\mathrm{div})$- and $H(\mathrm{curl})$-based spaces, but in fact the pullbacks may be defined uniformly in a manner guided by the FEEC [138, p. 35], [12, Section 6.2.5]; we here employ terminology for which we refer the reader to [12, Ch. 6].[17]

Let us regard the physical and reference cells $K, \hat{K}$ as submanifolds of dimension d in $\mathbb{R}^d$, with $F : \hat{K} \to K$ a diffeomorphism. Denote by $\mathrm{Alt}^k\,\mathbb{R}^d$ the space of alternating k-linear forms on $\mathbb{R}^d$, and for $M \in \{K, \hat{K}\}$ let $\Lambda^k(M)$ denote the space of differential k-forms on M, of which functions in the Sobolev spaces we consider will be scalar, vector, and tensor proxies, and the operators of vector calculus will be proxies for the exterior derivative $\mathrm{d} : \Lambda^k \to \Lambda^{k+1}$. Scalar fields may be identified with 0-forms or d-forms, and vector fields with 1-forms or $(d-1)$-forms. We may specify L^2-integrability of differential form coefficients with $L^2\Lambda^k(\Omega) := L^2(\Omega; \mathrm{Alt}^k\,\mathbb{R}^d)$; Sobolev

[17] We remark that much of the literature employing Piola transforms does little to motivate their definition, beyond stating the *consequences* of the definitions.

spaces of differential forms may be defined as $H\Lambda^k := \{\omega \in L^2\Lambda^k \mid \mathrm{d}\omega \in L^2\Lambda^{k+1}\}$, and correspond to the conventional spaces of vector calculus via $H\Lambda^0 \simeq H^1, H\Lambda^1 \simeq H(\mathrm{curl}), H\Lambda^{d-1} \simeq H(\mathrm{div})$, and $H\Lambda^d \simeq L^2$.[18]

An elastic stress field $\mathcal{T}$ on M may naturally be identified with an $(\mathrm{Alt}^{d-1}\mathbb{R}^d)$-valued $(d-1)$-form $\tau \in \Lambda^{d-1}(M; \mathrm{Alt}^{d-1}\mathbb{R}^d)$, which by the proxy of $\mathbb{R}^d$ for $\mathrm{Alt}^{d-1}\mathbb{R}^d$ may be identified with $\Lambda^{d-1}(M;\mathbb{R}^d)$, since when integrated over a codimension-1 submanifold (such as the boundary of a subdomain), it should give a vector representing force [19][96, p. 618]. Applying the Hodge star gives an element $\star\tau \in \Lambda^1(M;\mathbb{R}^d)$, i.e. a linear map $\mathbb{R}^d \to \mathbb{R}^d$ (hence, a matrix) at every point of M, which is the classical characterisation of stress. Alternatively, $\mathcal{T}$ may be identified with a (symmetric) *co*variant 2-tensor field in $\Lambda^1(M; \mathrm{Alt}^1\mathbb{R}^d)$, which to each point assigns a (symmetric) bilinear form on $\mathbb{R}^d$ [138, p. 10].

Given $\hat{\omega} \in \Lambda^k(\hat{K})$, the derivative of the inverse diffeomorphism $J^{-1}(\mathbf{x}) = (F^{-1})'(\mathbf{x})$ at $\mathbf{x} \in K$ induces an element $\omega = J^{-*}\hat{\omega} \in \Lambda^k(K)$ pointwise via $(J^{-*}\hat{\omega})_{\mathbf{x}} := J^{-1}(\mathbf{x})^*\hat{\omega}_{F^{-1}(\mathbf{x})}$, the *pullback* of $\hat{\omega}$ under F^{-1}, where * denotes the algebraic pullback of a linear map $L : \mathbb{R}^d \to \mathbb{R}^d$ given by $L^*\eta(v_1,\dots,v_k) := \eta(Lv_1,\dots,Lv_k)$ for $\eta \in \Lambda^K(M), v_i \in \mathbb{R}^d$. For scalar fields representing 0-forms $\hat{\omega} \in H\Lambda^0(\hat{K})$ (i.e. a constant map at each point), the scalar proxy for the resulting 0-form ω is easily seen to be given simply by precomposition with F^{-1}, because $(J^{-*}\hat{\omega})_{\mathbf{x}} = \hat{\omega}_{F^{-1}(\mathbf{x})}$, which for the proxy gives exactly the standard pullback (1.3.3). For a vector field $\hat{w}$ representing a 1-form $\hat{\omega} \in H\Lambda^1(\hat{K})$, the canonical identification is $\hat{\omega} = \sum_{i=1}^d \hat{w}_i \mathrm{d}\hat{\mathbf{x}}^i$, so that $\hat{\omega}_{\hat{\mathbf{x}}}(v) = \hat{w}(\hat{\mathbf{x}}) \cdot v$ (i.e. $\hat{w}$ is the pointwise Riesz representative of $\hat{\omega}$), so

$$(J^{-*}\hat{\omega})_{\mathbf{x}}(v) = \hat{\omega}_{F^{-1}(\mathbf{x})}(J^{-1}(\mathbf{x})v) = \hat{w}(F^{-1}(\mathbf{x})) \cdot (J^{-1}(\mathbf{x})v) = (J^{-\top}(\mathbf{x})\hat{w}(F^{-1}(\mathbf{x}))) \cdot v, \tag{1.6.1}$$

hence the transformed proxy is given by $\mathcal{F}^{\mathrm{curl}}(\hat{w})$. A vector field $\hat{w}$ can alternatively represent a $(d-1)$-form via

$$\begin{aligned}\hat{\omega}_{\hat{\mathbf{x}}}(v_1,\dots,v_{d-1}) = \det[\hat{w}(\hat{\mathbf{x}})|v_1|\dots|v_{d-1}] &=: \sum_{i=1}^d \hat{w}_i(\hat{\mathbf{x}})\phi_i(v_1,\dots,v_{d-1}) \\ &= \hat{w}(\hat{\mathbf{x}}) \cdot \phi(v_1,\dots,v_{d-1}),\end{aligned} \tag{1.6.2}$$

for which

$$\begin{aligned}(J^{-*}\hat{\omega})_{\mathbf{x}}(v_1,\dots,v_{d-1}) &= \det[\hat{w}(F^{-1}(\mathbf{x}))|J^{-1}v_1|\dots|J^{-1}v_{d-1}] \\ &= \det(J^{-1})\det[J\hat{w}(F^{-1}(\mathbf{x}))|v_1|\dots|v_{d-1}] \\ &= \det[\mathcal{F}^{\mathrm{div}}(\hat{w})(\mathbf{x})|v_1|\dots|v_{d-1}].\end{aligned} \tag{1.6.3}$$

[18] We already employ $\mathbb{R}^d$ as a proxy for the tangent spaces $\{T_{\mathbf{x}}M\}_{\mathbf{x}\in M}$ on which the alternating forms are defined.

The derivation of the tensor transforms are analogous; a (symmetric) covariant 2-tensor field $\hat{\tau} \in \Lambda^1(\hat{K}; \operatorname{Alt}^1 \mathbb{R}^d)$ has as proxy a (symmetric) matrix field $\hat{\mathcal{T}}$ via the identification $\hat{\tau}_{\hat{\mathbf{x}}}(v_1, v_2) = v_1^\top \hat{\mathcal{T}}(\hat{\mathbf{x}}) v_2$, so that $(J^{-*}\hat{\tau})_{\mathbf{x}}(v_1, v_2) = v_1^\top J^{-\top} \hat{\mathcal{T}}(F^{-1}(\mathbf{x})) J^{-1} v_2 = v_1^\top \mathcal{F}^{\mathrm{curl},\mathrm{curl}}(\hat{\mathcal{T}})(\mathbf{x}) v_2$.

We now provide a novel derivation of the double contravariant Piola map (1.3.6). A (symmetric) matrix field $\hat{\mathcal{T}}$ may instead serve as a proxy for a (symmetric) form $\hat{\tau} \in \Lambda^{d-1}(\hat{K}; \operatorname{Alt}^{d-1} \mathbb{R}^d)$ via the identification

$$\hat{\tau}_{\hat{\mathbf{x}}}(v_1, \dots, v_{d-1})(z_1, \dots, z_{d-1}) = \phi(v_1, \dots, v_{d-1})^\top \hat{\mathcal{T}}(\hat{\mathbf{x}}) \phi(z_1, \dots, z_{d-1}), \tag{1.6.4}$$

where ϕ is defined by (1.6.2).[19] By definition of ϕ it is easily checked that $\phi(J^{-1}v_1, \dots, J^{-1}v_{d-1}) = \frac{1}{\det J} J^\top \phi(v_1, \dots, v_{d-1})$, and hence

$$\begin{aligned} &(J^{-*}\hat{\tau})_{\mathbf{x}}(v_1, \dots, v_{d-1})(z_1, \dots, z_{d-1}) \\ &\qquad = \phi(J^{-1}v_1, \dots, J^{-1}v_{d-1})^\top \hat{\mathcal{T}}(F^{-1}(\mathbf{x})) \phi(J^{-1}z_1, \dots, z_{d-1}) \\ &\qquad = \phi(v_1, \dots, v_{d-1})^\top \mathcal{F}^{\mathrm{div},\mathrm{div}}(\hat{\mathcal{T}})(\mathbf{x}) \phi(z_1, \dots, z_{d-1}). \end{aligned} \tag{1.6.5}$$

Note that neither tensor transform is given by the row-wise application of the corresponding vector transform.

We hereafter assume that J is spatially constant, so that the pullback commutes with the exterior derivative. In this case, a crucial property is that moments of the exterior derivatives against appropriate fields are preserved, a primary motivation for the use of the Piola pullbacks in mixed finite elements [40, Lemmas 2.1.6, 2.1.9]. Let $\omega \in H\Lambda^k(K), \mu \in H\Lambda^{d-k-1}(K)$ with pullbacks $\hat{\omega}, \hat{\mu}$, then since the pullback respects the exterior product and commutes with the exterior derivative,

$$\int_K \mu \wedge \mathrm{d}\omega = \int_K J^{-*}\hat{\mu} \wedge \mathrm{d}J^{-*}\hat{\omega} = \int_K J^{-*}\hat{\mu} \wedge J^{-*}\mathrm{d}\hat{\omega} = \int_K J^{-*}(\hat{\mu} \wedge \mathrm{d}\hat{\omega}) = \pm \int_{\hat{K}} \hat{\mu} \wedge \mathrm{d}\hat{\omega}. \tag{1.6.6}$$

Note that since we have chosen to allow F to reverse orientation, in general the moment preservation (1.6.6) will only be up to sign. By Stokes' theorem, it also follows that

$$\int_{\partial K} \mu \wedge \omega = \pm \int_{\partial \hat{K}} \hat{\mu} \wedge \hat{\omega}, \tag{1.6.7}$$

where the boundary integrands are meant in the trace sense.

Combining these identities with the characterisation of constrained finite element spaces by kernels of constraint functionals, as in §1.4.4, also allows for a more elegant

[19] While the paper [28] corresponding to this chapter was under review, the preprint [64] was released, which offers a framework for identifying the (alternating-form-valued) differential forms to which tensor-valued functions are proxy; our formula (1.6.4) for $H(\mathrm{div}; \mathbb{S})$ functions coincides (up to signs of terms) with the identification proposed in [64, p. 18].

verification of their preservation by the Piola maps; the constraints on the divergence of the AW^{c} element is preserved in light of (1.6.6), while the preservation of boundary constraints follows from the identity (1.6.7) applied to appropriate $L^2(\partial K)$-orthogonal polynomials, as constructed e.g. in [155, Section 3].[20]

That the pullback commutes with the exterior derivative also implies the preservation of the kernel of the operators defining the spaces, a property implicit in the classical presentation of the Piola operators (e.g. [149, Section 3.9]). For example, if $K, \hat{K} \subseteq \mathbb{R}^2$ (respectively, $\mathbb{R}^3$), note that if $\hat{\phi} \in H^1(\hat{K})$ and $\phi \in H^1(K)$ is its standard pullback given by (1.3.3), then by the chain rule we have $\nabla\phi = J^{-\top}\hat{\nabla}\hat{\phi}$. Since $\operatorname{rot}\nabla \equiv 0$ (resp. $\operatorname{curl}\nabla \equiv 0$), certainly both $\hat{\nabla}\hat{\phi} \in H(\operatorname{rot}, \hat{K})$ (resp. $H(\operatorname{curl}, \hat{K})$) and $\nabla\phi \in H(\operatorname{rot}, K)$ (resp. $H(\operatorname{curl}, K)$), and the covariant map (1.3.7) "transform[s] vectors of $H(\operatorname{curl}; \Omega)$ like gradients" [40, p. 61], which, on simply connected domains, form the kernel of rot or curl by exactness of an appropriate de Rham sequence; hence

$$\ker(\operatorname{rot}) = \mathcal{F}^{\operatorname{curl}}\left(\ker\left(\widehat{\operatorname{rot}}\right)\right) \text{ in 2D and } \ker(\operatorname{curl}) = \mathcal{F}^{\operatorname{curl}}\left(\ker\left(\widehat{\operatorname{curl}}\right)\right) \quad \text{in 3D.} \tag{1.6.8}$$

Analogously, by a direct computation,

$$\operatorname{curl}\phi = \frac{1}{\det J} J\widehat{\operatorname{curl}}\ \hat{\phi}, \tag{1.6.9}$$

which is reflected in (1.3.5).

We now extend the discussion in [149, Section 3.9] to the tensor-valued case in 2D. For the matrix-valued curl of a vector field in 2D,

$$\mathbf{curl}\ v := \begin{pmatrix} \dfrac{\partial v_1}{\partial y} & -\dfrac{\partial v_1}{\partial x} \\ \dfrac{\partial v_2}{\partial y} & -\dfrac{\partial v_2}{\partial x} \end{pmatrix}, \tag{1.6.10}$$

we have

$$\mathbf{curl}\ v = \frac{1}{\det J}\widehat{\mathbf{curl}}\ \hat{v}\ J^{\top}. \tag{1.6.11}$$

Then, recalling that $\operatorname{airy} = \mathbf{curl}\operatorname{curl}$, we have for $\hat{\phi} \in H^2(\hat{K})$ with pullback $\phi \in H^2(K)$ that

$$\operatorname{airy}\phi = \frac{1}{(\det J)^2} J\left(\widehat{\operatorname{airy}}\ \hat{\phi}\right)J^{\top} = \mathcal{F}^{\operatorname{div},\operatorname{div}}\left(\widehat{\operatorname{airy}}\hat{\phi}\right), \tag{1.6.12}$$

so by exactness of the 2D stress complex (1.2.23), we obtain that $\ker(\operatorname{div}) = \mathcal{F}^{\operatorname{div},\operatorname{div}}(\ker(\widehat{\operatorname{div}}))$. Similarly, for the rot of a symmetric matrix field applied rowwise, we calculate that $\nabla^2\phi = \mathcal{F}^{\operatorname{curl},\operatorname{curl}}(\hat{\nabla}^2\hat{\phi})$, where $\nabla^2 H^2$ forms the kernel of rot on $H(\operatorname{rot}; \mathbb{S})$ by exactness of the 2D Hessian complex (e.g. [161, Remark 3.16]).

[20] The calculation for the divergence of $\hat{\tau}$ in the first half of §1.4.4 also reduces to the observation that the pullback commutes with the exterior derivative and preserves polynomial degree.

This observation of kernel preservation may also be connected to the (albeit trivial) topologies of K and $\hat{K}$: the pullbacks are isomorphisms between appropriate complexes on K and $\hat{K}$, which moreover commute with d, hence are cochain maps which preserve the cohomology of each domain.[21][22]

1.6.2 Kernel-capturing and robust multigrid

It is now well-established that the characterisation of the kernels of discretised differential operators is crucial for the design of robust multigrid schemes [18, 89, 90, 169]; for AW-type elements, this is given precisely by their positions in the discrete exact complex (1.2.23), as we now explain. We describe multigrid relaxation in the framework of subspace correction methods [188]. Given a finite-dimensional Hilbert space V of functions on a mesh, consider a decomposition

$$V = \sum_i V_i, \tag{1.6.13}$$

where the sum need not be direct. The variational problem to be solved over V often takes the form of a symmetric, coercive operator, perturbed by a positive semidefinite singular operator (such as a discretised divergence) which is scaled by some parameter $\alpha > 0$, a physical or penalty parameter which, as it increases, renders the problem difficult to solve. The seminal work of Schöberl [169, Theorem 4.1] revealed sufficient conditions for α-robustness of the parallel subspace correction preconditioner induced by the decomposition (1.6.13); a key insight is that, if $\mathcal{N}$ denotes the kernel of the

[21] One may naïvely relate some properties of the transformation F^{-1} to properties of the coordinate transformation from reference to deformed configurations in (hyper)elasticity. If $\rho : \Omega_0 \to \Omega$ denotes the deformation from current to reference configurations and σ denotes the Cauchy (or 'true') stress, which is over the deformed configuration, then the first Piola–Kirchhoff stress over the reference configuration (measuring the force per unit *un*deformed area) is given by $\mathcal{T} := \det(\nabla\rho)\sigma(\nabla\rho)^{-\top}$. The definition of the second Piola–Kirchhoff stress is typically motivated by wishing to work with a symmetric tensor [9, p. 439][46, p. 283][118, p. 219]:

$$\Sigma := \det(\nabla\rho)(\nabla\rho)^{-1}\sigma(\nabla\rho)^{-\top}.$$

Thus, viewing F^{-1} as an elastic deformation from physical to reference cell, then up to scale factor, the tensor Piola map (1.3.6) is formally equivalent to symmetrising the first Piola–Kirchhoff stress as above. Such guesswork may have been the historical origins of the transformation formulae (1.3.5)–(1.3.8).

[22] Identification of the tensor to which given Sobolev functions are proxy is useful for applying the correct notion of pullback, but for the purpose of standard finite element computations, in the end, the mesh is always a subset of standard Euclidean space, with one globally defined coordinate chart. To the author's knowledge, no existing FEM libraries allow for the coordinate-free construction of finite element spaces.

singular operator, the subspaces should satisfy the *kernel-capturing property*

$$\mathcal{N} = \sum_i (V_i \cap \mathcal{N}). \tag{1.6.14}$$

For an $H(\mathrm{div})$-based space V such as the AW stress space in the elasticity complex (1.2.23), one choice of relaxation method is given by the *vertex star iteration* [92], which is induced by the subspaces

$$V_i = \{v \in V \mid \mathrm{supp}(v) \subseteq K_i\}, \tag{1.6.15}$$

where K_i denotes the patch of cells in the mesh sharing vertex i. In abstract notation, given $v \in V$ with $\mathrm{div}\, v = 0$, where now $V = \Sigma_h$ denotes one of the canonical AW spaces, by exactness of the associated discrete complex when Ω is simply connected, we may write $\mathcal{C}\phi = v$ for some potential $\phi \in W$, where $(W, \mathcal{C}) = (Q_h, \mathrm{airy}_h)$. Let now $\{\phi_i\}_i$ denote a basis for W, and write $\phi = \sum_i c_i \phi_i$. Then a divergence-free decomposition of v is given by $v_i = c_i \mathcal{C}\phi_i$, since $v = \sum_i v_i$ and $v_i \in \mathcal{N}$ for each i, so it suffices to find subspaces V_i with $\mathcal{C}\phi_i \in V_i$ for each i. That the vertex star (1.6.15) fulfils this property follows from inspection of the basis functions of W.

Schöberl's hypotheses also require that the splitting (1.6.13) be stable in the V-norm and that the kernel splitting (1.6.14) be stable in the energy norm induced by the Galerkin projection of the coercive form, which does not follow automatically from the exactness of the discrete complex; typically, such bounds hold for the infinite-dimensional spaces, and hold also for the discrete complex if bounded commuting projections exist.

1.7 Multigrid for the Hellinger–Riessner system

To demonstrate the effectiveness of our mapping techniques in practical numerical simulations, it is necessary to consider preconditioners for the partial differential equations discretised by the AW elements, and to exhibit composability of our implementation with the associated software stack [131]. As indicated in the previous subsection, the application of patch-based multigrid smoothers is natural for the $H(\mathrm{div}; \mathbb{S})$-discretising elements we consider in this chapter.

Building on the work of Benzi and Olshanskii [37], Schöberl [169], and Hong et al. [115, 116] among others, Farrell and coauthors have successfully developed parameter- and mesh-robust preconditioners of augmented Lagrangian (AL) type, with specialised multigrid algorithms, for a host of nonlinear PDEs with saddle point

structure [86–88, 90–92, 135, 187]; we illustrate the AL method for AW elements. It consists of augmenting the Hellinger–Reissner Lagrangian (1.5.1) with a penalty term

$$\mathcal{H}_{h,\alpha}(\sigma, u) := \mathcal{H}_h(\sigma, u) + \frac{\alpha}{2}\int_\Omega \|\operatorname{div}_h \sigma - f\|^2 \, \mathrm{d}x \tag{1.7.1}$$

for $\alpha \geq 0$. The AL term penalises deviation from the set constrained by the momentum balance (1.2.7b), but does not change the exact solution. Its more significant benefit is that it allows the control of the Schur complement of the discretised system, as we now explain. The stationarity condition of the augmented energy (1.7.1) gives rise to a saddle point system for the stress-displacement pair, which, by a block factorisation, admits the well-known solution formula [36, Eq. 3.1]

$$\begin{pmatrix} A_\alpha & B^\top \\ B & \end{pmatrix}^{-1} = \begin{pmatrix} \mathbb{I} & -A_\alpha^{-1}B^\top \\ & \mathbb{I} \end{pmatrix} \begin{pmatrix} A_\alpha^{-1} & \\ & S_\alpha^{-1} \end{pmatrix} \begin{pmatrix} \mathbb{I} & \\ -BA_\alpha^{-1} & \mathbb{I} \end{pmatrix}, \tag{1.7.2}$$

where $A, B^\top, B$ are discrete compliance, symmetric gradient, and divergence operators respectively, $S = -BA^{-1}B^\top$ is the (in general, dense) Schur complement, and the subscript α denotes the same quantities but of the augmented system (so that $A_0 = A$ etc.). We wish to precondition this system for GMRES Krylov iterations. In analogy to the velocity-pressure Stokes problem, for which the Schur complement is spectrally equivalent to the viscosity-weighted pressure mass matrix [172], it can be shown (denoting by M_u the displacement mass matrix) that

$$\tilde{S}^{-1} := -\alpha M_u^{-1} \sim S_\alpha^{-1} \tag{1.7.3}$$

serves as an approximate inverse to the augmented Schur complement, at least for fixed mesh size, with the approximation improving as $\alpha \to \infty$. Preconditioning the Schur complement with (1.7.3) is however in tradeoff with the augmented stress solve A_α^{-1}; the AL term in A_α has a large kernel consisting of the infinite-dimensional affine space of tensor fields with divergence f, rendering standard multigrid relaxation schemes ineffective. We propose the vertex star relaxation as an α-robust multigrid algorithm for this block.

Remark 1.7.1. Both the AW^{c} and $\mathrm{AW}^{\mathrm{nc}}$ are non-nested under uniform refinement (in particular giving rise to non-nested bilinear forms); we employed the default prolongation operator of Firedrake, which involves (i) lossless projection of the coarse function onto a DG space of the same degree, (ii) lossless natural injection of the coarse projection, from the coarse grid to the fine DG space, (iii) projection from the fine DG space to the fine finite element space. Based on the success of the AL techniques described

in §1.7, we conjecture that multigrid convergence behaviour observed in §1.8 may be improved by the construction of specialised prolongation operators for each element which preserve, at least approximately, the kernel of the discrete divergence, in the style of [91, 92], this being the other component of the parameter-robust multigrid framework of Schöberl.

Remark 1.7.2. Let $\tau_h \in \mathrm{AW}^{\mathrm{c}}(K)$ denote a local AW^{c} basis function dual to a vertex DOF for a given cell K. Because all other nodes vanish at τ_h, its full normal component vanishes along each edge, and its components have vanishing mean. Since $\varepsilon(\operatorname{div}\tau_h)$ is a constant matrix,

$$\|\operatorname{div}\tau_h\|_{0,K} = \int_{\partial K} (\tau_h \mathbf{n}) \cdot (\operatorname{div}\tau_h)\,\mathrm{d}s - \int_K \tau_h : \varepsilon(\operatorname{div}\tau_h)\mathrm{d}x = 0; \tag{1.7.4}$$

thus, compared to $\mathrm{AW}^{\mathrm{nc}}$, the nodal AW^{c} basis functions arising from the 'extra' vertex DOFs contribute only to the divergence-free subspace. It follows that similar multigrid transfer operators may work well for both these elements.

1.8 Numerical examples

For the case of affine rather than Piola transformations, the inclusion of this theory into the Firedrake code stack was described in [132], and since this stack already understands Piola transformation the process is quite analogous. We must implement each new reference element in FIAT [129] and wrap it into FInAT [112]. The FInAT wrapper also requires a function to construct abstract syntax for the basis transformation in terms of callbacks provided by the form compiler to obtain symbols for geometric quantities such as Jacobians, and physical and reference normal and tangent vectors. The new elements must also be registered with UFL [1] and `tsfc` [113]. We now consider several test problems to validate our implementation and demonstrate its capabilities.

Linear systems in the manufactured solution examples, and on the coarsest grid in the multigrid examples, were solved by sparse LU factorisation with MUMPS [3] via PETSc [32].

1.8.1 Manufactured solutions

We now consider the canonical Hellinger–Reissner problem (1.5.2) and verify the convergence results proved by Arnold and Winther [24, Theorem 5.1][25, Theorem 4.1], summarised in Table 1.1. The approximation order m varies because in some

cases, higher-order convergence may be obtained if the exact solution pair admits improved Sobolev regularity.

Variable	AW^{c}	$\mathrm{AW}^{\mathrm{nc}}$
σ	$1 \leq m \leq 3$	1
$\operatorname{div}\sigma$	$0 \leq m \leq 2$	$0 \leq m \leq 2$
u	$1 \leq m \leq 2$	1

Table 1.1: Ranges of approximation order m by the AW elements of the elasticity variables in the L^2-norm.

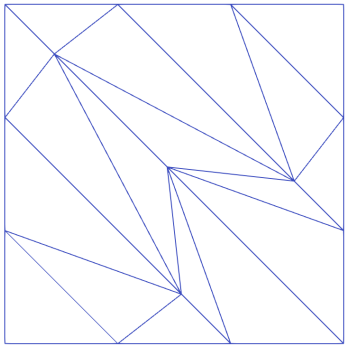


Figure 1.6: A warped mesh employed to check convergence under refinement.

On the unit square $\Omega = (0,1)^2$, we consider the displacement from Bramwell et al. [47]: $u(x,y) = (\sin(\pi x)\sin(\pi y), \sin(\pi x)\sin(\pi y))^\top$, which satisfies an unphysical homogeneous boundary condition, and the stress field

$$\sigma(x,y) = \begin{pmatrix} \cos(\pi x)\cos(3\pi y) & y + 2\cos(\frac{\pi}{2}x) \\ y + 2\cos(\frac{\pi}{2}x) & -\sin(3\pi x)\cos(2\pi x) \end{pmatrix}. \tag{1.8.1}$$

In order to show that the mapping techniques apply on general unstructured meshes, we perturb the interior vertices of the coarsest mesh as pictured in Figure 1.6; further refinements are obtained uniformly. In Tables 1.2 and 1.3, we check the experimental orders of convergence (EOCs) of $\mathrm{AW}^{\mathrm{nc}}$ in the L^2-norms in the incompressible limit $\nu \nearrow \frac{1}{2}$:

N	u error	u EOC	σ error	σ EOC	$\mathrm{div}_h(\sigma)$ error	$\mathrm{div}_h(\sigma)$ EOC
2^0	1.05×10^{-1}	–	5.51×10^{-1}	–	8.32×10^{-1}	–
2^1	2.78×10^{-2}	1.91	2.54×10^{-2}	1.12	2.68×10^{-1}	1.64
2^2	7.07×10^{-3}	1.98	1.18×10^{-1}	1.10	7.15×10^{-2}	1.91
2^3	1.77×10^{-3}	2.00	5.76×10^{-2}	1.04	1.82×10^{-2}	1.98
2^4	4.43×10^{-4}	2.00	2.85×10^{-2}	1.02	4.56×10^{-3}	1.99
2^5	1.11×10^{-4}	2.00	1.42×10^{-2}	1.00	1.14×10^{-3}	2.00

Table 1.2: Errors and convergence rates in the L^2-norms using $\mathrm{AW}^{\mathrm{nc}}$ for the model problem (1.5.2), with $\nu = 0.25, \mu = 1$. Here and below, N denotes the uniform refinement factor with respect to the original mesh.

N	u error	u EOC	σ error	σ EOC	$\mathrm{div}_h(\sigma)$ error	$\mathrm{div}_h(\sigma)$ EOC
2^0	1.05×10^{-1}	–	6.53×10^{-1}	–	8.32×10^{-1}	–
2^1	2.78×10^{-2}	1.91	3.07×10^{-1}	1.09	2.68×10^{-1}	1.64
2^2	7.05×10^{-3}	1.98	1.49×10^{-1}	1.04	7.15×10^{-2}	1.91
2^3	1.77×10^{-3}	2.00	7.38×10^{-2}	1.02	1.82×10^{-2}	1.98
2^4	4.42×10^{-4}	2.00	3.66×10^{-2}	1.01	4.56×10^{-3}	1.99
2^5	1.11×10^{-4}	2.00	1.83×10^{-2}	1.00	1.14×10^{-3}	2.00

Table 1.3: Errors and convergence rates with $\mathrm{AW}^{\mathrm{nc}}$ near the incompressible limit $\nu = 0.4999999, \mu = 1$.

Note that the observed order of convergence in the displacement is one higher than proved, but 2^{nd}-order convergence for the displacement is proved for the 3D analogue of $\mathrm{AW}^{\mathrm{nc}}$, the nonconforming Arnold–Awanou–Winther element [15], by applying a duality argument in the case of full elliptic regularity $(\sigma, u) \in H^1(\Omega; \mathbb{S}) \times H^2(\Omega; \mathbb{R}^d)$.

Tables 1.4–1.5 exhibit convergence behaviour of the AW^{c} element, applied to $u(x, y) = (-\mathrm{e}^{\sin(\frac{\pi}{2}y)}, 3\cos(\pi x))^\top$, and exact stress $\sigma = \mathbb{C}\varepsilon(u)$.

N	u error	u EOC	σ error	σ EOC	$\mathrm{div}(\sigma)$ error	$\mathrm{div}(\sigma)$ EOC
2^0	1.50×10^{-1}	–	1.16×10^{1}	–	1.47×10^{0}	–
2^1	3.81×10^{-2}	1.97	1.60×10^{-2}	2.85	3.75×10^{-1}	1.97
2^2	9.57×10^{-3}	1.99	2.09×10^{-3}	2.94	9.44×10^{-2}	1.99
2^3	2.40×10^{-3}	2.00	2.65×10^{-4}	2.98	2.36×10^{-2}	2.00
2^4	5.99×10^{-4}	2.00	3.34×10^{-5}	2.99	5.91×10^{-3}	2.00
2^5	1.50×10^{-4}	2.00	4.19×10^{-6}	3.00	1.48×10^{-3}	2.00

Table 1.4: Errors and convergence rates using AW^{c} with $\nu = 0.25, \mu = 1$.

N	u error	u EOC	σ error	σ EOC	div(σ) error	div(σ) EOC
2^0	1.49×10^{-1}	–	1.70×10^{-1}	–	1.47×10^{0}	–
2^1	3.81×10^{-2}	1.97	1.99×10^{-2}	3.09	3.75×10^{-1}	1.97
2^2	9.57×10^{-3}	1.99	2.31×10^{-3}	3.12	9.44×10^{-2}	1.99
2^3	2.40×10^{-3}	2.00	2.80×10^{-4}	3.05	2.36×10^{-2}	2.00
2^4	5.99×10^{-4}	2.00	3.46×10^{-5}	3.01	5.91×10^{-3}	2.00
2^5	1.50×10^{-4}	2.00	4.32×10^{-6}	3.00	1.48×10^{-3}	2.00

Table 1.5: AW^c near the incompressible limit $\nu = 0.4999999, \mu = 1$.

We manifestly see robustness in the incompressible regime for both elements. The comparative magnitudes of the errors show that the AW^c element provides a markedly more accurate approximation to the stress field. Note also that convergence behaviour in the divergence of the stress is the same for both elements, since their divergences have the same degree; this is also consistent with the 'extra' AW^c vertex basis functions being solenoidal as observed in Remark 1.7.2.

1.8.2 Li, 2018

Having validated both AW elements, we consider a more complex example, which moreover includes traction conditions, from the PhD thesis of Li [138, p. 111], who proposed and implemented the generalised Regge element which we shall study in §3. The domain, pictured in Figure 1.7, consists of the rectangle $\Omega = [0, 3] \times [0, 1]$ with three disks removed, occupied by a material assumed to be isotropic and homogeneous with $\nu = 0.2$ and Young's modulus $E = 10$:

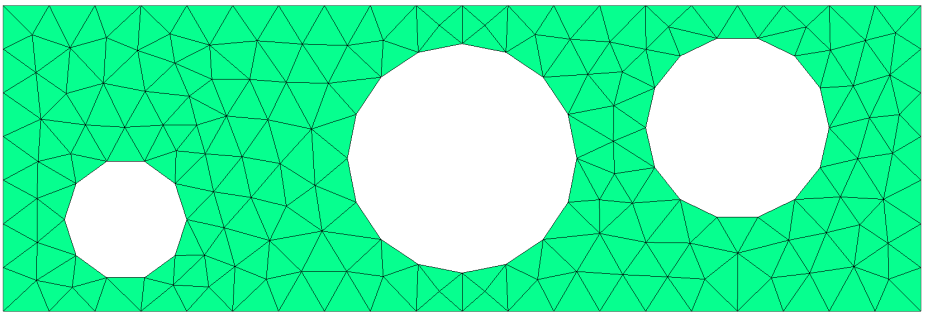


Figure 1.7: Domain with a coarser initial mesh than that employed in [138] so that multigrid may be performed.

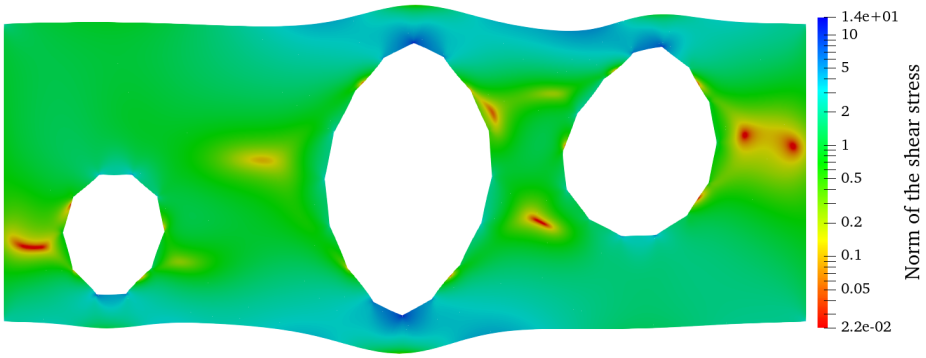


Figure 1.8: A traction-free condition, except at both ends.

The prescribed displacement is fixed $(0,0)^\top$ at the left-hand end and compressed $(-1,0)^\top$ at the right end, which together form Γ_D, with a stress-free condition $\sigma\mathbf{n} = 0$ on $\Gamma_N = \partial\Omega \setminus \Gamma_D$ given by the top, bottom, and the boundaries of the holes; there is no external force f. We combine the Nitsche and augmented Lagrangian penalties, seeking critical points (σ_h, u_h) of

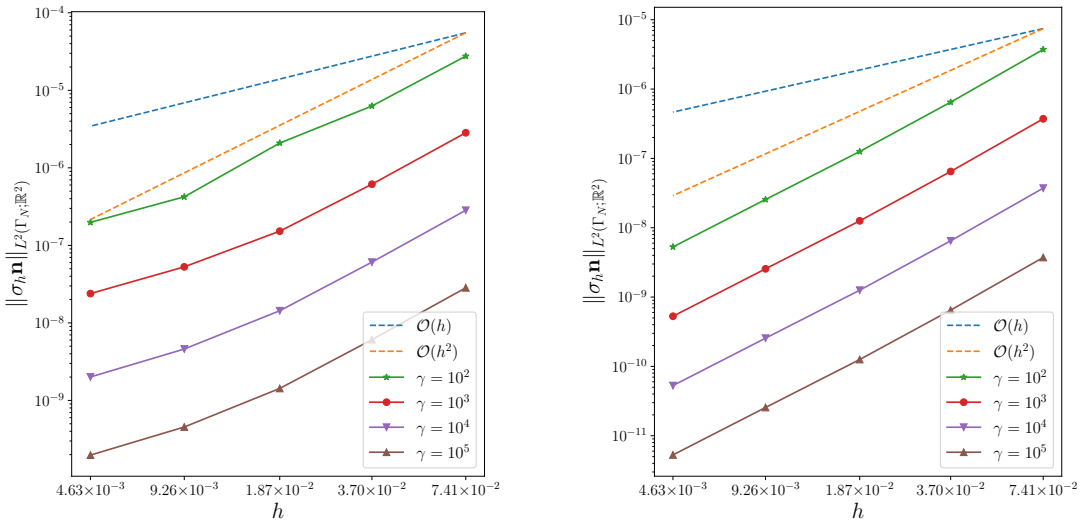
$$\mathcal{H}_{h,\gamma,\alpha}(\sigma_h, u_h) := \mathcal{H}_{h,\gamma}(\sigma_h, u_h) + \frac{\alpha}{2}\int_\Omega \|\operatorname{div}_h \sigma_h\|^2 \mathrm{d}x. \tag{1.8.2}$$

This was carried out with residual ℓ^2-norm tolerance 10^{-9} for the outermost Krylov iterations.[23] Table 1.6 exhibits the behaviour of GMRES for AW^c, with multigrid for the augmented stress block employing vertex star relaxation with Chebyshev smoother on each multigrid level, with fixed Nitsche and AL parameters $\gamma = 100, \alpha = 1$. We verify in Figure 1.8, which is coloured by the size of the shear stress $\|\operatorname{dev}\sigma_h\|$, that the AW^c solution on the finest mesh, with almost five million degrees of freedom, is free from numerical artifacts. Figure 1.9 shows convergence of the traction residual to zero in $L^2(\Gamma_N;\mathbb{R}^2)$ as $h \to 0$ using AW^c with $\alpha = 1$, and AW^{nc} (using LU factorisation) with $\alpha = 0$ respectively, for various values of the Nitsche parameter γ. Although we have proved convergence of the Nitsche penalty for any $\gamma \geq 1$, in practice we find the solver most effective at $\gamma = \mathcal{O}(100)$, and that increasing γ further will enforce the traction condition more strongly (if desired), at the cost of a more ill-conditioned system. Note that due to the equilibrium relation $\operatorname{div}\Sigma_h \subseteq V_h$ for both AW elements, the unpenalised AW method (1.5.2) will exactly enforce a divergence-free stress in the absence of an external force; this is no longer the case for the Nitsche scheme (1.5.6), but the divergence of the stress fields was found to be acceptably small even for $\alpha = \mathcal{O}(1)$.

[23] Due to the Nitsche boundary terms, which at time of writing cannot be treated with the `PCPATCH` [89] implementation of the vertex star relaxation, the application of the vertex star necessitated the use of `PCASM`.

N	DOFs	Krylov iterations
2^1	2.01×10^4	12
2^2	7.90×10^4	12
2^3	3.13×10^5	12
2^4	1.25×10^6	12
2^5	4.98×10^6	11

Table 1.6: Moderate and approximately constant outer Krylov iteration counts for the solution of (1.2.7) with the AW^c element, after preconditioning via the vertex star relaxation described in §1.6.2.



AW^c with $\alpha = 1$ AW^{nc} with $\alpha = 0$

Figure 1.9: Convergence to the traction-free condition in $L^2(\Gamma_N;\mathbb{R}^2)$ for the conforming and nonconforming AW elements, with and without AL penalisation respectively.

The observed order of convergence for the traction residual in Figure 1.9 is higher than that predicted by Proposition 1.5.2, which itself makes an artificial regularity assumption on the stress field, and which we therefore conjecture could be improved, for example via duality arguments.

Remark 1.8.1. The unpenalised Hodge Laplace problem (1.0.5) is ill-posed on the choice of Ω in Figure 1.7, which is not simply connected, implying nonexactness of the stress complex and nontriviality of the kernel of the HL operator, the *harmonic forms* $L^2(\Omega;\mathbb{R}^2)/(\operatorname{div} H_{\Gamma_N}(\operatorname{div};\mathbb{S})) \simeq \ker(\varepsilon; H^1_{\Gamma_D}(\Omega;\mathbb{R}^2))$; this is consistent with (unreported) divergent numerical results in the case $\gamma = \alpha = 0$. The Nitsche penalisation (1.5.5) thus has the incidental effect of regularising the problem to exclude this nullspace.

The conforming and nonconforming Arnold–Winther elements, with the modifications suggested by §1.4.3, were incorporated into the main branch of the publicly available Firedrake library as part of this work.[24][25]

[24]For reproducibility, the exact software versions used to generate the numerical results in this chapter are archived at https://zenodo.org/record/5596313 [191]; the code, and scripts for the associated plots, are available at https://bitbucket.org/FAznaran/piola-mapped.

[25]**Acknowledgements.** The author is grateful to Kaibo Hu for comments on §1.6.1, and to the two anonymous referees of [28] for their valuable suggestions.

Chapter 2

Application to linear irreversible thermodynamics

In the previous chapter, our emphasis was on abstract transformation theory and the broader goals of software automation and composability; the actual linear elastic PDE (1.2.7) solved was of importance, but decidedly classical. However, recall that one of our motivations was the fact that symmetric stress tensor fields often arise in continuum mechanics not only as variables of interest in their own right, but as coupling variables for other physical phenomena. We now demonstrate this in thorough detail by applying our stress element implementations to the nonlinear Onsager–Stefan–Maxwell (OSM) equations governing the molecular diffusion of single-phase multicomponent fluids, which we couple with compressible Stokes flow in stress-velocity-pressure form, in order to incorporate momentum into multicomponent flow in the steady state. The compressible Stokes system is essentially equivalent to the load Hodge Laplacian (1.0.5) in mixed weak form, by replacing the elastic displacement field with the fluid velocity and the full Cauchy stress with the viscous stress.

This chapter is structured as follows. In §2.1 we discuss the thermodynamic framework, the coupling, and relevant literature. In §2.2, we derive a novel variational formulation of the fully coupled nonlinear *Stokes–Onsager–Stefan–Maxwell* system, for which a linearisation is proposed and proved to be well-posed under physically reasonable assumptions in §2.3. We identify a structure-preserving discretisation of this linearisation in §2.4, and prove its convergence. The full scheme is validated numerically in §2.5, and illustrated with the simulation of the microfluidic mixing of

benzene and cyclohexane.[26]

2.1 Overview of the Stokes–Onsager–Stefan–Maxwell system

It is easy to motivate the numerical simulation of molecular diffusion due to its ubiquity as a mode of mass transport in physical processes on which we rely every day. If you are reading this on a portable device, then its LCD screen is powered by the energy differential occurring when lithium ions, migrating across a circuit in a manner described approximately by the OSM PDEs, undergo redox reactions at the anodes of battery cells. The broader field of battery electrochemistry plays an increasingly central role in modern concerns about the energy industry and the sustainability of major industrial processes. The same mathematical framework extended to incorporate thermodiffusive effects can be used to model the Haber–Bosch process for ammonia synthesis, the main enabler of fertiliser manufacture, which accounts for around 2% of all energy consumption worldwide [93]. Besides such well-known applications of molecular diffusion as battery electrochemistry and chemical reactor design, the OSM equations for multispecies transport which we will describe, and related models, also encompass phenomena ranging from the circulation of gaseous mixtures in the lungs [44] and the desalination of seawater [99], to the enrichment of weapons-grade uranium isotopes [142].

Despite the wide applicability of OSM-like systems in practical industrial applications, they do not frequently appear in the playgrounds of continuum mechanics in which most numerical analysis is traditionally done; consequently, in this chapter we are able (at least for our choice of formulation) to both ask and answer fundamental questions – concerning linearisations, well-posedness, Galerkin discretisation, error estimates, and even the correct choice of Sobolev space in which to take different fields – for the very first time.

2.1.1 Convection-diffusion in multicomponent flows

The fluids mentioned above in our motivations are all united in consisting of *mixtures* of multiple species. In many physical applications, such as the flow of air (and its many

[26] **Declaration.** The work of this chapter was done in collaboration with fellow DPhil candidate A. J. Van-Brunt, who is primarily responsible for the proof of Lemma 2.3.1 and the numerical code, plot generation, and (omitted) nondimensionalisation used for §2.5. The current author is primarily responsible for §2.2.1, the spaces and estimates introduced in §2.2.2, and the discussion concerning diagram (2.4.4); the rest is joint work.

constituents) over an aircraft wing, there is no special need to track the motions of each of these individual species. In this chapter, we are interested in scenarios where, on the contrary, it is important to resolve the motions of individual species, whose behaviour may in general greatly differ; we describe this situation as a *multicomponent flow*, where a fluid is composed of $n \geq 2$ distinct chemical species occupying a common thermodynamic phase.

We consider multicomponent flow in the *concentrated solution regime*, in contrast to the simpler and more well-known *dilute solution regime*. The dilute approximation describes mixtures for which a species known as the *solvent* (by convention assigned index $i = n$) whose concentration overwhelms that of all other $n - 1$ species, each of which is called a *solute*; for example, a classical problem in computational fluid dynamics (CFD) concerns the tracking of *tracers*, present in small proportions in a solvent by which they are convected. Thus, if $\Omega \subseteq \mathbb{R}^d, d \in \{2, 3\}$, denotes the medium across which the species are diffusing, the fluid density $\rho : \Omega \to \mathbb{R}$ is essentially independent of the solutes, and approximately coincides with the mass density of the pure solvent. This decouples the overall 'flow' (the material's bulk motion) from the *mass transport* (the motion of individual molecular constituents). One can thus solve for the pure bulk velocity field, and then use this simply as data to solve in parallel a system of independent advection-diffusion equations for the mass transport of each species. A typical dilute solution problem – which, we emphasise, we do *not* solve in this chapter – at low Mach number, so that the density ρ is assumed constant, is

$$\operatorname{div}(\rho u \otimes u) - \operatorname{div}(2\mu\varepsilon(u)) + \nabla p = \rho f, \tag{2.1.1a}$$

$$\operatorname{div} u = 0, \tag{2.1.1b}$$

$$\operatorname{div}(c_i u) + \operatorname{div} J_i = r_i, \qquad i = 1, \ldots, n-1, \tag{2.1.1c}$$

$$J_i = -D_i \nabla c_i, \quad i = 1, \ldots, n-1, \tag{2.1.1d}$$

where $u : \Omega \to \mathbb{R}^d$ is the flow velocity, $\mu > 0$ the shear viscosity, $p : \Omega \to \mathbb{R}$ the pressure, $f : \Omega \to \mathbb{R}^d$ the body acceleration induced within Ω due to the action of external fields, $c_i : \Omega \to \mathbb{R}$ the concentration of solute i in the solvent, $J_i : \Omega \to \mathbb{R}^d$ its diffusive flux, $r_i : \Omega \to \mathbb{R}$ its volumetric rate of generation or depletion, and $D_i > 0$ its Fickian diffusivity coefficient. The velocity $u_i : \Omega \to \mathbb{R}^d$ of each individual species is given by

$$u_i = u + \frac{J_i}{c_i}, \tag{2.1.2}$$

decomposing the transport of each species into a convective and a diffusive contribution. The dilute solution regime is characterised by the approximation $u \approx u_n$, i.e. that the bulk motion of the fluid coincides with the motion of the solvent.

This dilute solution approximation has been applied to great effect [39, 76, 78, 137], but fails for mixtures in which all of the species are present in comparable proportions. A number of issues arise when attempting to apply dilute solution models to concentrated solutions. For a start, the very notion of 'flow velocity' of the combined fluid becomes ambiguous, as the fluid's overall bulk motion need not coincide with any particular species velocity, and these species velocities may all be distinct in general. The fluid density is given by

$$\rho := \sum_{i=1}^{n} M_i c_i \tag{2.1.3}$$

in which $M_i > 0$ is the molar mass of species i. Using (2.1.2), the *species continuity equations* (2.1.1c) may be rephrased in terms of species velocities as

$$\operatorname{div}(c_i u_i) = r_i, \quad i = 1, \ldots, n. \tag{2.1.4}$$

The premise that homogeneous chemical reactions conserve atoms requires that $\sum_i M_i r_i = 0$; multiplying (2.1.4) by M_i and taking the sum over i thus gives

$$0 = \sum_i M_i(\operatorname{div}(c_i u_i) - r_i) = \operatorname{div}\left(\sum_i M_i c_i u_i\right). \tag{2.1.5}$$

This equation may be seen to be consistent with a more common understanding of mass continuity, however, because the canonical choice of flow velocity in the concentrated solution regime was identified by Hirschfelder et al. [111, p. 454] as the *mass-average velocity*

$$u = \sum_i \omega_i u_i, \tag{2.1.6}$$

a convex combination with coefficients the *mass fractions*

$$\omega_i := \frac{M_i c_i}{\rho}. \tag{2.1.7}$$

Rewriting (2.1.5) in terms of the mass-average velocity yields

$$\operatorname{div}(\rho u) = 0, \tag{2.1.8}$$

recovering the mass continuity equation familiar from fluid mechanics. In our formulation, we will solve for both the mass-average velocity and the individual species velocities.

A further issue to address in passing to the concentrated solution regime is the choice of constitutive law prescribing the relation between the thermodynamic forces

and their conjugate fluxes, whose pairwise products can be used to calculate the local entropy generation of the system. In dilute solutions, each solute interacts at a molecular level almost solely with solvent molecules, and so the diffusive solute fluxes J_i can each be modelled by Fick's law (2.1.1d) [94]. In the concentrated solution regime, even in the case of simple diffusion (meaning $u = 0$ uniformly), the diffusive flux of a given species can generally be driven by a concentration gradient of any other species in the solution, a phenomenon known as *cross-diffusion*. We therefore instead require a successor theory to Fick's which takes into account the cross-diffusion of all species. This will be the framework of linear irreversible thermodynamics pioneered by Onsager [156–158], which enables the thermodynamically consistent generalisation of Fick's law (2.1.1d) to the concentrated solution regime. This formalism is described in the next subsection.

2.1.2 Thermodynamic setting and the Onsager–Stefan–Maxwell system

In systems sufficiently close to thermodynamic equilibrium, Onsager's theory postulates a linear constitutive relation between thermodynamic forces and fluxes via

$$d_i = \sum_j \mathbf{M}_{ij} u_j, \quad i = 1, \dots, n, \tag{2.1.9}$$

where $d_i : \Omega \to \mathbb{R}^d$ denotes the *diffusional driving force* exerted by species i, conjugate to the species velocities $\{u_i\}_i$, and $\mathbf{M}$ is the Onsager transport coefficient matrix. The diffusion driving forces incorporate the effects of state variable gradients and external forces [101, Eq. (2.5.4)].

The Stefan–Maxwell system [146, 174] with which we will concretely specify the diffusive fluxes is given by the following constitutive law

$$d_i = \sum_{\substack{j=1 \\ j \neq i}}^{n} \frac{\mathcal{R} T c_i c_j}{\mathscr{D}_{ij} c_{\mathrm{T}}} (u_i - u_j), \tag{2.1.10}$$

where

$$c_{\mathrm{T}} := \sum_i c_i \tag{2.1.11}$$

denotes the total concentration, $\mathcal{R} > 0$ the ideal gas constant, $T > 0$ the absolute temperature, and the (experimentally measured) material parameter $\mathscr{D}_{ij}$ denotes the *Stefan–Maxwell diffusivity* of species i through species $j \neq i$. In the present discussion

we restrict attention to the case where every $\mathscr{D}_{ij}$ is constant, which in turn requires each to be positive [180].

The Stefan–Maxwell model preceded Onsager's theory, but was later reconciled with the latter in [139] by identifying

$$\mathbf{M}_{ij} = \begin{cases} -\frac{\mathcal{R}Tc_ic_j}{\mathscr{D}_{ij}c_T} & \text{if } i \neq j, \\ \sum_{k=1,k\neq i}^{n} \frac{\mathcal{R}Tc_ic_k}{\mathscr{D}_{ik}c_T} & \text{if } i = j. \end{cases} \tag{2.1.12}$$

Onsager's famous *reciprocal relations* [157] require symmetry of $\mathbf{M}$, which follows from the Stefan–Maxwell hypothesis $\mathscr{D}_{ij} = \mathscr{D}_{ji}$. The resulting *Onsager*–Stefan–Maxwell framework for isothermal but nonisobaric media postulates diffusion driving forces of the form [111][39, Eq. (24.1-8)]

$$d_i = -c_i\nabla\mu_i + \omega_i\nabla p, \tag{2.1.13}$$

where $\mu_i : \Omega \to \mathbb{R}$ is the chemical potential of species i. The chemical potential represents the partial derivative of the Gibbs free energy (a quantity describing the total amount of work a system can deliver to isothermal, isobaric surroundings) with respect to the number of moles of a given species i, and is related to the concentrations and pressure via a constitutive law, discussed below in §2.1.5.

An important aspect of the constitutive relation (2.1.9) is that dissipation should occur only as a result of *relative* motion between species, not their collective motion; if a fluid consists of n species collectively travelling at some high velocity, but which are in fact static relative to one another, then clearly no diffusion is occurring. Hence, the constitutive law (2.1.9) should be 'translation invariant at each point', i.e. invariant under replacing each u_i by $u_i - u^*$ for any choice of vector field $u^* \colon \Omega \to \mathbb{R}^d$; this is easily seen to be true of the Stefan–Maxwell law (2.1.10). This physically intuitive fact is incorporated into the spectrum of $\mathbf{M}$:

$$\sum_j \mathbf{M}_{ij} = 0, \qquad \text{i.e. } (1,\dots,1)^\top \in \ker(\mathbf{M}) \text{ a.e.} \tag{2.1.14}$$

Making such a shift in (2.1.9) by the mass-average velocity u, we have

$$d_i = \sum_j \mathbf{M}_{ij}\,(u_j - u)\,, \quad i = 1,\dots,n, \tag{2.1.15}$$

so that the transport matrix acts on terms proportional to the diffusive flux J_i. Thus, equation (2.1.9) can be understood as an implicit constitutive relation for the diffusive fluxes [51].

The nullspace (2.1.14) moreover implies the thermodynamically fundamental (isothermal, nonisobaric) *Gibbs–Duhem relation*

$$\sum_i d_i = 0, \tag{2.1.16}$$

which is naturally interpretable as a consequence of Newton's third law of motion, in that the net dissipative force exerted by all species upon each other should vanish.

Due to the nullspace (2.1.14), the OSM system is *a priori* ill-posed unless a choice of reference velocity is made, which one may think of as the convective velocity of the fluid which the species collectively occupy. While it is possible to fix such a choice by for example prescribing mass fluxes [180], we instead obtain a fuller description of the overall convection-diffusion transport process by solving also for the unknown reference velocity, for which we make the canonical choice of the convective velocity which is constrained to be the molar-mass-weighted species velocity in (2.1.6). We specify the compressible Stokes equations which it satisfies in the next subsection.

2.1.3 Stokes momentum balance

Motivated by the need for a reference velocity field to describe the convection of the fluid collectively occupied by multiple diffusing species, and which we take to be the mass-average velocity (2.1.6), we now describe the momentum balance which it satisfies, with which the OSM system (2.1.10) will be coupled.

Convection describes the bulk motion of a fluid subject to external body forces (incorporating prescribed velocity and traction conditions). In the stationary case, this is classically governed by the Cauchy equation

$$\operatorname{div}(\rho u \otimes u) - \operatorname{div}\tau + \nabla p = \rho f, \tag{2.1.17}$$

where $\tau : \Omega \to \mathbb{S}$ is the dissipative (viscous) stress tensor, to be specified with a constitutive law relating it to the strain rate, which we denote by E. If Newton's law of viscosity is used, then (2.1.17) reduces to the Navier–Stokes momentum equation (2.1.1a).

Compressible Newtonian fluids are, in the isothermal case, characterised by a Cauchy stress of the form [102, p. 337]

$$\sigma = \tau - p\mathbb{I}, \tag{2.1.18}$$

where the viscous stress is given by

$$\tau = 2\mu\left(E - \frac{\operatorname{tr}(E)}{d}\mathbb{I}\right) + \zeta \operatorname{tr}(E)\mathbb{I} = \mathbb{C}E, \tag{2.1.19}$$

where $\zeta > 0$ is the bulk viscosity, and the strain rate is given by the standard linearisation $E = \varepsilon(u)$. We write (2.1.19) equivalently as

$$\varepsilon(u) = \mathcal{A}\tau = \frac{1}{2\mu}\tau + \left(\frac{1}{d^2\zeta} - \frac{1}{2\mu d}\right)(\mathrm{tr}\tau)\mathbb{I}. \tag{2.1.20}$$

Here the elasticity tensor $\mathbb{C}$ (2.1.19) and compliance tensor $\mathcal{A}$ (2.1.20) are written with coefficients in terms of the Stokes parameters. We further consider steady-state creeping flow, under which assumptions Stokes' equation,

$$\mathrm{div}\,\tau - \nabla p = -\rho f, \tag{2.1.21}$$

follows from the momentum balance (2.1.17).

The Onsager constitutive equations (2.1.9) are written in *force-explicit* form: the equations express the driving forces explicitly, in terms of the species velocities (fluxes) as implicit variables. We choose also to write the Newtonian constitutive equation (2.1.19) in this manner, expressing the thermodynamic force (the linearised strain rate) in terms of the corresponding flux (the viscous stress) [111]. Typically in CFD, in analogy to the linear elasticity problem of the previous chapter, a flux-explicit formulation is obtained by using explicit rheology such as (2.1.19) to eliminate the Cauchy and viscous stresses in the first instance. For our overall coupled system (stated later in (2.1.29)), we do not eliminate the viscous stress, but include it as an implicit variable to be solved for. While this renders the resulting system more expensive overall, there are substantial benefits; the viscous stress plays a fundamental role in the calculation of local entropy production, but more significantly, we show in §2.2 that the resulting system of equations can be cast as a symmetric perturbed saddle point-like system, which is conducive to both abstract analysis and (we anticipate) efficient linear solvers.

2.1.4 Augmentation of the transport matrix and Stokes momentum balance

The variational formulation of our equations must enforce the relation (2.1.6), between the bulk (mass-average) velocity and the species velocities. We employ the augmentation approach introduced by Helfand [82, 100, 101, 107]; we augment each OSM equation (2.1.10) by adding the mass-average velocity constraint (2.1.6) to both sides with prefactor $\gamma > 0$:

$$d_i + \gamma\omega_i u = \sum_{j\neq i} \frac{\mathcal{R}Tc_ic_j}{\mathscr{D}_{ij}c_{\mathrm{T}}}(u_i - u_j) + \gamma\omega_i \sum_j \omega_j u_j. \tag{2.1.22}$$

Define the augmented transport matrix by

$$\mathbf{M}^{\gamma} := \mathbf{M} + \gamma(\omega_i)_{i=1}^{n} \otimes (\omega_j)_{j=1}^{n}, \tag{2.1.23}$$

so that (2.1.22) can be stated as $d_i + \gamma\omega_i u = \sum_{j\neq i} \mathbf{M}^{\gamma}_{ij} u_j$. In addition to the enforcement of the mass-average constraint by penalisation, this was motivated by the computation [180, Eq. 1.14–1.17]

$$\sum_{i,j} u_i \cdot \mathbf{M}^{\gamma}_{ij} u_j = \frac{1}{2} \sum_{j\neq i} \frac{\mathcal{R}Tc_i c_j}{\mathcal{D}_{ij} c_T} \|u_i - u_j\|^2 + \gamma \left\| \sum_j \omega_j u_j \right\|^2, \tag{2.1.24}$$

showing that the augmented transport matrix is symmetric positive definite, which allowed the work [180] to construct coercive bilinear forms for the pure Stefan–Maxwell diffusion problem.

The augmentation (2.1.22) modifies a constitutive law of the system, which will induce coercivity of a certain bilinear form below. However, this comes at the cost of symmetry of the eventual fully coupled system. To enforce symmetry, we add a 'dual' augmentation to the Stokes equation (2.1.21)

$$\operatorname{div} \tau - \nabla p = -\rho f + \gamma \sum_j \omega_j (u - u_j). \tag{2.1.25}$$

These augmentations are principally for thermodynamic structure-preservation; the transport matrix is *a priori* singular, but one can nevertheless recover the species velocities from the driving forces by coupling with the convective constraint (2.1.6). However, one is also 'rewarded' in that an important bilinear form defined later in (2.3.3a) will be both symmetric and coercive on an appropriate kernel. This greatly aids the continuous and discrete well-posedness analyses, as we demonstrate in §2.3.2 and §2.4.1.

2.1.5 The chemical potential and the thermodynamic equation of state

In an ideal gas, intermolecular forces can be neglected, for example between the solutes in the dilute solution regime; the thermodynamic constitutive laws relating pressure, concentrations, chemical potentials, and temperature have a particularly simple mathematical form.

Our variational formulation will solve for the chemical potential μ_i of each species i. This has several advantages. First, this allows for a general formula for the diffusion driving forces (2.1.13), independent of the materials considered. The concentrations

c_i are typically the quantities of practical interest; if we were to make the (perhaps more obvious) choice of solving for the c_i as the primary variables instead, the form of the diffusion driving forces would change in a material-dependent manner. Second, our choice allows for a decoupling in the linearisation we employ: the primary mixed system to solve only depends on the material via the diffusion coefficients and viscosities, with any non-ideality confined to the computation of concentrations and density postprocessed at every iteration using material-dependent thermodynamic constitutive relations discussed below. Third, together with the choice to solve for the viscous stress as described in §2.1.3, this decoupling endows the equations to solve with a symmetric perturbed saddle point-like structure.[27]

Generally each species concentration c_i can be inferred from $\{\mu_i\}_{i=1}^n$ and p, given thermodynamically consistent constitutive laws for the chemical potential, and the equation of state. Within an isothermal ideal gas, this relation is given by

$$c_i = \frac{p^\ominus}{\mathcal{R}T} \exp\left(\frac{\mu_i - \mu_i^\ominus}{\mathcal{R}T}\right), \tag{2.1.26}$$

for some known reference pressure $p^\ominus$ and a set of reference chemical potentials $\{\mu_i^\ominus\}_i$. A general relation for non-ideal systems is

$$\mu_i = \mu_i^\ominus + \mathcal{R}T \ln(\gamma_i x_i), \tag{2.1.27}$$

where $x_i := c_i/c_\mathrm{T}$ is the *mole fraction*, and γ_i the *activity coefficient*, of species i. To obtain the concentrations, an additional equation of state for the system as a whole is required, which may be expressed in volumetric form as

$$c_\mathrm{T} = \frac{1}{\sum_i V_i x_i}, \tag{2.1.28}$$

in which $V_i > 0$ is the *partial molar volume* of species i. Formally, the partial molar volume is the change in total fluid volume with respect to the number of moles of a species i at constant temperature and pressure.

Our linearisation below is such that the concentrations, and the density (2.1.3) and mass fractions (2.1.7) which depend on them, are postprocessed from the chemical potentials and pressure within each nonlinear iteration. This trivially guarantees positivity of concentrations, but more significantly, the model is able to incorporate non-ideality by employing constitutive laws more general than (2.1.26), such

[27] Very extensive (but unreported) investigations into alternative tuples of fields for which to solve, and ways to weakly formulate the resulting fully coupled system, gave rise to ill-posed or analytically intractable Picard linearisations when the concentrations c_i, or their normalisations the mole fractions x_i, were solved for as primary unknowns.

as (2.1.27). We intend for this choice to facilitate future research into convection-diffusion problems with alternative equations of state, for which c_i may (for example) depend on *all* μ_j, and on temperature.

2.1.6 Coupled problem statement

Our goal is to find and analyse a variational formulation and structure-preserving finite element discretisation of the following problem: given data f and $\{r_i\}_{i=1}^n$, find chemical potentials $\{\mu_i\}_{i=1}^n$, viscous stress τ, pressure p, species velocities $\{u_i\}_{i=1}^n$, and convective velocity u satisfying

$$-c_i\nabla\mu_i + \omega_i\nabla p + \gamma\omega_i u = \sum_j \mathbf{M}_{ij}^{\gamma} u_j \ \forall i, \quad (\textit{augmented OSM equations}) \tag{2.1.29a}$$

$$\mathcal{A}\tau = \varepsilon(u), \quad (\textit{viscous stress constitutive law}) \tag{2.1.29b}$$

$$\operatorname{div}\tau - \nabla p - \gamma\sum_j \omega_j(u - u_j) = -\rho f, \quad (\textit{augmented Stokes momentum balance}) \tag{2.1.29c}$$

$$\operatorname{div}(c_i u_i) = r_i \ \forall i, \quad (\textit{species continuity}) \tag{2.1.29d}$$

$$\operatorname{div}\left(u - \sum_j \omega_j u_j\right) = 0, \quad (\textit{mass-average velocity constraint}) \tag{2.1.29e}$$

for an augmentation parameter $\gamma \geq 0$, where $\{c_i, \omega_i\}_{i=1}^n, \rho$ are functions of the unknowns via chemical potential constitutive laws such as (2.1.27) and (2.1.28) and algebraic relations (2.1.3), (2.1.7). We shall introduce appropriate boundary conditions in (2.2.2). We call the system (2.1.29) the (augmented) *Stokes–Onsager–Stefan–Maxwell* (SOSM) system. When the convection term $\operatorname{div}(\rho u \otimes u)$ is incorporated into (2.1.29c), we call this the *Navier–Stokes–Onsager–Stefan–Maxwell* (NSOSM) system.

Note that in the system we only directly enforce the *divergence* of the mass-average velocity constraint (2.1.29e), which may be interpreted as the compressible generalisation of the standard divergence constraint (2.1.1b); this choice gives rise to a saddle point-like structure, as we show in the next section. Nevertheless, the full constraint (2.1.6) is incorporated via the augmentations (2.1.22) and (2.1.25), as discussed further in Remark 2.2.1. This constraint reduction, combined with the augmentations, may be regarded as the main novelty of the system (2.1.29).

2.1.7 Relation to existing numerical literature

For dilute solutions with constant solvent concentration (and no volumetric generation or the depletion of the solvent, $r_n = 0$), the (N)SOSM equations reduce to the incompressible (Navier–)Stokes equations, as well as convection-diffusion equations constituted by Fick's law for each solute. These are standard workhorses of CFD; for an overview of their extensive existing numerical analysis, see [81, 126, 176, 179]. In this regime, the momentum solve and the equation for the transport of concentration are decoupled using incompressibility.

Our formulation (2.1.29) solves for the viscous stress as an unknown variable. Of most relevance to this aspect of our approach is the work [60], which solves the stress-velocity Stokes system, in the incompressible limit but using Carstensen's alternative implementation, described in the previous chapter, of the Arnold–Winther stress elements which we shall use.

Numerical methods for solving the NSOSM equations have received much less attention. The only works of which we are aware are those of Ern, Giovangigli, and coauthors, including a monograph [82] and a series of other works [83–85, 101] which apply multicomponent transport to combustion modelling for ideal gas mixtures. These schemes use sophisticated finite difference methods, with the important exception of reference [85], which uses a finite element method with additional least-squares terms to stabilise the formulation. We are unaware of any literature that addresses numerical methods for SOSM or NSOSM systems in the non-ideal case.

For OSM models of isobaric ideal gases under simple diffusion, there has been slightly more work addressing numerical approaches; these include a finite element method proposed by McLeod & Bourgault [147], a finite volume method by Cancés et al. [55], and a finite difference scheme by Bondesan et al. [41]. Such works typically employ a reference velocity as prescribed data.

In particular, structure-preserving mixed FEM for the purely diffusional OSM subsystem for an ideal phase was recently developed in [180]. This approach solved the augmented OSM equations (2.1.22) combined with the species continuity equations (2.1.29d). We build on this work by incorporating momentum, non-ideality, and pressure-driven diffusion. In contrast to this prior work, we are able to avoid a generalised saddle point formulation, and in §2.3 will derive a symmetric perturbed saddle point system to be solved at each nonlinear iteration, a far more classical linear algebraic structure for which many solvers have been proposed [36]. However, due to our more complex form of driving force (2.1.13), and since we do not solve directly

for the species concentrations (to allow for non-ideality), we are not able to enforce the Gibbs–Duhem relation (2.1.16) to machine precision, as achieved in [180].

Remark 2.1.1. We shall repeatedly emphasise the utility of the positive semidefinite structure of the diffusion matrix (2.1.9) for the analysis, which motivates the augmented Lagrangian-type approach described in §2.1.4, and lies in contrast to many other cross-diffusion systems, for example describing multiagent systems in mathematical biology [57], which admit a formal gradient flow structure associated with an entropy (or *free energy*) functional; Although the Stefan–Maxwell system admits an associated thermodynamic energy, the *Gibbs free energy*, we are not able to show equivalence of the (S)OSM system to the Euler–Lagrange stationarity condition of any energy or Lagrangian functional, and hence cannot exploit any gradient flow structure. With our augmentations of the equations, the Picard scheme we propose below in §2.3 nevertheless gives rise to symmetric linearised problems to solve at each nonlinear iteration.

2.2 Variational formulation

2.2.1 Pressure regularity in the stress complex

In the isobaric, isothermal, purely diffusional problems originally considered by Stefan [174] and Maxwell [146], it was sufficient to work with driving forces

$$d_i = -\mathcal{R}T\nabla c_i. \tag{2.2.1}$$

In our nonisobaric setting, we recall that the OSM framework gives rise to driving forces (2.1.13) of the form

$$d_i = -c_i\nabla\mu_i + \omega_i\nabla p. \tag{2.2.2}$$

We wish to derive a variational formulation of the problem. That ω_i is spatially varying makes equation (2.2.2) difficult to integrate by parts when tested against a test function; formally, one may 'absorb' ω_i into a species velocity test function v (omitting surface terms for simplicity),

$$\int_\Omega v\cdot(\omega\nabla p)\,\mathrm{d}x = -\int_\Omega \operatorname{div}(v\omega_i)p\,\mathrm{d}x = -\int_\Omega(\omega_i\operatorname{div}v + v\cdot\nabla\omega_i)p\,\mathrm{d}x, \tag{2.2.3}$$

suggesting v be taken from a space containing at most $H(\mathrm{div})$; however, seeking species velocities only in $L^2(\Omega;\mathbb{R}^d)$ is at least consistent with the analysis of [180] in exploiting the coercivity with respect to $\|\cdot\|_0$ of the form induced by the augmented Onsager transport matrix, as in (2.1.24).

In order to rigorously incorporate the effect of pressure-driven diffusion, the analyst is therefore forced to leave at least the latter term of (2.2.2) untouched and instead consider the rather unorthodox possibility of formulating the Stokes subproblem with pressure lying in $H^1(\Omega)$. Looking back at the Stokes system, typically such a fact may be available in the form of elliptic regularity results for the pressure field, but to the author's knowledge, the *a priori* square-integrability of pressure gradients (i.e. for which, we emphasise, pressure is *defined* to lie in $H^1(\Omega)$) has not been considered for the Stokes system, except at the discrete level for the *in*compressible case in [175].

This condition is also suggested naturally in the ideal subcase of pure Stefan–Maxwell diffusion for nonisobaric gases, for which the driving forces are

$$d_i = -\mathcal{R}T\nabla c_i + \omega_i \nabla p, \tag{2.2.4}$$

which suggests considering each c_i (and hence c_T) to lie in $H^1(\Omega)$, forcing pressure to lie in at least the same space due to the ideal equation of state $p = c_T \mathcal{R}T$.

In general, one must distinguish between the *thermodynamic* pressure p which we use throughout this chapter, and the *mechanical* pressure $p_m := -\frac{\operatorname{tr}\sigma}{d}$, where the latter is related to the spherical Cauchy stress by $\operatorname{sph}\sigma = \frac{\operatorname{tr}\sigma}{d}\mathbb{I} = -p_m\mathbb{I}$, and to p by

$$p = p_m + \zeta \operatorname{div} u. \tag{2.2.5}$$

(In the context of multicomponent flow, this decomposition is discussed in further detail by Bothe & Dreyer [42].) Since no formulation of the compressible Stokes equations (or different formulations, corresponding to different Hodge Laplacians, of the linear elasticity problem) seek displacement with regularity greater than $H^1(\Omega)$, we see that none of the three terms in (2.2.5) need lie in $H^1(\Omega)$ *a priori*. One is therefore tempted to delete the offending term in (2.2.5) by passing to the incompressible limit, so that thermodynamic and mechanical pressures coincide. In this simpler setting (for which the pressure solves a Poisson-like problem, again readily amenable to elliptic regularity results), we still cannot expect any *a priori* extra regularity of $\nabla p = \nabla p_m = -\operatorname{div}(\operatorname{sph}\sigma)$ because $H(\operatorname{div};\mathbb{S})$ is not closed under taking spherical parts.[28] This suggests a mild incompatibility between the standard deviatoric-spherical decomposition of the Cauchy stress (whose physical relevance

[28] In any case, the incompressible regime, for which ρ is constant, is physically irrelevant to the OSM framework for mass diffusion which in particular implies spatial heterogeneity of the density.

we emphasised in §1.2.2) and its Hodge decomposition.[29] More precisely, viewing pressure as a component of the full Cauchy stress, then provided that Ω is simply connected, the Hodge decomposition of the base stress space [12, Theorem 4.5]

$$L^2(\Omega;\mathbb{S}) = \varepsilon H^1_0(\Omega;\mathbb{R}^d) \oplus_{L^2} \begin{cases} \operatorname{airy} H^2(\Omega), & d=2, \\ \operatorname{inc} H^2(\Omega;\mathbb{S}), & d=3, \end{cases} \tag{2.2.6}$$

does not endow that component with any extra regularity.[30]

Consequently, we do not take $p \in H^1(\Omega)$ but as a compromise consider the weaker condition defined by the combined viscous stress-pressure space

$$\{(\tau,p) \in L^2(\Omega;\mathbb{S}) \times L^2(\Omega) \mid \operatorname{div}\tau - \nabla p \in L^2(\Omega;\mathbb{R}^d)\} \left(\supsetneq H(\operatorname{div};\mathbb{S}) \times H^1(\Omega)\right), \tag{2.2.7}$$

and assign to it the weaker norm $\|\tau\|_0^2 + \|p\|_0^2 + \|\operatorname{div}\tau - \nabla p\|_0^2$. This space and norm were previously employed by Manouzi & Farhloul in an analysis of monotonically-constituted incompressible Stokes flow [144], for which τ is simply the shear stress $\operatorname{dev}\sigma$. Membership of (2.2.7) is naturally interpretable as the square-integrability of the divergence of the full Cauchy stress, i.e. that $\sigma = \tau - p\mathbb{I} \in H(\operatorname{div};\mathbb{S})$. Together with an analogous condition for the chemical potential gradient to be detailed next in §2.2.2, this weaker condition will account for the pressure gradient in the driving forces.[31]

2.2.2 Fully coupled nonlinear variational formulation

In this subsection, we derive a variational formulation for the stationary problem as a nonlinear perturbed saddle point-like system. We have found the following statement of the problem to be a feasible tradeoff between the (often competing) goals of: physical relevance of variables, physical realism of boundary data, regularity assumptions, numerical implementability and effectiveness, analytic tractability of

[29] Moreover, it is heuristically clear that there can be no formulation of the stress-velocity-pressure Stokes problem which gives $p \in H^1(\Omega)$ and is well-posed; alternative well-posed formulations may be formally derived from each other, trading regularities between different fields via integration by parts. Since both the mixed-dual (Cauchy stress $\in H(\operatorname{div};\mathbb{S})$, velocity $\in L^2(\Omega;\mathbb{R}^d)$, pressure $\in L^2(\Omega)$) and mixed-primal (Cauchy stress $\in L^2(\Omega;\mathbb{S})$, velocity $\in H^1(\Omega;\mathbb{R}^d)$, pressure $\in L^2(\Omega)$) formulations are well-posed, it is not clear what 'price we must pay' to obtain $p \in H^1(\Omega)$.

[30] For the domain stress space, this decomposition becomes (for example in 2D) $H(\operatorname{div};\mathbb{S}) = \operatorname{airy} H^2(\Omega) \oplus_{L^2} \left(\varepsilon H^1_0(\Omega;\mathbb{R}^2) \cap H(\operatorname{div};\mathbb{S})\right)$; functions in this right-hand summand may be taken from $\varepsilon(H^2 \cap H^1_0)(\Omega;\mathbb{R}^2)$, but (again) only in the case of elliptic regularity for the operator $-\operatorname{div}\circ\varepsilon$.

[31] One alternative approach is provided by attempting to construct a smoother analogue of the stress elasticity complex associated with the Cauchy stress space (2.2.7), for which equation (2.2.7) is replaced by some superspace of $H(\operatorname{div};\mathbb{S}) \times H^1(\Omega)$, just as the Stokes complex is precisely a smoothing of the de Rham complex, but we do not pursue this here.

continuous and discrete well-posedness, enforcement of fundamental thermodynamic relations and constraints, and extensibility to the transient, anisothermal, and non-ideal settings.

We use the notation $\tilde{q} = \{q_i\}_{i=1}^n$ to denote an n-tuple of functions. For boundary data, let $\Gamma = \partial\Omega$. We prescribe mass flux and molar fluxes:

$$\rho u = g_{\mathrm{u}} \in H^{1/2}(\Gamma_N; \mathbb{R}^d) \text{ on } \Gamma, \tag{2.2.8a}$$

$$c_i u_i \cdot \mathbf{n} = g_i \in H^{-1/2}(\Gamma) \qquad \text{on } \Gamma, \quad i = 1, \dots, n. \tag{2.2.8b}$$

For consistency with the mass-average velocity constraint (2.1.6), we require the compatibility condition

$$\sum_i M_i g_i = g_{\mathrm{u}} \cdot \mathbf{n}, \tag{2.2.9}$$

with equality in $H^{-1/2}(\Gamma)$. We impose the further conditions

$$\int_\Omega p \, \mathrm{d}x = \int_\Omega \mu_i \, \mathrm{d}x = 0, \quad i = 1, \dots, n. \tag{2.2.10}$$

Typically, the equation of state will require or imply strict positivity of p everywhere, in which case this condition should be understood as $⨍_\Omega p \, \mathrm{d}x = p^\ominus > 0$ and that p be shifted by the known value $p^\ominus$ as a postprocessing step.

Let $Q = L^2(\Omega; \mathbb{R}^d)^n \times L^2(\Omega; \mathbb{R}^d)$ with norm $\|(\tilde{v}, v)\|_Q^2 := \|\tilde{v}\|_0^2 + \|v\|_0^2$. For formal derivation of the weak form, we assume the solution tuple $(\tilde{\mu}, \tau, p, \tilde{v}, v)$ to be smooth on $\overline{\Omega}$. Consider choosing $(\tilde{w}, s, q)$ from the *solution-dependent* potential-stress-pressure test space

$$\Theta := \left\{ (\tilde{w}, s, q) \in L_0^2(\Omega)^n \times L^2(\Omega; \mathbb{S}) \times L_0^2(\Omega) \;\middle|\; \begin{array}{c} \operatorname{div} s - \nabla q \in L^2(\Omega; \mathbb{R}^d), \\ -c_i \nabla w_i + \omega_i \nabla q \in L^2(\Omega; \mathbb{R}^d) \ \forall i \end{array} \right\}. \tag{2.2.11}$$

Here it is understood that the $\{c_i, \omega_i\}_i$ are computed from the solution tuple. Multiplying the i^{th} continuity equation (2.1.29d) by w_i, the divergence of the mass-average velocity constraint (2.1.29e) by q, and contracting the stress constitutive law (2.1.29b) with s, we obtain

$$\sum_i \left(\operatorname{div}(c_i u_i) - r_i\right) w_i + \operatorname{div}\left(u - \sum_i \omega_i u_i\right) q + (\mathcal{A}\tau - \varepsilon(u)) : s = 0, \tag{2.2.12}$$

and hence

$$\int_\Omega \sum_i (\operatorname{div}(c_i u_i) w_i - \operatorname{div}(\omega_i u_i) q) + \mathcal{A}\tau : s - (s - q\mathbb{I}) : \varepsilon(u) \, \mathrm{d}x = \int_\Omega \sum_i r_i w_i \, \mathrm{d}x. \tag{2.2.13}$$

Integrating by parts yields

$$\begin{aligned}\int_\Omega \mathcal{A}\tau : s + \sum_i (-c_i \nabla w_i + \omega_i \nabla q) \cdot u_i + (\operatorname{div} s - \nabla q) \cdot u \, \mathrm{d}x \\ = \langle (s - q\mathbb{I})\mathbf{n}, u \rangle_\Gamma + \sum_i \left\langle c_i u_i \cdot \mathbf{n}, -w_i + \frac{\omega_i}{c_i} q \right\rangle_\Gamma + \int_\Omega \tilde{r} \cdot \tilde{w} \, \mathrm{d}x \\ = \left\langle (s - q\mathbb{I})\mathbf{n}, \frac{g_u}{\rho} \right\rangle_\Gamma + \sum_i \left\langle g_i, -w_i + \frac{M_i}{\rho} q \right\rangle_\Gamma + \int_\Omega \tilde{r} \cdot \tilde{w} \, \mathrm{d}x.\end{aligned} \tag{2.2.14}$$

Now for each i, we take the scalar product of $v_i \in L^2(\Omega; \mathbb{R}^d)$ with the augmented OSM equation (2.1.29a), and integrate over Ω to obtain

$$\int_\Omega (-c_i \nabla \mu_i + \omega_i \nabla p) \cdot v_i - v_i \cdot \sum_j \mathbf{M}_{ij} u_j - \gamma \omega_i \sum_j \omega_j (u_j - u) \cdot v_i \, \mathrm{d}x = 0. \tag{2.2.15}$$

Taking the inner product of the augmented Cauchy momentum balance (2.1.29c) with $v \in L^2(\Omega; \mathbb{R}^d)$ yields

$$\int_\Omega (\operatorname{div} \tau - \nabla p) \cdot v - \gamma \left(\sum_j \omega_j (u - u_j) \right) \cdot v \, \mathrm{d}x = - \int_\Omega \rho f \cdot v \, \mathrm{d}x. \tag{2.2.16}$$

We sum equation (2.2.15) over i and add equation (2.2.16) to derive

$$\begin{aligned}\int_\Omega \sum_i (-c_i \nabla \mu_i + \omega_i \nabla p) \cdot v_i + (\operatorname{div} \tau - \nabla p) \cdot v \\ - \sum_{i,j} v_i \cdot \mathbf{M}_{ij} u_j - \gamma \left(\sum_i \omega_i (u_i - u) \right) \cdot \left(\sum_j \omega_j (v_j - v) \right) \, \mathrm{d}x = \int_\Omega -\rho f \cdot v \, \mathrm{d}x.\end{aligned} \tag{2.2.17}$$

Note that both augmentations (2.1.22) and (2.1.25) were involved in deriving this expression.

Finally, we observe that by definition we have $\omega_i \in L^\infty(\Omega)$ with $\|\omega_i\|_{L^\infty(\Omega)} \leq 1$. Moreover, we make the physically reasonable assumptions that the concentrations associated with the solution are uniformly bounded, $c_i \in L^\infty(\Omega)$, with $c_i \geq \kappa > 0$ a.e., as in [180] (which in turn implies $\mathbf{M}_{ij}^\gamma, \rho \in L^\infty(\Omega)$, and $\rho \geq \kappa \sum_i M_i > 0$ a.e.), and that the density gradient is uniformly bounded, $\nabla \rho \in L^\infty(\Omega; \mathbb{R}^d)$.[32]

Definition 2.2.1. (Weak solution to the SOSM equations). We define a *weak solution to the augmented Stokes–Onsager–Stefan–Maxwell system* to be a $(2n+3)$-tuple

$$(\{\mu_i\}_{i=1}^n, \tau, p, \{u_i\}_{i=1}^n, u) \in L_0^2(\Omega)^n \times L^2(\Omega; \mathbb{S}) \times L_0^2(\Omega) \times \underbrace{L^2(\Omega; \mathbb{R}^d)^n \times L^2(\Omega; \mathbb{R}^d)}_{Q} \tag{2.2.18}$$

[32] A comparable condition, that $\rho \in (H^1 \cap W^{1,\infty})(\Omega)$ is bounded below with $\frac{\nabla \rho}{\rho} \in L^\infty(\Omega; \mathbb{R}^d)$, was used to analyse a compressible Stokes flow in [62].

inducing concentrations $\{c_i\}_{i=1}^n$ through a constitutive law (such as (2.1.26)) implicitly defining $c_i = c_i(\{\mu_i\}_{i=1}^n, p) \geq \kappa > 0$ a.e. for $i = 1, \ldots, n$, such that

$$\|c_i\|_{L^\infty(\Omega)} < \infty, \ i = 1, \ldots, n, \tag{2.2.19a}$$

$$\|\nabla \rho\|_{L^\infty(\Omega;\mathbb{R}^d)} < \infty, \tag{2.2.19b}$$

$$\|\operatorname{div} \tau - \nabla p\|_0^2 < \infty, \tag{2.2.19c}$$

$$\| - c_i \nabla \mu_i + \omega_i \nabla p\|_0^2 < \infty, \ i = 1, \ldots, n, \tag{2.2.19d}$$

and satisfying (2.2.14), (2.2.17) for all test tuples $(\{w_i\}_{i=1}^n, s, q, \{v_i\}_{i=1}^n, v) \in \Theta \times Q$, where Θ is defined in (2.2.11).

Observe that the solution tuple does not reside in any standard Sobolev space, but that the regularity assumptions placed on the solution tuple and test spaces ensure that the surface terms in (2.2.14) are well-defined. Recall that condition (2.2.19c) is the square-integrability of the Cauchy stress σ (as in [144]). The nonlinear integrability condition (2.2.19d) is to our knowledge a novel requirement, but also has a natural interpretation, namely the square-integrability of the diffusion driving forces:[33]

$$d_i \in L^2(\Omega; \mathbb{R}^d). \tag{2.2.20}$$

Moreover, we emphasise that this unorthodox formulation allows the rigorous incorporation of pressure diffusion via the pressure gradient on the left side of (2.1.29a), despite the fact that the pressure field is not *a priori* H^1-regular in the Stokes subsystem. Later in §2.5 we observe convergence of the diffusion driving forces in $\|\cdot\|_0$ and of the pressure in $\|\cdot\|_1$, but otherwise leave this consideration, and further investigation into the yet more subtle question of the optimal nonlinear formulation of the SOSM system, as intriguing open questions.

Remark 2.2.1. In the derivation of (2.2.12), we used the distributional divergence of the mass-average velocity constraint (2.1.29e), which ignores the curl component in the Helmholtz decomposition of the mass-average velocity relationship (2.1.6). This choice ensures that the number of equations matches the number of unknown variables, and the full constraint is nevertheless incorporated via the augmentations (2.1.22) and (2.1.25).

[33] We conjecture that one could alternatively derive a formulation of the SOSM system dual to ours which takes $d_i \in L^2(\Omega; \mathbb{R}^d)$ as a primary unknown. We also conjecture that the integrability assumptions in Definition 2.2.1 could potentially be relaxed, for example via Sobolev embeddings.

2.3 Linearisation and well-posedness

2.3.1 Generalised Picard scheme

In this section we derive a variational formulation of a generalised Picard linearisation. Given a previous estimate for the potentials $\tilde{\mu}^k$ and pressure p^k for $k \geq 0$, we regard these as fixed quantities which determine the concentrations $\tilde{c}^k$ via chemical potential constitutive laws and an appropriate equation of state such as (2.1.26). This in turn determines the density ρ^k, mass fractions $\tilde{\omega}^k$, total concentration c_{T}^k, and transport matrix $\mathbf{M}^k$ defined via (2.1.3), (2.1.7), (2.1.11), and (2.1.12), respectively. We then construct a linear system to solve for the next iterate $((\tilde{\mu}^{k+1}, \tau^{k+1}, p^{k+1}), (\tilde{u}^{k+1}, u^{k+1}))$. The heuristic behind this update strategy is that the gradients of chemical potential, pressure, and mass-average velocity primarily drive the dynamics of multicomponent flow; the role of the species concentrations is mostly confined to the effect of altering the drag coefficients in the transport matrix. We make the following physically reasonable assumptions about each iterate, in analogy to Definition 2.2.1.

Assumption 2.3.1. (Uniform positivity of concentrations.) For each $k \geq 0$, we assume that $c_i^k \in L^\infty(\Omega), \rho^k \in W^{1,\infty}(\Omega)$, and that $c_i^k \geq \kappa > 0$ a.e. for each i.

This again implies $\rho^k \geq \kappa \sum_i M_i > 0$ a.e. We also assume henceforth that $\gamma > 0$.

Given $\tilde{c}^k$ and the corresponding $\tilde{\omega}^k$, we define the *iteration-dependent* weighted function space

$$\Theta^k := \left\{ (\tilde{w}, s, q) \in L_0^2(\Omega)^n \times L^2(\Omega; \mathbb{S}) \times L_0^2(\Omega) \,\middle|\, \begin{array}{rl} \operatorname{div} s - \nabla q & \in L^2(\Omega; \mathbb{R}^d), \\ -c_i^k \nabla w_i + \omega_i^k \nabla q & \in L^2(\Omega; \mathbb{R}^d)\ \forall i \end{array} \right\}, \tag{2.3.1}$$

whose defining conditions linearise those in (2.2.11). This mixed space is Hilbert with graph norm

$$\|(\tilde{w}, s, q)\|_{\Theta^k}^2 := \sum_i \|w_i\|_0^2 + \|s\|_0^2 + \|q\|_0^2 + \|\operatorname{div} s - \nabla q\|_0^2 + \sum_i \| - c_i^k \nabla w_i + \omega_i^k \nabla q\|_0^2. \tag{2.3.2}$$

We now formulate our linearised problem as a symmetric perturbed saddle point

problem. Define $A_k : Q \to Q^*, \Lambda : \Theta^k \to (\Theta^k)^*, B_k : \Theta^k \to Q^*$ by

$$A_k(\tilde{u}, u; \tilde{v}, v) := \int_\Omega \sum_{i,j} u_i \cdot \mathbf{M}_{ij}^k v_j \, \mathrm{d}x + \gamma \int_\Omega \left(\sum_i \omega_i^k (u_i - u) \right) \cdot \left(\sum_j \omega_j^k (v_j - v) \right) \mathrm{d}x, \tag{2.3.3a}$$

$$\Lambda(\tilde{\mu}, \tau, p; \tilde{w}, s, q) := \int_\Omega \mathcal{A}\tau : s \, \mathrm{d}x, \tag{2.3.3b}$$

$$B_k(\tilde{\mu}, \tau, p; \tilde{v}, v) := \int_\Omega \sum_i (-c_i^k \nabla \mu_i + \omega_i^k \nabla p) \cdot v_i + (\operatorname{div} \tau - \nabla p) \cdot v \, \mathrm{d}x, \tag{2.3.3c}$$

and the functionals

$$\begin{aligned} \ell_k^1(\tilde{w}, s, q) &:= \left\langle (s - q\mathbb{I})\mathbf{n}, \frac{g_\mathrm{u}}{\rho^k} \right\rangle_\Gamma + \sum_i \left\langle g_i, -w_i + \frac{M_i}{\rho^k} q \right\rangle_\Gamma + \int_\Omega \tilde{r} \cdot \tilde{w} \, \mathrm{d}x, \\ \ell_k^2(\tilde{v}, v) &:= -\int_\Omega \rho^k f \cdot v \, \mathrm{d}x. \end{aligned} \tag{2.3.4}$$

Note that under Assumption 2.3.1, each of the bilinear functionals is continuous; we denote their operator norms by $\|A_k\|$, $\|\Lambda\|$, and $\|B_k\|$. Our linearised problem is posed as follows: find $((\tilde{\mu}^{k+1}, \tau^{k+1}, p^{k+1}), (\tilde{u}^{k+1}, u^{k+1})) \in \Theta^k \times Q$ such that

$$\begin{aligned} \Lambda(\tilde{\mu}^{k+1}, \tau^{k+1}, p^{k+1}; \tilde{w}, s, q) + B_k(\tilde{w}, s, q; \tilde{u}^{k+1}, u^{k+1}) &= \ell_k^1(\tilde{w}, s, q) \quad \forall \ (\tilde{w}, s, q) \in \Theta^k, \\ B_k(\tilde{\mu}^{k+1}, \tau^{k+1}, p^{k+1}; \tilde{v}, v) - A_k(\tilde{u}^{k+1}, u^{k+1}; \tilde{v}, v) &= \ell_k^2(\tilde{v}, v) \quad \forall \ (\tilde{v}, v) \in Q, \end{aligned} \tag{2.3.5}$$

i.e., defining the transpose $B_k^\top : Q \to (\Theta^k)^*$ in the canonical way,

$$\left(\begin{array}{c|c} \Lambda & B_k^\top \\ \hline B_k & -A_k \end{array}\right) \left(\begin{array}{c} \tilde{\mu}^{k+1} \\ \tau^{k+1} \\ p^{k+1} \\ \hline \tilde{u}^{k+1} \\ u^{k+1} \end{array}\right) = \left(\begin{array}{c} \ell_k^1 \\ \hline \ell_k^2 \end{array}\right). \tag{2.3.6}$$

We note that the variational terms involving chemical potential and pressure gradients are precisely of the same variational form as the species continuity equations and the divergence of the mass-average velocity constraint, which can be seen by inspecting (2.2.14) and (2.2.17). This key insight is what leads to a symmetric system.

Our nonlinear iteration scheme is as follows: for an initial estimate of the concentrations $\tilde{c}^0$, we solve the system (2.3.5) for the updated variables $((\tilde{\mu}^{k+1}, \tau^{k+1}, p^{k+1}), (\tilde{v}^{k+1}, v^{k+1})) \in \Theta^k \times Q$, for $k = 0, 1, 2, \ldots$. By the relations detailed in §2.1.5, these variables are used to calculate the updated concentrations $\tilde{c}^{k+1}$. This is iterated until for some set tolerance $\varepsilon > 0$,

$$\left(\|(\tilde{\mu}^{k+1}, \tau^{k+1}, p^{k+1}) - (\tilde{\mu}^k, \tau^k, p^k)\|_{\Theta^k}^2 + \|(\tilde{u}^{k+1}, u^{k+1}) - (\tilde{u}^k, u^k)\|_Q^2 \right)^{1/2} \leq \varepsilon. \tag{2.3.7}$$

2.3.2 Well-posedness of the linearised system

We will now prove that the saddle point system (2.3.5) is well-posed under Assumption 2.3.1. This will require the following beautiful Lemma due mostly to our collaborator, a Poincaré-type inequality for the following seminorm on Θ^k:

$$|(\tilde{w}, s, q)|^2_{\Theta^k} := \|s\|_0^2 + \|\operatorname{div} s - \nabla q\|_0^2 + \sum_i \| - c_i^k \nabla w_i + \omega_i^k \nabla q\|_0^2. \tag{2.3.8}$$

Lemma 2.3.1. (Poincaré inequality for the driving force; Van-Brunt, 2021.) *Let Ω be a Lipschitz domain. Under Assumption 2.3.1, for all $(\tilde{\mu}, \tau, p) \in \Theta^k$,*

$$\|(\tilde{\mu}, \tau, p)\|_{\Theta^k} \lesssim |(\tilde{\mu}, \tau, p)|_{\Theta^k}. \tag{2.3.9}$$

Proof of Lemma 2.3.1. The first step of the proof is to show that

$$\|p\|_0 \lesssim \|\tau\|_0 + \|\operatorname{div} \tau - \nabla p\|_0, \tag{2.3.10}$$

following and mildly generalising [144, Lemma 4]. Set $\theta = \tau - p\mathbb{I} - r\mathbb{I}$ where $r = \frac{1}{d|\Omega|}\int_\Omega \operatorname{tr}\tau \, \mathrm{d}x$. Then

$$\|\tau - p\mathbb{I}\|_0 \leq \|\theta\|_0 + \|r\mathbb{I}\|_0. \tag{2.3.11}$$

As $\int_\Omega \operatorname{tr}\theta \, \mathrm{d}x = 0$, we can use [40, Proposition 9.1.1] to derive

$$\|\tau - p\mathbb{I}\|_0 \lesssim \|\operatorname{dev}\theta\|_0 + \|\operatorname{div}\theta\|_0 + \|r\mathbb{I}\|_0 \lesssim \|\tau\|_0 + \|\operatorname{div}\tau - \nabla p\|_0, \tag{2.3.12}$$

with deviator $\operatorname{dev}\theta = \operatorname{dev}\tau$. Now using

$$\sqrt{d}\|p\|_0 \leq \|\tau - p\mathbb{I}\|_0 + \|\tau\|_0, \tag{2.3.13}$$

the result (2.3.10) follows. For the second stage of the proof, we will show that

$$\|\mu_i\|_0 \lesssim \|p\|_0 + \| - c_i^k \nabla \mu_i + \omega_i^k \nabla p\|_0. \tag{2.3.14}$$

This combined with (2.3.10) gives (2.3.9). To prove this second inequality, for each i we take the unique $z_i \in H_0^1(\Omega;\mathbb{R}^d)/\ker(\operatorname{div})$ such that $\operatorname{div} z_i = \mu_i$. Then $u_i := z_i/c_i^k \in L^2(\Omega;\mathbb{R}^d)$ with $\operatorname{div}(c_i^k u_i) = \mu_i$. With integration by parts we deduce

$$\int_\Omega (-c_i^k \nabla \mu_i + \omega_i^k \nabla p) \cdot u_i \, \mathrm{d}x = \int_\Omega |\mu_i|^2 - M_i p \left(\frac{\mu_i}{\rho^k} - \frac{\nabla \rho^k}{(\rho^k)^2} \cdot c_i^k u_i \right) \mathrm{d}x. \tag{2.3.15}$$

Upon rearrangement, we can derive the inequality

$$\begin{aligned}\|\mu_i\|_0^2 &\leq M_i \|p\|_0 \left(\frac{\|\mu_i\|_0}{\kappa \sum_j M_j} + \|u_i\|_0 \|c_i^k\|_0 \left\| \frac{\nabla \rho^k}{(\rho^k)^2} \right\|_{L^\infty(\Omega;\mathbb{R}^d)} \right) + \| - c_i^k \nabla \mu_i + \omega_i \nabla p\|_0 \|u_i\|_0 \\ &\leq \kappa^{-1} \|p\|_0 \left(\|\mu_i\|_0 + \|u_i\|_0 \|c_i^k\|_{L^\infty(\Omega)} \|\nabla \ln \rho^k\|_{L^\infty(\Omega;\mathbb{R}^d)} \right) + \| - c_i^k \nabla \mu_i + \omega_i \nabla p\|_0 \|u_i\|_0.\end{aligned} \tag{2.3.16}$$

By the bounded inverse theorem, div admits a bounded left inverse, so $\|z_i\|_1 \lesssim \|\mu_i\|_0$ and thus

$$\|u_i\|_0 \leq \kappa^{-1}\|z_i\|_0 \lesssim \kappa^{-1}\|\mu_i\|_0. \tag{2.3.17}$$

Combining this with (2.3.16), we can divide through by $\|\mu_i\|_0$ to derive

$$\|\mu_i\|_0 \lesssim \kappa^{-1}\|p\|_0 \left(1 + \kappa^{-1}\|c_i^k\|_{L^\infty(\Omega)}\|\nabla \ln \rho^k\|_{L^\infty(\Omega)}\right) + \kappa^{-1}\| - c_i^k\nabla\mu_i + \omega_i^k\nabla p\|_0. \tag{2.3.18}$$

□

Note that in particular, the two steps of this proof imply that

$$\left.\begin{aligned} \operatorname{div}\tau - \nabla p &= 0 \\ -c_i^k\nabla\mu_i + \omega_i^k\nabla p &= 0 \end{aligned}\right\} \Longrightarrow \left\{\begin{aligned} \|p\|_0 &\lesssim \|\tau\|_0, \\ \|\mu_i\|_0 &\lesssim \|p\|_0. \end{aligned}\right. \tag{2.3.19}$$

This has the physical interpretation that in the absence of (at least this linearisation of) the driving force, one can recover the chemical potentials from the pressure. In this sense it is a generalisation to the OSM framework of [144, Lemma 4], which is exactly the first line of (2.3.19): that in the absence of external forces, one can recover the pressure from the viscous stress. Since also the constant in (2.3.18) depends unfavourably on κ (the uniform lower bound on concentrations), we see also that such 'recovery' of the potentials becomes more unstable near the singular regime in which concentrations approach zero. Provided κ (and the relative variation of the density) are well-behaved across iterations, so will be the resulting constant.

A further intermediate lemma we need to prove well-posedness is the following.

Lemma 2.3.2. (Coercivity of a perturbation to A_k.) *Under* Assumption 2.3.1, *there is* $L = L(\gamma, k)$ *s.t. for all* $(\tilde{u}, u) \in Q$,

$$\left(\frac{n+1}{2}\right) L\|u\|_0^2 + A_k(\tilde{u}, u; \tilde{u}, u) \geq \frac{L}{2}\|(\tilde{u}, u)\|_Q^2. \tag{2.3.20}$$

Proof. Defining $\delta_i = u_i - u$ for each i, we compute that

$$A_k(\tilde{u}, u; \tilde{u}, u) = \int_\Omega \sum_{i,j} \delta_i \mathbf{M}_{ij}^{k,\gamma}\delta_j \, \mathrm{d}x, \tag{2.3.21}$$

where $\mathbf{M}^{k,\gamma}$ is defined using $\tilde{c}^k$ via (2.1.23). It follows from [180, Lemma 4.1] that the right-hand expression is a coercive bilinear form in $\tilde{\delta}$, i.e. for some $L > 0$,

$$A_k(\tilde{u}, u; \tilde{u}, u) \geq \frac{L}{2}\sum_i \|\delta_i\|_0^2 = \sum_i \|u_i - u\|_0^2, \tag{2.3.22}$$

so

$$\begin{aligned}\left(\frac{n+1}{2}\right) L\|\tilde{u}\|_0^2 + A_k(\tilde{u}, u; \tilde{u}, u) &\geq \frac{L}{2}\sum_i \left(\|u_i - u\|_0^2 + \|u\|_0^2\right) + \frac{L}{2}\|u\|_0^2 \\ &\geq \frac{L}{2}\left(\sum_i \|u_i\|_0^2 + \|u\|_0^2\right) = \frac{L}{2}\|(\tilde{u}, u)\|_Q^2.\end{aligned} \tag{2.3.23}$$

□

Despite the complexity of the original fully coupled physics problem, our constructed formulation allows us to invoke standard Babuška theory for well-posedness [31].

Theorem 2.3.1. (Well-posedness of the Picard linearisation). *Under* Assumption 2.3.1*, there exists a unique solution to the perturbed saddle point system* (2.3.5)*.*

Proof. We use the shorthand $(\mathfrak{p}, \mathfrak{q}) := ((\tilde{\mu}, p, \tau), (\tilde{u}, u)), (\mathfrak{s}, \mathfrak{v}) := ((\tilde{w}, s, q), (\tilde{v}, v)) \in \Theta^k \times Q$. Define the bounded bilinear form $\mathcal{G} : (\Theta^k \times Q)^2 \to \mathbb{R}$ by

$$\mathcal{G}(\mathfrak{p}, \mathfrak{q}; \mathfrak{s}, \mathfrak{v}) := \Lambda(\mathfrak{p}, \mathfrak{s}) + B_k(\mathfrak{s}; \mathfrak{q}) + B_k(\mathfrak{p}; \mathfrak{v}) - A_k(\mathfrak{q}; \mathfrak{v}). \tag{2.3.24}$$

We prove the Babuška condition for $\mathcal{G}$, namely that there exists $C > 0$ such that for each $(\mathfrak{p}, \mathfrak{q}) \in \Theta^k \times Q$ there is $(\mathfrak{s}, \mathfrak{v}) \in \Theta^k \times Q$ such that

$$\frac{\mathcal{G}(\mathfrak{p}, \mathfrak{q}; \mathfrak{s}, \mathfrak{v})}{\|(\mathfrak{s}, \mathfrak{v})\|_{\Theta^k \times Q}} \geq C\|(\mathfrak{p}, \mathfrak{q})\|_{\Theta^k \times Q}, \tag{2.3.25}$$

with product norm $\|(\mathfrak{p}, \mathfrak{q})\|_{\Theta^k \times Q}^2 := \|\mathfrak{p}\|_{\Theta^k}^2 + \|\mathfrak{q}\|_Q^2$. Since $\mathcal{G}$ is defined on the product of a space with itself and is symmetric, only the one inf-sup condition (2.3.25) need be verified. We show that for constants $L_1, L_2 > 0$, for each $(\mathfrak{p}, \mathfrak{q}) \in \Theta^k \times Q$, there is $(\mathfrak{s}, \mathfrak{v}) \in \Theta^k \times Q$ such that $\mathcal{G}(\mathfrak{p}, \mathfrak{q}; \mathfrak{s}, \mathfrak{v}) \geq L_1\|(\mathfrak{p}, \mathfrak{q})\|_{\Theta^k \times Q}^2$ with

$$\|(\mathfrak{s}, \mathfrak{v})\|_{\Theta^k \times Q} \leq L_2\|(\mathfrak{p}, \mathfrak{q})\|_{\Theta^k \times Q}. \tag{2.3.26}$$

Fix $(\mathfrak{s}, \mathfrak{v})$ as the ansatz

$$\begin{aligned} w_i &= C_1\mu_i, \qquad & s &= C_1\tau + C_2 s_u, \qquad & q &= C_1 p, \\ v_i &= C_3(-c_i^k \nabla u_i + \omega_i^k \nabla p) - C_1 u_i, \qquad & v &= -C_1 u + C_4(\operatorname{div}\tau - \nabla p). \end{aligned} \tag{2.3.27}$$

Here the C_j are constants to be chosen, and s_u is chosen (by closedness of the stress complex (1.0.3)) as the unique element of $H(\operatorname{div}; \mathbb{S})/\ker(\operatorname{div})$ satisfying $\operatorname{div} s_u = u$,

and by the bounded inverse theorem $\|s_u\|_{\mathrm{div}} \leq C_*\|u\|_0$. It is clear that (2.3.26) holds. We compute

$$\begin{aligned}\mathcal{G}(\mathfrak{p},\mathfrak{q};\mathfrak{s},\mathfrak{v}) = \int_\Omega \mathcal{A}\tau : (C_1\tau + C_2 s_u)\ \mathrm{d}x + C_3\sum_i \| - c_i^k\nabla\mu_i + \omega_i^k\nabla p\|_0^2 \\ + C_4\|\operatorname{div}\tau - \nabla p\|_0^2 + C_2\|u\|_0^2 - A_k(\tilde{u},u;\tilde{v},v),\end{aligned} \tag{2.3.28}$$

and observe that the final term may be written as

$$C_1 A_k(\tilde{u},u;\tilde{u},u) - A_k(\tilde{u},u;C_3(-c_i^k\nabla\mu_i + \omega_i^k\nabla p)_i, C_4(\operatorname{div}\tau - \nabla p)). \tag{2.3.29}$$

With L now given by Lemma 2.3.2, we choose $C_2 = \|A_k\|^2(n+1)L$ and assume $C_1 \geq 2\|A_k\|^2$. Then

$$C_2\|u\|_0^2 + C_1 A_k(\tilde{u},u;\tilde{u},u) \geq \|A_k\|^2 L\|(\tilde{u},u)\|_Q^2. \tag{2.3.30}$$

The compliance tensor is uniformly positive definite: there is $c_{\mathcal{A}}$ with $\int_\Omega \mathcal{A}s : s\ \mathrm{d}s \geq c_{\mathcal{A}}\|s\|_0^2\ \forall s \in L^2(\Omega;\mathbb{S})$. Together with the estimate on s_u and boundedness of Λ, A_k, we bound (2.3.28) from below as

$$\begin{aligned}\mathcal{G}(\mathfrak{p},\mathfrak{q};\mathfrak{s},\mathfrak{v}) \geq c_{\mathcal{A}}C_1\|\tau\|_0^2 + L\|A_k\|^2\|(\tilde{u},u)\|_Q^2 + C_3\sum_i \| - c_i^k\nabla\mu_i + \omega_i^k\nabla p\|_0^2 \\ + C_4\|\operatorname{div}\tau - \nabla p\|_0^2 - LC_*(n+1)\|A_k\|^2\|\Lambda\|\|u\|_0\|\tau\|_0 \\ - \|A_k\|\|(\tilde{u},u)\|_Q\left(C_3^2\sum_i \| - c_i^k\nabla\mu_i + \omega_i^k\nabla p\|_0^2 + C_4^2\|\operatorname{div}\tau - \nabla p\|_0^2\right)^{1/2}.\end{aligned} \tag{2.3.31}$$

The desired bound now follows with the choice

$$C_1 = \left(\frac{LC_*^2\|\Lambda\|^2(n+1)^2}{c_{\mathcal{A}}} + 2\right)\|A_k\|^2, \qquad C_3 = C_4 = L, \tag{2.3.32}$$

application of Lemma 2.3.1, and the weighted Young inequality:

$$\begin{aligned}\mathcal{G}(\mathfrak{p},\mathfrak{q};\mathfrak{s},\mathfrak{u}) &\geq 2c_{\mathcal{A}}\|A_k\|^2\|\tau\|_0^2 + \frac{L}{6}\|A_k\|_0^2\|(\tilde{u},u)\|_Q^2 \\ &\quad + \frac{L}{4}\left(\sum_i \| - c_i^k\nabla\mu_i + \omega_i^k\|_0^2 + \|\operatorname{div}\tau - \nabla p\|_0^2\right) \\ &\gtrsim |\mathfrak{p}|_{\Theta^k}^2 + \|\mathfrak{q}\|_Q^2 \gtrsim \|(\mathfrak{p},\mathfrak{q})\|_{\Theta^k\times Q} \gtrsim \|(\mathfrak{p},\mathfrak{q})\|_{\Theta^k\times Q}^2\|(\mathfrak{s},\mathfrak{v})\|_{\Theta^k\times Q}.\end{aligned} \tag{2.3.33}$$

□

2.4 Discretisation

We now assume that Ω is polytopal, and admits a quasi-uniform triangulation $\mathcal{T}_h$ with maximal element diameter h. Denote conforming finite element spaces for the discrete solution tuple by

$$\begin{aligned}\underbrace{(X_h^n \times \Sigma_h \times P_h)}_{=:\,\Theta_h^k} \times \underbrace{(W_h^n \times V_h)}_{=:\,Q_h} \\ \subset \underbrace{(L_0^2(\Omega)^n \times L^2(\Omega;\mathbb{S}) \times L_0^2(\Omega))}_{\supseteq\,\Theta^k} \times \underbrace{(L^2(\Omega;\mathbb{R}^d)^n \times L^2(\Omega;\mathbb{R}^d))}_{=\,Q}.\end{aligned} \tag{2.4.1}$$

Here Θ_h^k is independent of k as a set, but inherits an iteration-dependent norm described below; Q_h inherits the norm of Q. Our discretised linear problem after $k \geq 0$ nonlinear iterations therefore reads: seek $((\tilde{\mu}_h, \tau_h, p_h), (\tilde{u}_h, u_h)) \in \Theta_h^k \times Q_h$ such that

$$\begin{aligned}\Lambda(\tilde{\mu}_h, \tau_h, p_h; \tilde{w}_h, s_h, q_h) + B_{k,h}(\tilde{w}_h, s_h, q_h; \tilde{u}_h, u_h) &= \ell_{k,h}^1(\tilde{w}_h, s_h, q_h) \forall (\tilde{w}_h, s_h, q_h) \in \Theta_h^k, \\ B_{k,h}(\tilde{\mu}_h, \tau_h, p_h; \tilde{v}_h, v_h) - A_{k,h}(\tilde{u}_h, u_h; \tilde{v}_h, v_h) &= \ell_{k,h}^2(\tilde{v}_h, v_h) \qquad \forall (\tilde{v}_h, v_h) \in Q_h,\end{aligned} \tag{2.4.2}$$

where $A_{k,h}, B_{k,h}$ are obtained from A_k, B_k, and $\ell_{k,h}^1, \ell_{k,h}^2$ from ℓ_k^1, ℓ_k^2, respectively, by replacing the discretely computed concentrations c_i^k and inverse density $(\rho^k)^{-1}$ with discrete approximations; we use these to define a norm $\|\cdot\|_{\Theta_h^k}$ for Θ_h^k in analogy to (2.3.2). In block form, the linearised discrete problem reads

$$\left(\begin{array}{c|c} \Lambda & B_{k,h}^\top \\ \hline B_{k,h} & -A_{k,h} \end{array}\right) \left(\begin{array}{c} \tilde{\mu}_h \\ \tau_h \\ p_h \\ \hline \tilde{v}_h \\ v_h \end{array}\right) = \left(\begin{array}{c} \ell_{k,h}^1 \\ \hline \ell_{k,h}^2 \end{array}\right). \tag{2.4.3}$$

2.4.1 Structure-preservation and well-posedness

We have already emphasised that pressure is an H^1-like variable, for which we therefore employ the continuous Lagrange element of degree $t \geq 1$, $X_h = \mathrm{CG}_t(\mathcal{T}_h)$. It appears natural to take the chemical potential space X_h to be CG elements of at least the same degree, $X_h = \mathrm{CG}_r$ for $r \geq t$, from the diffusion driving forces (2.1.13), and since the chemical potentials are used to calculate the concentrations, which one would like to approximate to high order due to their physical importance. The mass-average velocity constraint (2.1.6) suggests that the species velocity space be contained in the space used for convective velocity, $W_h \subseteq V_h$.

For the Stokes subsystem, it is desirable that the pair $(\Sigma_h \times P_h, V_h)$ be inf-sup compatible, for which it is sufficient to have that the full divergence $(\tau, p) \mapsto \operatorname{div}\tau - \nabla p$ is surjective onto V_h. By the regularity choice (2.2.7) for the pressure, it is thus natural to apply div-conforming tensor elements such as our implemented AW^{c} element to discretise the viscous stress. By the decomposition (2.1.18), symmetry of the viscous stress is equivalent to the conservation of angular momentum; we consider exactly symmetric stress elements such as the Arnold–Winther [24] and Arnold–Awanou–Winther elements [14], since this obviates the need for a symmetry-enforcing Lagrange multiplier, which would add a further field to our already $(2n+3)$-field formulation.

However, if one would like to repeat at the discrete level the proof of Theorem 2.3.1, it is necessary for $\operatorname{div} : \Sigma_h \to V_h$ to be surjective, allowing us to construct the discrete analogue of the tensor field s_u in the ansatz (2.3.27). This is stronger than surjectivity of $(\tau, p) \mapsto \operatorname{div}\tau - \nabla p, \Sigma_h \times P_h \to V_h$, but in practice is equivalent because many appropriate choices of Σ_h are designed to discretise the *full* Cauchy stress. Furthermore, the discrete analogue of the constant C_* (and hence the resulting inf-sup constant) will *a priori* depend on h; it is therefore necessary to assume that such s_u can be constructed stably.

Assumption 2.4.1. (Stable right inverse for the divergence.) There exists C^* independent of h such that for each $v_h \in V_h$ and for the unique $s_h \in \Sigma_h / \ker(\operatorname{div})$ with $\operatorname{div} s_h = v_h$, there holds $\|s_h\|_{\operatorname{div}} \leq C^* \|v_h\|_0$.

This is true for (for example) stress elements discretising a stress complex which admits bounded commuting projections to the subcomplex, as is the case for the Arnold–Winther elements (1.2.23) as summarised above Lemma 1.5.1 [24], and the Arnold–Awanou–Winther elements [14]. The other relations are summarised below:[34]

$$\begin{array}{ccc} \underset{\substack{\text{chemical}\\\text{potential}}}{X_h} & & \underset{\substack{\text{species}\\\text{velocity}}}{W_h} \\ \pi_2 \uparrow & & \downarrow \subseteq \\ \underset{\text{stress}\times\text{pressure}}{\Sigma_h \times P_h} & \xrightarrow{(\tau,p)\mapsto \operatorname{div}\tau} & \underset{\substack{\text{convective}\\\text{velocity}}}{V_h} \end{array} \tag{2.4.4}$$

The bottom row corresponds to the load segment of a discrete stress complex such as (1.2.23), refined for Stokes flow due to the decomposition (2.1.18). We will need the conditions of Lemma 2.3.1 to hold exactly in the discretisation. This will in general require that we approximate the concentrations c_i^k, and *density reciprocal* $(\rho^k)^{-1}$, in

[34] Here π_i denotes projection onto the i^{th} component.

specific discrete function spaces. The interpolation of these terms will be denoted by $c_{i,h}^k$ and $\rho_h^{k,-1}$, respectively. We now show that the discrete linear problems are well-posed under a final condition which does not fit neatly onto (2.4.4).

Assumption 2.4.2. (Discrete driving force.) The operator given by

$$\mathrm{d}_h^{i,k}(w_h, q_h) := -c_{i,h}^k \nabla w_h + \omega_{i,h}^k \nabla q_h, \tag{2.4.5}$$

where $\omega_{i,h}^k := M_i c_{i,h}^k \rho_h^{k,-1}$, is well-defined as a map $\mathrm{d}_h^{i,k} : X_h \times P_h \to W_h$, i.e., it takes values in W_h.

Remark 2.4.1. Note that Lemma 2.3.1 required a differentiation of ρ^{-1}, and so $\rho_h^{k,-1}$ should at least be a continuous piecewise linear function. In order to minimise the polynomial degree for W_h arising from Assumption 2.4.2, it is advantageous to interpolate $c_{i,h}^k$ onto the space DG_0. These coefficients do not affect the accuracy of the discretisation, only the accuracy of the linearisation, and nonlinear convergence appears robust regardless of this approximation.

Theorem 2.4.1. (Discrete inheritance of well-posedness.) *Under* Assumptions 2.4.1 *and* 2.4.2 *and the relations specified in* (2.4.4)*, the system* (2.4.2) *is well-posed, uniformly in* h*.*

Proof. Due to the structural conditions demanded in the Assumptions, by inspection the choices of test functions (2.3.27) are valid. As a consequence, we may completely replicate the argument presented in the infinite-dimensional case, and derive the analogue of condition (2.3.25) with constant independent of h. □

2.4.2 Error estimates

Following [189, Theorem 2], for fixed k we infer the abstract error estimate

$$\|(\underline{\tilde{\mu}}^{k+1}, \underline{\tau}^{k+1}, \underline{p}^{k+1}) - (\tilde{\mu}_h, \tau_h, p_h)\|_{\Theta_h^k} + \|(\underline{\tilde{u}}^{k+1}, \underline{u}^{k+1}) - (\tilde{u}_h, u_h)\|_Q \lesssim \mathbb{E}_{\Theta_h^k} + \mathbb{E}_{Q_h}, \tag{2.4.6}$$

where

$$\begin{aligned} \mathbb{E}_{\Theta_h^k} &:= \inf_{(\tilde{w}_h, s_h, q_h) \in \Theta_h^k} \|(\underline{\tilde{\mu}}^{k+1}, \underline{\tau}^{k+1}, \underline{p}^{k+1}) - (\tilde{w}_h, s_h, q_h)\|_{\Theta_h^k}, \\ \mathbb{E}_{Q_h} &:= \inf_{(\tilde{v}_h, v_h) \in Q_h} \|(\underline{\tilde{u}}^{k+1}, \underline{u}^{k+1}) - (\tilde{v}_h, v_h)\|_Q. \end{aligned} \tag{2.4.7}$$

Here the tuple $((\underline{\tilde{\mu}}^{k+1}, \underline{\tau}^{k+1}, \underline{p}^{k+1}), (\underline{\tilde{u}}^{k+1}, \underline{u}^{k+1}))$ is defined as the exact solution to (2.3.5) but with $B_k, A_k, \ell_k^1, \ell_k^2$ replaced with $B_{k,h}, A_{k,h}, \ell_{k,h}^1, \ell_{k,h}^2$, respectively – that is, the solution of the system (2.3.5) with the estimates of the concentrations and inverse density replaced by $c_{i,h}^k$ and $\rho_h^{k,-1}$, respectively.

To derive a practical error estimate, we need to bound the quantities $\mathbb{E}_{\Theta_h^k}$ and $\mathbb{E}_{Q_h}$ by interpolation estimates specific to the choice of finite element spaces, by estimating $\|\cdot\|_{\Theta_h^k}, \|\cdot\|_Q$ in terms of standard Sobolev norms. To this end, we readily check that

$$\begin{aligned}\mathbb{E}_{\Theta_h^k} &\lesssim \max\left(1, \sum_i \|c_{i,h}^k\|_{L^\infty(\Omega)}\right) \inf_{\tilde{w}_h \in X_h^n} \|\underline{\tilde{\mu}}^{k+1} - \tilde{w}_h\|_1 \\ &\quad + \max\left(1, \sum_i \|\omega_{i,h}^k\|_{L^\infty(\Omega)}\right) \inf_{q_h \in P_h} \|\underline{p}^{k+1} - q_h\|_1 + \inf_{s_h \in \Sigma_h} \|\underline{\tau}^{k+1} - s_h\|_{\mathrm{div}}, \\ \mathbb{E}_{Q_h} &\lesssim \inf_{\tilde{v}_h \in W_h^n} \|\underline{\tilde{u}}^{k+1} - \tilde{v}_h\|_0 + \inf_{v_h \in V_h} \|\underline{u}^{k+1} - v_h\|_0.\end{aligned} \tag{2.4.8}$$

2.4.3 Examples of suitable finite elements

Having derived abstract error estimates, we now consider two simple combinations of finite elements satisfying the structural conditions (2.4.4) and Assumptions 2.4.1 and 2.4.2 in 2D. Denote by AW_3^c the lowest-order $H(\mathrm{div};\mathbb{S})$-conforming Arnold–Winther element studied in the previous chapter, with Clément-like interpolant $\Pi_h : H^1(\Omega;\mathbb{S}) \to \mathrm{AW}_3^c(\mathcal{T}_h;\mathbb{S})$. Specifying

$$X_h = P_h = \mathrm{CG}_1(\mathcal{T}_h) \cap L_0^2(\Omega), \tag{2.4.9a}$$
$$\Sigma_h = \mathrm{AW}_3^c(\mathcal{T}_h;\mathbb{S}), \tag{2.4.9b}$$
$$W_h = V_h = \mathrm{DG}_1(\mathcal{T}_h;\mathbb{R}^2), \tag{2.4.9c}$$

and further assuming that the discretely computed c_i^k and $(\rho^k)^{-1}$ have been interpolated into DG_0 and CG_1, respectively, then this discretisation satisfies the structural properties (2.4.4) and Assumptions 2.4.1 and 2.4.2, hence we deduce the error estimate (2.4.6).

Let $\Pi_h^{\mathrm{CG}_1} : H^2(\Omega) \to \mathrm{CG}^1(\mathcal{T}_h)$ and $\Pi_h^{\mathrm{DG}_1^2} : H^1(\Omega;\mathbb{R}^2) \to \mathrm{DG}_1(\mathcal{T}_h;\mathbb{R}^d)$ be the associated interpolation operators. We then have the following interpolation rates under sufficient regularity assumptions [40, p. 72][140, Ch. 3]:

$$\|\tilde{\mu} - \Pi_h^{\mathrm{CG}_1}\tilde{\mu}\|_1 \lesssim h|\tilde{\mu}|_2, \tag{2.4.10a}$$
$$\|p - \Pi_h^{\mathrm{CG}_1} p\|_1 \lesssim h|p|_2, \tag{2.4.10b}$$
$$\|\tau - \Pi_h\tau\|_0 + h\|\operatorname{div}(\tau - \Pi_h\tau)\|_0 \lesssim h^2|\tau|_2, \tag{2.4.10c}$$
$$\|(\tilde{u}, u) - \Pi_h^{\mathrm{DG}_1^d}(\tilde{u}, u)\|_Q \lesssim h^2|(\tilde{u}, u)|_1, \tag{2.4.10d}$$

where $\Pi_h^{\mathrm{CG}_1}, \Pi_h^{\mathrm{DG}_1^d}$ have been applied componentwise. Using these estimates for the interpolation operators and the error estimate (2.4.6), we can derive the error bound

$$\|(\underline{\tilde{\mu}}^{k+1}, \underline{\tau}^{k+1}, \underline{p}^{k+1}) - (\tilde{\mu}_h, \tau_h, p_h)\|_{\Theta_h^k} + \|(\underline{\tilde{u}}^{k+1}, \underline{u}^{k+1}) - (\tilde{u}_h, u_h)\|_Q \lesssim h. \tag{2.4.11}$$

We will see in practice that the order of convergence for several fields is actually higher, but the error in the species velocities and the driving forces remains $\mathcal{O}(h)$.

A higher-order class of finite elements is provided by replacing (2.4.9a) with

$$X_h = \mathrm{CG}_2(\mathcal{T}_h) \cap L^2_0(\Omega), P_h = \mathrm{CG}_1(\mathcal{T}_h) \cap L^2_0(\Omega), \tag{2.4.12}$$

and leaving the others unchanged; again the structural conditions are satisfied if c_i^k and $(\rho^k)^{-1}$ are interpolated into DG_0 and CG_1, respectively. A similar error analysis again confers an error bound of only $\mathcal{O}(h)$, but shortly we will see that this is higher in practice.

Remark 2.4.2. These estimates bound the error between the discrete solutions at iteration $k+1, ((\tilde{\mu}_h, \tau_h, p_h), (\tilde{u}_h, u_h))$ and the continuous solution of the nonlinear scheme $((\underline{\tilde{\mu}}^{k+1}, \underline{\tau}^{k+1}, \underline{p}^{k+1}), (\underline{\tilde{u}}^{k+1}, \underline{u}^{k+1}))$ with the same (discrete) coefficients, but ideally one would derive error estimates against the continuous solution $((\tilde{\mu}^{k+1}, \tau^{k+1}, p^{k+1}), (\tilde{u}^{k+1}, u^{k+1}))$ at iteration $k+1$ with the exact (continuous) coefficients. Estimates on such consistency errors were analysed for a simpler system in [180] and some rationale was provided as to why in practice this is not an issue, based on the formal order of the consistency error being strictly less than the discretisation error. We expect a similar (if tedious) analysis could be performed following the strategy in [180]. In general the consistency errors are expected to be $\mathcal{O}(h^2)$, which will be borne out in the numerical examples.

Remark 2.4.3. In analogy to the previous chapter, we emphasise that we have aimed to identify appropriate structural conditions between finite element spaces in order to preserve desirable properties of the SOSM system, and in particular which allow mimicry of well-posedness proofs from the infinite-dimensional problem, rather than to advocate specifically for the elements used here. We expect that it is possible to alternatively use a Lagrange multiplier to weakly enforce the symmetry of the viscous stress as described in §1.2.3.

The system matrix of our discrete linearised system (2.4.3) has symmetric perturbed saddle point structure, and although indefinite, is such that both the blocks $\Lambda, A_{k,h}$ are symmetric positive semidefinite. These matrix properties hold independently of the particular material considered. We expect that this structure should be conducive to the development of fast solvers.

2.5 Numerical experiments

We now verify our scheme, implemented in Firedrake [164]. Since extensions of §1 giving software implementations of symmetry-enforcing stress elements in 3D are yet to be carried out (see §4.1.2), we restrict ourselves to the case $d = 2$. Throughout these experiments we chose the penalty parameter $\gamma = 0.1$ and constant functions for the initial guesses.

2.5.1 Validation with manufactured solutions

We at first verify our error estimates via the method of manufactured solutions for an ideal gas on the unit square $\Omega = (0,1)^2$. If $\mathcal{R}T = 1$, the diffusivities are given by $\mathscr{D}_{ij} = D_i D_j$ for $D_j > 0$, and $g : \mathbb{R}^2 \to \mathbb{R}$ is smooth, then one can check that an analytic solution to the OSM subsystem (2.1.10) is given by

$$c_i = \exp\left(\frac{g}{D_i}\right), \quad v_i = D_i \nabla g, \tag{2.5.1}$$

which together implicitly define every other quantity (for given shear and bulk viscosities), apart from the chemical potentials which we compute by inverting the ideal gas relation (2.1.26) with $p^{\ominus} = \fint_\Omega p \, \mathrm{d}x, \mu_i^{\ominus} = \fint_\Omega c_i \, \mathrm{d}x \ \forall i$. The molar mass of each species was set to 1, and ζ, μ to 0.1. The initial guesses for the concentrations $\tilde{c}^0$ were set as $c_i^0 = \fint_\Omega c_i \, \mathrm{d}x$, i.e. as the means of the exact concentrations.

We used $D_i = \frac{1}{2} + \frac{i}{4}, i = 1, 2, 3$, and $g(x, y) = \frac{xy}{5}(1-x)(1-y)$ to generate Figure 2.1, which simultaneously demonstrates the negligible effect of the consistency error induced by the discrete interpolations $c_{i,h}^k, \rho_h^{k,-1}$ and verifies the error estimate (2.4.11).

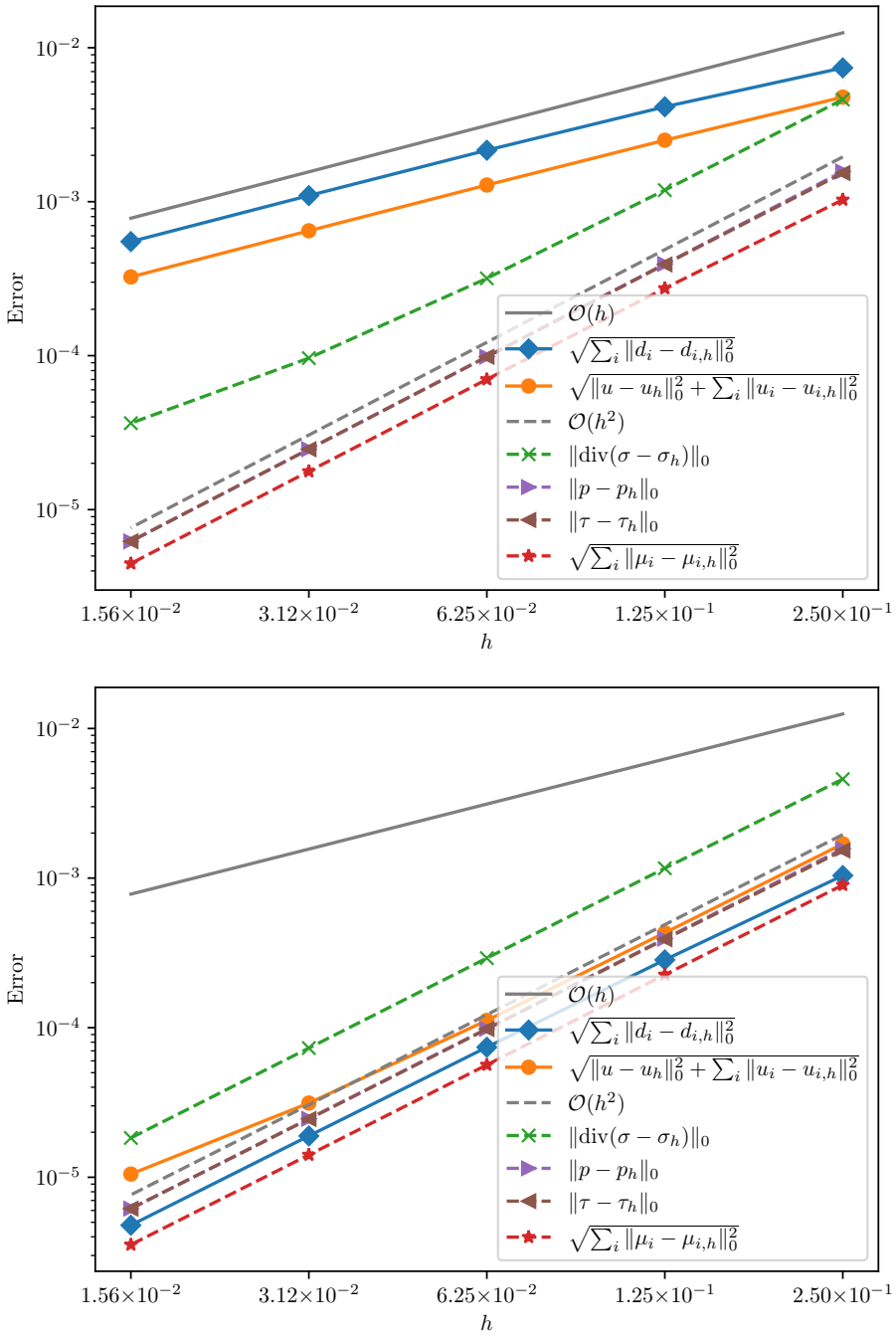


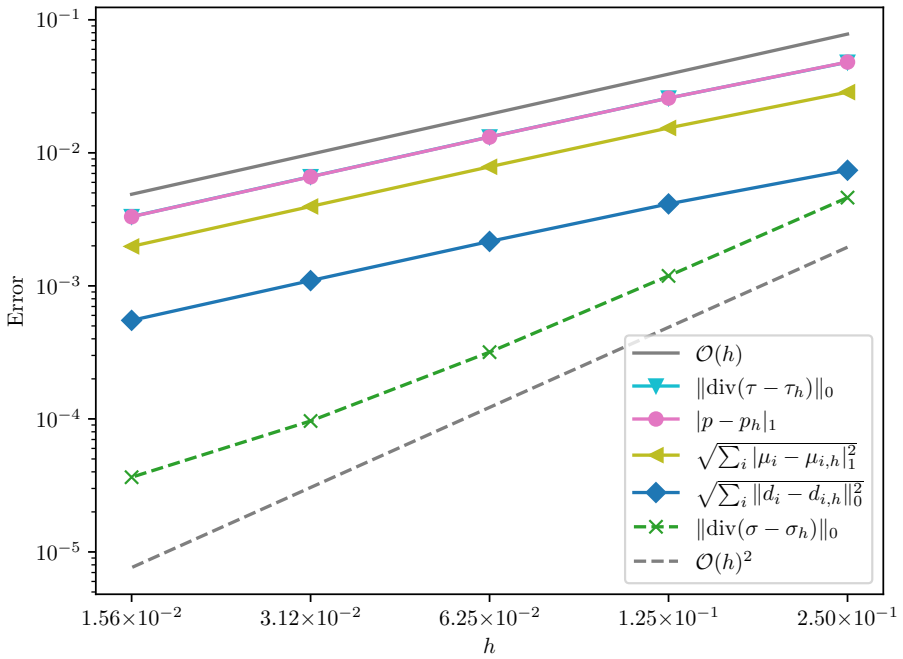
Figure 2.1: Error plots for two finite element families: (2.4.9) (top) and (2.4.12) (bottom).

The outer solver tolerance was 10^{-7} in the ℓ^2 norm, and took 6 nonlinear iterations on the coarsest mesh of 4×4, to 7 iterations on finest mesh of 32×32. We have denoted in Fig. 2.1 $d_{i,h}$ as the discrete driving force defined by (2.4.5) at the final iteration, and $\sigma_h := \tau_h - p_h\mathbb{I}$. As could be expected, the observed convergence rates

of $\mathcal{O}(h^2)$ in the $\|\cdot\|_0$ norms of the chemical potential, stress, and pressure, are even higher than those which we are able to prove in §2.4, once again suggesting that our error estimates could be improved, for example by duality arguments.

2.5.2 Convergence of thermodynamic forces and the pressure gradient

We also test the convergence of the thermodynamic forces underlying the SOSM system. Due to our construction of the 'linearised' function space (2.3.1), it is the norm $\|\cdot\|_{\Theta_h^k}$ with respect to which we have proved convergence of the solution tuple. It is natural to wonder whether this is an artefact of our constructed function spaces. To answer this, we measure convergence of the chemical potential gradients $\nabla\mu_i$, pressure gradient ∇p, and divergence $\operatorname{div}\tau$ of the non-equilibrium stress to their true values, compared to the convergence of the nonlinear diffusion driving forces, and of the div of the full Cauchy stress. For the former quantities, there is *a priori* no reason to expect any convergence at all.



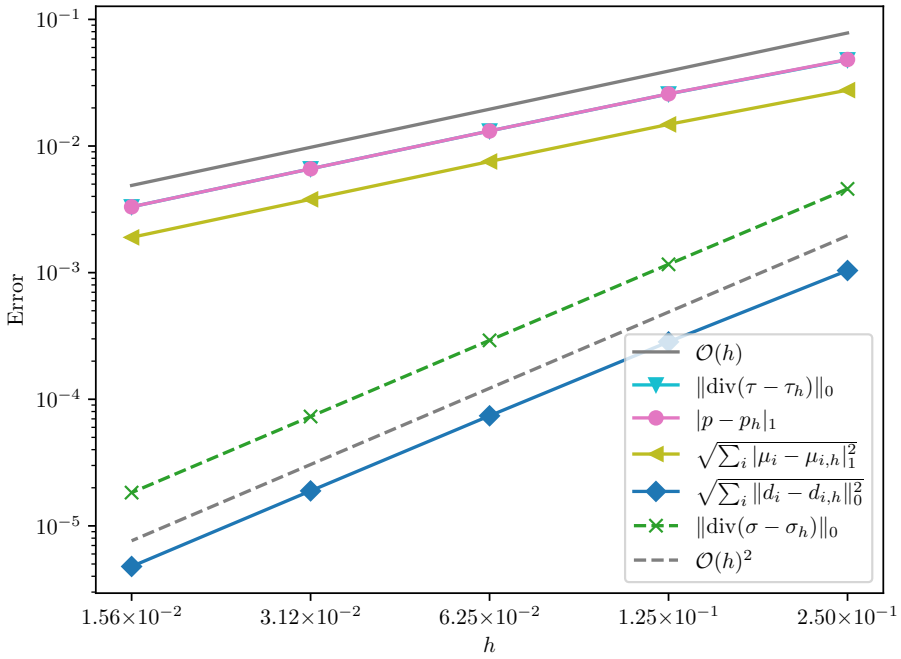


Figure 2.3: Higher-order convergence in L^2 of the divergence of the full Cauchy stress, and driving forces, for two finite element families, (2.4.9) (top) and (2.4.12) (bottom), providing circumstantial evidence towards their nonlinear integrability in (2.2.19c)–(2.2.19d).

Remarkably, we observe in Figure 2.3 that not only do the components $\nabla\mu_i, \nabla p, \mathrm{div}\,\tau$ converge, but there is convergence of the nonlinear diffusion driving forces and divergence of the full Cauchy stress, and in fact at a rate one order higher than these individual components; this suggests that, rather than being a mathematical artefact of our novel formulation, the conditions defining the Θ^k space capture the underlying thermodynamic quantities of interest. This also provides intriguing (if circumstantial) evidence towards the physical relevance of our nonlinear formulation in Definition 2.2.1.

2.5.3 Microfluidic mixing of benzene and cyclohexane

Cyclohexane is important in the petrochemical industry, where it is mainly used for nylon synthesis. It is primarily produced through the dehydrogenation of benzene, resulting in a benzene-cyclohexane mixture, but the extraction of cyclohexane from this mixture is difficult due to the similar vaporisation temperatures of the two components [183]. This provides a tractable non-ideal example for our scheme to simulate, since its relatively high industrial importance makes most of the required material

and thermodynamic parameter data readily available in the literature. We consider a microfluidic chamber in which the Stokes flows of benzene and cyclohexane mix.

The transport parameters, measured at $T = 298.15\text{K}$, may be found in [105]; we observe from these data that the diffusivity between the constituents, and their shear viscosities, are essentially constant, and will be taken as $\mathscr{D}_{12} = 2.1 \times 10^{-9}\text{m}^2/\text{s}$ and $\mu = 6 \times 10^{-4}\text{Pa}\cdot\text{s}$ respectively. In the absence of accurate data for the bulk viscosities of either chemical, we set them to essentially vanish at $\zeta = 10^{-7}\text{Pa}\cdot\text{s}$. The molar masses are taken as 0.078kg/mol for benzene and 0.084kg/mol for cyclohexane. Ambient pressure was taken as $p^{\ominus} = 10^5\text{Pa}$. The benzene-cyclohexane mixture forms a non-ideal solution, for which a relation between the chemical potentials is therefore required. We employ a Margules model [104], whose parameters were reported in [178].

Stiffness arises in the interaction between the species velocities, since the mixtures are almost fully separated at the inlets to the domain; we therefore employ a relaxation parameter of 0.1 in the update direction with respect to the concentrations, i.e. iteration $k+1$ updates the concentrations to $c_i^{*,k+1} := 0.9c_i^k + 0.1c_i^{k+1}$.

We consider a 2D pipe configuration bringing two inlets to a single outlet. At the top, pure benzene enters, and at the bottom, pure cyclohexane. A parabolic axial velocity profile is prescribed at inlets and outlet, as is consistent with planar Poiseuille flow. Simulated results are visualised in Figures 2.4 and 2.5.

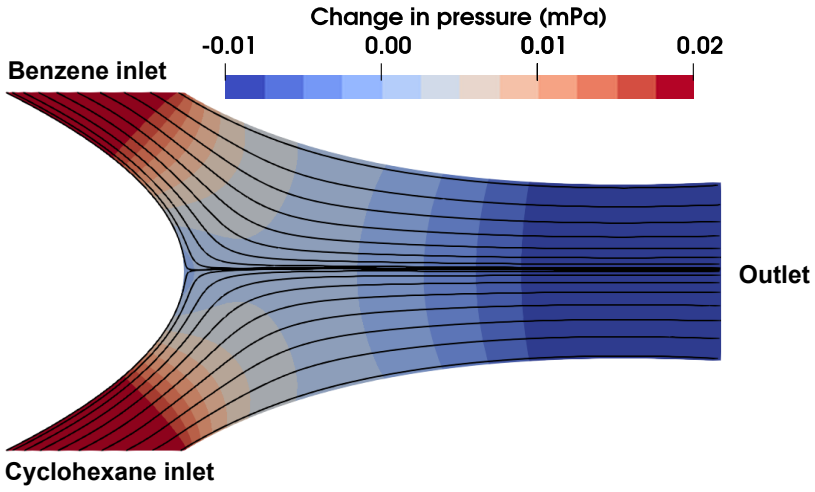


Figure 2.4: Plot of change in pressure in the mixing chamber, with streamlines computed from the mass-average velocity.

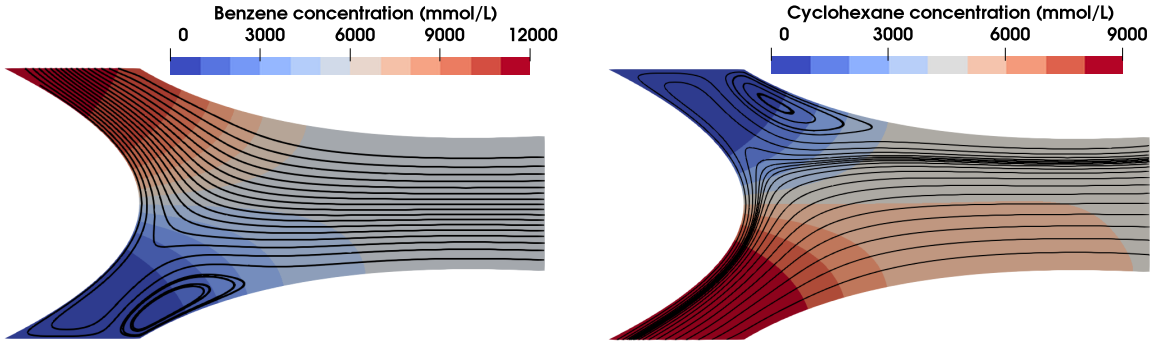


Figure 2.5: Concentrations of benzene (left) and cyclohexane (right), with streamlines computed from their velocities.

We may observe that the pressure profile is smooth. Although the mass-average velocity exhibits rather simple, predictable behaviour, we are also able to resolve the flow fields of the individual species, which are significantly more complex; moreover, these three flow profiles are cleanly distinguished. We see that both species streamlines develop convective rolls, behaviour markedly different from the convective flow.[35]

[35]For reproducibility, the exact software versions used to generate the numerical results in this chapter are archived at https://zenodo.org/record/7017917 [192]; the code, and scripts for the associated plots, are available at https://bitbucket.org/FAznaran/sosm-numerics/. Our implementation of the microfluids problem employs a nondimensionalisation of the SOSM system, which may be detailed in forthcoming work.

Chapter 3

The strain Hodge Laplacian

We now turn to the Hodge Laplacian boundary value problem arising from the strain space $H(\mathrm{inc};\mathbb{S})$ in the strain elasticity complex in 2D:

$$0 \longrightarrow \underset{\text{displacement}}{H^1_{\Gamma_D}(\Omega;\mathbb{R}^2)} \xrightarrow{\varepsilon} \underset{\text{strain}}{H_{\Gamma_D}(\mathrm{inc};\mathbb{S})} \xrightarrow{\mathrm{inc}} \underset{\substack{\text{incompatibility}\\ \text{/curvature}}}{L^2(\Omega)} \longrightarrow 0. \tag{3.0.1}$$

When $|\Gamma_N| = 0$, this is replaced with

$$0 \longrightarrow \underset{\text{displacement}}{H^1_0(\Omega;\mathbb{R}^2)} \xrightarrow{\varepsilon} \underset{\text{strain}}{H_0(\mathrm{inc};\mathbb{S})} \xrightarrow{\mathrm{inc}} \underset{\substack{\text{incompatibility}\\ \text{/curvature}}}{L^2(\Omega)/\mathcal{P}_1(\Omega)} \longrightarrow 0, \tag{3.0.2}$$

and when $|\Gamma_D| = 0$ with

$$0 \longrightarrow \underset{\substack{\text{rigid}\\ \text{motions}}}{RM} \xrightarrow{\subseteq} \underset{\text{displacement}}{H^1(\Omega;\mathbb{R}^2)} \xrightarrow{\varepsilon} \underset{\text{strain}}{H(\mathrm{inc};\mathbb{S})} \xrightarrow{\mathrm{inc}} \underset{\substack{\text{incompatibility}\\ \text{/curvature}}}{L^2(\Omega)} \longrightarrow 0. \tag{3.0.3}$$

Here, as in §1, we assume $\partial\Omega = \Gamma_D \sqcup \Gamma_N$, and Γ_D, Γ_N are each relatively open and Lipschitz with $0 < |\Gamma_D|, |\Gamma_N| < |\partial\Omega|$. The *incompatibility* operator $\mathrm{inc} := \mathrm{rot}\,\mathrm{rot}$ is the linearised Gaussian curvature of the strain field, considered as a metric tensor. Of central interest will be the characterisation of its associated Sobolev space, denoted by $H(\mathrm{inc}) := H(\mathrm{inc};\mathbb{S}) = \mathrm{dom}(\mathrm{inc})$. Its formal adjoint in 2D is the Airy stress operator $\mathrm{airy} := \mathbf{curl}\,\mathrm{curl}$.

Note that we formally have the dualities between the stress and strain complexes (1.0.1)$\longleftrightarrow$(3.0.1), (1.0.2)$\longleftrightarrow$(3.0.2), and (1.0.3)$\longleftrightarrow$(3.0.3), except that the trace operator associated with $H(\mathrm{inc})$ is yet to be clarified – one of the contributions made by this chapter. We therefore focus on the sequence without boundary conditions (3.0.3).

In primal strong form, for given $\mathbb{S}$-valued data f, the strain HL of (3.0.3) seeks a tensor field E, in a space we shall specify, such that

$$\operatorname{airy}\operatorname{inc} E - \varepsilon(\operatorname{div} E) = f \quad \text{in } \Omega. \tag{3.0.4}$$

We denote by $\operatorname{dom}(\operatorname{airy}) := H(\operatorname{airy})$ the domain of the Airy operator. Clearly $H(\operatorname{airy}) = H^2(\Omega)$ by the classical Poincaré inequality for ∇, with the equivalence $\|\cdot\|^2_{\operatorname{airy}} \equiv \|\cdot\|^2_0 + |\cdot|^2_2 \simeq \|\cdot\|^2_2$, but we now retain the former notation in order to emphasise the duality with inc.

In this chapter, we propose a discretisation of the mixed weak form of (3.0.4), based on the adaptation of discontinuous Galerkin FEM (DGFEM) to the incompatibility operator using the symmetric-tensor-valued *Regge* finite element. This strain-displacement formulation serves as a simple candidate model problem for intrinsic linear elasticity in the presence of defects.

First, we describe our motivations, before writing down the problem (3.0.4) precisely in §3.2. Then §3.3 studies the scalar incompatibility operator, clarifying why most results of this chapter do not follow automatically from any existing FEEC framework. In §3.4, we discuss discrete analogues of inc in a DGFEM context and motivate the use of the Regge element, before describing a well-posed DG method in §3.5, providing among the first nonconforming discretisations of the inc operator.

3.1 Motivations: Kröner's theory of defect elasticity

The sequence (3.0.1) in particular encodes as a complex property the differential identity

$$\operatorname{inc} \circ \varepsilon = 0, \tag{3.1.1}$$

and in fact if Ω is simply connected then (3.0.1) is exact at $H(\operatorname{inc})$, giving the integrability condition

$$\ker(\operatorname{inc}; H(\operatorname{inc})) = \varepsilon H^1(\Omega; \mathbb{R}^d). \tag{3.1.2}$$

This is precisely a restatement (with Sobolev regularity) of the classical *St Venant compatibility condition* of linear elasticity, derived in 1860, which models (compatible) strain fields as symmetric gradients: that a tensor field E is inc-free if and only if it is a symmetric gradient. The inc operator is thus sometimes denoted sven.

The pioneering work of Kröner [134] took this further by modelling the presence of defects and dislocations at the microscopic scale precisely by the violation of St Venant compatibility by the strain field, formally deriving $\operatorname{inc} E = \operatorname{curl}\left(\Lambda - \frac{\operatorname{tr}\Lambda}{2}\mathbb{I}\right)$,

where Λ is the (in general, tensor-valued) *density of dislocations*; the presence of defects is therefore formally incorporated into the PDE (3.0.4) by violation of the St Venant compatibility condition, i.e.

$$\operatorname{inc} E \neq 0. \tag{3.1.3}$$

Indeed, the elasticity complex is sometimes called the *Kröner complex*.

Due to its interpretation as a linearised notion of curvature, the inc operator also arises naturally in the Einstein equations of general relativity [138] and the Ricci flow [182]. The inc operator and its discretisation with finite elements have not been studied widely, but extensive functional analysis has been carried out for the 3D, matrix-valued operator $\operatorname{inc} := \operatorname{curl} \circ \top \circ \operatorname{curl}$ by van Goethem and coauthors [4–6, 141]. The same authors propose linearised models of defect elasticity and elasto-plastic behaviour, to be discussed in §3.2.2, based on the incompatibility concept in Kröner's framework, and the models recover standard compatible linear elasticity in a parameter limit; they have observed these models to produce physically realistic simulations at least in academic examples [7].

Such models are *intrinsic* in the sense of solving for the strain tensor, rather than (just) the displacement, as a primary unknown. This perspective goes back to Ciarlet [73, p. 115], who modelled strain fields as identically compatible, $\operatorname{inc} E = 0$ [74], and who identifies the strain field as inducing a Riemannian metric on the reference configuration of the elastic body, the displacement field as an immersion, and the incompatibility tensor as a linearisation of the Riemannian curvature [5].

This chapter is thus motivated by the observation that several other formulations of elasticity arise as Hodge Laplacians from other points in the complexes (1.0.1)–(3.0.1), a canonical example being the Hellinger–Reissner Hodge Laplacian on which we focused in §1, in addition to the pure primal displacement formulation arising from the displacement space $H^1(\Omega;\mathbb{R}^d)$. Many important PDEs (or their linearisations) arise as the HL problem from a space in an appropriately chosen complex, as emphasised in §0.

However, there is no consensus in the literature on a canonical PDE model of linear elasticity in the presence of defects, and we shall mostly regard this application as downstream from this work. We do not claim that (3.0.4) will accurately model defects but only that we are discretising the appropriate operators and spaces for that eventual goal, instead regarding the PDE as of interest in its own right, since numerical solution of HL problems is in any case a topic of central interest in the FEEC [12, p. 39].

3.2 Problem formulation

3.2.1 A strain-displacement formulation

In primal strong formulation, for given $f \in L^2(\Omega;\mathbb{S})$, we seek

$$\begin{aligned} E &\in \operatorname{dom}(\operatorname{airy}\operatorname{inc} - \varepsilon \operatorname{div}) \\ &= \{F \in H(\operatorname{inc}) \cap H_0(\operatorname{div};\mathbb{S}) \mid \operatorname{inc} F \in H_0(\operatorname{airy}), \operatorname{div} F \in H^1(\Omega;\mathbb{R}^2)\} \\ &= \left\{ F \in (H(\operatorname{inc}) \cap H(\operatorname{div}))(\Omega;\mathbb{S}) \;\middle|\; \begin{array}{c} \operatorname{airy}\operatorname{inc} F, \varepsilon \operatorname{div} F \in L^2(\Omega;\mathbb{S}), \\ \operatorname{inc} F = \partial_{\mathbf{n}}(\operatorname{inc} F) = 0 \text{ and } F\mathbf{n} = 0 \text{ on } \partial\Omega \end{array} \right\} \end{aligned} \tag{3.2.1}$$

such that

$$\operatorname{airy}\operatorname{inc} E - \varepsilon(\operatorname{div} E) = f \text{ in } \Omega, \tag{3.2.2}$$

where

$$H_0(\operatorname{airy}) := H^2_0(\Omega) = \{v \in H^2(\Omega) \mid v = \partial_{\mathbf{n}} v = 0 \text{ on } \partial\Omega\}. \tag{3.2.3}$$

Note that the space (3.2.1) encodes strongly imposed boundary conditions, and that its constraints are not assumptions of elliptic regularity. As a result, the boundary value problem (3.2.2) is equivalent (not just formally) to the primal weak form, which one may consider for Galerkin discretisation:[36] seek $E \in H(\operatorname{inc}) \cap H_0(\operatorname{div};\mathbb{S})$ such that

$$\int_\Omega (\operatorname{inc} E)(\operatorname{inc} F) + \operatorname{div} E \cdot \operatorname{div} F \, \mathrm{d}x = \int_\Omega f : F \, \mathrm{d}x \qquad \forall\, F \in H(\operatorname{inc}) \cap H_0(\operatorname{div};\mathbb{S}). \tag{3.2.4}$$

As is typical with primal HL problems arising not from the 'first' or 'last' space in a complex, note that the test and trial space in (3.2.4) does not arise directly in any version of the complexes (1.0.1)–(1.0.3), (3.0.1)–(3.0.3), and appears difficult to discretise. We therefore consider the following equivalent, amenable mixed weak formulation of the problem, with dual variable $u := -\operatorname{div} E$ interpreted as the elastic displacement: seek the strain-displacement pair $(E, u) \in H(\operatorname{inc}) \times H^1(\Omega;\mathbb{R}^2)$ such that

$$\int_\Omega (\operatorname{inc} E)(\operatorname{inc} F) + \varepsilon(u) : F \, \mathrm{d}x = \int_\Omega f : F \, \mathrm{d}x \quad \forall\, F \in H(\operatorname{inc}), \tag{3.2.5a}$$

$$\int_\Omega \varepsilon(v) : E - u \cdot v \, \mathrm{d}x = 0 \qquad \forall\, v \in H^1(\Omega;\mathbb{R}^2). \tag{3.2.5b}$$

[36] By analogy, observe that by definition the domain of the Neumann–Laplace problem at $H^1(\Omega)$ for the de Rham sequence (0.1.2) has HL operator with domain $\{u \in H^1(\Omega) \mid \nabla u \in H_0(\operatorname{div})\} = \{u \in H^1(\Omega) \mid \Delta u \in L^2(\Omega), \partial_{\mathbf{n}} u = 0 \text{ on } \partial\Omega\}$.

The strain tensor is classically viewed as a metric tensor; in geometric terms this means it is the matrix proxy to a symmetric covariant 2-tensor field, which moreover is everywhere positive definite. As identified back in §1.6.1, the correct notion of pullback for the $H(\mathrm{inc})$ space, and any FE space by which it is discretised, is therefore given by the double covariant Piola map (1.3.8).

3.2.2 Comparison to the linear models of van Goethem et al.

We now compare the model problem (3.2.5) to a linearised intrinsic model of defect elasticity proposed by van Goethem and coauthors, and argue that implicit in some of this existing work are concepts readily provided already by the structure of the elasticity complexes (0.1.3) and (3.0.3).

Observe that Kröner's condition (3.1.3) is naturally interpretable in terms of the Hodge decomposition of the base strain space (2.2.6),

$$L^2(\Omega;\mathbb{S}) = \varepsilon H_0^1(\Omega;\mathbb{R}^2) \oplus_{L^2} \text{airy}\, H(\text{airy}) = \varepsilon H^1(\Omega;\mathbb{R}^2) \oplus_{L^2} \text{airy}\, H_0(\text{airy}), \tag{3.2.6}$$

revealing that the incompatible component of a strain field is exactly its divergence-free component. The three-dimensional analogue of the orthogonal decomposition (3.2.6), i.e. the Hodge decomposition of $L^2(\Omega;\mathbb{S})$ in (0.1.3), has been generalised in [141] to tensor fields in $L^p(\Omega;\mathbb{S}), 1 < p < \infty$, and proposed by van Goethem (by its classical name, the *Beltrami decomposition*) as an alternative to the classical elasto-plastic decomposition of the strain tensor from plasticity theory [5]. For example, it is observed to be preferable in being unique upon prescribing boundary conditions for the displacement field; indeed, this is *always* true of the Hodge decomposition, as may be seen from *both* decompositions in the special case (3.2.6). Analogously, the application of this general case in the same work [141] to prove the Korn inequality for vector fields in $W^{1,p}(\Omega;\mathbb{R}^3), 1 < p < \infty$, is, in FEEC terms, a generalisation to the non-Hilbertian case of the Poincaré inequality associated with $H^1(\Omega;\mathbb{R}^3)$ in the sequence (0.1.3), which follows automatically by the bounded inverse theorem and the closedness of (0.1.3).

Recently in [7], the same authors proposed an intrinsic model of small-strain incompatible elasticity given by seeking the strain field $E \in \mathcal{H}$ with

$$\int_\Omega \mathbb{C}E : F + \mathbb{D}\,\mathrm{inc}\,E : \mathrm{inc}\,F \,\mathrm{d}x = \int_\Omega \mathcal{K} : F \,\mathrm{d}x \qquad \forall\, F \in \mathcal{H}, \tag{3.2.7}$$

where $\mathbb{C}$ is the elasticity tensor, $\mathbb{D}$ is symmetric and uniformly positive definite, and $\mathcal{K}$ is a tensor field representing external work. Here in 3D, the partially trace-free

space $\mathcal{H}$ is defined as $\{F \in H(\mathrm{inc}) \mid \mathcal{T}_0(E) = \mathcal{T}_1(E) = 0 \text{ on } \Gamma \subseteq \partial\Omega\}$, where $\mathcal{T}_0, \mathcal{T}_1$ are trace operators discussed below in (3.3.1). The deformed solid body is endowed with metric induced by the matrix field $g = \mathbb{I} + 2E$, whose Riemannian curvature tensor in the small strain regime is $\mathrm{inc}\, E$ (up to constants in each component). Equation (3.2.7) is then obtained as the Newton linearisation of a proposed plastic flow rule.

Observe that up to the identification of the symmetric positive definite tensors $\mathbb{C}, \mathbb{D}$ with the identity, equation (3.2.7) is essentially equivalent to solving the $H(\mathrm{inc})$ Riesz map $(E, F)_{H(\mathrm{inc})} = \langle \mathcal{K}, F \rangle \ \forall\ F \in H(\mathrm{inc})$, where $\langle \cdot, \cdot \rangle$ denotes the dual pairing of $H(\mathrm{inc})^*$. Such an identification between tensors is exactly the equivalence between the mixed form of the Poisson Hodge Laplacian and Darcy flow, as pointed out in §0.2.1. Its leading-order operator essentially coincides with that in our formulation of interest (3.2.4), subject to the constraint $\mathrm{div}\, E = 0$, which encodes incompatibility as already argued; this may be thought of as 'half' a HL operator, and in fact will turn out to be crucial to our analysis in §3.5.2. The zeroth-order perturbation term $(\mathbb{C}E, F)_{L^2}$ is moreover natural to weight with the elasticity tensor $\mathbb{C}$, as the base strain space $L^2(\Omega; \mathbb{S})$ in (3.0.3) may be weighted with $\mathbb{C} = \mathcal{A}^{-1}$ in duality with the weighting of the base stress space with $\mathcal{A}$ as specified back in §1; in FEEC terms, the constitutive law which relates the strain to the stress, and the strain complex to the stress complex, is in analogy to the Hodge star between differential forms [12, Section 8.6].

For finite element appoximation, the Beltrami decomposition is used to derive a mixed displacement-strain-displacement formulation in $H^1(\Omega; \mathbb{R}^3) \times H(\mathrm{inc}) \times H^1(\Omega; \mathbb{R}^3)$, the secondary displacement field arising also as a potential for $\mathcal{K}$ which is not directly known. The resulting mixed weak formulation [7, p. 14] is still recognisably comparable to our mixed weak form (3.2.5), apart from low-order cross terms arising from the zeroth-order perturbation and the secondary displacement field.

In [141], the authors draw analogy between the St Venant condition and determining whether a curl-free vector field is conservative, a question answered by the classical Poincaré lemma and equivalent to exactness of the de Rham sequence (0.1.2) at $H(\mathrm{curl})$, but draw no further connection to the FEEC. The Hodge Laplace problem (3.2.2) is anticipated to be a problem of interest in its own right, and with it we may apply the theoretical FEEC machinery discussed in §0.2 and §1.6.1 to inherit well-posedness and give clues to discretisation.

3.3 The incompatibility operator

3.3.1 Green's formulae

We first make note of the following theorem in 3D due to van Goethem & Amstutz [4]: for $\Omega \subseteq \mathbb{R}^3$ with smooth boundary, $E \in C^2\left(\overline{\Omega}; \mathbb{S}\right), S \in H^2(\Omega; \mathbb{S})$,

$$\int_\Omega E : \operatorname{inc}(S)\ \mathrm{d}x = \int_\Omega \operatorname{inc}(E) : S\ \mathrm{d}x + \int_{\partial\Omega} \mathcal{T}_1(E) : S + \mathcal{T}_0(E) : \partial_{\mathbf{n}} S\ \mathrm{d}s, \tag{3.3.1}$$

where

$$\begin{aligned} \mathcal{T}_0(E) &:= (E \times \mathbf{n})^\top \times \mathbf{n} \in H^{-1/2}(\partial\Omega; \mathbb{S}), \\ \mathcal{T}_1(E) &:= \operatorname{sym}(\operatorname{curl}(E \times \mathbf{n})^\top) + \\ &\qquad ((\partial_{\mathbf{n}} + k)E \times \mathbf{n})^\top \times \mathbf{n} + \operatorname{sym}((\operatorname{curl} E)^\top \times \mathbf{n}) \in H^{-3/2}(\partial\Omega; \mathbb{S}), \end{aligned} \tag{3.3.2}$$

and k is twice the mean (extrinsic) curvature of $\partial\Omega$. For the two-dimensional case, we now derive novel Green's formulae which relate the scalar inc operator to its formal adjoint, the Airy operator. For $\mathbf{n}$ the outward pointing unit normal to a given boundary, let $\mathbf{t} := \mathbf{n}^\perp = L\mathbf{n}$ denote the unit tangent, where

$$L = \begin{pmatrix} & -1 \\ 1 & \end{pmatrix} \tag{3.3.3}$$

is anticlockwise rotation. For the remainder of this section, we assume $\Omega \subseteq \mathbb{R}^2$ is a bounded domain, with trivial topology, and that $\partial\Omega$ is at least C^2. For all $E \in C^2(\overline{\Omega}; \mathbb{S}), S \in C^2(\overline{\Omega})$, we compute that

$$\begin{aligned} \int_\Omega (\operatorname{inc} E) S\ \mathrm{d}x &= \int_\Omega (\operatorname{rot} E) \cdot \operatorname{curl} S\ \mathrm{d}s + \int_\Gamma ((\operatorname{rot} E) \cdot \mathbf{t}) S\ \mathrm{d}s \\ &= \int_\Omega E : \operatorname{airy} S\ \mathrm{d}x + \int_\Gamma ((\operatorname{rot} E) \cdot \mathbf{t}) S + (\operatorname{curl} S) \cdot E\mathbf{t}\ \mathrm{d}s, \end{aligned} \tag{3.3.4}$$

where $\Gamma := \partial\Omega$. Decomposing the final surface term, we have

$$\int_\Gamma (L^{-1}\nabla S) \cdot E\mathbf{t}\ \mathrm{d}s = \int_\Gamma -(\partial_{\mathbf{n}} S)(E\mathbf{t} \cdot \mathbf{t}) + (\partial_{\mathbf{t}} S)(E\mathbf{t} \cdot \mathbf{n})\, \mathrm{d}s, \tag{3.3.5}$$

and by the divergence theorem for the tangential gradient $\nabla_\Gamma := (\partial_{\mathbf{t}} \cdot)\mathbf{t}$ and the tangential divergence $\operatorname{div}_\Gamma \mathbf{f} := \nabla_\Gamma \cdot \mathbf{f}$ (e.g. [80, Theorem 2.10]),

$$\begin{aligned} \int_\Gamma (\partial_{\mathbf{t}} S)(E\mathbf{t} \cdot \mathbf{n})\, \mathrm{d}s &= \int_\Gamma (\nabla_\Gamma S) \cdot E^\top \mathbf{n}\ \mathrm{d}s \\ &= \int_\Gamma (\mathbf{n} \cdot E^\top \mathbf{n}) S\kappa - S \operatorname{div}_\Gamma (E^\top \mathbf{n})\, \mathrm{d}s + \int_{\partial\Gamma} S(E^\top \mathbf{n}) \cdot \pi\ \mathrm{d}s \\ &= \int_\Gamma (\mathbf{n} \cdot E\mathbf{n}) S\kappa - S\partial_{\mathbf{t}} (\mathbf{n} \cdot E\mathbf{t})\, \mathrm{d}s + \int_{\partial\Gamma} S(E\mathbf{n}) \cdot \pi\ \mathrm{d}s, \end{aligned} \tag{3.3.6}$$

where $\kappa(\mathbf{x}) = -\frac{1}{2}\operatorname{div}_\Gamma \mathbf{n}(\mathbf{x})$ is the curvature of Γ at $\mathbf{x} \in \Gamma$, and π is the conormal to Γ, a term we may drop since Γ is a compact hypersurface (giving $\partial\Gamma = \emptyset$). This gives the overall Green's formula

$$\int_\Omega E : \operatorname{airy} S \, \mathrm{d}x = \int_\Omega (\operatorname{inc} E) S \, \mathrm{d}x + \int_\Gamma \mathcal{T}_0(E)\partial_{\mathbf{n}} S + \mathcal{T}_1(E) S \, \mathrm{d}s, \tag{3.3.7}$$

where, comparing with (3.3.1), we have defined

$$\mathcal{T}_0(E) := \mathbf{t} \cdot E\mathbf{t}, \tag{3.3.8a}$$

$$\mathcal{T}_1(E) := \partial_{\mathbf{t}}(\mathbf{n} \cdot E\mathbf{t}) - (\mathbf{n} \cdot E\mathbf{n})\kappa - (\operatorname{rot} E) \cdot \mathbf{t}. \tag{3.3.8b}$$

3.3.2 Traces and exactness

We now characterise the correct notion of traces for the $H(\operatorname{inc})$ space, which is necessary to even define the vanishing-trace subspaces in (3.0.1), (3.0.2). We follow *mutatis mutandis* the procedure for normal traces of $H(\operatorname{div})$ functions in [12, Section 3.4].

Proposition 3.3.1. (Annihilator of $H_0(\operatorname{airy})$). *If $L \in H(\operatorname{airy})^*$ vanishes on $H_0(\operatorname{airy})$, then there exists a unique $(\mathfrak{t}_0, \mathfrak{t}_1) \in (H^{1/2} \times H^{-3/2})(\partial\Omega)$ such that*

$$Lv = \langle \partial_{\mathbf{n}} v, \mathfrak{t}_0 \rangle_{\partial\Omega} + \langle \mathfrak{t}_1, v \rangle_{\partial\Omega} \ \ \forall\ v \in H(\operatorname{airy}), \tag{3.3.9}$$

and $\|(\mathfrak{t}_0, \mathfrak{t}_1)\|_{\frac{1}{2}\times-\frac{3}{2},\partial\Omega} \lesssim \|L\|_{H(\operatorname{airy})^*}$.

Proof. Define $j : H(\operatorname{airy}) \to (H^{-1/2} \times H^{3/2})(\partial\Omega)$ by the traces $j(S) = (\partial_{\mathbf{n}} S, S)$. Then j is bounded linear with kernel $H_0(\operatorname{airy})$. Let $(y, Y) \in (H^{-1/2} \times H^{3/2})(\partial\Omega)$; we show that j is surjective.

There exists $w \in H(\operatorname{div})$ with $y = w \cdot \mathbf{n}$. Choose $z \in H^2(\Omega)/\mathbb{R}$ to be the unique solution of

$$-\Delta z = -\operatorname{div} w \ \text{ in } \Omega, \qquad \partial_{\mathbf{n}} z = 0 \ \text{ on } \partial\Omega. \tag{3.3.10}$$

Then $\operatorname{div}\nabla z = \operatorname{div} w$, i.e. $w, \nabla z$ coincide up to a curl, so for all $b \in H^1(\Omega)$,

$$\langle y, b \rangle_{\partial\Omega} = \int_\Omega (\operatorname{div} w) b + w \cdot \nabla b \, \mathrm{d}x = \int_\Omega (\operatorname{div}\nabla z) b + \nabla z \cdot \nabla b \, \mathrm{d}x, \tag{3.3.11}$$

and hence $\nabla z \cdot \mathbf{n} = y$. A minor subtlety in working with this higher-order trace, familiar from the analysis of biharmonic problems and already clear from the definition of $H_0(\operatorname{airy})$ (3.2.3), is that the zeroth-order trace is enough to specify tangential derivative traces, and *a priori* the subspaces of $H(\operatorname{airy})$ mapping surjectively onto

$H^{1/2}$ and $H^{-3/2}$ could be orthogonal. This is corrected simply by solving the Laplace problem

$$-\Delta z' = 0 \ \text{ in } \Omega, \qquad z' = Y \ \text{ on } \partial\Omega \tag{3.3.12}$$

for $z' \in H^2(\Omega)$, so that $j(z + z') = (y, Y)$.

Identifying $H^{-1/2}(\partial\Omega)^* = H^{1/2}(\partial\Omega)$ and by [12, Lemma 3.10], the dual $j^* : (H^{1/2} \times H^{-3/2})(\partial\Omega) \to H(\text{airy})^*$ is therefore a bounded injection with image the annihilator of $H_0(\text{airy})$, which gives the statement. □

Theorem 3.3.1. (Traces in $H(\text{inc})$). *The map* $E \mapsto (\mathcal{T}_0(E), \mathcal{T}_1(E)), C^2(\overline{\Omega}; \mathbb{S}) \to C^0(\partial\Omega)^2$, *extends to a bounded linear trace operator* $\mathcal{T} : H(\text{inc}) \to (H^{1/2} \times H^{-3/2})(\partial\Omega)$ *which moreover satisfies the Green's formula* (3.3.7) *for all* $S \in H(\text{airy})$.

Proof. Fix $E \in H(\text{inc})$ and define $L_E \in H(\text{airy})^*$ by

$$L_E(S) = \int_\Omega E : \text{airy}\, S - (\text{inc}\, E)S \ \mathrm{d}x, \tag{3.3.13}$$

which vanishes on $C_c^\infty(\Omega)$ by (3.3.7), and by density also on $H_0(\text{airy})$. Proposition 3.3.1 gives a unique pair $\mathcal{T}E = (\mathfrak{t}_0(E), \mathfrak{t}_1(E)) \in (H^{1/2} \times H^{-3/2})(\partial\Omega)$ with

$$\int_\Omega E : \text{airy}\, S - (\text{inc}\, E)S \ \mathrm{d}x = \langle \partial_{\mathbf{n}} S, \mathfrak{t}_0(E)\rangle_{\partial\Omega} + \langle \mathfrak{t}_1(E), S\rangle_{\partial\Omega} \ \forall\, E \in H(\text{inc}), S \in H(\text{airy}), \tag{3.3.14}$$

and

$$\|\mathcal{T}E\|_{\frac{1}{2}\times-\frac{3}{2},\partial\Omega} = \sup_{S\in H(\text{airy})} \frac{\int_\Omega E : \text{airy}\, S - (\text{inc}\, E)S \ \mathrm{d}x}{\|S\|_{\text{airy}}} \leq \sqrt{2}\|E\|_{\text{inc}}. \tag{3.3.15}$$

To interpret $\mathcal{T}$, we see that for fixed $E \in C^2(\overline{\Omega}; \mathbb{S})$, each integral in (3.3.7) is $\|\cdot\|_{\text{airy}}$-bounded as a function of $S \in C^2(\overline{\Omega})$, so (3.3.7) holds for all $S \in H(\text{airy})$ by density of $C^\infty(\overline{\Omega})$ in $H(\text{airy})$. Since the pair $\mathcal{T}E$ is uniquely determined by the relation (3.3.14), we have

$$(\mathfrak{t}_0(E), \mathfrak{t}_1(E)) = (\mathcal{T}_0(E), \mathcal{T}_1(E)) \tag{3.3.16}$$

whenever $E \in C^2(\overline{\Omega}; \mathbb{S})$. □

Definition 3.3.1. (Vanishing on the boundary in $H(\text{inc})$). The trace-free subspace of $H(\text{inc})$ is defined as $H_0(\text{inc}) := \{E \in H(\text{inc}) \mid \mathcal{T}_0(E) = \mathcal{T}_1(E) = 0 \text{ on } \partial\Omega\}$.

With this structure in place, the following result is elementary; it is not surprising, as exactness of a complex is typically inherited by its adjoint sequence, but we explicitly prove the following special case, as adjoints and exactness for the elasticity complexes have only partially been clarified in the literature.

Lemma 3.3.1. (Exactness of the strain complex with boundary conditions). *The strain complex with boundary conditions* (3.0.2) *is exact, provided* Ω *is simply connected.*

Proof. If $E = \varepsilon(u)$ for some $u \in H^1_0(\Omega;\mathbb{R}^2)$, then for all $S \in H(\mathrm{airy})$,

$$\begin{aligned}\langle \partial_{\mathbf{n}} S, \mathcal{T}_0(E)\rangle_{\partial\Omega} + \langle \mathcal{T}_1(E), S\rangle_{\partial\Omega} &= \int_\Omega E : \mathrm{airy}\, S - (\mathrm{inc}\, E)S \,\mathrm{d}x = \int_\Omega \varepsilon(u) : \mathrm{airy}\, S \,\mathrm{d}x \\ &= \langle (\mathrm{airy}\, S)\mathbf{n}, u\rangle_{\partial\Omega} - \int_\Omega \mathrm{div}(\mathrm{airy}\, S)\cdot u \,\mathrm{d}x = 0,\end{aligned} \tag{3.3.17}$$

i.e. $(\mathcal{T}_1(E), \mathcal{T}_1(E))$ vanish in $(H^{1/2}\times H^{-3/2})(\partial\Omega)$. Conversely if $E \in \ker(\mathrm{inc}; H_0(\mathrm{inc}))$, then $E \perp_{L^2} \mathrm{airy}\, H(\mathrm{airy})$, so by the Hodge decomposition of the strain complex without boundary conditions (3.0.3), we have $E = \varepsilon(u)$ for some $u \in H^1(\Omega;\mathbb{R}^2)$. For all $S \in H(\mathrm{airy})$,

$$0 = \int_\Omega \varepsilon(u) : \mathrm{airy}\, S \,\mathrm{d}x = \langle (\mathrm{airy}\, S)\mathbf{n}, u\rangle_{\partial\Omega} - \int_\Omega \underbrace{\mathrm{div}(\mathrm{airy}\, S)}_{=0}\cdot u \,\mathrm{d}x. \tag{3.3.18}$$

By surjectivity of $S \mapsto (\mathrm{airy}\, S)\mathbf{n}, H(\mathrm{airy}) \to H^{-1/2}(\partial\Omega)$, we can choose $(\mathrm{airy}\, S)\mathbf{n}$ to be the Hahn–Banach norming functional of $u|_{\partial\Omega} \in H^{1/2}(\partial\Omega)$, i.e. we must have $u|_{\partial\Omega} = 0$.

If $E \in H_0(\mathrm{inc})$, then (3.3.7) clearly gives $\mathrm{inc}\, E \perp_{L^2(\Omega)} \mathcal{P}_1(\Omega)$. Conversely, let $S \in \mathcal{P}_1(\Omega)^{\perp_{L^2(\Omega)}}$. Observe that for scalar fields w, r we have the identity

$$\mathrm{airy}\, w : \mathrm{airy}\, r \equiv \nabla^2 w : \nabla^2 r, \tag{3.3.19}$$

so by the regularity theory of the biharmonic problem with homogeneous boundary conditions, there exists a unique $w \in H^4(\Omega)\cap H_0(\mathrm{airy})$ with

$$\int_\Omega \mathrm{airy}\, w : \mathrm{airy}\, r \,\mathrm{d}x = \int_\Omega Sr \,\mathrm{d}x \qquad \forall r \in H_0(\mathrm{airy}), \tag{3.3.20}$$

so $w = \partial_{\mathbf{n}} w = 0$ on $\partial\Omega$ with $S = \mathrm{inc}\,\mathrm{airy}\, w$. □

3.3.3 A remark on abstract Hilbert traces

We discuss our result, Theorem 3.3.1, in the context of the very recent framework [110] for trace operators on abstract Hilbert complexes. There is no notion of 'boundary' in an abstract Hilbert space, so given an abstract closed Hilbert complex, the work [110] (in the notation of page iv) uses relations of the form $H(\mathrm{op};\mathbb{X})/H_0(\mathrm{op};\mathbb{X}) \simeq TH(\mathrm{op};\mathbb{X})$ (which hold in $\mathbb{R}^d$ for $\partial\Omega$ of sufficient regularity)

to *define* the trace spaces, and the notion of 'boundary' is subsumed into an assumption of the existence of an L^2-dense closed subcomplex of spaces $H_*(\mathrm{op};\mathbb{X})$ playing the role of the trace-free subspaces $H_0(\mathrm{op};\mathbb{X})$ [110, Eq. (2.8a)]. The framework makes precise the observation that for a given operator, passing to the trace space commutes with taking the dual, as is easily seen in Theorem 3.3.1. However, to our knowledge this abstraction does not provide a classical interpretation of the trace operator on a smoother subspace in the sense of (3.3.8), which justifies its computation by hand.

A further potential criticism of [110] is the apparently arbitrary manner in which the trace operator is 'hidden' in assuming the existence of the dense subcomplex, whose closed subspaces $H_*(\mathrm{op};\mathbb{X})$ could *a priori* encode conditions other than being trace-free. However, due to the density assumption, this may still be seen to be inherent to the notion of traces in the following sense. In the abstract setting of sequences of smooth differential k-forms (to which functions in the de Rham complex are proxy) as introduced in §1.6.1, Brüning & Lisch [50] observe that $H_0\Lambda^k := \overline{C_c^\infty\Lambda^k}^{\|\cdot\|_{\mathrm{d}}}$ is the domain of the minimal closed extension of d, while $H\Lambda^k$ is the domain of its maximal closed extension. For the Sobolev functions proxy to these differential forms, it follows that the Sobolev space playing the role of the (trace-free) dense subspace $H_*(\mathrm{op};\mathbb{X})$ must, indeed, lie 'between' $H_0(\mathrm{op};\mathbb{X})$ and $H(\mathrm{op};\mathbb{X})$, which corresponds to (for example) the subspace vanishing in the trace sense on only a part of the boundary $\Gamma \subsetneq \partial\Omega$ (for Γ of sufficient regularity).

3.4 Discrete incompatibility and the Regge element

For discretisation of the model problem, symmetric tensor elements conforming to the $H(\mathrm{inc})$ space have been recently constructed [72], but in this section, we argue why a DG-type method is appropriate specifically for the strain HL.

In [117], a framework is provided for the DGFEM discretisation of HL problems arising in the de Rham complex in arbitrary dimensions. It is known that the elasticity complex may be constructed via the de Rham complex [20], but this connection is nontrivial and we prefer to attack (3.0.4) directly.

We assume now that Ω is polygonal, and let $\mathcal{T}_h$ denote a quasi-uniform triangulation thereof. We proceed with the DG notation $\mathcal{E}_h^\circ, \Lambda_h, [\![\cdot]\!]$ introduced in §1.5; in addition, for a given cell K, denote the set of its edges by $\mathcal{E}(K)$, and by $\mathcal{E}_h = \cup_{K\in\mathcal{T}_h}\cup_{\mathbf{e}\in\mathcal{E}(K)}\mathbf{e}$ the set of all edges of $\mathcal{T}_h$. On an interior edge $\mathbf{e} = \partial K \cap \partial K'$, let $\{v_h\} := \frac{1}{2}(v_h|_K + v_h|_{K'})$ denote the average, defined as the identity on an exterior

edge $\mathbf{e} \subseteq \partial\Omega$. We introduce the shorthand $\int_{\mathcal{T}_h} := \sum_{K\in\mathcal{T}_h} \int_K$, $\int_{\mathcal{E}_h^{(\circ)}} := \sum_{\mathbf{e}\in\mathcal{E}_h^{(\circ)}} \int_{\mathbf{e}}$, and the corresponding inner products induce norms $\|\cdot\|_{0,\mathcal{T}_h}, \|\cdot\|_{\mathcal{E}_h^{(\circ)}}$.

3.4.1 The Regge finite element

It is natural to first consider C^0-interior penalty methods for the airy inc operator due to its 4^{th} order nature, as have been very successful for the biharmonic problem [49]. The comparable model detailed above in §3.2.2 was solved for a strain tensor with the scalar $H^2(\Omega)$-conforming Hsieh–Clough–Tocher element in each component in order to avoid the direct discretisation of $H(\text{inc})$. However, the exact solution to the primal problem (3.0.4) might not lie in $H^1(\Omega;\mathbb{S})$, and we anticipate an incompatible strain field to be of low regularity, so that an even weakly $H^1(\Omega;\mathbb{S})$-conforming numerical solution could be spurious. Such a situation is familiar in being even a motivation for the invention of what is now called the FEEC, in that spurious solutions arise from the use of Lagrange (rather than Nédélec) elements for the Maxwell eigenproblem [12, p. 9], or more generally for high-order curl source and eigenproblems, due to the lack of discrete cohomological structure [125]; this lies in analogy with the Lavrentiev gap phenomenon.

Secondly, in anticipation of application to the scheme to fracture mechanics, the fully discontinuous Galerkin method is well-known to incorporate the possibility of shock-/singularity-capture through the development of Riemann solvers or slope limiters. In particular, the Lagrangian associated with a DG scheme will include normed jumps of the solution tuple across element boundaries, as for example in (1.5.8), which may be interpreted as the energetic cost of crack creation or propagation [77].

Thirdly, motivated to discretise the mixed formulation (3.2.5), to resolve the $-\varepsilon\,\mathrm{div}$ term it is in addition essential to be guided by the structure of a discrete elasticity complex, for which proof of the inf-sup compatibility condition is tractable. Discrete elasticity complexes more regular than the Regge complex (see (3.4.2) below, which we shall use) which provide a $H^1(\Omega;\mathbb{S})$-conforming metric tensor do exist (in analogy to the Stokes complex and its subcomplexes as smoothed versions of the de Rham complex), but to date, only on specialised meshes, such as the Alfeld/Worsey–Farin split [70].

We propose the symmetric-tensor-valued *generalised Regge finite element* to discretise the strain field. Regge [165] postulated a formalism for producing simplicial approximations to spacetimes in general relavitity, the so-called *Regge calculus*, using piecewise constant metric tensors; this produced a corresponding discrete formulation of the Einstein equations which made them amenable to numerical simulation.

This method has been interpreted in FEEC terms, in particular as a concrete finite element space in 3D nonconforming to $\{F \in L^2(\Omega;\mathbb{S}) \mid \operatorname{inc} F \in H^{-1}(\Omega;\mathbb{S})\}$, by Christiansen [67, 69], and then generalised to arbitrary polynomial order and dimension in the recent PhD thesis of Li [138], who applied them to discretise the metric tensor of general relativity. A Regge-valued finite element solution thus inherits a clear interpretation as a metric. The simplicial Riemannian metric and corresponding Gaussian curvature induced by the Regge space can be understood in a distributional sense [38], as we touch on in the next subsection.

The Regge element is characterised by tangential-tangential continuity. It is globally defined for degree $k \geq 0$ as

$$\mathbb{REG}_h^k := \{F \in \mathrm{DG}_k(\mathcal{T}_h;\mathbb{S}) \mid [\![\mathbf{t} \cdot F\mathbf{t}]\!] = 0 \text{ on } \mathcal{E}_h^\circ\}. \tag{3.4.1}$$

Consequently, the Regge space is partially inc-conforming in that it is $\mathcal{T}_0$-continuous over mesh edges. By a rotation of its rows, at lowest order it coincides with the HHJ element in 2D and forms a strict subset of the TDNNS element in 3D, each described in §1.2.3. In this lowest order case, for which a schematic is provided in Figure 3.1, the degrees of freedom are given by the mean of the tangential-tangential components on each edge. On a cell K, DOFs for the kth-degree element are given by tangential-tangential moments up to degree k over edges, and internal moments $F \mapsto \int_K F : B \, \mathrm{d}x$ against elements B of a basis of $\mathcal{P}_{k-1}(K;\mathbb{S})$.

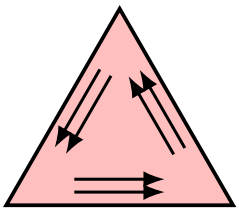


Figure 3.1: The 0^{th}-order generalised Regge finite element [138].

The associated Regge complex may be connected to the 2D strain complex via appropriate densely defined commuting interpolants, in the lowest-order case as

$$\begin{array}{ccccccccc}
0 & \longrightarrow & RM & \xrightarrow{\subseteq} & H^1(\Omega;\mathbb{R}^2) & \xrightarrow{\varepsilon} & H(\mathrm{inc}) & \xrightarrow{\mathrm{inc}} & L^2(\Omega) & \longrightarrow & 0 \\
 & & \downarrow{\scriptstyle \mathrm{id}} & & \downarrow{\scriptstyle I_h^0} & & \downarrow{\scriptstyle I_h^1} & & \downarrow{\scriptstyle I_h^2} & & \\
0 & \longrightarrow & RM & \xrightarrow{\subseteq} & \mathrm{CG}_1(\mathcal{T}_h;\mathbb{R}^2) & \xrightarrow{\varepsilon} & \mathbb{REG}_h^0 & \xrightarrow{\mathrm{inc}} & X_h & \longrightarrow & 0.
\end{array} \tag{3.4.2}$$

Here $X_h := \{\delta_{\mathbf{x}} \mid \mathbf{x} \in \Lambda_h\}$ is a distributional element whose shape functions are measures, the Dirac masses supported on mesh vertices Λ_h, hence is not a finite element in the classical Ciarlet sense. This structure follows from [69] and explicit computations which we provide in the next subsection.

3.4.2 Discrete Green's formulae

As the Regge space is $H(\mathrm{inc})$-nonconforming, in this subsection we carefully consider mesh-dependent analogues of the inc operator in the framework of DGFEM.

We cannot apply cell-by-cell the Green's formula (3.3.7), because on the edges of triangular cells one cannot compute curvature in the classical sense; edges have no curvature other than that arising from the discontinuous jump in the normal vector $\mathbf{n}$ at the vertices. Instead, given a cell $K \in \mathcal{T}_h$ and $E \in C^2(\overline{K}; \mathbb{S}), S \in C^2(\overline{K})$, we apply edge-wise the formula (3.3.6). Thus, curvature vanishes, but one cannot drop the conormal term:

$$\int_{\partial K} (\partial_{\mathbf{t}} S)(E\mathbf{t} \cdot \mathbf{n}) \, \mathrm{d}s = \sum_{\mathbf{e} \in \mathcal{E}(K)} \int_{\mathbf{e}} -S \partial_{\mathbf{t}} (\mathbf{n} \cdot E\mathbf{t}) \, \mathrm{d}s + \int_{\partial \mathbf{e}} S(E\mathbf{n}) \cdot \pi \ \mathrm{d}s, \tag{3.4.3}$$

in which $\mathcal{E}(K)$ denotes the set of edges of K. We thus obtain the discrete Green's formula

$$\begin{aligned} \int_K E : \operatorname{airy} S \ \mathrm{d}x = \int_K \operatorname{inc}(E) S \ \mathrm{d}x + \sum_{\mathbf{e} \in \mathcal{E}(K)} \int_{\mathbf{e}} \mathcal{T}_0(E) \partial_{\mathbf{n}} S + (\partial_{\mathbf{t}} (\mathbf{n} \cdot E\mathbf{t}) - \mathbf{t} \cdot \operatorname{rot} E) S \ \mathrm{d}s \\ + \sum_{\mathbf{e} \in \mathcal{E}(K)} \sum_{\mathbf{x} \in \partial \mathbf{e}} (-1)^{[\mathbf{e}, \mathbf{x}]} (\mathbf{n} \cdot E\mathbf{t})(\mathbf{x}) S(\mathbf{x}), \end{aligned} \tag{3.4.4}$$

with Iverson bracket negating the sign only if $\mathbf{e}$ starts at $\mathbf{x}$:

$$[\mathbf{e}, \mathbf{x}] := [\mathbf{x} \text{ is the start point of } \mathbf{e}] = \begin{cases} 1 & \text{if } \mathbf{e} \text{ starts at } \mathbf{x}, \\ 0 & \text{if } \mathbf{e} \text{ ends at } \mathbf{x}. \end{cases} \tag{3.4.5}$$

This recovers [65, Eq. 34]; we place terms in order of codimension of their 'integration domain'.

Consequently if $E_h \in \mathrm{DG}_k(\mathcal{T}_h; \mathbb{S})$ and $\phi \in C_c^\infty(\Omega)$, then the distributional incompatibility of E_h across the mesh, $\operatorname{inc} E_h \in \mathcal{D}'(\Omega)$, is given by taking the sum over all cells in (3.4.4):

$$\begin{aligned} \langle \operatorname{inc} E_h, \phi \rangle &:= \int_\Omega E_h : \operatorname{airy} \phi \ \mathrm{d}x \\ &= \int_{\mathcal{T}_h} \operatorname{inc}_h(E_h) \phi \ \mathrm{d}x + \int_{\mathcal{E}_h} [\![\mathcal{T}_0(E_h)]\!] \partial_{\mathbf{n}} \phi + [\![\partial_{\mathbf{t}} (\mathbf{n} \cdot E_h \mathbf{t}) - \mathbf{t} \cdot \operatorname{rot} E_h]\!] \phi \ \mathrm{d}s \\ &\quad + \sum_{K \in \mathcal{T}_h} \sum_{\mathbf{e} \in \mathcal{E}(K)} \sum_{\mathbf{x} \in \partial \mathbf{e}} (-1)^{[\mathbf{e}, \mathbf{x}]} (\mathbf{n} \cdot E_h(\mathbf{x}) \mathbf{t}) \phi(\mathbf{x}), \end{aligned} \tag{3.4.6}$$

i.e.

$$\begin{aligned}\operatorname{inc} E_h = \operatorname{inc}_h E_h + \sum_{\mathbf{e}\in\mathcal{E}_h} [\![\mathcal{T}_0(E_h)]\!]\delta^{\mathbf{n}}_{\mathbf{e}} + [\![\partial_{\mathbf{t}}(\mathbf{n}\cdot E_h\mathbf{t}) - \mathbf{t}\cdot\operatorname{rot} E_h]\!]\delta_{\mathbf{e}} \\ + \sum_{K\in\mathcal{T}_h}\sum_{\mathbf{e}\in\mathcal{E}(K)}\sum_{\mathbf{x}\in\partial\mathbf{e}}(-1)^{[\mathbf{e},\mathbf{x}]}(\mathbf{n}\cdot E_h\mathbf{t})\delta_{\mathbf{x}},\end{aligned} \tag{3.4.7}$$

where for $\theta \in C^\infty(\mathbf{e})$,

$$\langle\theta\delta_{\mathbf{e}}, S\rangle := \int_{\mathbf{e}} \theta S \ \mathrm{d}s, \quad \langle\theta\delta^{\mathbf{n}}_{\mathbf{e}}, S\rangle := \int_{\mathbf{e}} \theta\partial_{\mathbf{n}} S \ \mathrm{d}s. \tag{3.4.8}$$

The discontinuous Galerkin method may be thought of as comparing an operator (inc) with its element-wise version (inc_h), and then considering what spaces lie in the kernel of the error terms, contributed by jumps in the fluxes across interior cell edges (or more generally, positive-codimensional facets). Tangential-tangential continuity of the Regge space means the $\mathcal{T}_0$ jump term vanishes identically, and the 0^{th} order Regge element is piecewise constant, so that its piecewise inc and its edge jump in derivatives must vanish. Thus, it may be seen from (3.4.7) that $\operatorname{inc} : \mathbb{REG}^0_h \to X_h$ is well-defined and surjective. These Dirac masses may be rigorously interpreted as the measure-valued curvature of the cell boundary [38], the quantity κ in the continuous Green's formula (3.3.7), so in this simple lowest-order case, the calculation (3.4.7) is consistent with the intuition that the incompatibility operator encodes the existence of singularities in the curvature of the domain.

Since the product of Dirac masses is ill-defined, this also demonstrates the subtlety of interpreting the airy inc operator "$\langle\text{airy inc}\, E, S\rangle = \langle\operatorname{inc} E, \operatorname{inc} S\rangle$" if one would like to take both arguments from the Regge space, in analogy to the div operator acting on the TDNNS stress-displacement element in §1.2.3.

3.4.3 Codimension-2 curvature

Consider the localisation of the vertex term in (3.4.7). At a given $\mathbf{x} \in \Lambda_h$, let $P^{\mathbf{x}}_h := \{K \in \mathcal{T}_h \mid \mathbf{x} \in \partial K\}$ denote the patch of cells sharing $\mathbf{x}$ as a vertex. The *angle defect*

$$\sum_{K\in P^{\mathbf{x}}_h}\sum_{\mathbf{e}\in\mathcal{E}(K)}\sum_{\mathbf{x}\in\partial\mathbf{e}}(-1)^{[\mathbf{e},\mathbf{x}]}\delta_{\mathbf{x}}(\mathbf{n}\cdot E_h\mathbf{t}) = \sum_{K\in P^{\mathbf{x}}_h}\sum_{\mathbf{e}\in\mathcal{E}(K)}\sum_{\mathbf{x}\in\partial\mathbf{e}}(-1)^{[\mathbf{e},\mathbf{x}]}\mathbf{n}\cdot E_h(\mathbf{x})\mathbf{t} \tag{3.4.9}$$

is then a 2-codimensional analogue of the classical DG jump over mesh edges, whose cancellation quantifies the inc-nonconformity of a tensor field.

The following combinatorial identity, which can be proved by hand assuming sufficient regularity of a matrix field near a vertex, therefore means something rather concrete in terms of inc-conformity.

Corollary 3.4.1. ("Kirchhoff's law".) *For all* $E \in C^\infty(\overline{\Omega}; \mathbb{S})$,

$$\sum_{K \in P_h^{\mathbf{x}}} \sum_{\mathbf{e} \in \mathcal{E}(K)} \sum_{\mathbf{x} \in \partial \mathbf{e}} (-1)^{[\mathbf{e},\mathbf{x}]} \mathbf{n} \cdot E(\mathbf{x}) \mathbf{t} = 0 \tag{3.4.10}$$

at each $\mathbf{x} \in \Lambda_h$.

3.5 Interior penalisation in $H(\mathrm{inc})$

3.5.1 A codimension-1 approach

For $k \geq 0$, let $V_h^k := \mathrm{CG}_{k+1}(\mathcal{T}_h; \mathbb{R}^2)$ denote the discrete displacement space in the Regge complex. We consider the following DG formulation of the strain HL on the Regge element pair: seek $(E_h, u_h) \in \mathbb{REG}_h^k \times V_h^k$ such that

$$a_h(E_h, F_h) + \int_\Omega F_h : \varepsilon(u_h) \, \mathrm{d}x = \int_\Omega f : F_h \, \mathrm{d}x \qquad \forall \, F_h \in \mathbb{REG}_h^k, \tag{3.5.1a}$$

$$\int_\Omega E_h : \varepsilon(v_h) - u_h \cdot v_h \, \mathrm{d}x = 0 \qquad \forall \, v_h \in V_h^k, \tag{3.5.1b}$$

where now, in light of §3.4.2, $a_h(\cdot, \cdot)$ is a carefully chosen mesh-dependent airy inc operator. We must decrease the regularity requirement of the argument E_h in (3.4.7), so as to derive a well-defined bilinear form on the Regge space.

We now specify the choice of trace formula to use for this purpose. Although we have argued that the Regge element is the natural choice for a DG discretisation of the model problem, its degrees of freedom only match the trace operator $\mathcal{T}_0$, and not $\mathcal{T}_1$ nor its discrete analogue. We thus choose to partially reverse the integration by parts in (3.4.6): for $E_h \in \mathrm{DG}_k(\mathcal{T}_h; \mathbb{S})$, we have

$$\mathrm{inc}\, E_h = \mathrm{inc}_h \, E_h + \sum_{\mathbf{e} \in \mathcal{E}_h} -[\![\mathrm{rot}\, E_h \cdot \mathbf{t}]\!] \delta_{\mathbf{e}} + [\![\mathbf{t} \cdot E_h \mathbf{t}]\!] \delta_{\mathbf{e}}^{\mathbf{n}} - [\![\mathbf{n} \cdot E_h \mathbf{t}]\!] \delta_{\mathbf{e}}^{\mathbf{t}}, \tag{3.5.2}$$

where for $\theta \in C^\infty(\mathbf{e})$,

$$\langle \theta \delta_{\mathbf{e}}^{\mathbf{t}}, S \rangle := \int_{\mathbf{e}} \theta \partial_{\mathbf{t}} S \, \mathrm{d}s, \tag{3.5.3}$$

so if $E_h \in \mathbb{REG}_h^k$ then

$$\begin{aligned} \mathrm{inc}\, E_h &= \mathrm{inc}_h \, E_h - \sum_{\mathbf{e} \in \mathcal{E}_h} \Big([\![\mathrm{rot}\, E_h \cdot \mathbf{t}]\!] \delta_{\mathbf{e}} + [\![\mathbf{n} \cdot E_h \mathbf{t}]\!] \delta_{\mathbf{e}}^{\mathbf{t}} \Big) \\ &= \mathrm{inc}_h \, E_h - \sum_{K \in \mathcal{T}_h} \sum_{\mathbf{e} \in \mathcal{E}(K)} \Big((\mathrm{rot}\, E_h \cdot \mathbf{t}) \delta_{\mathbf{e}} + (\mathbf{n} \cdot E_h \mathbf{t}) \delta_{\mathbf{e}}^{\mathbf{t}} \Big). \end{aligned} \tag{3.5.4}$$

This form of the inc operator is thus amenable to approximation or regularisation, but without the 2-codimensional jump terms suggested by the previous subsection (although vertex jump terms have been applied for the biharmonic operator [49]).

Note that the final term in (3.5.4) counts interior edges twice, but using the classic identity $[\![uv]\!] = \frac{1}{2}\left([\![u]\!]\{v\}+\{u\}[\![v]\!]\right)$ is readily simplified to

$$\begin{aligned}
&\sum_{K\in\mathcal{T}_h}\int_{\partial K}((\operatorname{rot} E_h\cdot\mathbf{t})S+(\mathbf{n}\cdot E_h\mathbf{t})\partial_{\mathbf{t}}S)\,\mathrm{d}s\\
&=\int_\Gamma((\operatorname{rot} E_h\cdot\mathbf{t})S+(\mathbf{n}\cdot E_h\mathbf{t})\partial_{\mathbf{t}}S)\,\mathrm{d}s+\int_{\mathcal{E}_h^\circ}[\![\operatorname{rot} E_h\cdot\mathbf{t}]\!]\{S\}+\{\operatorname{rot} E_h\cdot\mathbf{t}\}[\![S]\!]\\
&\qquad\qquad+[\![\mathbf{n}\cdot E_h\mathbf{t}]\!]\{\partial_{\mathbf{t}}S\}+\{\mathbf{n}\cdot E_h\mathbf{t}\}[\![\partial_{\mathbf{t}}S]\!]\,\mathrm{d}s.
\end{aligned}\tag{3.5.5}$$

We define the mesh-dependent discrete seminorm

$$|E_h|_h^2 := \|\operatorname{inc}_h E_h\|_{0,\mathcal{T}_h}^2+\frac{1}{h^3}\|[\![\operatorname{rot} E_h\cdot\mathbf{t}]\!]\|_{0,\mathcal{E}_h^\circ}^2+\frac{1}{h}\|[\![\mathbf{n}\cdot E_h\mathbf{t}]\!]\|_{0,\mathcal{E}_h^\circ}^2,\tag{3.5.6}$$

with kernel the distributionally inc-free tensor fields, and the mesh-dependent airy inc operator

$$\begin{aligned}
a_h(E_h,F_h) := &\int_{\mathcal{T}_h}(\operatorname{inc}_h E_h)(\operatorname{inc}_h F_h)\,\mathrm{d}x\\
&-\int_{\mathcal{E}_h}\Big([\![\mathbf{t}\cdot\operatorname{rot} E_h]\!]\{\operatorname{inc} F_h\}+\{\operatorname{inc} E_h\}[\![\mathbf{t}\cdot\operatorname{rot} F_h]\!]\Big)\,\mathrm{d}s\\
&-\int_{\mathcal{E}_h}\Big([\![\mathbf{n}\cdot E_h\mathbf{t}]\!]\{\operatorname{inc} F_h\}+\{\operatorname{inc} E_h\}[\![\mathbf{n}\cdot F_h\mathbf{t}]\!]\Big)\,\mathrm{d}s\\
&+\frac{1}{h^3}\int_{\mathcal{E}_h^\circ}[\![\mathbf{t}\cdot\operatorname{rot} E_h]\!][\![\mathbf{t}\cdot\operatorname{rot} F_h]\!]\,\mathrm{d}s\\
&+\frac{1}{h}\int_{\mathcal{E}_h^\circ}[\![\mathbf{n}\cdot E_h\mathbf{t}]\!][\![\mathbf{n}\cdot F_h\mathbf{t}]\!]\,\mathrm{d}s.
\end{aligned}\tag{3.5.7}$$

As is standard in DGFEM, we add consistent terms to symmetrise the bilinear form, and penalisation terms to weakly enforce the inc-conformity requirement and to make the form coercive with respect to an appropriate mesh-dependent norm. By construction,

$$|a_h(E_h,F_h)|\le|E_h|_h|F_h|_h.\tag{3.5.8}$$

3.5.2 A discrete Poincaré inequality

A fundamental tool in DG analysis is the establishment of a *discrete Poincaré inequality*

$$\|E\|_0\lesssim|E|_h\tag{3.5.9}$$

for all piecewise polynomial fields. Clearly, such an inequality can be true only on a subspace orthogonal to the kernel of inc, which by the discrete Hodge decomposition of $\mathbb{RE}\mathbb{G}_h^k$ will be equivalent to the gauge condition $\mathrm{div}^h E = 0$, where div^h denotes some appropriate notion of discrete divergence. This is to be expected, as typically a bilinear form arising on the diagonal of a saddle point system need only be coercive on some (possibly infinite-codimensional) kernel, as has been the case for the saddle point systems already studied in both §1 and §2.

Typically, such results on nonconforming polynomial spaces are available by employing the space $BV(\mathbb{R}^d)$ of functions of bounded variation in an intermediate estimate (e.g. [79, Theorem 5.3]), whose norm agrees with the $W^{1,1}(\mathbb{R}^d)$ seminorm $|\nabla(\cdot)|_{L^1(\mathbb{R}^d)}$ on an $\|\cdot\|_{L^1(\mathbb{R}^d)}$-dense subspace [2, Theorem 3.9]. However, an heuristic problem in this setting lies, as mentioned above, in the infinite-dimensional kernel of inc, in contrast to those of ∇ or ε which are trivially fixed by imposing Dirichlet boundary conditions or requiring finite integrability on all of $\mathbb{R}^d$; moreover, it is unclear how to generalise Sobolev embeddings to the inc operator as, unlike ∇, it is *a priori* well-defined only in dimension 2 or 3. Thus, adaptations of standard DG well-posedness theory, for example using an analogue of the BV space for the inc operator, would require significant modification for the present case.

Typically, the operation of passing to a subcomplex of a given complex commutes with taking the Hodge Laplace equations; this is for example true of the conforming Arnold–Winther method for the Hellinger–Reissner principle as in (1.5.2). Indeed, in the case of a subcomplex for which bounded commuting interpolations can be constructed, Poincaré inequalities may then be inherited from the infinite-dimensional spaces with constants independent of h, as required already for the previous chapter in Assumption 2.4.1.

For the *non*conforming subcomplex (3.4.2), a Poincaré inequality could be derived by applying the bounded inverse theorem directly to the closedness of the Regge sequence, but the resulting constant (which will arise in convergence estimates) will *a priori* depend on h. Moreover, any scheme of the form (3.5.1) cannot be interpreted as a Hodge Laplacian associated with the exact Regge complex (3.4.2) at $\mathbb{RE}\mathbb{G}_h^k$ (which would render its well-posedness automatic), as the space X_h is not Hilbertian. We therefore proceed with direct analysis of the scheme (3.5.1).

We now motivate the 'halved' Hodge Laplace problem. In the special case that the data f in the abstract HL problem (0.2.6) is chosen from the subspace $\ker((\mathrm{d}^{k-1})^*)$, then f admits a potential in the space V^{k+1}, $f = (\mathrm{d}^k)^* g$ for some $g \in V^{k+1}$, and it may be checked that the solution to (0.2.6) with data f can be obtained as $u = (\mathrm{d}^k)^* v$,

where $v \in V^{k+1}$ solves the HL $\mathcal{L}^{k+1}v = g$ [12, Section 4.4.3]. In what follows, we shall place the following strong assumption on a discrete analogue of this PDE at $H(\mathrm{inc})$, where $(\mathrm{d}^{k-1})^* = -\operatorname{div}$, to account for the infinite-dimensional kernel of inc.

Define $\operatorname{div}^h : L^2(\Omega;\mathbb{S}) \to V_h^k$ as the Hilbert space adjoint of $-\varepsilon$, i.e.

$$\int_\Omega (\operatorname{div}^h E_h) \cdot v_h := -\int_\Omega E_h : \varepsilon(v_h)\, \mathrm{d}x \quad \forall\, v_h \in V_h^k, \tag{3.5.10}$$

so that vanishing div^h of the data is a compatibility condition for well-posedness of what follows.

Assumption 3.5.1. (Elliptic regularity of the 'half' strain Hodge Laplacian). Assume Ω is such that for every $f \in \mathbb{RE}\mathbb{G}_h^k$ with $\operatorname{div}^h f = 0$, a solution $\Xi \in H(\mathrm{inc})$ to the system

$$\begin{aligned} \operatorname{airy}\operatorname{inc}\Xi &= f && \text{in } \Omega, \\ \operatorname{div}^h \Xi &= 0 && \text{in } \Omega, \\ \operatorname{inc}\Xi = \partial_{\mathbf{n}}(\operatorname{inc}\Xi) &= 0 && \text{on } \Gamma, \\ \Xi\mathbf{n} &= 0 && \text{on } \Gamma, \end{aligned} \tag{3.5.11}$$

exists and satisfies $\Xi \in H^4(\Omega;\mathbb{S})$, and moreover that $\|\Xi\|_4 \lesssim \|f\|_0$.

This (strong) assumption may be viewed as a statement of elliptic regularity for the continuous Hodge Laplacian, but constrained by the discrete divergence (3.5.10).

Note that in the case of the HL (3.5.11), the displacement may thus be interpreted as the Lagrange multiplier enforcing that the strain field is completely incompatible, i.e. (by the Hodge decomposition (3.2.6)) that it is divergence-free.

Lemma 3.5.1. (Poincaré inequality for the discrete incompatibility). *Let Ω satisfy* Assumption 3.5.1. *Then for all $E \in \mathbb{RE}\mathbb{G}_h^k$ with $\operatorname{div}^h E = 0$,*

$$\|E\|_0 \lesssim |E|_h. \tag{3.5.12}$$

Norming V_h^k with $\|\cdot\|_0$, we see that by the Babuška theory of perturbed saddle point systems [31], well-posedness of the scheme (3.5.1) follows from (3.5.8) and that $a_h(\cdot,\cdot)$ is bounded below by $|\cdot|_h$.

Proof. We adapt the proof of [10, Lemma 2.1] (for scalar fields) to tensor fields, which moreover are div^h-free. Define $\Xi \in H^4(\Omega;\mathbb{S})$ to be the unique solution to (3.5.11) with

right-hand side data E. Then by (3.5.5),

$$\|E\|_0^2 = \int_\Omega E : \operatorname{airy}\operatorname{inc}\Xi \,\mathrm{d}x \tag{3.5.13a}$$

$$= \int_{\mathcal{T}_h} (\operatorname{inc} E)(\operatorname{inc}\Xi)\,\mathrm{d}x - \int_{\mathcal{E}_h} (\llbracket \operatorname{rot} E\cdot\mathbf{t}\rrbracket \operatorname{inc}\Xi + \llbracket \mathbf{n}\cdot E\mathbf{t}\rrbracket \partial_{\mathbf{t}}(\operatorname{inc}\Xi))\,\mathrm{d}s \tag{3.5.13b}$$

$$\lesssim \left(\|\operatorname{inc}_h E\|_{0,\mathcal{T}_h}^2 + \frac{1}{h^3}\|\llbracket \operatorname{rot} E_h\cdot\mathbf{t}\rrbracket\|_{0,\mathcal{E}_h^\circ}^2 + \frac{1}{h}\|\llbracket \mathbf{n}\cdot E_h\mathbf{t}\rrbracket\|_{0,\mathcal{E}_h^\circ}^2\right)^{\frac{1}{2}} \tag{3.5.13c}$$

$$\times \left(\|\operatorname{inc}_h \Xi\|_{0,\mathcal{T}_h}^2 + h^3\|\operatorname{rot}\Xi\cdot\mathbf{t}\|_{0,\mathcal{E}_h^\circ}^2 + h\|\mathbf{n}\cdot\Xi\mathbf{t}\|_{0,\mathcal{E}_h^\circ}^2\right)^{\frac{1}{2}}. \tag{3.5.13d}$$

By the scalings $\|\operatorname{rot}\Xi\cdot\mathbf{t}\|_{0,\mathbf{e}} \lesssim h^{-3/2}\|\Xi\|_{0,K}$, $\|\mathbf{n}\cdot\Xi\mathbf{t}\|_{0,\mathbf{e}} \lesssim h^{-1/2}\|\Xi\|_{0,K}$ for $\mathbf{e}\in\mathcal{E}(K)$, we see that the final term (3.5.13d) may be bounded in terms of $\|E\|_0$. The claim follows.[37] □

[37] The author is grateful to Ari Stern for a discussion concerning §3.3.3.

Chapter 4

Concluding remarks and outlook

The three thrusts of this thesis are somewhat disjoint – the price to be paid, perhaps, for actually diving into the myriad applications which we claimed the elasticity complex would have back in the Introduction. We here review natural avenues for future work. There is much to be said, because the triad of themes – automated finite element transformations, structure-preserving finite elements for novel problems in thermodynamics, and analysis for the spaces and operators of defect elasticity models – are each of a 'fundamental' flavour.

4.1 Exotic finite elements

In our first chapter, we generalised Piola transformation theory to incorporate nonstandard elements discretising $H(\mathrm{div};\mathbb{S})$, developing techniques in 2D for two representative, exotic elements for elastic stress due to Arnold and Winther which discretise the symmetric Cauchy stress tensor in planar linear elasticity. This has ranged from the axiomatic considerations of why such a tensor even *exists*, to concrete numerical experiments verifying the accuracy of implementations which are newly enabled by our approach. We have also demonstrated the composability of our implementations with existing patch-based smoothers in Firedrake.

We emphasise that our theory aims to demonstrate that unusual or nonstandard elements, with desirable features but perhaps complicated transformation properties, can be used in an inexpensive, composable, and automated way, rather than to advocate for the use of AW^{c} or $\mathrm{AW}^{\mathrm{nc}}$ specifically. Indeed, the calculations for the transformation theory in §1 are mostly elementary, but there remains a large gap between structure-preserving elements currently being devised by the FEEC community, and the extent of their actual implementation and use in solving concrete problems. We hope that our didactic treatment of the transformation theory provides an example

for those wishing to implement schemes with other sophisticated elements and/or in other software ecosystems.

In the long term, one would like to be able to implement any (reference-based) finite element just by providing its DOFs and a constructive definition of its local shape space, although this places a burden on the user to provide a unisolvent set. One should also consider the notion of finite element with which to work, as in Remark 1.3.4. Future software generalisations could even aim to automate *all calculations* carried out in (for example) §1.3.2, §1.4.1, §1.4.2, but would have to avoid premature optimisation, in the sense of ensuring that these computations for additional finite elements would not be outweighed in effort by such an automation.

4.1.1 Solvers for symmetry-enforcing discretisations

In keeping with Remark 1.7.1, it is likely that specialised kernel-preserving transfer operators for the AW elements could be constructed to make the vertex star iteration even more robust, and the two elements have the same elastostatic subspace as per Remark 1.7.2. Note that in [87], an AL preconditioner was developed for a shear stress-velocity-pressure formulation of implicitly-constituted incompressible flow, but the shear stress was taken only in $L^2(\Omega;\mathbb{S})$.

Of independent interest is the application of Nitsche's method to dual mixed problems, and further investigation is merited by the interaction between the Nitsche and augmented Lagrangian penalties, whose efficacy when combined together we have observed numerically when applied to AW elements.[38]

4.1.2 Symmetric elements and Piola transforms in 3D

The 3D analogues of the AW spaces, namely the conforming and nonconforming Arnold–Awanou–Winther elements [14, 15], are of dimension 162 and 42 respectively when restricted to a single cell, and are presented in the understanding that "[t]he complexity of the elements may very well limit their practical significance" [14, p. 1231], although the nonconforming element is amenable to hybridisation [15]. A cheaper alternative is provided by the conforming Hu–Zhang element, which in 3D is of dimension only 48, while many nonconforming efforts in 3D are rectangular [119, 190]; in keeping with Remark 1.3.2, we conjecture that the mapping properties of these 3D

[38] Furthermore, there is the possibility of extension to nonlinear and/or complementarity problems such as the Signorini contact problem, which to date (in this formulation) has, to the author's knowledge, only been solved using FOSLS [26].

elements would be analogous to our analysis in §1.3.3, if perhaps more involved due to the complexity of the geometry used to define their DOFs.

In 3D, one also has that the co- and contravariant cases are genuinely distinct (see Remark 1.3.3); the covariant maps are used for the $H(\mathrm{curl})$ and $H(\mathrm{curl};\mathbb{S})$ spaces, typically arising in computational electromagnetism. Our work in §1 could provide an example for future work if elements are proposed with bases not preserved by the covariant Piola map.

4.1.3 The curvilinear case

The zany transformation theory could be extended to spaces defined on curved meshes, which corresponds to choosing the diffeomorphism F in (1.3.1) to be non-affine. That a given finite element method easily extends to curved elements is a common claim in papers, but 'composing' these issues with the dual transformations described here would be nontrivial; relations between physical and reference components would not be as succinct as in §1.3.2 because of spatial variation in the Jacobian J. Moreover, an issue arising on curved geometries for the elasticity complex (which is absent from the de Rham case) is a nonvanishing cross term in the commutator $\mathrm{d}J^{-*} - J^{-*}\mathrm{d}$ [124], so that §1.4.4 ceases to apply.

Non-affine approximation of Piola-mapped symmetric tensor fields has been considered in [23, 170], although with elements such as HHJ or TDNNS, so that the Piola map suffices in the standard manner as explained in §1.3.2.

4.2 Multicomponent diffusion

In §2, we proposed a formulation and numerical method for the Stokes–Onsager–Stefan–Maxwell equations of multicomponent flow, proving continuous and discrete inf-sup conditions for a linearisation of the system with saddle point structure. This structure arises from the duality between the diffusion driving forces, and the combination of species continuity equations with the divergence of the mass-average velocity constraint. The resulting error estimates were (modulo interpolation of the coefficients) a straightforward application of the approximation theory of perturbed saddle point problems.

We saw that the subcomplex structure for the stress elements gave h-independent discrete inf-sup constants. Alternative discretisations may be pursued via, for example, weak imposition of the symmetry of the viscous stress, which at the time of writing would provide a first avenue to extending §2 to 3D or to higher polynomial

degree. In any case, we hope that this work plays some role in exhibiting Onsager's theory of thermodynamics as an exciting new application area of the FEM and FEEC.

4.2.1 Refinements of the model

Future work could incorporate tertiary physical phenomena by relaxing the physical assumptions placed on the model discretised in §2. Of particular interest would be the full incorporation of thermal effects based on the framework proposed in [181].

Rigorous investigation into a notion of weak solution more refined than Definition 2.2.1 incorporating (for example) integrability of thermodynamic pressure gradients, and weak form of linearisation, would also be of significant interest. We also remark that a proof of convergence of the Picard iteration could be used to prove the existence of a solution tuple for the infinite-dimensional nonlinear SOSM system.

4.2.2 Multicomponent CFD

Many concepts and methods from the classical CFD literature on numerical methods for Navier–Stokes problems in the dilute solution regime merit generalisation to our formulation of the SOSM problem, for example boundary layers, new scalings and nondimensionalisations relating the species velocities to each other and to the convective velocity, pressure-robustness [127], flow-following smoothers [81, Ch. 7], gradient jump penalisation for the convective term [150], and the Q-criterion, a turbulence statistic for the detection of eddies [193].

4.2.3 Preconditioning

As repeatedly emphasised, the perturbed saddle point structure (2.4.3) should be amenable to the development of fast solvers, potentially building on the techniques for AL-type preconditioners as described in §1.7. It is interesting to note that the operator blocks in the linearised coupled SOSM system (2.3.6) do not correspond to the Stokes and OSM subsytems, so that development of a multigrid scheme for one does not reduce the problem to developing a solver for the other.

4.3 The incompatibility operator and defect elasticity

Finally in §3, we studied the incompatibility operator in 2D and the strain Hodge Laplacian problem, drawing links between the compatibility condition encoded in the

strain complex and Kröner's theory of incompatible strain fields. A DG method was presented, using the Regge element for metric tensors and bypassing a vertex-jump formulation.

This DG scheme is not hybridisable as is, but the HL problem discretised with a local DG method may be amenable to weak enforcement of $H(\mathrm{inc})$-conformity via Lagrange multipliers on the skeleton $\mathcal{E}_h$ [75], and to hybridisation of the abstract HL problem as proposed in [27]. Future work could consider a fuller physical interpretation of the model problem, extension to the 3D elasticity complex, and the identification of problematic parameter regimes in analogy to the incompressible limit in primal linear elasticity.

The method presented in §3 in addition may not be the most competitive, due to ill-conditioning of the Regge element (and indeed many FEEC-based elements); multigrid schemes may partially deal with this via the construction of kernel-preserving transfer operators as explained in §1.7.

4.4 How far can we take the FEEC and the Hodge Laplace concept?

Even if one believes that the Hodge Laplacian is useful as an abstraction, there is a temptation to 'shoehorn' – to identify HL structure where in fact there is none. Recall however that we already encountered such a situation in §2; as in Remark 2.1.1, the Stefan–Maxwell equations are not (or not obviously) the Euler-Lagrange stationarity condition of any associated functional, and hence in particular their Newton linearisation cannot have HL structure. For our discrete structural conditions, the bottom of (2.4.4) is simply a segment in a discrete stress complex, but we were not able to provide a similar sequence for the Stefan–Maxwell variables, or draw an analogous sequence for the five Sobolev spaces (2.4.1) in infinite dimensions.

4.4.1 Construction of finite element complexes

The recent framework due to Arnold and Hu [22] presents a systematic method to derive new complexes from old, using the Bernstein–Gelfand–Gelfand (BGG) resolution from Lie representation theory. Although we emphasised in §0 (and demonstrated throughout the thesis) how much structure is provided by the existence of a discrete subcomplex to a given sequence, there is to date no systematic way to construct such a discrete subcomplex. Discrete analogues of the BGG construction have been used

to reinterpret the Arnold–Winter element [20], and have been constructed for the Hessian, elasticity, and div div complexes in 2D [123].

4.4.2 General relativity

In §3 we drew on the work [138], which applied the Regge calculus and element to the discretisation of the Riemannian metric tensor which encodes the geometry of spacetime in the fully nonlinear Einstein field equations. Indeed, numerical relativity, like elasticity, is becoming an increasingly successful application area of the FEEC [162]. This is partly because the same complexes arise in both problems – for example, the smooth analogue of the elasticity complex (0.1.3) also arises when considering the stable discretisation of the time derivative of the metric tensor in the linearised Einstein equations [11]. This is at least consistent with the observation that spacetime may be formally modelled as a 4-dimensional elastic medium [177].

4.4.3 Implicitly-constituted continuum mechanics

We began §1 by observing that Hellinger–Reissner linear elasticity arises as a HL if the base stress space $L^2(\Omega;\mathbb{S})$ is weighted with the compliance tensor; later in §3.2.2 we pointed out that this corresponds to the Hodge star operator, in d dimensions mapping isometrically between differential k-forms and $(d-k)$-forms, which may be observed from §1.6.1 upon comparison of the forms to which stress and strain are proxy. It is therefore natural to consider whether the theory of continua with implicitly-constituted rheological laws, for which one of the stress or (rate of) strain cannot be eliminated purely in terms of the other, can also be interpreted in FEEC terms – for example, via an implicitly defined Hodge star operator.

4.4.4 Nonlinear complexes of Riemannian geometry

For $\Omega \subseteq \mathbb{R}^3$ in reference configuration, let $\phi \in C^\infty(\Omega;\mathbb{R}^3)$ denote a deformation of Ω to some domain in $\mathbb{R}^3$. Let $\mathcal{D}\phi := \nabla\phi(\nabla\phi)^\top$ denote the corresponding right Cauchy–Green strain tensor, precisely the metric induced by the embedding ϕ, taking values in $C^\infty_+(\Omega;\mathbb{S})$, which we define to be the symmetric positive definite cone in $C^\infty(\Omega;\mathbb{S})$. For a flat metric on $\mathbb{R}^3$, we have $\mathrm{Riem}\circ\mathcal{D} = 0$, where Riem denotes the Riemannian curvature tensor, and the second Bianchi identity states that $\mathrm{div}\circ\mathrm{Riem} = 0$. The *fundamental theorem of Riemannian geometry* gives for $g \in C^\infty_+(\Omega;\mathbb{S})$ with $\mathrm{Riem}\, g = 0$ the existence of an embedding $\phi \in C^\infty(\Omega;\mathbb{R}^3)$, unique up to isometry, with $g = \mathcal{D}\phi$.

It will not surprise the reader that we are now tempted to write down the following sequence [122]:

$$0 \longrightarrow C^\infty(\Omega;\mathbb{R}^3) \xrightarrow{\mathcal{D}} C^\infty_+(\Omega;\mathbb{S}) \xrightarrow{\text{Riem}} C^\infty(\Omega;\mathbb{S}) \xrightarrow{\text{div}} C^\infty(\Omega) \longrightarrow 0, \tag{4.4.1}$$

whose linearisation about the identity is the smooth version of precisely the linear elasticity complex (0.1.3) with which this thesis began. This is purely formal, however, and it is not clear what 'exactness' would amount to at the penultimate space, since the definition of div involves covariant derivatives and thus a metric in the first place. The intriguing possibilities of seeking nonlinear generalisations of Hodge Laplace operators, inf-sup conditions, and Hodge decompositions now arise. The nonlinear generalisation of the Poincaré inequalities, for example, may unify known results such as nonlinear Korn inequalities due to Ciarlet [73, p. 57].

References

[1] M. S. Alnæs, A. Logg, K. B. Ølgaard, M. E. Rognes, and G. N. Wells, *Unified Form Language: a Domain-Specific Language for weak formulations of partial differential equations*, ACM Transactions on Mathematical Software, Feb. 2014, pp. 1–37, https://doi.org/10.1145/2566630.

[2] L. Ambrosio, N. Fusco, and D. Pallara, *Functions of bounded variation and free discontinuity problems*, Oxford Mathematical Monographs, Clarendon Press, 2000.

[3] P. R. Amestoy, I. S. Duff, J.-Y. L'Excellent, and J. Koster, *A fully asynchronous multifrontal solver using distributed dynamic scheduling*, SIAM Journal on Matrix Analysis and Applications, Apr. 2001, pp. 15–41, https://doi.org/10.1137/S0895479899358194.

[4] S. Amstutz and N. Van Goethem, *Analysis of the incompatibility operator and application in intrinsic elasticity with dislocations*, SIAM Journal on Mathematical Analysis, 2016, pp. 320–348, https://doi.org/10.1137/15M1020113.

[5] ——, *The incompatibility operator: from Riemann's intrinsic view of geometry to a new model of elasto-plasticity*, in Topics in Applied Analysis and Optimisation, Springer, 2019, pp. 33–70, https://doi.org/10.1007/978-3-030-33116-0_2.

[6] ——, *Existence and asymptotic results for an intrinsic model of small-strain incompatible elasticity*, Discrete & Continuous Dynamical Systems-B, 2020, p. 3769, https://doi.org/10.3934/dcdsb.2020240.

[7] ——, *A second-order model of small-strain incompatible elasticity*, Feb. 2022, https://hal.archives-ouvertes.fr/hal-03581050.

[8] R. Anderson, J. Andrej, A. Barker, J. Bramwell, J.-S. Camier, J. Cerveny, V. Dobrev, Y. Dudouit, A. Fisher, T. Kolev, et al., *MFEM: A modular finite element methods library*, June 2019, https://arxiv.org/abs/1911.09220.

[9] S. S. Antman, *Nonlinear problems of elasticity*, vol. 107 of Applied Mathematical Sciences, Springer, New York, 2nd ed., 2005, https://doi.org/10.1007/0-387-27649-1.

[10] D. N. Arnold, *An interior penalty finite element method with discontinuous elements*, SIAM Journal on Numerical Analysis, 1982, pp. 742–760, https://doi.org/10.1137/0719052.

[11] ——, *From exact sequences to colliding black holes: Differential complexes in numerical analysis*. Plenary address at the International Congress of Mathematics, Beijing, Aug. 2002. https://www-users.math.umn.edu/~arnold//talks/icm2002.pdf.

[12] ——, *Finite element exterior calculus*, no. 93 in CBMS-NSF Regional Conference Series in Applied Mathematics, SIAM, Philadelphia, 2018, https://doi.org/10.1137/1.9781611975543.

[13] ——, *Lecture notes on numerical analysis of partial differential equations*. University of Minnesota, Mar. 2018. http://www-users.math.umn.edu/~arnold/8445/notes.pdf.

[14] D. N. Arnold, G. Awanou, and R. Winther, *Finite elements for symmetric tensors in three dimensions*, Mathematics of Computation, July 2008, pp. 1229–1251, https://doi.org/10.1090/S0025-5718-08-02071-1.

[15] ——, *Nonconforming tetrahedral mixed finite elements for elasticity*, Mathematical Models and Methods in Applied Sciences, 2014, pp. 783–796, https://doi.org/10.1142/s021820251350067x.

[16] D. N. Arnold, F. Brezzi, and J. Douglas, *PEERS: A new mixed finite element for plane elasticity*, Japan Journal of Applied Mathematics, May 1984, pp. 347–367, https://doi.org/

10.1007/BF03167064.
[17] D. N. Arnold, R. Falk, and R. Winther, *Mixed finite element methods for linear elasticity with weakly imposed symmetry*, Mathematics of Computation, Oct. 2007, pp. 1699–1723, https://doi.org/10.1090/S0025-5718-07-01998-9.
[18] D. N. Arnold, R. S. Falk, and R. Winther, *Multigrid in $H(\mathrm{div})$ and $H(\mathrm{curl})$*, Numerische Mathematik, Jan. 2000, pp. 197–217, https://doi.org/10.1007/PL00005386.
[19] ——, *Finite element exterior calculus, homological techniques, and applications*, Acta Numerica, May 2006, pp. 1–155, https://doi.org/10.1017/S0962492906210018.
[20] ——, *Differential complexes and stability of finite element methods II: The elasticity complex*, in Compatible Spatial Discretizations, Springer, Jan. 2007, pp. 47–67, https://doi.org/10.1007/0-387-38034-5_3.
[21] ——, *Geometric decompositions and local bases for spaces of finite element differential forms*, Computer Methods in Applied Mechanics and Engineering, May 2009, pp. 1660–1672, https://doi.org/10.1016/j.cma.2008.12.017.
[22] D. N. Arnold and K. Hu, *Complexes from complexes*, Foundations of Computational Mathematics, 2021, pp. 1–36, https://doi.org/10.1007/s10208-021-09498-9.
[23] D. N. Arnold and S. W. Walker, *The Hellan–Herrmann–Johnson method with curved elements*, SIAM Journal on Numerical Analysis, 2020, pp. 2829–2855, https://doi.org/10.1137/19M1288723.
[24] D. N. Arnold and R. Winther, *Mixed finite elements for elasticity*, Numerische Mathematik, Sept. 2002, pp. 401–419, https://doi.org/10.1007/s002110100348.
[25] ——, *Nonconforming mixed elements for elasticity*, Mathematical Models and Methods in Applied Sciences, Mar. 2003, pp. 295–307, https://doi.org/10.1142/s0218202503002507.
[26] F. S. Attia, Z. Cai, and G. Starke, *First-order system least squares for the Signorini contact problem in linear elasticity*, SIAM Journal on Numerical Analysis, 2009, pp. 3027–3043, https://doi.org/10.1137/080726975.
[27] G. Awanou, M. Fabien, J. Guzmán, and A. Stern, *Hybridization and postprocessing in finite element exterior calculus*, Oct. 2021, https://arxiv.org/abs/2008.00149.
[28] F. R. A. Aznaran, P. E. Farrell, and R. C. Kirby, *Transformations for Piola-mapped elements*, SMAI Journal of Computational Mathematics, 2023. (to appear), https://arxiv.org/abs/2110.13224.
[29] F. R. A. Aznaran, P. E. Farrell, C. W. Monroe, and A. J. Van-Brunt, *Finite element methods for multicomponent convection-diffusion*, Aug. 2022, https://arxiv.org/abs/2208.11949.
[30] F. R. A. Aznaran and K. Hu, *The strain Hodge Laplacian*. In preparation.
[31] I. Babuška, *Error-bounds for finite element method*, Numerische Mathematik, Jan. 1971, pp. 322–333, https://doi.org/10.1007/BF02165003.
[32] S. Balay, S. Abhyankar, M. F. Adams, J. Brown, P. Brune, K. Buschelman, L. Dalcin, V. Eijkhout, W. D. Gropp, D. Karpeyev, D. Kaushik, M. G. Knepley, D. May, L. C. McInnes, R. T. Mills, T. Munson, K. Rupp, P. Sanan, B. F. Smith, S. Zampini, H. Zhang, and H. Zhang, *PETSc Users Manual*, Tech. Report ANL-95/11 - Revision 3.11, Mar. 2019.
[33] W. Bangerth, R. Hartmann, and G. Kanschat, *deal.II – A general-purpose object-oriented finite element library*, ACM Transactions on Mathematical Software (TOMS), 2007, pp. 24/1–24/27, https://doi.org/10.1145/1268776.1268779.
[34] S. Bartels, *Numerical methods for nonlinear partial differential equations*, vol. 47 of Springer Series in Computational Mathematics, Springer, 2015, https://doi.org/10.1007/978-3-319-13797-1.
[35] P. Bastian, M. Blatt, C. Engwer, A. Dedner, R. Klöfkorn, S. Kuttanikkad, M. Ohlberger, and O. Sander, *The Distributed and Unified Numerics Environment (DUNE)*, in Proceedings of the 19th Symposium on Simulation Technique in Hannover, vol. 123, Aug. 2006.
[36] M. Benzi, G. H. Golub, and J. Liesen, *Numerical solution of saddle point problems*, Acta Numerica, Apr. 2005, pp. 1–137, https://doi.org/10.1017/S0962492904000212.

[37] M. Benzi and M. A. Olshanskii, *An augmented Lagrangian-based approach to the Oseen problem*, SIAM Journal on Scientific Computing, Dec. 2006, pp. 2095–2113, https://doi.org/10.1137/050646421.

[38] Y. Berchenko-Kogan and E. S. Gawlik, *Finite element approximation of the Levi-Civita connection and its curvature in two dimensions*, Nov. 2021, https://arxiv.org/abs/2111.02512.

[39] R. B. Bird, W. E. Stewart, and E. N. Lightfoot, *Transport phenomena*, no. 1 in Transport Phenomena, Wiley, 2nd ed., 2002.

[40] D. Boffi, F. Brezzi, and M. Fortin, *Mixed finite element methods and applications*, vol. 44 of Springer Series in Computational Mathematics, Springer, Berlin, 2013, https://doi.org/10.1007/978-3-642-36519-5.

[41] A. Bondesan, L. Boudin, and B. Grec, *A numerical scheme for a kinetic model for mixtures in the diffusive limit using the moment method*, Numerical Methods for Partial Differential Equations, Jan. 2019, pp. 1184–1205, https://doi.org/10.1002/num.22345.

[42] D. Bothe and W. Dreyer, *Continuum thermodynamics of chemically reacting fluid mixtures*, Acta Mechanica, June 2015, pp. 1757–1805, https://doi.org/10.1007/s00707-014-1275-1.

[43] N. Bottasso, *Experimental methods for measuring the mechanical properties of soft tissues under large deformations*, master's thesis, Polytechnic University of Turin, Mar. 2020. https://webthesis.biblio.polito.it/14104/1/tesi.pdf.

[44] L. Boudin, D. Götz, and B. Grec, *Diffusion models of multicomponent mixtures in the lung*, in ESAIM: Proceedings, vol. 30, EDP Sciences, 2010, pp. 90–103, https://doi.org/10.1051/proc/2010008.

[45] D. Braess, *Finite elements: Theory, fast solvers, and applications in solid mechanics*, Cambridge University Press, Cambridge, 3rd ed., 2007, https://doi.org/10.1088/0957-0233/13/9/704.

[46] D. Braess and P. Ming, *A finite element method for nearly incompressible elasticity problems*, Mathematics of Computation, 2005, pp. 25–52, https://doi.org/10.1090/S0025-5718-04-01662-X.

[47] J. Bramwell, L. Demkowicz, J. Gopalakrishnan, and W. Qiu, *A locking-free hp DPG method for linear elasticity with symmetric stresses*, Numerische Mathematik, Dec. 2012, pp. 671–707, https://doi.org/10.1007/s00211-012-0476-6.

[48] S. Brenner and R. Scott, *The mathematical theory of finite element methods*, vol. 15 of Texts in Applied Mathematics, Springer Science & Business Media, New York, 3rd ed., 2007, https://doi.org/10.1007/978-0-387-75934-0.

[49] S. C. Brenner, T. Gudi, and L.-Y. Sung, *A weakly over-penalized symmetric interior penalty method for the biharmonic problem*, Electronic Transactions on Numerical Analysis, 2010, pp. 214–238, https://etna.math.kent.edu/vol.37.2010/pp214-238.dir/pp214-238.pdf.

[50] J. Brüning and M. Lesch, *Hilbert complexes*, Journal of Functional Analysis, Aug. 1992, pp. 88–132, https://doi.org/10.1016/0022-1236(92)90147-B.

[51] M. Bulíček, E. Maringová, and J. Málek, *On nonlinear problems of parabolic type with implicit constitutive equations involving flux*, Mathematical Models & Methods in Applied Sciences, Aug. 2021, pp. 2039–2090, https://doi.org/10.1142/s0218202521500457.

[52] E. Burman and R. Puppi, *Two mixed finite element formulations for the weak imposition of the Neumann boundary conditions for the Darcy flow*, Journal of Numerical Mathematics, June 2022, pp. 141–162, https://doi.org/10.1515/jnma-2021-0042.

[53] Z. Cai, J. Korsawe, and G. Starke, *An adaptive least squares mixed finite element method for the stress-displacement formulation of linear elasticity*, Numerical Methods for Partial Differential Equations: An International Journal, 2005, pp. 132–148, https://doi.org/10.1002/num.20029.

[54] Z. Cai and G. Starke, *Least-squares methods for linear elasticity*, SIAM Journal on Numerical Analysis, June 2004, pp. 826–842, https://doi.org/10.1137/S0036142902418357.

[55] C. Cancés, V. Ehrlacher, and L. Monasse, *Finite volumes for the Stefan–Maxwell*

cross-diffusion system, July 2020, https://arxiv.org/abs/2007.09951.

[56] A. Čap and K. Hu, *BGG sequences with weak regularity and applications*, Mar. 2022, https://arxiv.org/abs/2203.01300.

[57] J. A. Carrillo, Y. Huang, and M. Schmidtchen, *Zoology of a nonlocal cross-diffusion model for two species*, SIAM Journal on Applied Mathematics, Apr. 2018, pp. 1078–1104, https://doi.org/10.1137/17M1128782.

[58] C. Carstensen, M. Eigel, and J. Gedicke, *Computational competition of symmetric mixed FEM in linear elasticity*, Computer Methods in Applied Mechanics and Engineering, Oct. 2011, pp. 2903–2915, https://doi.org/10.1016/j.cma.2011.05.013.

[59] C. Carstensen, D. Gallistl, and M. Schedensack, *L^2 best approximation of the elastic stress in the Arnold–Winther FEM*, IMA Journal of Numerical Analysis, July 2016, pp. 1096–1119, https://doi.org/10.1093/imanum/drv051.

[60] C. Carstensen, J. Gedicke, and E.-J. Park, *Numerical experiments for the Arnold–Winther mixed finite elements for the Stokes problem*, SIAM Journal on Scientific Computing, Aug. 2012, pp. A2267–A2287, https://doi.org/10.1137/100802906.

[61] C. Carstensen, D. Günther, J. Reininghaus, and J. Thiele, *The Arnold–Winther mixed FEM in linear elasticity. Part I: Implementation and numerical verification*, Computer Methods in Applied Mechanics and Engineering, Feb. 2008, pp. 3014–3023, https://doi.org/10.1016/j.cma.2008.02.005.

[62] S. Caucao, D. Mora, and R. Oyarzúa, *A priori and a posteriori error analysis of a pseudostress-based mixed formulation of the Stokes problem with varying density*, IMA Journal of Numerical Analysis, Apr. 2016, pp. 947–983, https://doi.org/10.1093/imanum/drv015.

[63] A.-L. B. Cauchy, *Recherches sur l'équilibre et le mouvement intérieur des corps solides ou fluides, élastiques ou non élastiques*, Bulletin de la Société Philomatique, 1823, pp. 9–13. https://gallica.bnf.fr/ark:/12148/bpt6k901948/f308.image.

[64] L. Chen and X. Huang, *Geometric decompositions of* div*-conforming finite element tensors*, Dec. 2021, https://arxiv.org/abs/2112.14351.

[65] ——, *Finite elements for* divdiv*-conforming symmetric tensors*, Mathematics of Computation, 2022, pp. 1107–1142.

[66] C. Cherubini, S. Filippi, A. Gizzi, A. Loppini, and R. Ruiz-Baier, *Modelling thermo-electro-mechanical effects in orthotropic cardiac tissue*, Communications in Computational Physics, Jan. 2020, pp. 87–115, https://doi.org/10.4208/cicp.OA-2018-0253.

[67] S. H. Christiansen, *A characterization of second-order differential operators on finite element spaces*, Mathematical Models and Methods in Applied Sciences, 2004, pp. 1881–1892, https://doi.org/10.1142/S0218202504003854.

[68] ——, *A construction of spaces of compatible differential forms on cellular complexes*, Mathematical Models and Methods in Applied Sciences, May 2008, pp. 739–757, https://doi.org/10.1142/S021820250800284X.

[69] ——, *On the linearization of Regge calculus*, Numerische Mathematik, Dec. 2011, pp. 613–640, https://doi.org/10.1007/s00211-011-0394-z.

[70] S. H. Christiansen, J. Gopalakrishnan, J. Guzmán, and K. Hu, *A discrete elasticity complex on three-dimensional Alfeld splits*, Sept. 2020, https://arxiv.org/abs/2009.07744.

[71] S. H. Christiansen, J. Hu, and K. Hu, *Nodal finite element de Rham complexes*, Numerische Mathematik, June 2018, pp. 411–446, https://doi.org/10.1007/s00211-017-0939-x.

[72] S. H. Christiansen and K. Hu, *Finite element systems for vector bundles: elasticity and curvature*, Foundations of Computational Mathematics, Feb. 2022, pp. 1–52, https://doi.org/10.1007/s10208-022-09555-x.

[73] P. G. Ciarlet, *An introduction to differential geometry with applications to elasticity*, Journal of Elasticity, 2005, pp. 1–215, https://doi.org/10.1007/s10659-005-4738-8.

[74] P. G. Ciarlet, L. Gratie, and C. Mardare, *Intrinsic methods in elasticity: A mathematical survey*, Discrete & Continuous Dynamical Systems, 2009, pp. 133–164, https://doi.org/10.3934/dcds.2009.23.133.

[75] B. Cockburn, J. Gopalakrishnan, and R. Lazarov, *Unified hybridization of discontin-*

uous Galerkin, mixed, and continuous Galerkin methods for second order elliptic problems, SIAM Journal on Numerical Analysis, 2009, pp. 1319–1365, https://doi.org/10.1137/070706616.

[76] E. L. Cussler, *Diffusion: Mass transfer in fluid systems*, Cambridge Series in Chemical Engineering, Cambridge University Press, 2009, https://doi.org/10.1017/CBO9780511805134.

[77] L. De Luca, R. Scala, and N. Van Goethem, *A new approach to topological singularities via a weak notion of Jacobian for functions of bounded variation*, May 2022, https://arxiv.org/abs/2205.14746.

[78] W. M. Deen, *Introduction to chemical engineering fluid mechanics*, Cambridge Series in Chemical Engineering, Cambridge, 2016, https://doi.org/10.1017/CBO9781316403464.

[79] D. A. Di Pietro and A. Ern, *Mathematical aspects of discontinuous Galerkin methods*, vol. 69 of Mathématiques et Applications, Springer, 2011, https://doi.org/10.1007/978-3-642-22980-0.

[80] G. Dziuk and C. M. Elliott, *Finite element methods for surface PDEs*, Acta Numerica, 2013, pp. 289–396, https://doi.org/10.1017/S0962492913000056.

[81] H. C. Elman, D. J. Silvester, and A. J. Wathen, *Finite elements and fast iterative solvers: With applications in incompressible fluid dynamics*, Numerical Mathematics and Scientific Computation, Oxford University Press, 2nd ed., 2014, https://doi.org/10.1093/acprof:oso/9780199678792.001.0001.

[82] A. Ern and V. Giovangigli, *Multicomponent transport algorithms*, vol. 24 of Lecture Notes in Artificial Intelligence, Springer-Verlag, 1994, https://doi.org/10.1007/978-3-540-48650-3.

[83] ——, *Thermal diffusion effects in hydrogen-air and methane-air flames*, Combustion Theory and Modelling, Dec. 1998, pp. 349–372, https://doi.org/10.1088/1364-7830/2/4/001.

[84] ——, *Impact of detailed multicomponent transport on planar and counterflow hydrogen/air and methane/air flames*, Combustion Science and Technology, Jan. 1999, pp. 157–181, https://doi.org/10.1080/00102209908952104.

[85] A. Ern and J.-L. Guermond, *Theory and practice of finite elements*, vol. 159 of Applied Mathematical Sciences, Springer Science & Business Media, New York, 2004, https://doi.org/10.1007/978-1-4757-4355-5.

[86] P. E. Farrell, L. F. Gatica, B. P. Lamichhane, R. Oyarzúa, and R. Ruiz-Baier, *Mixed Kirchhoff stress–displacement–pressure formulations for incompressible hyperelasticity*, Computer Methods in Applied Mechanics and Engineering, Feb. 2021, p. 113562, https://doi.org/10.1016/j.cma.2020.113562.

[87] P. E. Farrell and P. A. Gazca-Orozco, *An augmented Lagrangian preconditioner for implicitly-constituted non-Newtonian incompressible flow*, SIAM Journal on Scientific Computing, Nov. 2020, pp. B1329–B1349, https://doi.org/10.1137/20M1336618.

[88] P. E. Farrell, P. A. Gazca-Orozco, and E. Süli, *Finite element approximation and preconditioning for anisothermal flow of implicitly-constituted non-Newtonian flow*, Mathematics of Computation, Nov. 2021, pp. 659–697, https://doi.org/10.1090/mcom/3703.

[89] P. E. Farrell, M. G. Knepley, F. Wechsung, and L. Mitchell, *PCPATCH: software for the topological construction of multigrid relaxation methods*, ACM Transactions on Mathematical Software, Sept. 2021, pp. 1–22, https://doi.org/10.1145/3445791.

[90] P. E. Farrell, L. Mitchell, L. R. Scott, and F. Wechsung, *A Reynolds-robust preconditioner for the Scott–Vogelius discretization of the stationary incompressible Navier–Stokes equations*, SMAI Journal of Computational Mathematics, Mar. 2021, pp. 75–96, https://doi.org/10.5802/smai-jcm.72.

[91] ——, *Robust multigrid methods for nearly incompressible elasticity using macro elements*, IMA Journal of Numerical Analysis, Jan. 2022, https://doi.org/10.1093/imanum/drab083.

[92] P. E. Farrell, L. Mitchell, and F. Wechsung, *An augmented Lagrangian preconditioner for the 3D stationary incompressible Navier–Stokes equations at high Reynolds number*, SIAM Journal on Scientific Computing, Oct. 2019, pp. A3073–A3096, https://doi.org/10.1137/18M1219370.

[93] C. A. Fernandez and M. C. Hatzell, *Economic considerations for low-temperature elec-*

trochemical ammonia production: Achieving Haber–Bosch parity, Journal of the Electrochemical Society, Nov. 2020, p. 143504, https://doi.org/10.1149/1945-7111/abc35b.

[94] A. Fick, *Über Diffusion*, Annalen der Physik, 1855, pp. 59–86, https://doi.org/10.1002/andp.18551700105.

[95] B. M. Fraeijs de Veubeke, *Displacement and equilibrium models in the finite element method*, Stress Analysis, 1965, pp. 145–197, https://doi.org/10.1002/nme.339.

[96] T. Frankel, *The geometry of physics: An introduction*, Cambridge University Press, Cambridge, 2nd ed., 2003, https://doi.org/10.1017/CBO9780511817977.

[97] Y.-C. Fung, P. Tong, and X. Chen, *Classical and computational solid mechanics*, vol. 2 of Advanced Series in Engineering Science, World Scientific Publishing Company, Singapore, 2nd ed., July 2017, https://doi.org/10.1142/9744.

[98] J. Gedicke and A. Khan, *Arnold–Winther mixed finite elements for Stokes eigenvalue problems*, SIAM Journal on Scientific Computing, Oct. 2018, pp. A3449–A3469, https://doi.org/10.1137/17M1162032.

[99] S. A. A. Ghoreyshi, F. A. Farhadpour, and M. Soltanieh, *Multicomponent transport across nonporous polymeric membranes*, Desalination, 2002, pp. 93–101, https://doi.org/10.1016/S0011-9164(02)00295-3.

[100] V. Giovangigli, *Mass conservation and singular multicomponent diffusion algorithms*, IMPACT of Computing in Science and Engineering, Mar. 1990, pp. 73–97, https://doi.org/10.1016/0899-8248(90)90004-T.

[101] ——, *Multicomponent flow modeling*, Modeling and Simulation in Science, Engineering and Technology, Birkhäuser Basel, 1999, https://doi.org/10.1007/978-1-4612-1580-6.

[102] O. Gonzalez and A. M. Stuart, *A first course in continuum mechanics*, Cambridge Texts in Applied Mathematics, Cambridge University Press, Cambridge, 2008, https://doi.org/10.1017/CBO9780511619571.

[103] J. Gopalakrishnan and J. Guzmán, *A second elasticity element using the matrix bubble*, IMA Journal of Numerical Analysis, 2012, pp. 352–372, https://doi.org/10.1093/imanum/drq047.

[104] D. W. Green and R. H. Perry, *Perry's chemical engineers' handbook*, McGraw Hill Professional, McGraw-Hill Education, 8th ed., 2007.

[105] G. Guevara-Carrion, T. Janzen, Y. Muñoz-Muñoz, and J. Vrabec, *Mutual diffusion of binary liquid mixtures containing methanol, ethanol, acetone, benzene, cyclohexane, toluene, and carbon tetrachloride*, The Journal of Chemical Physics, Mar. 2016, p. 124501, https://doi.org/10.1063/1.4943395.

[106] J. S. Hale, M. Brunetti, S. P. A. Bordas, and C. Maurini, *Simple and extensible plate and shell finite element models through automatic code generation tools*, Computers & Structures, Oct. 2018, pp. 163–181, https://doi.org/10.1016/j.compstruc.2018.08.001.

[107] E. Helfand, *On inversion of the linear laws of irreversible thermodynamics*, The Journal of Chemical Physics, Aug. 1960, pp. 319–322, https://doi.org/10.1063/1.1731144.

[108] K. Hellan, *Analysis of elastic plates in flexure by a simplified finite element method*, Acta Polytechnica Scandinavica, Civil Engineering and Building Construction Series, Jan. 1967, pp. 1–29. Finnish Academy of Technology, Tekniikentie 12, FIN-02150 Espoo, Finland.

[109] L. R. Herrmann, *Finite-element bending analysis for plates*, Journal of the Engineering Mechanics Division, Oct. 1967, pp. 13–26.

[110] R. Hiptmair, D. Pauly, and E. Schulz, *Traces for Hilbert complexes*, Mar. 2022, https://arxiv.org/abs/2203.00630.

[111] J. O. Hirschfelder, C. F. Curtiss, and R. B. Bird, *The molecular theory of gases and liquids*, John Wiley & Sons, New York, 1954, https://doi.org/10.1002/pol.1955.120178311.

[112] M. Homolya, R. C. Kirby, and D. A. Ham, *Exposing and exploiting structure: Optimal code generation for high-order finite element methods*, Nov. 2017, https://arxiv.org/abs/1711.02473.

[113] M. Homolya, L. Mitchell, F. Luporini, and D. A. Ham, *TSFC: A structure-preserving form compiler*, SIAM Journal on Scientific Computing, June 2018, pp. C401–C428, https:

//doi.org/10.1137/17M1130642.
[114] Q. Hong, J. Hu, L. Ma, and J. Xu, *An extended Galerkin analysis for linear elasticity with strongly symmetric stress tensor*, Feb. 2020, https://arxiv.org/abs/2002.11664.
[115] Q. Hong and J. Kraus, *Uniformly stable discontinuous Galerkin discretization and robust iterative solution methods for the Brinkman problem*, SIAM Journal on Numerical Analysis, Sept. 2016, pp. 2750–2774, https://doi.org/10.1137/14099810X.
[116] Q. Hong, J. Kraus, J. Xu, and L. Zikatanov, *A robust multigrid method for discontinuous Galerkin discretizations of Stokes and linear elasticity equations*, Numerische Mathematik, Mar. 2015, pp. 23–49, https://doi.org/10.1007/s00211-015-0712-y.
[117] Q. Hong, Y. Li, and J. Xu, *An extended Galerkin analysis in finite element exterior calculus*, Mathematics of Computation, 2022, pp. 1077–1106, https://doi.org/10.1090/mcom/3707.
[118] P. Howell, G. Kozyreff, and J. Ockendon, *Applied solid mechanics*, vol. 43, Cambridge University Press, Cambridge, 2009, https://doi.org/10.1017/CBO9780511611605.
[119] J. Hu, *Finite element approximations of symmetric tensors on simplicial grids in $\mathbb{R}^n$: The higher order case*, Journal of Computational Mathematics, May 2015, pp. 283–296, https://doi.org/10.4208/jcm.1412-m2014-0071.
[120] J. Hu and S. Zhang, *A family of conforming mixed finite elements for linear elasticity on triangular grids*, Jan. 2015, https://arxiv.org/abs/1406.7457.
[121] ——, *Finite element approximations of symmetric tensors on simplicial grids in $\mathbb{R}^n$: The lower order case*, Mathematical Models and Methods in Applied Sciences, July 2016, pp. 1649–1669, https://doi.org/10.1142/S0218202516500408.
[122] K. Hu. Private communication, Nov. 2021.
[123] ——, *Oberwolfach report: Discretization of Hilbert complexes*, Aug. 2022, https://arxiv.org/abs/2208.03420.
[124] ——, *Spline Bernstein–Gelfand–Gelfand sequences*. Seminar at Heidelberg University, Mar. 2022.
[125] K. Hu, Q. Zhang, J. Han, L. Wang, and Z. Zhang, *Spurious solutions for high order* curl *problems*, Nov. 2021, https://arxiv.org/abs/2110.12481.
[126] W. Hundsdorfer and J. G. Verwer, *Numerical solution of time-dependent advection-diffusion-reaction equations*, Springer Series in Computational Mathematics, Springer Berlin Heidelberg, 2013, https://doi.org/10.1007/978-3-662-09017-6.
[127] V. John, A. Linke, C. Merdon, M. Neilan, and L. G. Rebholz, *On the divergence constraint in mixed finite element methods for incompressible flows*, SIAM Review, Aug. 2017, pp. 492–544, https://doi.org/10.1137/15M1047696.
[128] C. Johnson, *On the convergence of a mixed finite-element method for plate bending problems*, Numerische Mathematik, Feb. 1973, pp. 43–62, https://doi.org/10.1007/BF01436186.
[129] R. C. Kirby, *Algorithm 839: FIAT, a new paradigm for computing finite element basis functions*, ACM Transactions on Mathematical Software, Dec. 2004, pp. 502–516, https://doi.org/10.1145/1039813.1039820.
[130] ——, *A general approach to transforming finite elements*, SMAI Journal of Computational Mathematics, Apr. 2018, pp. 197–224, https://doi.org/10.5802/smai-jcm.33.
[131] R. C. Kirby and L. Mitchell, *Solver composition across the PDE/linear algebra barrier*, SIAM Journal on Scientific Computing, Feb. 2018, pp. C76–C98, https://doi.org/10.1137/17M1133208.
[132] ——, *Code generation for generally mapped finite elements*, ACM Transactions on Mathematical Software, Dec. 2019, pp. 1–23, https://doi.org/10.1145/3361745.
[133] J. Könnö, D. Schötzau, and R. Stenberg, *Mixed finite element methods for problems with Robin boundary conditions*, SIAM Journal on Numerical Analysis, Feb. 2011, pp. 285–308, https://doi.org/10.1137/09077970X.
[134] E. Kröner, *General continuum theory of dislocations and proper stresses*, Archive for Rational Mechanics and Analysis, 1960, pp. 273–334.
[135] F. Laakmann, P. E. Farrell, and L. Mitchell, *An augmented Lagrangian preconditioner for the magnetohydrodynamics equations at high Reynolds and coupling numbers*, SIAM Journal on Scientific Computing, Aug. 2022, pp. B1018–B1044, https://doi.org/10.1137/

21M1416539.

[136] M. Lange, L. Mitchell, M. G. Knepley, and G. J. Gorman, *Efficient mesh management in Firedrake using PETSc DMPlex*, SIAM Journal on Scientific Computing, 2016, pp. S143–S155, https://doi.org/10.1137/15M1026092.

[137] V. G. Levich, *Physicochemical hydrodynamics*, Prentice-Hall International Series in the Physical and Chemical Engineering Sciences, Prentice-Hall, Englewood Cliffs, New Jersey, 1962.

[138] L. Li, *Regge finite elements with applications in solid mechanics and relativity*, PhD thesis, University of Minnesota, May 2018, http://www-users.math.umn.edu/~arnold/papers/LiThesis.pdf.

[139] E. N. Lightfoot, E. L. Cussler, and R. L. Rettig, *Applicability of the Stefan–Maxwell equations to multicomponent diffusion in liquids*, AIChE Journal, 1962, pp. 708–710, https://doi.org/10.1002/aic.690080530.

[140] A. Logg, K.-A. Mardal, and G. N. Wells, *Automated solution of differential equations by the finite element method: The FEniCS book*, vol. 84 of Lecture Notes in Computational Science and Engineering, Springer, 2012, https://doi.org/10.1007/978-3-642-23099-8.

[141] G. B. Maggiani, R. Scala, and N. Van Goethem, *A compatible-incompatible decomposition of symmetric tensors in L^p with application to elasticity*, Mathematical Methods in the Applied Sciences, 2015, pp. 5217–5230, https://doi.org/10.1002/mma.3450.

[142] H. Makihara and T. Ito, *Centrifugal separation of uranium isotopes in presence of light gas*, Journal of Nuclear Science and Technology, 1989, pp. 1023–1037, https://doi.org/10.1080/18811248.1989.9734423.

[143] J. Málek, V. Průša, T. Skřivan, and E. Süli, *Thermodynamics of viscoelastic rate-type fluids with stress diffusion*, Physics of Fluids, 2018, p. 023101, https://doi.org/10.1063/1.5018172.

[144] H. Manouzi and M. Farhloul, *Mixed finite element analysis of a non-linear three-fields Stokes model*, IMA Journal of Numerical Analysis, Jan. 2001, pp. 143–164, https://doi.org/10.1093/imanum/21.1.143.

[145] K.-A. Mardal, X.-C. Tai, and R. Winther, *A robust finite element method for Darcy–Stokes flow*, SIAM Journal on Numerical Analysis, Oct. 2002, pp. 1605–1631, https://doi.org/10.1137/s0036142901383910.

[146] J. C. Maxwell, *IV. On the dynamical theory of gases*, Philosophical Transactions of the Royal Society of London, Jan. 1867, pp. 49–88, https://doi.org/10.1098/rstl.1867.0004.

[147] M. McLeod and Y. Bourgault, *Mixed finite element methods for addressing multi-species diffusion using the Maxwell–Stefan equations*, Computer Methods in Applied Mechanics and Engineering, Sept. 2014, pp. 515–535, https://doi.org/10.1016/j.cma.2014.07.010.

[148] L. A. Mihai and A. Goriely, *Numerical simulation of shear and the Poynting effects by the finite element method: An application of the generalised empirical inequalities in nonlinear elasticity*, International Journal of Non-Linear Mechanics, Mar. 2013, pp. 1–14, https://doi.org/10.1016/j.ijnonlinmec.2012.09.001.

[149] P. Monk, *Finite element methods for Maxwell's equations*, Numerical Mathematics and Scientific Computation, Oxford University Press, New York, 2003, https://doi.org/10.1093/acprof:oso/9780198508885.001.0001.

[150] R. C. Moura, A. Cassinelli, A. F. C. da Silva, E. Burman, and S. J. Sherwin, *Gradient jump penalty stabilisation of spectral/hp element discretisation for under-resolved turbulence simulations*, Computer Methods in Applied Mechanics and Engineering, Jan. 2022, p. 114200, https://doi.org/10.1016/j.cma.2021.114200.

[151] B. Müller, G. Starke, A. Schwarz, and J. Schröder, *A first-order system least squares method for hyperelasticity*, SIAM Journal on Scientific Computing, Sept. 2014, pp. B795–B816, https://doi.org/10.1137/130937573.

[152] M. Neilan, *Discrete and conforming smooth de Rham complexes in three dimensions*, Mathematics of Computation, Sept. 2015, pp. 2059–2081, https://doi.org/10.1090/S0025-5718-2015-02958-5.

[153] S. Nicaise, K. Witowski, and B. Wohlmuth, *An a posteriori error estimator for the Lamé equation based on $H(\mathrm{div})$-conforming stress approximations*, IMA Journal of Numerical

Analysis, Apr. 2008, pp. 331–353, https://doi.org/10.1.1.495.2057.

[154] J. Nitsche, *Über ein Variationsprinzip zur Lösung von Dirichlet-Problemen bei Verwendung von Teilräumen, die keinen Randbedingungen unterworfen sind*, in Abhandlungen aus dem mathematischen Seminar der Universität Hamburg, vol. 36, Springer, July 1971, pp. 9–15, https://doi.org/10.1007/BF02995904.

[155] S. Olver and Y. Xu, *Orthogonal structure on a wedge and on the boundary of a square*, Foundations of Computational Mathematics, June 2019, pp. 561–589, https://doi.org/10.1007/s10208-018-9393-0.

[156] L. Onsager, *Reciprocal relations in irreversible processes. I*, Physical Review, Feb. 1931, pp. 405–426, https://doi.org/10.1103/PhysRev.37.405.

[157] ——, *Reciprocal relations in irreversible processes. II*, Physical Review, Dec. 1931, pp. 2265–2279, https://doi.org/10.1103/PhysRev.38.2265.

[158] ——, *Theories and problems of liquid diffusion*, Annals of the New York Academy of Sciences, Nov. 1945, pp. 241–265, https://doi.org/10.1111/j.1749-6632.1945.tb36170.x.

[159] J. E. Pasciak and Y. Wang, *A multigrid preconditioner for the mixed formulation of linear plane elasticity*, SIAM Journal on Numerical Analysis, Mar. 2006, pp. 478–493, https://doi.org/10.1137/040617820.

[160] D. Pauly and M. Schomburg, *Hilbert complexes with mixed boundary conditions – Part 2: Elasticity complex*, Mathematical Methods in Applied Sciences, Aug. 2022, https://doi.org/10.1002/mma.8242.

[161] D. Pauly and W. Zulehner, *The* divDiv*-complex and applications to biharmonic equations*, Applicable Analysis, 2020, pp. 1579–1630, https://doi.org/10.1080/00036811.2018.1542685.

[162] V. Quenneville-Bélair, *A new approach to finite element simulations of general relativity*, PhD thesis, University of Minnesota, June 2015. https://www-users.cse.umn.edu/~arnold/papers/QuennevilleThesis.pdf.

[163] R. Rannacher and S. Turek, *Simple nonconforming quadrilateral Stokes element*, Numerical Methods for Partial Differential Equations, Mar. 1992, pp. 97–111, https://doi.org/10.1002/num.1690080202.

[164] F. Rathgeber, D. A. Ham, L. Mitchell, M. Lange, F. Luporini, A. T. T. McRae, G.-T. Bercea, G. R. Markall, and P. H. J. Kelly, *Firedrake: Automating the finite element method by composing abstractions*, ACM Transactions on Mathematical Software, Dec. 2016, pp. 1–27, https://doi.org/10.1145/2998441.

[165] T. Regge, *General relativity without coordinates*, Il Nuovo Cimento (1955–1965), Feb. 1961, pp. 558–571, https://doi.org/10.1007/BF02733251.

[166] E. Reissner, *On a variational theorem in elasticity*, Journal of Mathematics and Physics, 1950, pp. 90–95, https://doi.org/10.1002/sapm195029190.

[167] R. Riedlbeck, D. A. Di Pietro, A. Ern, S. Granet, and K. Kazymyrenko, *Stress and flux reconstruction in Biot's poro-elasticity problem with application to a posteriori error analysis*, Computers & Mathematics with Applications, Apr. 2017, pp. 1593–1610, https://doi.org/10.1016/j.camwa.2017.02.005.

[168] M. E. Rognes, R. C. Kirby, and A. Logg, *Efficient assembly of* $H(\mathrm{div})$ *and* $H(\mathrm{curl})$ *conforming finite elements*, SIAM Journal on Scientific Computing, Nov. 2009, pp. 4130–4151, https://doi.org/10.1137/08073901X.

[169] J. Schöberl, *Robust multigrid methods for parameter dependent problems*, PhD thesis, Johannes Kepler University, Linz, June 1999. https://www.asc.tuwien.ac.at/~schoeberl/wiki/publications/diss.pdf.

[170] J. Schöberl and A. S. Sinwel, *Tangential-Displacement and Normal-Normal-Stress continuous mixed finite elements for elasticity*, tech. report, Linz, Oct. 2007. https://ricamwww.ricam.oeaw.ac.at/files/reports/07/rep07-10.pdf.

[171] D. Shapero, *Nitsche's method*. https://shapero.xyz/posts/nitsches-method/, 2019. Accessed 2020.11.16.

[172] D. Silvester and A. Wathen, *Fast iterative solution of stabilised Stokes systems Part II: Using general block preconditioners*, SIAM Journal on Numerical Analysis, Oct. 1994,

pp. 1352–1367, https://doi.org/10.1137/0731070.

[173] A. Sky, I. Muench, and P. Neff, *On* $[H^1]^{3\times3}$, $[H(\mathrm{curl})]^3$ *and* $H(\mathrm{symCurl})$ *finite elements for matrix-valued* Curl *problems*, Feb. 2022, https://arxiv.org/abs/2202.08740.

[174] J. Stefan, *Über das Gleichgewicht und die Bewegung, insbesondere die Diffusion von Gasgemengen*, Sitzungsberichte der Mathematisch-Naturwissenschaftlichen Classe der Kaiserlichen Akademie der Wissenschaften Wien, 2$^{\text{te}}$ Abteilung, 1871, pp. 63–124.

[175] R. Stenberg, *Some new families of finite elements for the Stokes equations*, Numerische Mathematik, Aug. 1989, pp. 827–838, https://doi.org/10.1007/BF01405291.

[176] M. Stynes and D. Stynes, *Convection-diffusion problems*, Graduate Studies in Mathematics, American Mathematical Society, 2018, https://doi.org/10.1090/gsm/196.

[177] A. Tartaglia, *Fourdimensional elasticity: Is it general relativity?*, in Frontiers of Fundamental Physics, Springer, Boston, 1994, pp. 147–152, https://doi.org/10.1007/978-1-4615-2560-8_17.

[178] A. Tasić, B. Djordjević, D. Grozdanić, N. Afgan, and D. Malić, *Vapour–liquid equilibria of the systems acetone–benzene, benzene–cyclohexane and acetone–cyclohexane at 25°C*, Chemical Engineering Science, 1978, pp. 189–197, https://doi.org/10.1016/0009-2509(78)85053-2.

[179] V. Thomée, *Galerkin finite element methods for parabolic problems*, vol. 25 of Springer Series in Computational Mathematics, Springer Berlin Heidelberg, Berlin, 2$^{\text{nd}}$ ed., 2006, https://doi.org/10.1007/3-540-33122-0.

[180] A. J. Van-Brunt, P. E. Farrell, and C. W. Monroe, *Augmented saddle point formulation of the steady-state Stefan–Maxwell diffusion problem*, IMA Journal of Numerical Analysis, Oct. 2021, https://doi.org/10.1093/imanum/drab067.

[181] ——, *Consolidated theory of fluid thermodiffusion*, AIChE Journal, Jan. 2022, p. e17599, https://doi.org/10.1002/aic.17599.

[182] N. Van Goethem, *A multiscale model for dislocations: from mesoscopic elasticity to macroscopic plasticity*, ZAMM-Journal of Applied Mathematics and Mechanics/Zeitschrift für Angewandte Mathematik und Mechanik, 2012, pp. 514–535, https://doi.org/10.1002/zamm.201100076.

[183] J. Villaluenga and A. Tabe-Mohammadi, *A review on the separation of benzene/cyclohexane mixtures by pervaporation process*, Journal of Membrane Science, May 2000, pp. 159–174, https://doi.org/10.1016/S0376-7388(99)00337-3.

[184] S. W. Walker, *FELICITY: A MATLAB/C++ toolbox for developing finite element methods and simulation modeling*, SIAM Journal on Scientific Computing, 2018, pp. C234–C257, https://doi.org/10.1137/17M1128745.

[185] Y. Wang, *Preconditioning for the mixed formulation of linear plane elasticity*, PhD thesis, Texas A&M University, College Station, Aug. 2004. https://oaktrust.library.tamu.edu/bitstream/handle/1969.1/2781/etd-tamu-2004B-MATH-Wang.pdf.

[186] S. Wu and J. Xu, *Nonconforming finite element spaces for* $2m$*th order partial differential equations on* $\mathbb{R}^n$ *simplicial grids when* $m = n + 1$, Mathematics of Computation, Mar. 2019, pp. 531–551, https://doi.org/10.1090/mcom/3361.

[187] J. Xia, P. E. Farrell, and F. Wechsung, *Augmented Lagrangian preconditioners for the Oseen–Frank model of nematic and cholesteric liquid crystals*, BIT Numerical Mathematics, Mar. 2021, pp. 1–38, https://doi.org/10.1007/s10543-020-00838-9.

[188] J. Xu, *Iterative methods by space decomposition and subspace correction*, SIAM Review, Dec. 1992, pp. 581–613, https://doi.org/10.1137/1034116.

[189] J. Xu and L. Zikatanov, *Some observations on Babuška and Brezzi theories*, Numerische Mathematik, Mar. 2003, pp. 195–202, https://doi.org/10.1007/s002110100308.

[190] S.-Y. Yi, *Nonconforming mixed finite element methods for linear elasticity using rectangular elements in two and three dimensions*, Calcolo, July 2005, pp. 115–133, https://doi.org/10.1007/s10092-005-0101-5.

[191] *Software used in 'Transformations for Piola-mapped elements'*, Oct. 2021, https://doi.org/10.5281/zenodo.5596313.

[192] *Software used in 'Finite element methods for multicomponent convection-diffusion'*, Aug. 2022,

https://doi.org/10.5281/zenodo.7017917.

[193] J. Zhan, Y. Li, W. O. Wai, and W. Hu, *Comparison between the Q criterion and Rortex in the application of an in-stream structure*, Physics of Fluids, 2019, p. 121701, https://doi.org/10.1063/1.5124245.